THE ROLES OF GLUCOCORTICOIDS AND THE ANTERIOR CINGULATE CORTEX IN HUNTINGTON'S DISEASE SYMPTOMOLOGY AND THERAPEUTICS

By

Brett D. Dufour

A DISSERTATION

Presented to the Department of Behavioral Neuroscience
and Oregon Health & Science University
School of Medicine
in partial fulfillment of
the requirements for the degree of

Doctor of Philosophy

January 2018

School of Medicine

Oregon Health & Science University

CERTIFICATE OF APPROVAL

This is to certify that the PhD dissertation of
Brett D. Dufour
has been approved

_____
Andrey Ryabinin, Committee Chair

_____
Jodi McBride, Mentor/Advisor

_____
Deb Finn, Member

_____
Penny Hogarth, Member

_____
Charlie Meshul, Member

_____
Joe Quinn, Member

Table of Contents

List of Figures and Tables

Abbreviations

AAV – Adeno Associated Virus

ACC – anterior cingulate cortex

ACTH – adrenocorticotropin hormone

ADX – adrenalectomy

CORT – corticosterone and/or cortisol

CRF – Corticotropin Releasing Factor

Cre – Cre-recombinase

FST – forced swim test

HD – Huntington's disease

HTT – wild-type huntingtin (gene)

HTT – wild-type huntingtin (protein)

LD – light-dark test

m*HTT* – mutant huntingtin (gene)

mHTT – mutant huntingtin (protein)

PVN – paraventricular nucleus

SCN – suprachiasmatic nucleus

SP – sucrose preference (test)

Acknowledgements

First, I would like to thank my boyfriend, John Criscitello, for the tremendous amount of love, kindness, support, and patience that he always provides, for being a wonderful partner in life, and for always making me smile. I would also like to thank my family, particularly my parents Glenn and Beverly, who are two of the most selfless, loving, and kind people I have ever known, and who have always been endlessly supportive. I am incredibly lucky to have you as my parents. To the rest of my family: Mark, Matt, Kelly, Stacey, Michelle, Cameron, Ethan, Madison, Rylie, Austin, Julian, Mia, and Vincent – thank you and I love you. I would also like to thank Byrd McDonald and Doug Schick for being wonderful and supportive friends. And finally, to Bret Fuller - thank you for many years of love and companionship. You are my best friend and will always be a part of my family.

Professionally and academically - I would first like to thank Jodi McBride for giving me a chance and helping me get a start in neuroscience back in 2010. I can't thank you enough for all of the training, support, and patience that you have provided over many years. I have had many opportunities that aren't always afforded to other trainees, including the freedom in determining my own projects, and the financial and intellectual support in executing them. You have provided me with many tools that I will carry with me always, both personally and professionally. Also, thank you to Mark Pitzer for great stories and lots of support and training as I was getting started in the McBride lab. I would like to thank the greater McBride lab, with a particular acknowledgement of Jordan Lueras, Randy Clark, Dana Button, and Jackie Domire, as well as Alison Weiss and Will Liguore.

I would like to thank myself for assembling an amazing dissertation advisory committee. I sought to choose people who are intelligent, experienced, and uncompromising scientists who are also kind and supportive people that I knew would serve as great mentors. I knew you would

all provide me with excellent training and I was right. Andrey – thank you so much for chairing the committee, for great conversations about neuroscience, neuropeptides, region specific vasopressin receptor expression and social monogamy, the edinger-westphal nucleus, alcohol, voles, and molecular genetic tools. You have been incredibly giving over the years and have provided a tremendous amount of support (letters of rec, NRSA, help with talks, etc). I can't thank you enough. Charlie – thanks for always taking time for me and being an amazing advocate. Your support has been invaluable. Deb – thanks for your kindness and support. It's amazing all of the hard work you selflessly do, including teaching and being incredibly active in the department and graduate program. You've always been super kind and eager to help, and I appreciate it greatly. Penny – thank you so much for taking this on as your first dissertation advisory committee, for making time for meetings, and for providing an incredibly important clinical point of view.

I would also like to thank all of the other people that have provided help in my research and academic endeavors while here at OHSU: the Kievit lab and Rene Lindsley for help with metabolic chambers, the small laboratory animal unit at the ONPRC for lots of assistance broadly and for taking great care of my mice, Drew Martin for help in getting adrenalectomy surgeries up and running and providing other surgical assistance and support. Thank you so much Kris Thomason, Nicole Ernst, Jeanne Sutter – you all have helped tremendously in so many different ways. None of us students would be able to do this without you.

Lastly, I would like to thank my funding sources. In particular, I would like to thank Quentin and Bea Neufeld – you're both wonderful, and your donations to the lab have been incredibly generous and invaluable for me completing many of the experiments presented here. Of course, I would like to thank Jodi McBride (again) as she has provided a tremendous amount of financial investment and support in my endeavors. I would like to thank the NIH/NINDS for providing me with funding through the pre-doctoral NRSA program.

Abstract

The prognosis for patients with the genetic neurological disorder Huntington's disease (HD) is incredibly poor. HD onsets in midlife, causes a variety of severe and debilitating symptoms, progresses over 10-15 years, and always leads to death. There are currently no treatments that can slow the progression of the disease in any way. Thus, there is tremendous need to discover new therapeutic approaches that can slow or halt disease progression and thereby improve quality of life for patients. In the studies presented here, I characterized the roles of glucocorticoids and the anterior cingulate cortex in HD symptomology, with the overarching goal of assessing the suitability of these two systems as possible points of therapeutic intervention for HD. In Chapter 2, I verified that the R6/2 mouse HD model has elevated glucocorticoid levels, and demonstrated that chronically elevated glucocorticoid levels worsens HD symptomology in this model by exacerbating weight loss and shortening lifespan. In Chapter 3, I further demonstrated that not only do elevated glucorticoid contribute to HD symptomology, but that normalizing glucocorticoids to wild-type levels in R6/2 mice attenuates HD metabolic symptomology and neuropathology. In Chapter 4, I assessed the role of the anterior cingulate cortex (ACC) in HD mood symptoms. Here, I tested the hypothesis that reducing mHTT expression in the ACC in the BACHD mouse model of HD would reduce depressive- and anxiety-like behavior. These data show that reducing mHTT expression in the ACC leads to a reduction in depressive-like symptomology but has no effect on anxiety-like symptoms, thus confirming that mHTT toxicity in the ACC is causal to some HD mood symptomology. Accordingly, the findings from this dissertation confirm that both of these pathophysiological systems, elevated glucocorticoids and mHTT toxicity in the ACC, do directly contribute to HD symptomology and that ameliorating pathology in these systems could possibly lead to symptom improvement for patients.

Chapter 1 – Introduction

Huntington's disease (HD) is a fatal, genetic neurodegenerative disorder. The hallmark symptom of the disease is Huntington's chorea, whereby patients show uncontrollable hyperkinetic movements that become progressively more severe (Huntington Study Group, 1996; Ross *et al.*, 2014). Although typically conceptualized as a movement disorder, HD patients also suffer from severe cognitive, psychiatric, and metabolic symptoms (Anderson & Marder, 2001; Bamford *et al.*, 1995; Kirkwood *et al.*, 2001; Ross *et al.*, 2014; Ross & Tabrizi, 2011; van der Burg *et al.*, 2009). The disease typically onsets in the 3rd to 4th decade of life, progresses over 15-20 years, and always leads to death (Ross *et al.*, 2014). It is more common in individuals of European ancestry, with an estimated prevalence of 5.70 per 100,000 (Pringsheim *et al.*, 2012).

1.1 – HD Genetics and Pathology

Although HD had long been known to be a heritable disease, the gene that causes the disease was not identified until 1993. Linkage analysis studies in the early 1980s first associated the genetic mutation that causes HD to chromosome 4, although the exact locus remained unclear (Gusella *et al.*, 1983). Subsequent studies identified the IT15 locus as the disease causing gene, which was subsequently named the Huntingtin gene (*HTT*) (Huntington Disease Collaborative Research Group, 1993). *HTT* is a large 180kb gene consisting of 67 exons, and in turn codes for a large 348kd Huntingtin protein (Huntington Disease Collaborative Research Group, 1993). These authors (1993) further demonstrated that a mutation in exon 1 of the *HTT* gene, consisting of an expansion of the naturally occurring DNA bases cytosine-adenine-guanine (CAG) triplet region, is causal to the HD phenotype (Huntington Disease Collaborative Research Group, 1993). The mutated allele shows typical Mendelian inheritance and is autosomal dominant - thus a single

mutated copy is sufficient to cause disease. Average CAG repeat length for the wild-type Huntingtin allele in humans is between 17-20 (Kremer *et al.*, 1994). Alleles with 40 or more repeats result in a fully penetrant HD phenotype (ACMG/ASHG, 1998). A CAG repeat length of 36-39 results in incomplete penetrance, with some individuals (but not all) developing mild HD symptoms later in life (ACMG/ASHG, 1998). Age of onset is inversely proportional to the length of the CAG repeat, with extremely large expansions resulting in childhood onset (Andrew *et al.*, 1993). Characterizing the genetics of the disease was a turning point in HD research. It enabled genetic testing for individuals at risk for carrying the gene (ACMG/ASHG, 1998). It also enabled the development of transgenic animal models of HD (Chan *et al.*, 2015; Chang *et al.*, 2015; Mangiarini *et al.*, 1996), which have been indispensable for characterizing the mechanisms that underlie HD pathology and symptomology, as well as for the development of novel therapeutics.

The HTT gene is expressed ubiquitously, throughout the brain and peripheral tissues, although it is expressed at highest levels in the brain and testes (Moffitt *et al.*, 2009; Sharp *et al.*, 1995; Trottier *et al.*, 1995). The function of the wild-type allele is less characterized than the mutant allele, as developing a better understanding HD pathology has been of particular interest for researchers. However, the wild-type allele appears to be important for development, as full knockout of the wild-type allele is embryonic lethal in rodents (Nasir *et al.*, 1995). In adults, the wild-type allele appears to play an important role in intracellular transport and scaffolding (Caviston & Holzbaur, 2009; Caviston *et al.*, 2007), synaptic terminal integrity (Sun *et al.*, 2001), and gene expression (Cattaneo *et al.*, 2005). While there has been interest in whether the HD mutation leads to disease through a loss of function of the wild-type allele, this seems to largely not be the case (Ross & Tabrizi, 2011). In fact, the mutated HTT allele does retain some healthy endogenous function, as individuals that are homozygous for the *mHTT* allele develop normally and do not show an earlier age of disease onset relative to heterozygotes (Wexler *et al.*, 1987),

although they do show some worsening of symptomology once the disease onsets (Squitieri *et al.*, 2003).

Although there isn't much empirical support for loss of function mechanisms mediating HD symptomology, there is considerable evidence that the HD mutation leads to disease through a toxic gain of function (Miller *et al.*, 2010; Ross & Tabrizi, 2011). The polyglutamine expansion in mHTT protein causes alterations in protein folding and conformation, which results in mHTT existing in different forms: as soluble misfolded monomers, soluble intermediate sized oligomers, and large aggregated inclusion bodies (Ross & Tabrizi, 2011). There remains uncertainty over which species is the most toxic (Todd & Lim, 2013), with particular disagreement over the nature of inclusion bodies: whether they represent a neuroprotective mechanism by which the cell inactivates the more toxic soluble species (Arrasate *et al.*, 2004; Miller *et al.*, 2010), or whether they represent a more toxic mHTT form themselves. Although inclusion formation may offer some neuroprotective effects for the cell early in the disease process (Arrasate *et al.*, 2004), mHTT-positive inclusion bodies are indeed toxic – polyglutamine containing aggregates grown *in vitro* and introduced into the nucleus of cultured cells, but not the cytosol, leads to dramatic cell death (Yang *et al.*, 2002). However, consensus in the field seems to be moving more towards the concept that soluble oligomer species are even more toxic than aggregates or soluble monomers (Arrasate *et al.*, 2004; Miller *et al.*, 2010; Takahashi *et al.*, 2008), without precluding the idea that aggregates and monomers still confer a certain amount of toxicity (Nagai *et al.*, 2007; Ross & Tabrizi, 2011; Todd & Lim, 2013). mHTT protein is altered in many other ways than simply its conformation and tendency to aggregate. It is proteolytically cleaved into smaller n-terminal fragments of varying sizes, which contain the mutated polyglutamine expansion, and are also considered to be more toxic than full length mHTT (Landles *et al.*, 2010; Ratovitski *et al.*, 2009; Schilling *et al.*, 1999; Schilling *et al.*, 2007). mHTT also undergoes numerous post-translational modifications, including

phosphorylation, acetylation, ubiquitination, and sumolyation, which can have varying effects on mHTT toxicity, depending on the type and locus of peptide modification (Gu *et al.*, 2009; Rockabrand *et al.*, 2007; Schilling *et al.*, 2006). Wild-type HTT undergoes palmitoylation, which enhances membrane association, while mHTT protein loses the capacity for this modification which in turn results in increased unbound cytosolic levels and increased toxicity (Yanai *et al.*, 2006). Although many different mechanisms of toxicity have been identified on a molecular level, the sequence and progression of toxic events have yet to be clearly elucidated (Ross & Tabrizi, 2011). Regardless, there is a clear dose-response relationship between intracellular mHTT levels and mHTT toxicity (Arrasate *et al.*, 2004; Miller *et al.*, 2010), and this toxicity is further augmented by the fact that mHTT protein is degradation resistant, which further increases intracellular levels (Fu *et al.*, 2017; Tsvetkov *et al.*, 2013).

The toxic gain of function of mHTT protein leads to a progressive disruption in numerous cellular processes, and can eventually lead to cell death. mHTT impairs transcription, broadly (Cui *et al.*, 2006; Hodges *et al.*, 2006), both through direct interaction with DNA (Benn *et al.*, 2008), and indirectly by impairing the function of other transcription factors (Nucifora *et al.*, 2001; Schaffar *et al.*, 2004). One particularly important consequence is the downregulation of the anti-apoptotic neurotrophic factor BDNF (Zuccato *et al.*, 2001). Mitochondria are also negatively impacted by mHTT in many ways, including reduced mitochondrial biogenesis (Shirendeb *et al.*, 2012), direct inhibition of Complex II and IV of the electron transport chain leading to reduced ATP levels and impaired cellular metabolism (Benchoua *et al.*, 2006; Damiano *et al.*, 2010; Tabrizi *et al.*, 2000), and impaired CA++ buffering leading to increased cytosolic levels which in turn upregulate calpains and thus increase the likelihood of excitotoxic cell death (Milakovic & Johnson, 2005; Milakovic *et al.*, 2006). Reactive oxygen species are also increased in HD cells, and thus likely further exacerbate cellular toxicity, elevate CA++ levels, and increase the likelihood of

apoptosis (Damiano *et al.*, 2010; Tabrizi *et al.*, 2000). Cellular trafficking is disrupted by mHTT, including trafficking of mitochondria to nerve terminals (Shirendeb *et al.*, 2012). There are also many impairments in proteostasis, including reduced expression of chaperones (Hay *et al.*, 2004), as well as impairments in the ubiquitin-proteasome system and autophagy (Bence *et al.*, 2001), leading to increased levels and aberrant folding of mHTT, as well as impaired processing and degradation of other peptides (Ross & Tabrizi, 2011).

As mHTT expression levels are uniquely high in brain, both neurons and other non-neuronal cell types are particularly impacted by mHTT toxicity. In living neurons, mHTT toxicity results in abnormalities in resting membrane potential and capacitance (Cummings *et al.*, 2009; Klapstein *et al.*, 2001), altered spontaneous currents (EPSCs and IPSCs), increased firing rates (Cummings *et al.*, 2009; Klapstein *et al.*, 2001; Rebec *et al.*, 2006), and alterations in neurotransmitter synthesis and release (Cepeda *et al.*, 2014) – all of which lead to impaired neuronal communication (Cepeda *et al.*, 2010). There are also high rates of neuronal cell death (Vonsattel *et al.*, 1985), for which particular neuronal cell-types are selectively vulnerable (Cowan & Raymond, 2006; Graveland *et al.*, 1985; Richfield *et al.*, 1995), and which further disrupts functional circuitry. The medium spiny neurons (MSN) of the striatum are particularly vulnerable (Ehrlich, 2012), with some patients showing a loss of 95% or more of these neurons by end stages of disease (Vonsattel *et al.*, 1985). MSNs appear to be more vulnerable than other cell types to cell-autonomous mHTT toxicity (de Almeida *et al.*, 2002; Desplats *et al.*, 2006; Zala *et al.*, 2005), outlined above, while at the same time these cells are also at high risk of excitotoxic cell death by non-cell autonomous mechanisms. These two possible processes have been figuratively described as either MSN suicide (cell-autonomous mechanisms) or murder (non-cell autonomous mechanisms) (Ehrlich, 2012) – however it's likely that these processes work synergistically. MSNs are highly innervated by cortical glutamatergic projections, as well as dopaminergic projections

from the substantia nigra pars compacta, and in HD there is an increase in release of both neurotransmitters onto MSNs in HD (Andre *et al.*, 2010; Cepeda *et al.*, 2014; Garrett & Soares-da-Silva, 1992; Li *et al.*, 2004; Milnerwood *et al.*, 2010). Persistent elevations in glutamate and dopamine can result in excitotoxicity (Buisson *et al.*, 1992; Garside *et al.*, 1996; Hastings, 2009; Linden *et al.*, 1987), even in healthy neurons, and mHTT+ cells are even more vulnerable given their widespread cellular pathology (Andre *et al.*, 2010; Ehrlich, 2012; Jakel & Maragos, 2000; Wu *et al.*, 2016). Additionally, BDNF, which is released by the cortex to provide neurotrophic support for MSNs, is downregulated in HD and thus renders these cells even more vulnerable (Canals *et al.*, 2004; Xie *et al.*, 2010). In addition to direct mHTT induced pathology in neurons and neuronal circuits, mHTT is also expressed in astrocytes and other non-neuronal cell types, further disturbing cellular homeostasis throughout the brain (J. Bradford *et al.*, 2010; J. W. Bradford *et al.*, 2010).

Gross neuropathological analysis of the HD brain indicates that there are regional reductions in brain volume, dramatic neuronal cell loss, the presence of mHTT inclusion bodies, as well as markers of inflammation such as astrogliosis and microglial activation and proliferation (Rub *et al.*, 2015; Sapp *et al.*, 2001; Vonsattel *et al.*, 1985). In addition to dramatic reductions in striatal volume related to MSN cell loss, the rest of the basal ganglia also show particularly severe degeneration (Glass *et al.*, 2000; Vonsattel *et al.*, 1985). The cortex also shows loss of pyramidal cells and GABAergic interneurons, although there is heterogeneity in patients with respect to specific cortical regions that are affected (Heinsen *et al.*, 1994; Kim *et al.*, 2014; Thu *et al.*, 2010). While the basal ganglia and cortex are most affected, many other regions show significant pathology and cell loss, including the hypothalamus (Gabery *et al.*, 2010; Soneson *et al.*, 2010; Timmers *et al.*, 1996), cerebellum (Rodda, 1981; Rub *et al.*, 2013), hippocampus (Rosas *et al.*, 2003; Spargo *et al.*, 1993), amygdala (Kipps *et al.*, 2007; Rosas *et al.*, 2003), and brainstem nuclei (Zweig *et al.*, 1992). Patients also show neuroendocrine changes (Saleh *et al.*, 2009) and

autonomic nervous system hyperactivity (Andrich *et al.*, 2002; Aziz *et al.*, 2010; Bar *et al.*, 2008). Although lower than in brain, mHTT is also expressed in peripheral cells and tissues leading to significant pathology in muscle, bone, the digestive system, and other tissues (Goodman & Barker, 2011; Luthi-Carter *et al.*, 2002; Magnusson-Lind *et al.*, 2014; Moffitt *et al.*, 2009; Phan *et al.*, 2009; van der Burg *et al.*, 2009).

1.2 - HD Clinical Symptomology

HD symptoms are an emergent property of widespread mHTT induced impairment in neuronal and non-neuronal cell types, including progressive cell loss throughout the brain and periphery. As cellular level pathology varies widely between different cell types and tissues, some systems are more affected than others. The net result is a variety of progressive and severe symptoms, which can be somewhat idiosyncratic to individual patients (Kim *et al.*, 2014; Thu *et al.*, 2010), and that largely fall into four domains: motor, cognitive, psychiatric, and metabolic/peripheral (Anderson & Marder, 2001; Harrington *et al.*, 2014; Huntington Study Group, 1996; Kirkwood *et al.*, 2001; Nehl & Paulsen, 2004; Petersen & Bjorkqvist, 2006; Ross *et al.*, 2014; van der Burg *et al.*, 2009). While HD is often characterized primarily as a movement disorder, other non-motor symptom domains are also quite severe and may have an even more deleterious impact on quality of life (Anderson & Marder, 2001; Ho *et al.*, 2009). Disease onset is clinically defined as the onset of motor symptoms (Huntington Study Group, 1996), which tends to occur in the 4th decade of life (Aziz *et al.*, 2012; Ross *et al.*, 2014). Disease progression is typically characterized as five disease stages, reflecting increasing loss of function and symptom severity (See **Figure 1.1**) (Huntington Study Group, 1996; Ross *et al.*, 2014; Shoulson & Fahn, 1979), although some non-motor 'premanifest symptoms' are present before the onset of motor symptoms (Duff *et al.*, 2007; Kirkwood *et al.*, 2001; Paulsen *et al.*, 2008). Systems-level

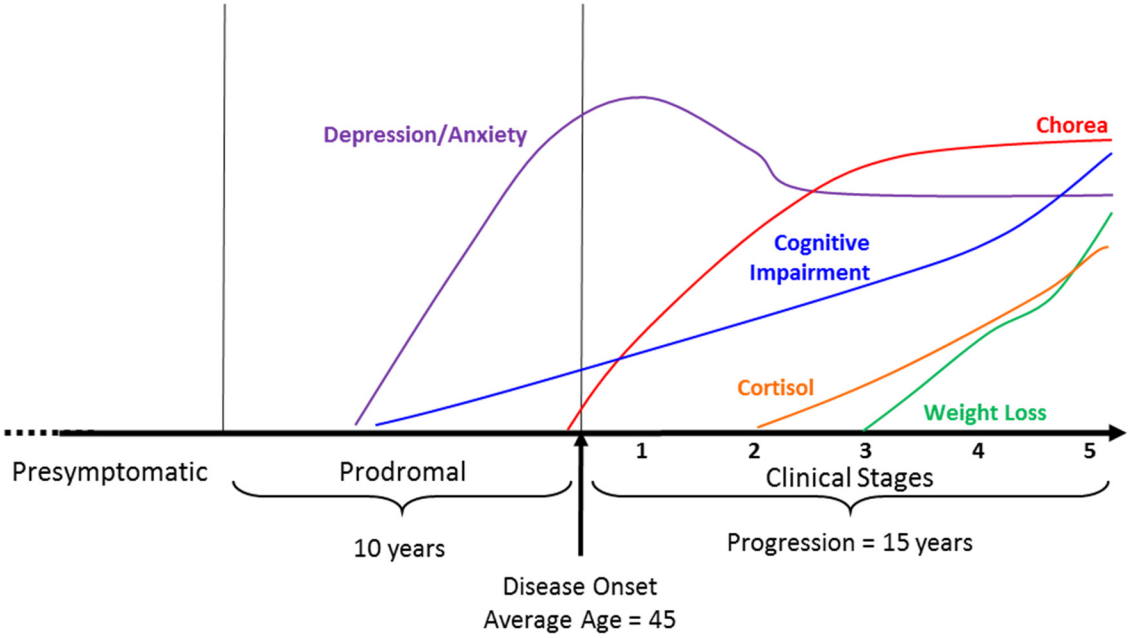

Figure 1.1 – Timecourse of Symptom Progression in Huntington's Disease. Clinical onset of Huntington's disease (HD) is defined by the onset of chorea in midlife (average age of onset is 45). Symptomology across all domains is progressive and increasing clinical stages are defined by increasing symptom severity, decreasing functional capacity, and ultimately death. Both cognitive and mood (depression/anxiety) symptoms first appear in the prodromal stage, before the onset of chorea. Mood symptom prevalence and severity increase into clinical stages 1 and 2, then attenuate slightly. Cognitive symptoms are progressive throughout disease progression. Weight loss and a progressive increase in cortisol begins in mid-stages and worsens through end stage. **Adapted and modified from Ross *et al.*, 2014; Kirkwood *et al.*, 2001; and Bjorkquist et al. 2006a**.

mechanisms that underlie motor symptoms are rather well characterized, while those that underlie HD cognitive, psychiatric, and metabolic symptom domains are less understood.

HD patients show a variety of severe motor symptoms, initially involving hyperkinetic and uncontrollable motor movements called chorea (Berardelli *et al.*, 1999; Thompson *et al.*, 1988), which worsen with time. Patients also suffer from other motor symptoms including a loss of fine motor skills, postural changes, irregular gait and difficulty walking, muscle weakness, difficulty chewing and swallowing, and respiratory difficulties (Berardelli *et al.*, 1999; Kirkwood *et al.*, 2001; Reyes *et al.*, 2014; Ross *et al.*, 2014; Thompson *et al.*, 1988; Trejo *et al.*, 2004). Towards late stages of the disease, hyperkinetic movements attenuate, and patients instead begin to show a hypokinetic phenotype, which includes dystonia, rigidity, bradykinesia, and a difficulty in initiating movement (Berardelli *et al.*, 1999; Hefter *et al.*, 1987; Kirkwood *et al.*, 2001; van Vugt *et al.*, 1996). Pathophysiological mechanisms that underlie these motor symptoms are well described. Hyperkinetic choreiform movements likely reflect a disinhibited striatum, mediated by preferential early loss of D2+ striatal indirect pathway MSNs (Albin *et al.*, 1992; Deng *et al.*, 2004; Galvan *et al.*, 2012). Elevated dopaminergic input into the striatum also contributes, and medications that reduce dopaminergic input (e.g. Tetrabenazine, a VMAT2 inhibitor) reduce chorea (Cepeda *et al.*, 2014; Garrett & Soares-da-Silva, 1992). The motor cortex is also impacted in HD, and more severe pathology there is associated with more severe motor symptoms (Thu *et al.*, 2010). In later stages, loss of D1+ direct pathway becomes more severe, and likely contributes to the hypokinetic phenotype (Deng *et al.*, 2004; Galvan *et al.*, 2012).

HD patients show a variety of severe and progressive cognitive deficits, often before the onset of motor symptoms (Snowden *et al.*, 2002; Stout *et al.*, 2011; Tabrizi *et al.*, 2011). During the premanifest stages a variety of deficits emerge, including impairments in emotional recognition, psychomotor speed, and executive function (Snowden *et al.*, 2002; Snowden *et al.*,

2015; Unmack Larsen *et al.*, 2015). Executive function is particularly impaired, with patients showing deficits in working memory, complex cognitive set-shifting tasks, as well as difficulty in everyday cognitive abilities such as goal planning, decision making, and sustaining attention (Dumas *et al.*, 2013; Lawrence *et al.*, 1996; Snowden *et al.*, 2002; You *et al.*, 2014). Patients often become cognitively disinhibited as the disease progresses, another type of executive function impairment, resulting in a variety of impulsive and unwanted behavioral actions (Johnson *et al.*, 2017). Executive function is largely mediated by interconnected frontal cortex and basal ganglia circuitry, and thus it is no surprise that these deficits are so severe in HD (Elliott, 2003; Heyder *et al.*, 2004; Joel, 2001). Indeed, many imaging studies have confirmed that frontal-corticostriatal abnormalities in HD corresponds to the severity of executive function deficits for patients (Bamford *et al.*, 1995; Joel, 2001; Lawrence *et al.*, 1998; Tabrizi *et al.*, 2011). In later disease stages, patients also show more global cognitive deficits, sometimes described as dementia, including general deficits in memory and reduced measures of intelligence (Dumas *et al.*, 2013; Peavy *et al.*, 2010; Snowden *et al.*, 2015).

The most deleterious symptoms for many HD patients, with respect to quality of life, are psychiatric symptoms and personality changes (Anderson & Marder, 2001; Ho *et al.*, 2009). Of the four HD symptom clusters, the mechanisms that underlie psychiatric symptoms in HD are the most poorly understood. Patients show increased levels of aggression and irritability, and paradoxically, feelings of apathy are also quite common (Anderson & Marder, 2001; Paulsen *et al.*, 2001; van Duijn *et al.*, 2010). Depression and anxiety are particularly prevalent in HD populations (See section 1.4 below for a more comprehensive review) (Paulsen *et al.*, 2005; Paulsen *et al.*, 2001; van Duijn *et al.*, 2010), and lead to a significant reduction in quality of life (Ho *et al.*, 2009). Suicide rates are particularly high in HD: approximately 27% attempt suicide, and 3-7% complete it (Anderson & Marder, 2001; Farrer, 1986). There is overlap with some cognitive

domains here, as increased impulsivity and emotional recognition can also interact with other aspects of psychopathology. For instance, it is postulated that increases in impulsivity may contribute to high rates of suicide in HD, in combination with depressive symptoms (Novak & Tabrizi, 2010). Some patients also show obsessive or compulsive symptoms, although they don't necessarily meet full DSM criteria for Obsessive Compulsive Disorder (Anderson & Marder, 2001; Marder *et al.*, 2000). Although rare, some HD patients also show psychotic symptoms (Paulsen *et al.*, 2001).

The fourth HD symptom domain is a heterogeneous grouping of symptomology relating to peripheral tissue pathology and whole body metabolic disturbance (Reviewed by van der Burg *et al.*, 2009). The best characterized of these symptoms is a metabolic phenotype, in which patients show progressive weight loss. Patients are in a state of negative energy balance (Gaba *et al.*, 2005; Goodman *et al.*, 2008), showing weight loss in spite of spontaneously increased hunger and caloric intake (Trejo *et al.*, 2004), although further caloric supplementation can help to slow weight-loss (Trejo *et al.*, 2005). There is an increase in sedentary energy expenditure in patients (Pratley *et al.*, 2000), suggesting that this state of negative energy balance is not simply due to the hyperkinetic movement phenotype, but perhaps due to a generalizable metabolic defect such as mHTT induced mitochondrial dysfunction (Damiano *et al.*, 2010). However, there is evidence energy expenditure can be further worsened by hyperkinetic movements (Gaba *et al.*, 2005). In addition to weight loss, patients also show severe skeletal muscle wasting. Cardiac muscle also shows pathology (Mihm *et al.*, 2007), and there appears to be an increased incidence of heart disease in patients (Lanska *et al.*, 1988; van der Burg *et al.*, 2009). Patients have reduced bone mineral density (osteoporosis) (Goodman & Barker, 2011), and also have higher rates of Type-II diabetes. Pathology has been documented throughout the digestive system, including the stomach, pancreas, and liver, although the consequences of that pathology on healthy function

(e.g. nutrient breakdown, absorption, and metabolic regulation) is poorly characterized in human patients.

Many of these metabolic/peripheral symptoms are likely multifactorial, resulting from a mixture of mHTT mediated pathological mechanisms, including: CNS pathology, neuroendocrine disturbance, and the direct consequences of mHTT expression and toxicity in peripheral tissues themselves. With respect to central (CNS) mechanisms of metabolic dysfunction, the hypothalamus is a key suspect (Petersen & Bjorkqvist, 2006). Hypothalamic pathology is severe and occurs early in HD, with volumetric reductions detectible up to 10 years before the onset of motor symptoms (Soneson *et al.*, 2010), and involving the loss of several neuropeptide cell populations (Gabery *et al.*, 2010). In particular, there is a dramatic loss of orexin+ neurons, key central regulators of metabolism (Petersen *et al.*, 2005). Additionally, HD patients show neuroendocrine disturbance – cortisol, growth hormone, and IGF-1 levels are elevated (Saleh *et al.*, 2009), which are regulated by separate corticotropic and somatotropic hypothalamic-pituitary axes. Both cortisol and GH levels are negatively correlated with body mass index in HD (Saleh *et al.*, 2009), suggesting that these hormonal abnormalities may mediate and/or further exacerbate HD metabolic symptoms. HD patients also have autonomic nervous system abnormalities, including both sympathetic and parasympathetic nervous system dysfunction (Andrich *et al.*, 2002; Bar *et al.*, 2008). Although likely driven by central mechanisms, possibly by locus coeruleus or hypothalamic pathology (Bar *et al.*, 2008; Zweig *et al.*, 1992), autonomic dysfunction could have dramatic downstream effects on innervated visceral targets and metabolism. However, some peripheral abnormalities may be driven by endogenous mHTT expression and toxicity alone. Testicular pathology in HD is a good example: there is severe and progressive degeneration of the testes leading to a reduction in testosterone levels in late stage male patients (Saleh *et al.*, 2009; Van Raamsdonk *et al.*, 2007). Testicular pathology does not seem to be due to reductions in

gonadotropic hormones, as these levels remain normal throughout life (Saleh *et al.*, 2009). Since mHTT expression levels is particularly high in the testes, comparable to brain expression levels (Strong *et al.*, 1993), it is likely that endogenous toxicity is severe and leads to widespread degeneration.

1.3 - Glucocorticoids and Huntington's disease

Elevated cortisol is a well-documented symptom in HD patients (Bjorkqvist *et al.*, 2006a; Heuser *et al.*, 1991; Saleh *et al.*, 2009; Shirbin, Chua, Churchyard, Hannan*, et al.*, 2013). However, the mechanisms that underlie this elevation, as well as the consequences of this elevation on HD symptomology, remain poorly characterized. Given the well characterized roles of glucocorticoids in health and disease, it has long been suspected that elevated glucocorticoid levels in HD contribute to symptomology, particularly with respect to cognitive, psychiatric, and metabolic symptom domains (Petersen & Bjorkqvist, 2006; Saleh *et al.*, 2009; Shirbin et al. 2013).

Cortisol is a steroid hormone produced in the zona fasciculata of the adrenal cortex and released into the blood stream in response to circulating levels of adrenocorticotropic hormone (ACTH). ACTH is released by the pituitary gland into the general circulation, and its release is in turn regulated by the upstream release of corticotropin releasing hormone (CRH) from the paraventricular nucleus of the hypothalamus into the pituitary (Whitnall, 1993). This system is referred to as the Hypothalamic-Pituitary-Adrenal (HPA) axis and is outlined in **Figure 1.2**. Like other steroid hormones, it is lipid soluble and thus able to diffuse through lipid based membranes easily, including the plasma membranes of cells as well as more complex multicellular membranes such as the blood brain barrier (Pardridge & Mietus, 1979). Cortisol is the main glucocorticoid hormone in humans and is the natural ligand of the glucocorticoid receptor (GR). However, cortisol is a somewhat promiscuous ligand and also has a high affinity for the mineralocorticoid

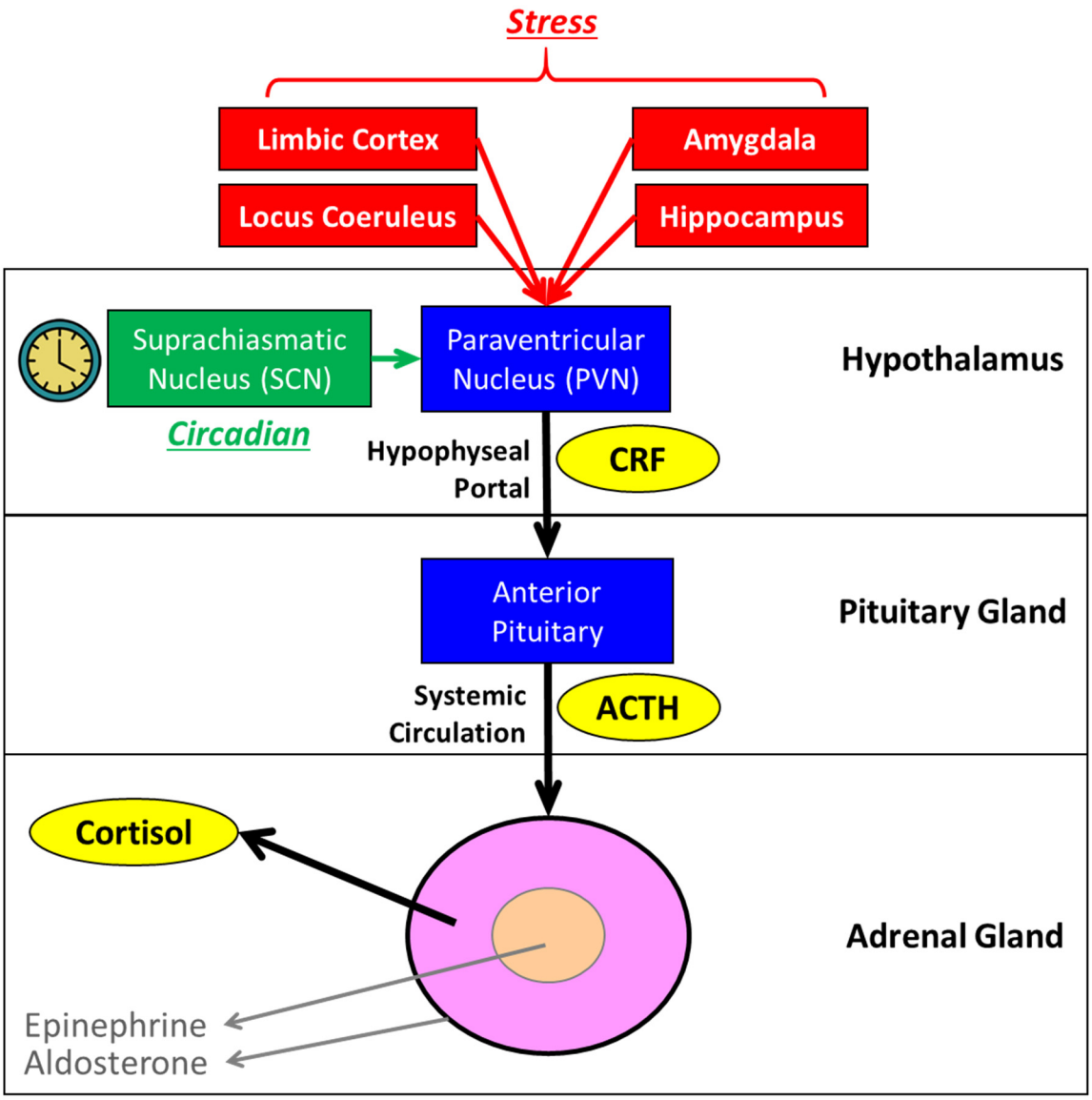

Figure 1.2 – Hypothalamic-Pituitary-Adrenal (HPA)Axis. Cortisol release is regulated by the HPA-axis, which is outlined here. Corticotropin Releasing Factor (CRF) is released by the paraventricular nucleus (PVN) of the hypothalamus into the hypophyseal portal vein, where it stimulates adrenocorticotropin hormone (ACTH) release from the anterior pituitary gland into systemic circulation. ACTH in-turn stimulates the release of the steroid hormone cortisol from the cortex of the Adrenal Gland into systemic circulation, whereby it exerts it numerous effects by signaling at the glucocorticoid receptor, which is expressed throughout the brain and body. Cortisol is released in a diurnal pattern, which is mediated by the suprachiasmatic nucleus (SCN) of the hypothalamus, which regulates a circadian pattern of CRF release. Cortisol is also released in response to acute stressors, which is caused by stress signals transduced by numerous limbic brain regions (including limbic cortex, locus coeruleus, amygdala, hippocampus, and others) which activate the HPA-axis by stimulating an acute release of CRF. Other hormones are also produced by the adrenal gland (indicated in gray), including epinephrine and aldosterone, but are not a part of the HPA-axis.

receptor (MR), the primary receptor for aldosterone (Arriza *et al.*, 1988; Gomez-Sanchez & Gomez-Sanchez, 2014). However, many cells expressing MRs also express 11 β-hydroxysteroid dehydrogenase type 2 (11-β-HSD2), and enzyme that inactivates cortisol by converting it to cortisone, and thus blocking its ability to signal at MRs in these cells (Tomlinson & Stewart, 2001). As with other steroid hormone receptors, the GR is a cytosolic peptide that is a transcription factor, with both a ligand binding domain and a DNA binding domain (Mangelsdorf *et al.*, 1995). GRs are bound to heat shock proteins (Hsp70 and Hsp90), which alter the conformation of the protein to expose the ligand binding domain and thus enable signaling by cortisol (Pratt, 1993). Once bound to ligand, GRs dimerize, translocate to the nucleus, form a complex with transcriptional co-regulators, and bind to glucocorticoid response elements (GREs - DNA sequences in the promoter regions of genes that bind the activated ligand-GR complex) to alter the expression of target genes (Mangelsdorf *et al.*, 1995; Weikum *et al.*, 2017).

Cortisol is released in a diurnal pattern, with levels increasing in the early morning in humans (shortly before waking), peaking at mid-day, and then returning to low levels in the evening/overnight (Engeland & Arnhold, 2005). This pattern of release is regulated by the suprachiasmatic nucleus (SCN) of the hypothalamus (Engeland & Arnhold, 2005). Acute stressors of any type, physiological or psychological, stimulate an acute release of cortisol, which slowly returns back to basal levels over a few hours. This is mediated by negative feedback of cortisol acting on GR receptors at the level of the hypothalamus and pituitary (Dallman *et al.*, 1992; Dallman & Jones, 1973), as well as more complex feedback at GRs and MRs in the hippocampus, amygdala, and locus coeruleus (Makino *et al.*, 2002). While cortisol is often conceptualized exclusively as a 'stress hormone', since it is released in response to stress and is often used as an unbiased indicator of stress response activation, it is actually a potent modulator of whole-organism metabolism, which occurs in the absence of stressors (i.e. normal diurnal oscillations),

but can be further upregulated in response to stress (Adams, 2007; Bass & Takahashi, 2010; Sapolsky *et al.*, 2000). Diurnal oscillations in cortisol levels modulate metabolism, putting an organism in a catabolic state when cortisol levels are high (active, daytime) and shifting the individual to an anabolic state when levels are low (inactive, nighttime) (Adams, 2007; Bass & Takahashi, 2010). More specifically, acute activation of the GR mobilizes nutrient stores so that they are readily available for use during a time of increased activity and metabolic demand. Glucocorticoid signaling increases blood glucose levels by stimulating glycogen breakdown (glycolysis), increasing glucose synthesis (gluconeogenesis), and decreasing insulin receptor sensitivity (Black *et al.*, 1982; Exton, 1979; Sapolsky *et al.*, 2000; Weinstein *et al.*, 1995). Amino acid and fatty acid utilization by tissues is reduced, and shunted towards the liver as a fuel for gluconeogenesis (Sapolsky *et al.*, 2000). When glucocorticoid levels are particularly high, they can lead to breakdown of fat stores and protein to further liberate fatty acids and amino acids for glucose production through gluconeogenesis (Lee *et al.*, 2005; Lofberg *et al.*, 2002; Sapolsky *et al.*, 2000; Xu *et al.*, 2009). It is theorized that these elevated glucose levels reflect a ready available energy store for increased metabolic demand, particularly for brain and muscle during active waking hours (Sapolsky *et al.*, 2000). In addition to this shift in nutrient form and utilization, processes that are of high metabolic demand but that are not of immediate need are suppressed by glucocorticoids. For instance, cell division and proliferation is reduced by acute glucocorticoid signaling (Moutsatsou *et al.*, 2012; Yu *et al.*, 2004). During non-waking hours and sleep, as glucocorticoids are low, the organism returns to an anabolic state, whereby glycogen and fatty acid stores can be replenished, amino acids can again be utilized predominately for protein synthesis, and cell division/proliferation can again proceed (Adams, 2007; Bass & Takahashi, 2010; Boden *et al.*, 1996; Sapolsky *et al.*, 2000). In addition to its potent regulatory role in metabolism and energy homeostasis, glucocorticoids also have profound anti-inflammatory and immune-

suppressant effects (Elenkov & Chrousos, 2002; Franchimont, 2004) – and synthetic glucocorticoids are one of the front line treatments to reduce inflammation and suppress the immune system across a variety of medical conditions.

While this glucocorticoid mediated oscillation between anabolic and catabolic states is adaptive, chronic elevations in glucocorticoids lead to a profound disturbance in homeostasis and can have severely deleterious effects on health. Cushing's syndrome describes the constellation of symptoms that occurs in individuals who have chronically elevated levels of circulating glucocorticoids (hypercortisolinemia), regardless of the mechanism that leads to this elevation (Orth, 1995; Valassi *et al.*, 2012). This hypercortisolinemia is typically caused by hypersecretion of ACTH due to pituitary tumors, or by chronic treatment with synthetic glucocorticoids, which are typically prescribed for their potent anti-inflammatory and immunosuppressive effects. Cushing's patients show widespread metabolic abnormalities, which lead to profound muscle wasting, a simultaneous accumulation of abdominal fat, and reduced bone mineral density (Braun *et al.*, 2013; Toth & Grossman, 2013; Valassi *et al.*, 2012). Chronically elevated glucocorticoids also lead to a variety of neuropathological symptoms, including regional reductions in brain volume, neuronal cell loss, and reduced dentate gyrus neurogenesis (Bourdeau *et al.*, 2005; Bourdeau *et al.*, 2002; Crochemore *et al.*, 2005; Gruver-Yates & Cidlowski, 2013). Symptomology in part reflects the cumulative effects of an organism being in a persistent state of catabolism, reducing essential and adaptive anabolic processes. Protein breakdown leading to muscle wasting is a likely example (Lofberg *et al.*, 2002). However, some Cushing's symptoms are paradoxical to the normal effects of acute GR signaling, including increased inflammation and immune-dysfunction (Barahona *et al.*, 2009; Shah *et al.*, 2017). These paradoxical symptoms are not surprising, given that chronically elevated glucocorticoids lead to profound receptor downregulation and

desensitization (Burnstein *et al.*, 1991), thus blocking the normal adaptive effects of glucocorticoids and in turn leading to these paradoxical symptoms.

There is tremendous overlap between the effects of chronically elevated glucocorticoids (Cushing's symptoms) and many HD symptoms (Outlined in **Figure 1.3**), including metabolic abnormalities (weight-loss, and muscle wasting), cognitive deficits, psychiatric symptoms, as well as neuropathological features such as reduced regional brain volume, neuronal cell loss, reductions in neurogenesis, and increased inflammation (Bourdeau *et al.*, 2005; Bourdeau *et al.*, 2002; Burt *et al.*, 2006; Cameron & Gould, 1994; Shah *et al.*, 2017; Toth & Grossman, 2013; Valassi *et al.*, 2012). While the effects of mHTT toxicity alone could be sufficient to result in these symptoms in HD, it is has long been suspected that elevated cortisol levels contribute to, and further worsen, cognitive, psychiatric, and metabolic symptoms (Bjorkqvist *et al.*, 2006a; Petersen & Bjorkqvist, 2006; Shirbin, Chua, Churchyard, Lowndes*, et al.*, 2013; Trejo *et al.*, 2004). Although quite plausible, direct evidence of a causal relationship between elevated glucocorticoids and worsened HD symptoms is lacking - the data supporting this suspicion are mostly circumstantial and correlational. For instance, Saleh *et al.* (2009) demonstrated that there is an inverse relationship of cortisol levels with body mass index (BMI) in HD patients, suggesting that elevated cortisol could be contributing to weight loss. Shirbin et al. (2013) also demonstrated an inverse correlation between cortisol levels and cognitive function in HD patients, suggesting that elevated cortisol levels could be exacerbating cognitive decline. Similarly, the R6/2 transgenic mouse HD model shows a progressive elevation in circulating corticosterone levels, the rodent homolog of cortisol, which worsens in parallel with the development of motor, cognitive, and metabolic symptoms (Bjorkqvist *et al.*, 2006a). While these clinical and rodent data are consistent with the suspicion that elevated cortisol worsens symptoms, they are not conclusive. It is also possible that glucocorticoid dysregulation simply worsens as a part of disease progression broadly, in parallel

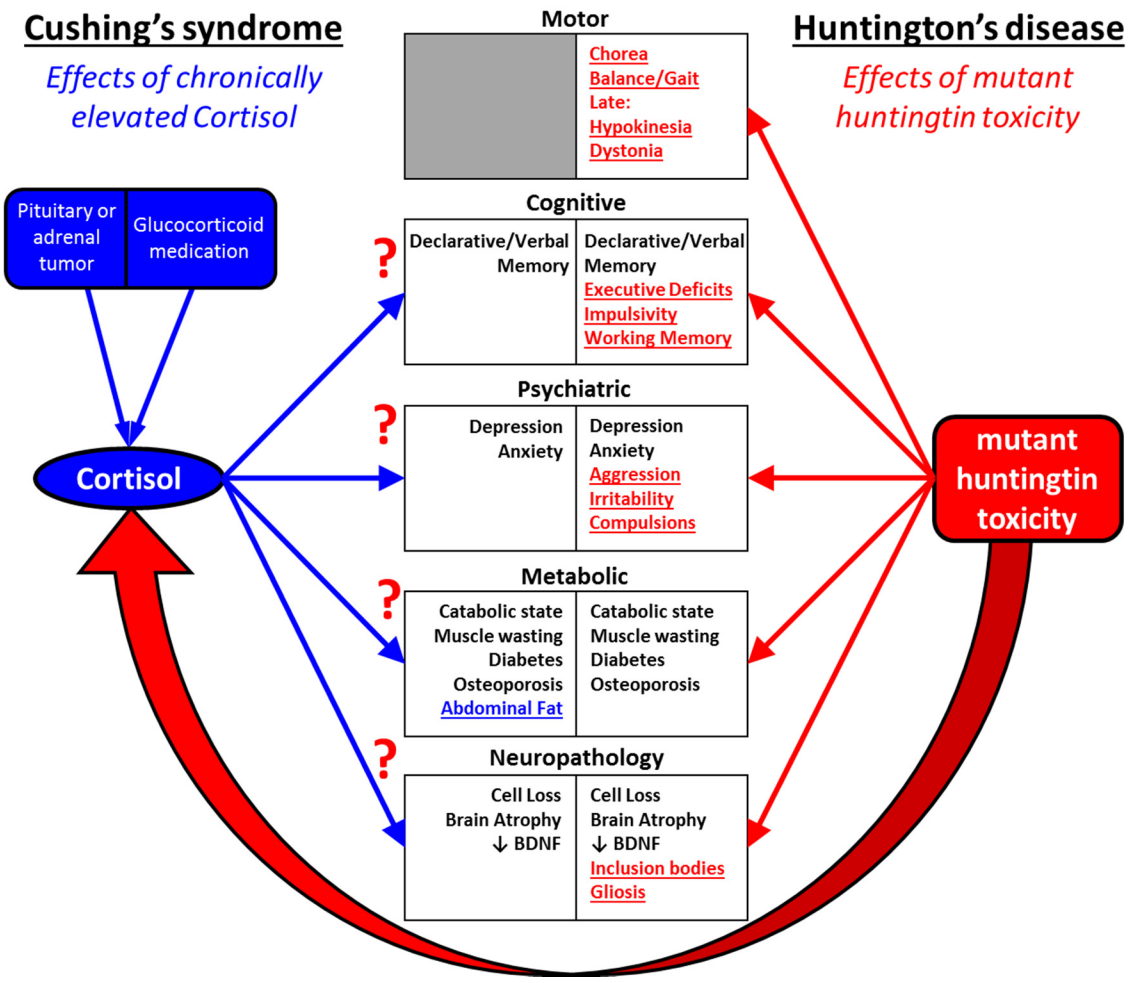

Figure 1.3 – Overlap in Huntington's Disease and Cushing's Syndrome Symptomology. Huntington's disease (HD) symptomology is largely caused by the deleterious effects of mutant huntingtin toxicity, leading to robust motor, cognitive, psychiatric, metabolic, and neuropathological symptoms (outlined in the right sides of boxes). Mutant huntingtin toxicity also leads to chronic elevations in the steroid hormone cortisol (a type of glucocorticoid). In non-HD populations, chronically elevated cortisol results in a spectrum of symptoms (outlined on left side of boxes) which is called Cushing's syndrome (CS). CS is typically caused by pituitary or adrenal tumors, or chronic administration of glucocorticoid medications. There is tremendous symptom overlap between HD and CS, as shown in parallel (in black) in the two sets of boxes. Given this overlap, it has long been speculated, but largely unexplored experimentally, that elevated cortisol in HD contributes to and/or worsens HD symptomology. The main focus of the experiments presented in Chapters 2 and 3 were to further assess empirically whether or not chronically elevated glucocorticoids do worsen HD symptomology, and whether normalizing glucocorticoid levels could be used as a therapeutic strategy for the disease.

with worsening metabolic and cognitive symptoms, without necessarily mediating them. Although limited, there is direct evidence of a relationship between elevated glucocorticoids and HD symptomology, which come from a handful of studies assessing the effects of experimentally elevated glucocorticoids in rodent HD models. In the R6/1 HD mouse model, experimentally elevated corticosterone slows weight gain and worsens cognitive symptoms (Mo, Pang*, et al.*, 2014), and acute stress in R6/1 mice can also worsen cognitive symptoms (Mo *et al.*, 2013). There are limitations to the experiments: R6/1 mice do not show an endogenous elevation in corticosterone and treatments in these mice were applied at early ages, before the typical onset of robust HD-like symptomology. Furthermore, while these findings indicate that experimental elevations in glucocorticoids can worsen symptoms, they do not demonstrate that typical elevations in glucocorticoids, inherent to the HD phenotype, further worsen symptoms.

The mechanisms that underlie elevated cortisol levels in HD are not clear - while there is robust hypothalamic pathology in HD, there is not an elevation in upstream tropic hormones (CRH, ACTH) that stimulate cortisol release (Saleh *et al.*, 2009), suggesting that adrenal pathology may be driving glucocorticoid elevations. Indeed, rodent models of HD show adrenal pathology, including hypertrophy and inclusion formation (Bjorkqvist *et al.*, 2006a; Moffitt *et al.*, 2009). The adrenal gland is also innervated by the autonomic nervous system through the splanchnic nerve, which can sensitize glucocorticoid producing cells of the adrenal cortex to ACTH (Ulrich-Lai *et al.*, 2006). Thus, autonomic hyperactivity is another possible mediator of elevated cortisol levels. If elevated glucocorticoids do in fact worsen HD symptomology, a better understanding of how mHTT toxicity leads to this elevation could serve as important point of therapeutic intervention for HD. It would also help with adapting current experimental therapeutics, such as gene silencing approaches, to include treating the mechanisms and consequences of hypercortisolinemia in HD.

1.4 - HD mood symptoms and the role of the anterior cingulate cortex

Mood symptoms are particularly prevalent in HD, including high rates of depression (30-70%), anxiety (30-60%), and suicide (3-7%) (Anderson & Marder, 2001; van Duijn *et al.*, 2008; van Duijn *et al.*, 2007). Although they are particularly deleterious for HD patients with respect to quality of life (Anderson & Marder, 2001; Ho *et al.*, 2009), the neurobiological mechanisms that underlie these symptoms remain poorly understood. While psychological factors likely contribute to mood symptoms for some patients (e.g. stress/worry about diagnosis, prodromal gene positive individuals stressed from caregiving of symptomatic parents and relatives with HD), there is good evidence that mood symptoms in HD have a biological basis. In at-risk individuals that do not know their HD gene status (offspring of HD patients, before disease onset) – HD gene carriers show a two-fold increase in rates of depression and anxiety compared to non-carriers, who had a similar rates to the general population (Julien *et al.*, 2007; van Duijn *et al.*, 2008). Thus, although both populations are at equal risk of developing HD and under similar psychological stress, the HD gene carriers show increased depression rates. Depression rates further increase from the prodromal stage and peak in the early stages (I/II) of the disease (Epping *et al.*, 2013; Epping & Paulsen, 2011; Paulsen *et al.*, 2005). While there is good evidence that mood symptoms have a biological origin in HD, the neurobiological mechanisms that underlie these symptoms are poorly characterized, particularly in contrast to HD motor and cognitive symptoms for which the neuropathological basis is better understood.

Many different limbic brain regions associated with anxiety and depression also show pathology in HD, including brain monoamine systems (dopamine, norepinephrine, and serotonin), the amygdala, hypothalamus, hippocampus, and limbic cortex (Rosas *et al.*, 2003; Soneson *et al.*, 2010; Thu *et al.*, 2010; Zweig *et al.*, 1992). It remains unclear whether pathology in a single brain region or a specific neurochemical disturbance (e.g. reduced serotonin signaling) is responsible

for the development of mood symptoms, or if these symptoms are mediated by simultaneous dysfunction in multiple limbic regions/systems. Many rodent models of HD also demonstrate depressive- and anxiety-like behavior (Hult Lundh *et al.*, 2013; Pouladi *et al.*, 2009; Wang *et al.*, 2014), as well as reduced dentate gyrus neurogenesis (Gil *et al.*, 2005) which is a biomarker for depression. However, while there have been numerous studies on HD mood symptoms in these rodent models, these findings are often inconclusive and contradictory, and have yet to lead to a consensus on putative mechanism. For instance, reducing striatal mHTT expression in the striatum leads to full rescue of depressive-like behavior in the YAC128 mouse HD model (Stanek *et al.*, 2014), but fails to improve depressive-like behavior in the BACHD model (Wang *et al.*, 2014). It's not clear why these two findings disagree - both models have similar genetics (artificial chromosome models carrying a full length mutant huntingtin transgene, with similar repeat lengths – 128 or 97, under the control of the human huntingtin promoter (Gray *et al.*, 2008; Slow *et al.*, 2003)) and both show similar depressive- and anxiety-like behavioral profiles (both strains show increased immobility in the forced swim test, which was used as a measure of depressive-like behavior for both of these studies). It is not due to the inability of the BACHD experimenters to detect improvements in depressive-like behavior – in the same study, Wang *et al*. (2014) demonstrated that silencing mHTT throughout the cortex in BACHD mice fully rescues both depressive- and anxiety-like behavior, as measured by the forced swim test and the light-dark test, respectively. In yet another study, silencing mHTT in the hypothalamus in BACHD mice led to a substantial improvement in depressive-like behavior in the forced swim test, although it had no effect on anxiety-like behavior in the elevated plus maze (Hult Lundh *et al.*, 2013). It is unclear which model and findings show good construct and predictive validity, with respect to human HD mood symptoms. Assessment of HD rodent model validity is further hampered by the limited understanding of the neuropathological basis HD mood symptoms in human cases. Identifying a

valid rodent HD model, with demonstrable construct validity is essential for further studies, which will involve showing a relationship between region specific neuropathology and mood symptoms that is shared between that particular rodent model and human clinical HD.

While the mechanisms that underlie mood symptoms in human HD are not well characterized, recent human clinical imaging studies and neuropathological assessments have identified pathology in the anterior cingulate cortex (ACC) as one possible contributor. The ACC is implicated in typical (i.e. non-HD) human cases of depression and anxiety. For instance, imaging studies show that individuals with either bipolar or unipolar depression show reduced grey matter volume and hypoactivity in the ACC (Drevets *et al.*, 1998; Drevets *et al.*, 1997; Drevets *et al.*, 2008). Similarly, individuals with generalized anxiety disorder show impaired activation of the ACC during emotional conflict (Etkin *et al.*, 2010). In HD, structural MRI studies show volumetric reductions in ACC grey matter and demonstrate that the severity of this reduction is inversely correlated with mood symptoms (Hobbs *et al.*, 2011). Additionally, HD patients with mood symptoms show reduced fractional anisotropy in the ACC, indicative of microstructural abnormalities, relative to both HD patients and healthy controls without mood symptoms (Sprengelmeyer *et al.*, 2014). fMRI studies also indicate alterations in brain networks related to depressive symptoms in HD, including increased activation of the default mode network (which includes the ACC) and reduced functional connectivity of the ACC with other cortical regions (McColgan *et al.*, 2017). However, while hypoactivity and volumetric reductions in the ACC correlate with mood symptoms in both HD and non-HD, these data do not necessarily provide a causal link between HD neuropathology and the development of mood symptoms - they simply show that ACC volume and activity is altered in mood symptoms, regardless of etiology. However, neuropathological assessments in postmortem HD cases provide a crucial link, suggesting that these abnormalities in ACC volume and activation, shown by MRI, are likely due to HD-specific neuropathology in the ACC. Thu et al

(2010) compared patterns of cortical degeneration in postmortem HD brains from individuals with different clinical symptom profiles: 1) Individuals with predominant motor symptoms, 2) Individuals with predominant mood symptoms, and 3) Individuals with both motor and mood symptoms. Those with mood symptoms (either alone or with combined motor symptoms) showed dramatic neuronal cell loss in the ACC, including a loss of pyramidal neurons, while those with motor symptoms did not show cell loss in the ACC (Kim *et al.*, 2014; Thu *et al.*, 2010). Further studies indicated that there is also a dramatic loss of GABAergic interneurons in the ACC that is specific to HD patients with mood symptoms (Kim *et al.*, 2014). In contrast, HD patients with motor symptoms (either alone or in combination with mood symptoms) showed similar degeneration in the motor cortex, including a loss of pyramidal neurons and to a lesser degree GABAergic interneurons (Kim *et al.*, 2014; Thu *et al.*, 2010). Those with mood symptoms only did not show any cell loss in the motor cortex (Kim *et al.*, 2014; Thu *et al.*, 2010). Thus, while cortical pathology had been long known to occur in HD, in addition to more robust striatal pathology, these studies demonstrated for the first time that heterogeneity in HD symptom profile may be related to heterogeneity in region-specific neurodegeneration. However, while all of these studies indicate that ACC pathology is associated with HD mood symptoms, including HD-characteristic neurodegeneration, they do not necessarily preclude the involvement of other brain regions.

1.5 – Characterizing the roles of glucocorticoids and the anterior cingulate cortex in Huntington's disease symptomology and therapeutics

The prognosis is incredibly poor for patients – HD is invariably fatal and no known treatments can slow or halt progression of the disease. Tetrabenazine and Deutetrabenazine are the only FDA approved medications for HD, which reduced chorea (Huntington Study Group, 2006; Huntington Study Group *et al.*, 2016). Separate from these medications, therapeutics for the disease largely consist of off-label pharmacotherapies utilized to treat specific symptoms (e.g.

SSRI's for depressive symptoms, neuroleptics for irritability (Ross & Tabrizi, 2011)), other types of non-pharmacological therapies to attenuate symptoms (e.g. high calorie nutritional supplementation to reduce weight loss (Trejo *et al.*, 2005)), and palliative care at end stages. Thus, there is tremendous need to develop novel therapeutics for these patients that can slow or halt the progression of the disease, instead of simply treating symptoms, and in turn result in sustained improvement in quality of life for patients. Inherent to this goal is to develop a better understanding of how mHTT toxicity leads to systems-level pathology, which in turn leads to symptomology. By doing so, therapeutics can be developed and tailored to target specific disease causing mechanisms and thus improve outcomes for patients.

In order to better characterize disease causing pathways, as well as novel therapeutic approaches for disease, rodent models are often utilized as they enable controlled experimentation that is not feasible in human clinical experiments. Many different transgenic mouse models of HD have been generated, which carry modified versions of the human mutant huntingtin gene (Genetics of HD rodent models utilized/addressed in this dissertation are outlined in **Table 1.1**), and model many of the symptoms of the disease (Symptoms of HD rodent models utilized/addressed in this dissertation are outlined in **Table 1.2**). No model is perfect and some of these transgenic lines model particular HD symptomology better than others. Thus, in the studies presented here, I utilized two different transgenic mouse models of HD to further characterize disease mechanisms and novel therapeutics for HD relating to neuroendocrine disturbance and HD psychiatric symptomology. For the first series of experiments, I utilized the R6/2 mouse model of HD which carries a fragment of the human mHTT gene (exon 1 only) which contains the CAG repeat expansion (160 repeats) that confers toxicity on encoded mutant huntingtin protein (Mangiarini *et al.*, 1996). R6/2 HD mice recapitulate many human HD symptoms including robust motor, cognitive, metabolic, and neuropathological symptomology, as well as a severely

shortened lifespan (Mangiarini *et al.*, 1996; Menalled *et al.*, 2009). Since R6/2 mice show such a severe and rapidly progressing phenotype they are sometimes considered a model of late stage HD. This model was chosen in particular in the studies presented here (Chapters 2 and 3), to assess the role of glucocorticoid dysregulation in HD symptomology and therapeutics, as it is the only HD mouse model that shows chronically elevated glucocorticoid levels (Bjorkqvist *et al.*, 2006a). One limitation to this strain is that R6/2 mice are poor models of HD psychiatric symptoms – they only show modest and transient depressive-like behavior (Ciamei *et al.*, 2015, and unpublished data) and they show a paradoxical decrease in anxiety-like behavior (File *et al.*, 1998; Hickey *et al.*, 2005), unlike HD patients who show increased anxiety as a part of their phenotype (Anderson & Marder, 2001). In a second set of studies (Chapter 4) I utilized the BACHD transgenic mouse model of HD, which carries a copy of the full length human mutant huntingtin gene bearing 97 CAG/CAA repeats (both CAG and CAA code for glutamine, but CAA repeats were used to increase stability of the repeat length) (Gray *et al.*, 2008). As with R6/2 mice, BACHD mice also show motor and cognitive symptomology. However, BACHD mice were utilized in these experiments as they are much better models of HD psychiatric symptoms, with mice showing robust depressive-like and anxiety-like behaviors (Hult Lundh *et al.*, 2013; Menalled *et al.*, 2009; Wang *et al.*, 2014). Unlike R6/2 mice, BACHD mice have a normal lifespan and only show very modest HD neuropathology (Gray *et al.*, 2008; Menalled *et al.*, 2009) – accordingly, they are sometimes considered a model of the early stages of HD for which motor and psychiatric symptoms predominate and neuropathology is less severe.

In the studies presented here in this dissertation, I characterized the roles of glucocorticoids and the anterior cingulate cortex in HD symptomology. The overarching goal of these experiments was to further assess the suitability of these two systems as possible points of therapeutic intervention for HD. In a series of experiments presented in Chapters 2 and 3, I

assessed whether elevated glucocorticoids in HD worsen symptomology. In Chapter 2, I characterized alterations in glucocorticoid homeostasis in the R6/2 mouse model, which provides some possible insights into the mechanisms that underlie the mHTT mediated elevation in corticosterone in HD. In both Chapters 2 and 3, I tested the hypothesis that normalizing glucocorticoids to wild-type levels in R6/2 mice would improve HD metabolic and neuropathological symptoms. The data from these studies do in fact support this hypothesis, and thus provide some of the first direct evidence that elevated glucocorticoids do in fact worsen HD symptoms. Furthermore, these data provides an initial characterization of which HD symptoms are worsened by this elevation, and which symptoms are unaffected. In Chapter 4, I assessed the role of the anterior cingulate cortex (ACC) in HD mood symptoms. Here, I tested the hypothesis that reducing mHTT expression in the ACC in the BACHD mouse model of HD would reduce depressive- and anxiety-like behavior. These data show that reducing mHTT expression in the ACC leads to a reduction in depressive-like symptomology but has no effect on anxiety-like symptoms, thus confirming that mHTT toxicity in the ACC is causal to some HD mood symptomology. Accordingly, the findings from this dissertation confirm that both of these pathophysiological systems, elevated glucocorticoids and mHTT toxicity in the ACC, do directly contribute to HD symptomology and that ameliorating pathology in these systems could possibly lead to symptom improvement for patients.

Table 1.1 - HD Rodent Models - Genetics

Line	Background	Promoter	Transgene	Exons	CAG repeats	Lifespan	Original Characterization
R6/2	B6 x CBA	HTT	fragment	Exon 1 only	160	10-13wks	Mangiarini et al., 1996
R6/1	B6 x CBA	HTT	fragment	Exon 1 only	113	32-40wks	Mangiarini et al., 1996
BACHD	FVB	HTT	full-length	Exons 1-67	97*	unaffected	Gray et al., 2008

*BACHD mice have a mixed CAG/CAA repeat (both code for glutamine), which increases CAG repeat length stability

Table 1.2 - HD Rodent Models - Symptomology

	Neuropathology						Motor		Cognitive			Psychiatric		Metabolic		Hormones		Paradoxical
	Shortened Lifespan	Inclusions	Reduced Brain Volume	Cell Death	Rotarod Deficits	Clasping	Open Field - Hypoactivity	Working Memory Deficits	Impulsivity	Depressive - Reduced SP	Depressive - FST Deficit	Anxiety - LD or EPM deficit	Weight Loss	Muscle Wasting	Increased Corticosterone	Decreased Testosterone (♂)	Weight Gain / Obesity	Lower Anxiety - LD/EPM	Sex Differences
R6/2	●	●	●	●	●	●	●	●	?	Tr	—	●	●	●	●	—	●	♀: 1wk delay symptoms
R6/1	●	●	●	●	●	●	?	?	●	●	—	●	?	—	●	—	●	♀only - FST and SP deficit
BACHD	—	few	mild	—	●	—	●	—	●	●	●	—	●	—	—	●	—	none here different	

Key

●	Present
—	Absent
?	Unknown, not investigated/reported
Tr	Transient/Mild
♀	Female Specific Symptomology
♂	Male Specific Symptomology
SP	Sucrose Preference Test (Anhedonia)
FST	Forced Swim Test (Behavioral Despair)
LD	Light Dark Box Task
EPM	Elevated Plus Maze

References

Giralt et al., 2012; Hannan & Ransome, 2011; Hult Lundh et al., 2013; Li et al., 2015; Menalled et al., 2009; Oakeshott et al., 2013, Pang et al., 2009; Pla et al., 2014; Renoir et al, 2011; Soylu-Kucharz et al, 2016; Valadao et al., 2017; Zielonka et al., 2014

Chapter 2: Corticosterone Dysregulation Exacerbates Disease Progression in the R6/2 Transgenic Mouse Model of Huntington's Disease[1]

2.1 - Introduction

Huntington's disease (HD) is an autosomal dominantly inherited neurological disorder that is caused by an expansion in the CAG region of the human *HTT* gene (Huntington Disease Collaborative Research Group, 1993). This expansion confers a toxic gain of function on the encoded protein, mutant huntingtin (mHTT). mHTT is expressed ubiquitously, but in particularly high levels in the brain, leading to widespread neurodegeneration. The striatum, cortex, hippocampus and hypothalamus are particularly affected and show inclusion body formation, cell loss, and gliosis (Gourfinkel-An *et al.*, 1998; Heinsen *et al.*, 1994; Vonsattel *et al.*, 1985). The hallmark symptom of HD is chorea, with patients showing uncontrollable hyperkinetic movements. However, patients also show particularly severe psychiatric, cognitive, and metabolic symptoms (Anderson & Marder, 2001 ; Lawrence *et al.*, 1996; Tabrizi *et al.*, 2009). Psychiatric symptoms are particularly prevalent, including high rates of depression and anxiety (Anderson & Marder, 2001; Levy *et al.*, 1998; Pflanz *et al.*, 1991). Cognitive symptoms include deficits in memory, executive function, and impulse control (Lawrence *et al.*, 1996; Tabrizi *et al.*, 2009). Patients also show metabolic symptoms, including severe weight loss and diabetes (Aziz *et al.*, 2008; Petersen & Bjorkqvist, 2006; Trejo *et al.*, 2004; van der Burg *et al.*, 2009). HD typically onsets in midlife, and symptoms become increasingly severe over 10-15 years, ultimately leading to death.

---

[1]This chapter was published previously and has been included in its entirety as Chapter 2.

Dufour BD & McBride JL. Corticosterone dysregulation exacerbates disease progression in the R6/2 transgenic mouse model of Huntington's disease. Experimental Neurology 2016; 283: 308-317.
doi: 10.1016/j.expneurol.2016.06.028.

HD patients show a two-fold increase in circulating basal levels of the glucocorticoid cortisol (Heuser *et al.*, 1991; Saleh *et al.*, 2009). Likewise, R6/2 transgenic HD mice show a three-fold elevation in corticosterone, the rodent homolog of cortisol (both now abbreviated CORT), and these levels increase in parallel with HD symptom progression (Bjorkqvist *et al.*, 2006a). R6/2 mice also show hypertrophy of the adrenal gland, consistent with HPA-axis hyperactivity (Bjorkqvist *et al.*, 2006a). However, the consequences of elevated CORT on HD symptoms, as well as the mechanisms that underlie it, are largely unexplored. Because chronic high levels of circulating CORT in the non-HD population leads to Cushing's disease, a disorder characterized by neuropathological changes and cognitive, psychiatric and metabolic disturbance (Orth, 1995; Valassi *et al.*, 2012), I postulated that elevated CORT in HD may be exacerbating HD symptom development and/or accelerating disease progression. There is recent empirical support that elevated CORT can exacerbate HD symptoms; Mo and colleagues (2014) showed that increasing CORT levels in R6/1 transgenic mice, a model wherein CORT is not naturally elevated, exacerbates cognitive deficits and reduces hippocampal neurogenesis (Mo, Pang*, et al.*, 2014). Additionally, female R6/1 mice, show an aberrant, persistent elevation in CORT following restraint stress (Du *et al.*, 2012). Thus, in the current chapter, I investigated the role of chronic, elevated CORT in metabolic symptom progression (weight loss), as well as broad HD symptom progression (motor dysfunction and lifespan) in the R6/2 mouse model, which more accurately mirrors the spontaneous elevation in CORT shown by HD patients. Additionally, I characterized the circadian pattern of plasma CORT release, as well as the stress induced CORT response, in the R6/2 transgenic mouse model of HD.

2.2 - Methods

Animals. All animals were group housed with littermates (3-5 mice per cage) under controlled conditions of temperature and light (12 hour light/dark cycle). Food and water were provided *ad libitum*. R6/2 mice (stock # 002810, carrying 160±5 CAG repeats) were obtained from Jackson Laboratories (Bar Harbor, ME) and bred in the vivarium at the Oregon National Primate Research Center (ONPRC). Wild-type males were mated with ovary transplanted wild-type females. Transgenic mice were genotyped using primers specific for the mutant human HTT transgene (forward primer 5' TCATCAGCTTTTCCAGGGTCGCCAT and reverse primer 5' CGCAGGCTAGGGCTGTCAATCATGCT), and age-matched wild-type littermates were used for the indicated experiments. A subset of mice from the colony that participated in the current studies were used to assess CAG repeat length (n=12), showing a mean length of 165 ± 5 (SD) repeats (Laragen Sequencing and Genotyping, Los Angeles, CA). Body weights of all animals were recorded weekly. All experimental procedures were performed according to ONPRC and OHSU Institutional Animal Care and Use Committee.

Adrenalectomy Surgery. Mice were anesthetized with 3% isoflurane. A 2cm x 2cm square was shaved on their lower dorsal surface and an incision was made in the skin at the animal's dorsal midline (this opening was used for the removal of both adrenal glands). Next, a small (3-5mm) incision in the muscular wall was made, directly above the kidney. Small tweezers were used to grasp and gently remove the adrenal gland. This procedure was repeated for the animal's contralateral side (bilateral adrenalectomy). The muscle incisions were closed using suture and the dorsal skin was closed with wound clips.

Corticosterone Replacement. Corticosterone replacement was provided in the animals' drinking water, which was available ad-libitum. Corticosterone (Sigma, cat. #27840) was dissolved in a

small volume of ethanol (0.6%), and then added to dH_20. Since the aldosterone producing cells of the adrenal gland are lost to adrenalectomy, NaCl (0.9%) was also added to replace salt loss. Sucrose (2.0%) was also added to increase palatability of the solution. A dose of 10ug/ml corticosterone was used for the physiological/WT level replacement group and 60ug/ml of corticosterone was used for the high/HD level replacement group. Vehicle alone (2% sucrose, 0.9% NaCl, and 0.6% ethanol in dH_20) was given to the sham surgery animals. All treatments were balanced for sex and genotype, with 2 WT and 2 HD age-matched mice randomized and caged together from the colony, into each male and female cage. A total of 48 mice were used in this study, with n=16 (4 HD males, 4 HD females, 4 WT males, and 4 WT females) for each of the three treatments. The experimenter was blind to the three different experimental conditions and genotypes. Replacement solution intake (volume) was monitored daily for each cage, and averaged over the week (and mathematically adjusted for all 4 mice in a weekly intake/mouse/week score – this was further adjusted with the loss of mice due to early death).

Restraint Stress. Mice were restrained for 30 minutes in modified 50mL conical tubes (Bale *et al.*, 2002). Several air-holes were drilled into the bottom of each tube, tubes were shortened to restrict forward and backward movement and were closed at the end. Tube lengths were 7.3cm (for mice ≤20g), 8.1cm (mice between 20g – 25g), and 9.0cm (for mice >25g). Mice underwent restraint stress at 4, 7, and 10 weeks of age.

Behavioral Measures – Open Field. Mice were placed singly in a dimly lit, automated infra-red activity arenas (40.64 x 40.64 cm) for 15 minutes (Med Associates, St. Albans, VT). Each open field arena was enclosed in a sound attenuating chamber. Mice were habituated to the room for 1 hour before testing, and all testing occurred in the afternoon between 4-6pm. Distance traveled during the 15 minute test period was measured. Mice were assayed in the open field at weeks 6, 8, and 10.

Blood Collection and processing. Blood was collected by saphenous venipuncture in the dose response and adrenalectomy studies. Mice were gently restrained, their left hind-limb extended and wiped with antibiotic ointment (to visualize the vein), the vein was punctured using a 30g needle, and whole blood was collected into heparinized collection tubes and processed for plasma. The tail clip method was utilized for serial blood measurements in the circadian CORT and stress-induced CORT studies. The tip of the tail was clipped (0.5mm), and approximately 20ul of whole blood was collected from the tip and collected into heparinized capillary tubes, and processed for plasma. The incision site was disrupted for subsequent sampling within the same week. Handling of mice during tail-clip method blood collection was minimized, and typically lasted approximately 30 seconds. All plasma was assayed for corticosterone by the ONPRC Endocrine Technology CORE using an in-house radio-immuno assay. For the circadian CORT experiment, blood was collected every 20 hours over 5 days for a total of 6 collections (6pm, 2pm, 10am, 6am, 2am, and 10pm). Blood was collected every 20 hours, versus every 4, to avoid artificially elevating plasma corticosterone levels due to frequent repeated handling stress. This procedure was repeated for each mouse included in the study, at each age (4, 7, and 10 weeks); thus, each mouse had a total of 18 blood collections. A total of 28 mice were used for the circadian CORT experiment, including 6 WT females, 5 WT males, 6 HD females, and 11 HD males. More HD than WT mice were included to account for possible premature deaths before the end of the experiment. For the stress-induced CORT experiment, blood was collected every 30 minutes, starting immediately before the mice were placed into restrainer tubes. Blood was collected 5 times (0, 30, 60, 90, 120min) for each mouse at 3 ages (4, 7, and 10 weeks of age), which was carried out between 11am and 2pm. A total of 30 mice were used in this experiment, including 4 WT females, 8 WT males, 12 HD females, and 6 HD males. For both the circadian and the stress-

induced CORT studies, the experimenter was blind to genotype at the time of blood collection and assay.

Statistical analysis. All statistical analyses were performed by using JMP Version 11 (SAS Institute Inc.). A repeated measures mixed-model was used for all repeated measures (dependent variables: bodyweight, open field, circadian corticosterone, stress-induced corticosterone; independent variables: genotype, sex, treatment, time-point and/or age). A proportional hazards model was used to analyze the survivorship data, which allows for post-hoc multiple pairwise comparisons between groups. A three-way ANOVA was used to assess the effects of genotype, sex, and treatment group on plasma corticosterone levels in the adrenalectomy experiment. Post-hoc contrasts were used to assess differences between WT and HD mice in the circadian CORT experiment at each possible age/time combination (i.e. HD vs WT mice at 10pm at 10 weeks of age), and alpha level was Bonferroni adjusted to 0.002 (.05/18 comparisons – p<.002 was considered statistically significant). For all other analyses, Tukey's post-hoc comparisons were performed when statistically significant fixed effects were detected (p < 0.05 was considered statistically significant).

2.3 - Results

Corticosterone Replacement Dose Response

Prior to assessing the effect of differing levels of corticosterone (CORT) on HD symptom progression, I performed an initial dose response study to establish CORT replacement doses that would achieve WT and HD-levels of plasma CORT following adrenalectomy surgery in R6/2 mice. Animals received CORT replacement in their drinking water. Target levels were based on previously published data demonstrating that basal CORT levels of 50-100ng/ml for WT R6/2 mice and 600ng/ml for transgenic R6/2 mice (Bjorkqvist *et al.*, 2006a). Additionally, I added low levels of sucrose to the CORT replacement solution to increase palatability and thus increase our likelihood of achieving target HD-levels of circulating CORT. Two concentrations of sucrose supplementation were tested (2% and 5%) in addition to four concentrations of CORT replacement (10, 20, 60, and 80ug/ml). CORT replacement solutions also contained sodium chloride (at 0.9%) to prevent salt-loss due to the removal aldosterone producing cells following the adrenalectomy.

Transgenic and wild-type R6/2 Mice were adrenalectomized at 8-9 weeks of age, and allocated to one of four CORT-replacement groups: 10, 20, 60, or 80ug/ml dose replacement. These solutions were first supplemented with 2% sucrose for the first week, then 5% for the second week. Blood was collected at midnight on the last night of supplementation and analyzed for plasma CORT. Replacement with 2% sucrose supplementation achieved the following plasma CORT levels: 65.1±14.7ng/ml for 10ug/ml dose, 145.1±47.1ng/ml for the 20ug/ml dose, 458.1±100.0ng/ml for the 60ug/ml dose, and 404.2±198.7ng/ml for the 80ug/ml dose. Replacement with 5% sucrose achieved the following plasma CORT levels: 63.4±19.5ng/ml for 10ug/ml dose, 147.5±83.5ng/ml for the 20ug/ml dose, 674.6±193.0ng/ml for the 60ug/ml dose,

and 1240.3±441.5ng/ml for the 80ug/ml dose (**Supplemental Fig. 2.1**). The 10ug/ml and 60ug/ml doses supplemented with 2% sucrose were selected for subsequent studies as they achieved plasma CORT within or near the desired range. 2% instead of 5% sucrose supplementation was selected with the goal of avoiding elevating plasma CORT above the levels described previously (Bjorkqvist *et al.*, 2006a).

Effect of adrenalectomy and corticosterone replacement on HD symptoms

R6/2 and wild-type mice underwent adrenalectomy surgery (ADX) at 6 weeks of age, followed by CORT replacement in water at physiological/WT levels (10ug/ml) or high/HD levels (60ug/ml). An additional group of R6/2 and WT mice underwent sham surgery at 6 weeks of age, and vehicle only (water, 2% sucrose and 0.9% NaCl) was provided instead of CORT replacement. Given that chronically elevated levels of glucocorticoids lead to metabolic abnormalities and muscle wasting in healthy individuals, I hypothesized that high level CORT replacement would exacerbate weight loss in HD mice. Indeed, R6/2 mice on the 60ug/ml CORT replacement showed a significant reduction in bodyweight (**Fig. 2.1b**) relative to sham mice starting at week 8, and continuing through the end of the study ($p<.05$ for each time-point); By week 11, HD mice on 60ug/ml CORT replacement showed a 15.4% reduction in bodyweight, while sham HD mice had yet to lose weight (4.1% increase over baseline level). Mice on HD-level (60ug/ml) replacement showed significantly reduced bodyweight relative to those on WT-level (10ug/ml) replacement at weeks 10 and 11 ($p<.05$), at which point they showed a 2.5% reduction from baseline. There was no difference in bodyweight between sham R6/2 mice and those on WT-level (10ug/ml) replacement ($p>.05$). In contrast to the R6/2 mice, all WT controls gained weight throughout the study, regardless of treatment. At the 11 week timepoint, there was a small but significant reduction in weight-gain in those WT mice on low-dose CORT, relative to those WT mice treated

with HD-level CORT replacement or sham surgery (**Supplemental Fig. 2.2**, $p<.05$ for both pairwise comparisons).

Changes in motor behavior were assessed in the open field, both before (baseline at 6 weeks of age) and following surgery/treatment at 8 and 10 weeks of age. R6/2 mice show a clear motor phenotype, as indicated by reductions in ambulatory activity in the open field. While the characteristic reduction in distance travelled was detected in the R6/2 mice here (894.17 ± 181.57 cm for R6/2 mice and 1609.05 ± 140.64 cm for WT, $p<.05$), there was no effect of CORT treatment on motor performance (i.e. no genotype*treatment interaction, $p>.05$, **Fig. 2.1d**). Thus, the progressive motor symptoms shown in R6/2 mice are not affected by changes in circulating glucocorticoid levels.

In addition to weight loss, I hypothesized that increased CORT levels would hasten the latency to death. R6/2 transgenic mice have a shortened lifespan compared to WT mice, typically dying between the ages of 12-14 weeks. I found a dramatic increase in mortality in the HD-level replacement group, with 100% of mice (8/8) dying before the pre-determined endpoint of the study at 12 weeks of age (**Fig. 2.1c**). In contrast, only 37% (3/8) of the HD mice on WT-level replacement and 13% (1/8) of the sham treated HD mice died before the study's endpoint. Using a proportional hazards survivorship analysis, which allows between group comparisons, there was a significant reduction in survivorship in the HD-level replacement group relative to the sham operated ($p<.001$) and the WT-level replacement ($p<.01$) groups. There was no difference in survivorship between the WT-level replacement and the sham groups ($p>.05$). Together these data demonstrate that high levels of CORT can exacerbate the weight-loss and early death phenotype of transgenic R6/2 mice, but does not affect their motor phenotype.

To confirm that CORT replacement doses achieved the desired target plasma levels, blood was collected from all mice at 10 weeks of age (**Fig. 2.1e**). Since mice drink water in a diurnal pattern, with most drinking occurring during the night/dark, blood was collected at midnight - the expected time of peak plasma CORT from drinking. I also measured CORT replacement solution intake in this experiment (See **Supplemental Fig. 2.3**), which showed that there was an increase in intake in the high-CORT replacement mice at the 10 week timepoint (Tukey's $p<.05$ for both comparisons). Although this likely elevated the plasma CORT levels in the high-dose group, there was still a very clear difference between low and high-dose treatment plasma levels, similar to the values expected. Mean plasma CORT values for mice on high/HD-level (60ug/ml) replacement was 768.9 ± 310.1 ng/ml for WT and 922.9 ± 239.5 ng/ml for R6/2, which were not statistically different between genotypes ($p>.05$). Mean plasma CORT values for mice on physiological/WT (10ug/ml) replacement was 96.2 ± 18.6 ng/ml for WT and 119.8 ± 30.5 ng/ml for R6/2, which was also not statistically different between genotypes ($p>.05$). I found that mice on high/HD-level replacement showed significantly higher plasma CORT levels relative to those on physiological/WT replacement ($p>.05$) and sham treated mice ($p<.05$). Interestingly, I found no genotype differences in the sham treatment group: WT mice had a mean of 116.3 ± 34.7 ng/ml, while R6/2 mice had a mean of 53.6 ± 28.0 ng/ml. I hypothesized that the lack of elevated CORT seen in the HD sham treated mouse, which was predicted to be elevated based on previously published data, resulted from the time of day that I chose for blood collection. Therefore, I performed a follow-up study to characterize the circadian pattern of CORT release in R6/2 mice.

Circadian corticosterone release

CORT is released from the adrenal gland in a circadian pattern, with peak levels occurring at the time an organism wakes (morning for humans, evening/lights-out for rodents). This pattern

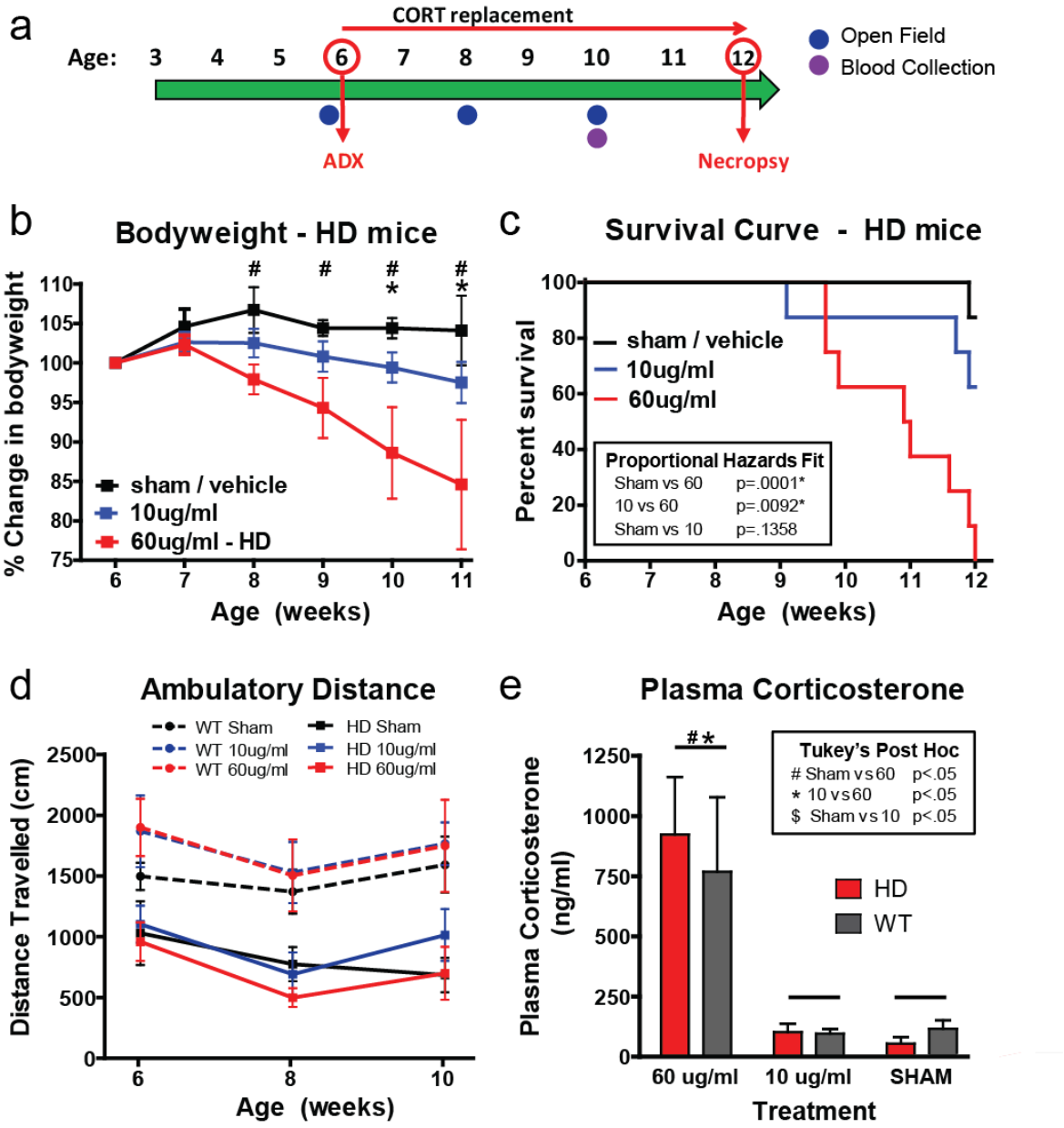

Figure 2.1 - Adrenalectomy and corticosterone replacement. (a) Timeline for experiment (b) HD mice on high/HD level replacement showed a progressive reduction in bodyweight starting at 8 weeks of age relative to sham HD mice (Tukey's post-hoc p<.05, indicated by #) and starting at week 10 relative to physiological/WT level replacement in adrenalectomized HD mice (Tukey's post-hoc, p<.05, indicated by *). (c) HD mice on high/HD level CORT replacement showed a significant reduction in survival relative to sham treated HD mice (p<.001) and HD mice on physiological/WT-level corticosterone replacement (p<.01). (d) Although R6/2 showed a reduction in distance traveled relative to WT mice, there was no effect of treatment on either R6/2 or WT mice (p>.05). (e) As expected, plasma CORT was higher in mice on the high/HD-level corticosterone replacement than the sham treated mice and physiological/WT-level corticosterone replacement groups. There was no difference in plasma corticosterone levels between R6/2 and WT mice in any of the treatment groups (p>.05). Values represent Mean ± SE. *#$ - Represent significant Tukey's posthoc comparisons.

of release is regulated by the suprachiasmatic nucleus (SCN), which regulates the HPA-axis at the level of the paraventricular nucleus of the hypothalamus. While R6/2 mice have been previously shown to have a progressive increase in plasma CORT levels at a single clock-time, it is unclear whether there is a change in the circadian pattern of CORT release. Given that R6/2 mice also have a progressive disruption in the SCN, and in circadian behavior (Morton *et al.*, 2005), I hypothesized that the circadian pattern of CORT release would likewise show a progressive disruption. Therefore, I characterized the circadian pattern of CORT release in R6/2 mice at 4, 7, and 10 weeks of age. Blood was collected at 6am, 10am, 2pm, 6pm, 10pm, and 2am at each age (**Fig. 2.2a**) from transgenic R6/2 mice and WT controls. Area under the curve (AUC) values were generated from the circadian profile for each mouse at each age, detailing the total amount of CORT that each mouse produces over a 24 hour period. I found that male WT mice had mean CORT AUC values of 1421 ±154, 1277 ± 130, and 1398 ± 245 at 4, 7, and 10 weeks of age, respectively, while male R6/2 mice had mean CORT AUC values of 1584 ± 170, 1156 ± 67 and 2575 ± 365 at 4, 7, and 10 weeks of age. Female WT mice had CORT AUC values of 3424 ± 642, 2182 ± 317 and 2117 ± 152 at 4, 7, and 10 weeks of age and female R6/2 mice had CORT AUC values of 2727 ± 440, 2327 ± 278 and 3230 ± 1057 at 4, 7, and 10 weeks of age, respectively. Percent change in CORT AUC values from week 4 were calculated and analyzed statistically. Relative to week 4, HD mice showed a significant 159.5 ± 24.3% increase in CORT AUC levels at week 10 (**Fig. 2.2b**, Tukey's $p<.05$), although there was no change at week 7 ($p>.05$). As expected, WT mice showed consistent AUC CORT levels across all ages (no significant difference in % change AUC CORT at 7 or 10 weeks, $p>.05$). Male and female mice did not show any differences in AUC CORT % change, regardless of age or genotype (Sex: $p=.78$; sex*genotype: $p=.51$; sex*age*genotype: $p=.15$).

The light-cycle for all mice was 12:12 (lights on at 6am and lights out at 6pm) and circadian CORT levels are expected to peak at 6pm when lights go out. I found no difference in the circadian

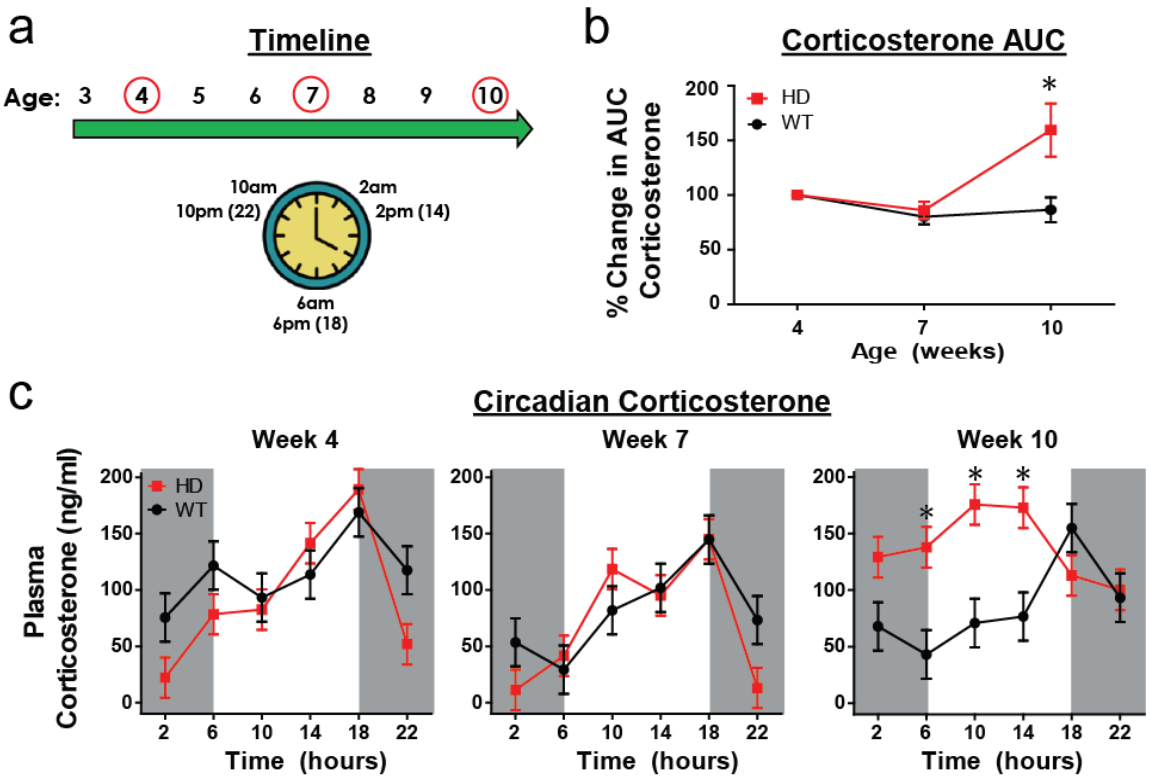

Figure 2.2 - Circadian corticosterone. (a) Timeline for data collection - mice underwent repeated blood collection at 4, 7, and 10 weeks of age. At each age, blood was collected from each mouse at 2am, 6am, 10am, 2pm (14hrs), 6pm (18hrs), and 10pm (22hrs). (b) R6/2 mice show an increase in area under the curve (AUC) corticosterone at 10 weeks of age relative to WT mice (p<.05). (c) R6/2 mice showed abnormalities in their circadian profile of plasma corticosterone at week 10 only. R6/2 mice showed elevated CORT levels at 6am, 10am, and 2pm (14hrs) relative to WT mice of the same age (Bonferroni adjusted alpha = 0.0028, significant contrasts all p<.001). At all other timepoints, within each age, there was no difference in plasma corticosterone between R6/2 and WT mice. There was no effect of sex (p>.05), and thus the data are collapsed across sex. Mice were on a 12:12 light cycle, with gray shading reflecting clock times with lights out (from 6pm to 6am). Values represent Mean ± SE. * Represents significant Tukey's posthoc comparisons.

CORT profile of WT and HD mice at 4 or 7 weeks of age, with both genotypes showing the expected peak level occurring at 6pm (18hrs) (**Fig. 2c**). However, at 10 weeks there is a clear and significant disruption in the circadian CORT profile in R6/2 mice – the peak mean level no longer occurs at 18hrs, but instead occurs at 10hrs (10am). Also at 10 weeks of age, R6/2 mice also showed significantly elevated CORT at 6, 10, and 14hrs (p<.001 for each pairwise contrast) relative to WT mice (Genotype*Age*Timepoint interaction: p<.05) **(Fig. 2.2C**). There was no significant effect of sex, or any of its interactions (all p>.05), and thus the data presented are collapsed across sex (values for males and females are presented separately in **Supplemental Fig. 2.4**). Although there is not a fragmentation of the circadian pattern of CORT release, the peak is clearly shifted to an earlier clock time and widened, with R6/2 mice showing a sustained elevation. Together, the circadian data demonstrate that there is indeed an alteration in the circadian pattern of CORT release in late-stage R6/2 mice, and that R6/2 mice do show an elevation in overall plasma CORT levels across a 24 hour period even when accounting for the disruption in circadian release.

Stress induced corticosterone release

In addition to the basal circadian pattern of CORT release, all types of stressors (psychological, physiological, etc.) also activate the HPA-axis, leading to a short-term release of CORT. Although R6/2 mice show an elevation in basal CORT release, it is unclear whether or not they show an exaggerated stress-induced activation of the HPA-axis leading to increased secretion of CORT. Thus, in a third experiment, I assessed whether restraint stress would lead to an acute increase in CORT release in R6/2 mice relative to WT mice and whether there is a disease-associated delay returning back to basal levels.

To address this, R6/2 and WT mice were subjected to 30 minutes of restraint stress at 4, 7, and 10 weeks of age (**Fig. 2.3a**). Blood was collected at baseline (prior to the stressor – 0min) and four subsequent times following the stressor (30, 60, 90, and 120min. – see **Fig. 2.3b**). There

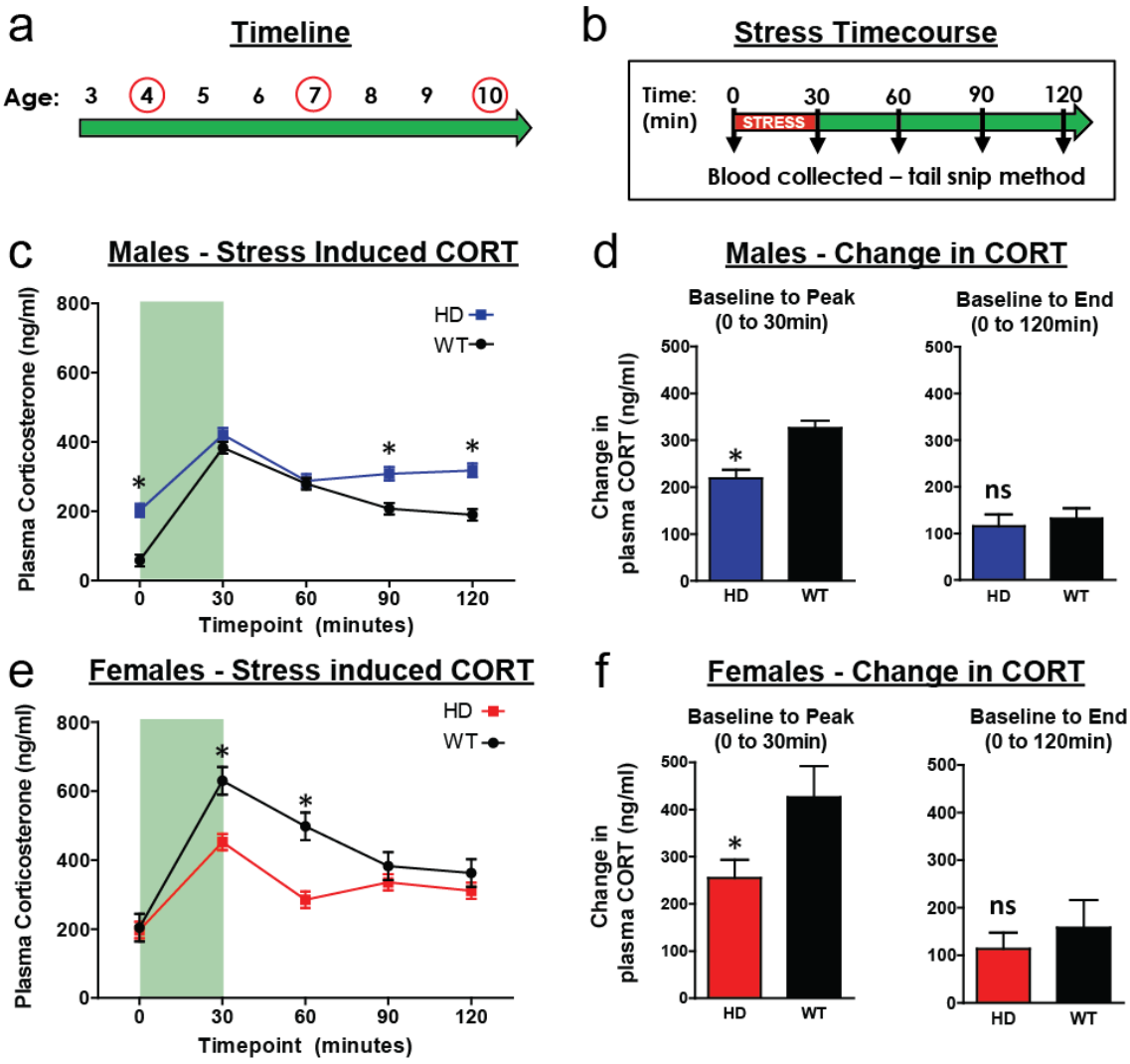

Figure 2.3 - Stress induced corticosterone release. (a) Mice underwent restraint stress and blood collection protocol at 4, 7, and 10 weeks of age. (b) Mice were placed in restrainer tubes for 30 minutes, with blood collected at baseline (time = 0min), immediately following restraint stress (30min), and for the next 90 minutes at 30 minute intervals (time 60, 90, 120min). There was not a significant effect of age (all p>.05), and thus data are collapsed across the three different ages. (c) Male R6/2 mice showed elevated CORT levels at time 0, 90, and 120 (Tukey's post-hoc, p<.05), relative to WT males. (d) Absolute difference from baseline to peak (30min) plasma CORT values shows that male R6/2 mice have a blunted CORT response to stress, when baseline differences are accounted for (p<.05). Absolute difference from baseline to end (0 to 120min) shows a small persistent elevation in CORT, that is not different between WT and R6/2 males (p>.05). (e) Female R6/2 mice showed lower plasma CORT values at time 30 and 60min, relative to WT females (Tukey's post-hoc, p<.05). (f) Absolute difference from baseline to peak (0 to 30min) plasma CORT values shows that female R6/2 mice have a blunted CORT response to stress (p<.05). Absolute difference from baseline to end (0 to 120min) shows a small persistent elevation in CORT at the end of the time-course, that is not different between WT and R6/2 females (p>.05). Light green shading in (c) and (d) reflects the time that the mice were undergoing restraint stress. Values represent Mean ± SE. * Represent significant Tukey's posthoc comparisons.

was no significant effect of age, or any of its interactions, on plasma CORT levels (all p>.05), and thus the data presented in **Fig. 2.3** are collapsed across age (data for both sexes at all ages and timepoints are provided in **Supplemental Fig. 2.5**). Relative to male WT mice, male R6/2 mice showed elevated plasma CORT levels at baseline (0min.), and at the 90min. and 120min. time-points (**Fig. 3c**, Tukey's p<.05 for all). Conversely, female R6/2 mice showed lower plasma CORT levels relative to WT females at the 30min. and 60min. time points (**Fig. 2.3f**, Tukey's p<.05 for both). To test my hypothesis that R6/2 mice show an augmented stress-induced CORT response, I accounted for the baseline difference shown between R6/2 and WT mice by calculating the absolute difference between baseline (0min) and peak (30min) plasma CORT levels. Contrary to my hypothesis, both male and female R6/2 mice have a blunted stress-induced CORT response relative to WT mice (**Fig. 2.3d and 2.3f,** p<.05). I also found that CORT values similarly returned to baseline for both WT and R6/2 mice, regardless of sex (difference between 0min. and 120min., **Fig. 2.3d and 2.3f**, p>.05). As with the males, female R6/2 and WT mice had a similar reduction towards baseline at the 120min. time point (**Fig. 2.3f**, p>.05). These data demonstrate that elevated CORT in R6/2 mice isn't simply due to general hyperactivity of the HPA-axis. If it were, I would expect there to be both an increase in resting CORT levels (which there is at 10 weeks), as well as stress-induced CORT release. In fact, these data demonstrate that R6/2 mice have an attenuated CORT response to restraint stress, and suggests that they have intact negative feedback of the HPA-axis as their levels normalized similarly to WT mice.

Adrenal gland weights

I collected adrenal glands from mice in both the circadian and stress induced CORT experiments to assess whether there is a change in adrenal gland weight due to genotype (circadian experiment) and whether this weight could be affected by exposure to repeated restraint stress (stress-induced CORT experiment). Previous studies have shown that R6/2 mice

demonstrate adrenal gland hypertrophy, as measured by an increase in adrenal gland weight. It is also well established that WT female mice have larger adrenal glands than males (Bielohuby *et al.*, 2007). Here, mice were sacrificed at 12 weeks of age and adrenal gland weights were measured at necropsy. The effect of experiment (circadian and stress), sex (male and female), and genotype (WT and HD), and their interactions on adrenal gland weight were assessed. There were no differences in adrenal gland weight between the two studies ($p>.05$ for experiment and all of its interactions), suggesting that repeated restraint stress did not have an effect on adrenal gland weight in either WT or HD mice. Since there was no difference between experiments, data were collapsed across the two studies (**Fig. 2.4**). I did, however, find that both sex and genotype influenced adrenal gland weight ($p<.05$ sex*genotype interaction). R6/2 male mice showed significantly larger adrenal gland weight relative to WT males (2.90±0.1mg for R6/2 and 2.35±0.12mg for WT; Tukey's post-hoc $p<.05$). Conversely, R6/2 females had significantly smaller adrenal weights than WT females (3.16±0.12mg for R6/2 and 3.92±0.14mg for WT; Tukey's post-hoc $p<.05$). As has been shown previously, female WT mice had significantly larger adrenal glands compared to male WT mice (Tukey's post-hoc $p<.05$). There was no statistical difference in adrenal gland weight between male and female R6/2 mice (Tukey's post-hoc $p>.05$). Together, these data show that there is a sex-specific difference in adrenal gland weight, with female HD mice showing adrenal atrophy and male HD mice showing adrenal hypertrophy.

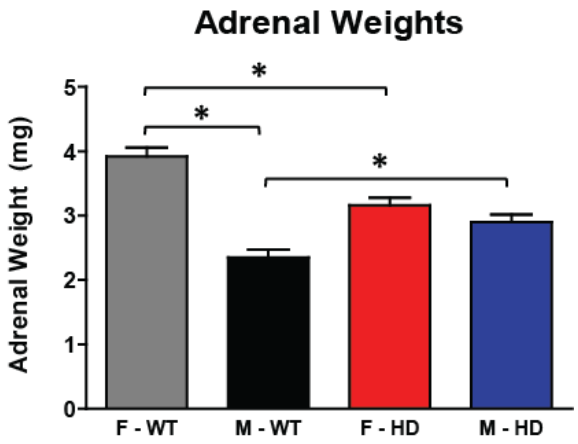

Figure 2.4 - Adrenal Gland Weights. Mice were sacrificed at 12 weeks of age in the Circadian and Stress-induced CORT experiments, and wet adrenal gland weights were measured. Female R6/2 mice had significantly smaller adrenal glands than did WT females, while male R6/2 mice had significantly larger adrenal glands compared to WT males (p<.05). There was no difference in adrenal gland weight between R6/2 males and females (p>.05), while WT females had larger adrenal glands than WT males (p<.05). There was no difference in adrenal gland weight between the two experiments, and thus data are collapsed across experiments. Values represent Mean ± SE. *Represent significant Tukey's posthoc comparisons.

2.4 - Discussion

Although numerous studies have shown that HD patients have elevated plasma cortisol (Aziz *et al.*, 2009; Bjorkqvist *et al.*, 2006a; Heuser *et al.*, 1991; Saleh *et al.*, 2009), the causes and consequences of this elevation remain largely unknown. Given that persistent hypercortisolinemia in otherwise healthy individuals can cause metabolic, cognitive, and psychiatric symptoms, it is possible that hypercortisolinemia is contributing to some of the same symptoms in HD patients. Abnormalities in corticosterone (CORT) homeostasis, the rodent homolog of cortisol, have been demonstrated in the R6/2 (Bjorkqvist *et al.*, 2006a) and the R6/1 (Du *et al.*, 2012) transgenic HD mouse models of HD. Experimental elevation of CORT in the male R6/1 HD mouse exacerbates cognitive symptoms, reduces hippocampal neurogenesis, and slows weight gain (Mo, Pang*, et al.*, 2014). Similarly, short-term stress in the R6/1 model exacerbates memory impairment in female HD mice (Mo *et al.*, 2013), while long term stress reduces weight gain in male and female HD mice, reduces saccharine preference in female HD mice (a depressive-like measure of anhedonia), and reduces olfactory sensitivity (Mo, Renoir*, et al.*, 2014). In the series of experiments presented here, I extend these findings and demonstrate that elevated CORT in the R6/2 model dramatically exacerbates the weight loss phenotype in these mice and also shortens lifespan. Additionally, I extended previous findings that CORT homeostasis is altered in R6/2 HD mice, confirming that CORT levels are elevated at end stage of disease. Further, I demonstrate that there is a clear disruption in the circadian pattern of CORT release and an attenuated CORT response to restraint stress in R6/2 HD mice.

One of the most significant findings from these experiments is that experimentally elevated CORT dramatically reduced bodyweight in transgenic R6/2 mice. Elevated CORT in human HD patients is significantly correlated with reduced BMI (Aziz *et al.*, 2008). Although this human study was correlational, our finding in R6/2 mice demonstrates causality – that artificially

elevated CORT has the ability to exacerbate the weight loss phenotype associated with the HD gene. HD patients, like R6/2 mice, are in a state of negative energy balance, showing increased hunger and food intake and simultaneous weight loss (Farrer & Yu, 1985; Trejo *et al.*, 2004; van der Burg *et al.*, 2008). Weight loss is progressive in patients, typically starting before the onset of motor symptoms, and by end stage leads to severe cachexia (Djousse *et al.*, 2002; Farrer & Yu, 1985; Kosinski *et al.*, 2007; van der Burg *et al.*, 2009). Although the weight loss phenotype is well documented in HD, the mechanisms by which mutant huntingtin toxicity leads to weight loss in patients is still poorly understood (van der Burg *et al.*, 2009). It is not caused by energy expenditure due to chorea, nor is it due to insufficient nutritional intake (Mochel *et al.*, 2007; Sanberg *et al.*, 1981). In fact, HD patients have significantly higher caloric intake than controls (Farrer & Yu, 1985; Trejo *et al.*, 2004). It has been speculated that mutant huntingtin toxicity in peripheral tissues, such as muscle, pancreas and adipose tissue may be the source of weight loss in HD (Bjorkqvist *et al.*, 2005; Phan *et al.*, 2009; van der Burg *et al.*, 2008; van der Burg *et al.*, 2009; van der Burg *et al.*, 2011). It has also been postulated that hypothalamic pathology may be causal to metabolic changes in patients (Hult *et al.*, 2011; Petersen *et al.*, 2005). As a steroid hormone, CORT reaches virtually all tissues in the brain and body, and has potent metabolic effects on an organism. In individuals with chronically elevated CORT there is a dramatic shift in whole body metabolism and composition, with a decrease in skeletal muscle mass (wasting), a simultaneous increase in body fat, and robust insulin resistance (Orth, 1995; Valassi *et al.*, 2012). Although it is likely that mutant huntingtin toxicity in the periphery and/or the hypothalamus is sufficient to cause a metabolic phenotype in HD, this phenotype is probably multifactorial and elevated CORT may play an important role.

Another key finding is that high dose CORT treatment significantly shortened lifespan in R6/2 mice. This transgenic mouse model of HD is one of the most severe - mice typically die

between 13-16 weeks of age, after developing a progressive motor, cognitive, and metabolic phenotype. Although lifespan is severely truncated, the immediate cause of death is unclear for these mice, as it has never been systematically evaluated (Li *et al.*, 2005). Considering that increased BMI is correlated with a slower progression of disease in human patients (Myers *et al.*, 1991), it may be possible that the converse is true – that elevated CORT hastens the progression to death in R6/2 mice by exacerbating the weight-loss phenotype.

One surprising finding from the adrenalectomy experiments was that I failed to detect an elevation in CORT in 10 week old sham treated (intact) R6/2 mice (**Fig. 2.1e**). It has been previously shown that R6/2 mice show a progressive elevation in circulating CORT, starting at approximately 6 weeks of age and resulting in approximately a three-fold increase by end stage (Bjorkqvist *et al.*, 2006a). In the same study, the authors found that late-stage human HD patients also show a progressive increase in urinary CORT, starting at clinical stage III and further worsening at clinical stage IV (Bjorkqvist *et al.*, 2006a). I hypothesized that our failure to detect an increase in our adrenalectomy experiment was due to the time that I collected blood (midnight). However, it remained unclear whether or not R6/2 mice simply show an increase in blood CORT only at the time it peaks (lights off), whether there is a persistent elevation in CORT at all clock times, or whether there is a dysregulation in the time of CORT peak in this transgenic line that has a progressive disturbance in circadian rhythms (Morton, 2013; Morton *et al.*, 2005). Thus, I decided to further characterize the circadian pattern of CORT release in R6/2 mice at three different ages: 4, 7, and 10 weeks of age.

I found a clear alteration in the circadian pattern of release of CORT in R6/2 mice at 10 weeks of age. This is a novel finding in HD mice, and may represent a generalized disruption in circadian rhythms which becomes pronounced in late stage R6/2 mice. In early stage human HD patients, the 24 hour profile of CORT release also shows an increase in AUC levels (Aziz *et al.*,

2009). While there was no difference in peak levels between human patients and controls, CORT levels became elevated earlier than expected and persisted at a level until later in the day (Aziz *et al.*, 2009). Our finding is similar, with R6/2 mice showing a persistent, significant elevation in CORT which starts at a much earlier clock time (6am) and lasting throughout most the day (until 2pm). At 6pm, the expected time of peak CORT levels, plasma levels in R6/2 mice lowered to the peak WT levels. As with the human studies, this early elevation and persistence in high CORT levels accumulates to an overall AUC increase in 24 hour CORT. From a practical point of view, these data demonstrate that measuring blood levels of CORT in individuals with HD may be more complicated than taking a single measure at a single clock time. Although there is an overall increase in CORT, as indicated by the AUC analysis, no differences would have been detected from samples taken at 6pm (lights-out) or 10pm alone. This likely explains our failure to detect a difference in the midnight CORT measure from sham treated mice in the adrenalectomy. Since the circadian rhythm of CORT release is altered, it might be more ideal to take a more long-term measure of the hormone, such as CORT from hair samples (Thomson *et al.*, 2010), which is not sensitive to diurnal variation. Although there are numerous human studies showing that HD patients show an elevation in CORT, there are also some that fail to detect an increase. It is possible that abnormalities in the circadian pattern of CORT release may have obscured what the true differences are between human HD subjects and controls in these studies. More studies investigating the circadian pattern of CORT release in human subjects across disease stages could provide great insight into the discrepancies in these studies, as well as offer a better understanding of how CORT may influence symptom progression in HD.

In contrast with the circadian CORT findings, I found that R6/2 mice show a reduction in stress-induced CORT release, and that they similarly return to baseline levels following the stressor (**Fig. 2.3d and 2.3f**). Unlike the circadian experiment, the pattern of stress-induced CORT

release was stable and did not change with age. Both of these findings were unexpected. Although stress-induced CORT release had never been previously investigated in R6/2 mice, I hypothesized that previous reports of elevated CORT in R6/2 mice reflected a general hyperactivity of the HPA-axis. I therefore expected to see an increase in both basal and stress-induced CORT release in these mice, as well as longer time for CORT levels to normalize in mice undergoing stress. The restraint-stress paradigm has been utilized in R6/1 studies investigating CORT homeostasis at an early (pre-motor dysfunction) stage (Du *et al.*, 2012). These studies demonstrated that there was not a different response in stress-induced peak CORT levels between WT and HD R6/1 mice, although female HD mice failed to normalize to pre-stress CORT levels following the stressor (Du *et al.*, 2012). While there is no clear explanation for the divergent findings between the two strains, it is possible that the R6/2 is simply a better model of CORT disruption in the human disease, as they show a spontaneous increase in CORT levels, similar to human HD patients. It is also possible that alterations in CORT homeostasis may simply occur at a later stage in R6/1 mice than have been previously investigated. One unexpected finding was that female mice showed high basal CORT (approximately 200ng/ml), which was not different between genotypes. Although it is possible that this elevation is associated with stress at handling, I purposefully used a blood collection method that is rapid (blood collection from tail tip, which takes less than 30 seconds) and doesn't require anesthesia. This method is similar, if not quicker, to the tail-incision method described by Sadler and Bailey (2013), which is designed to reduce the possibility of elevating CORT levels through handling. Interestingly, I did not find a sex difference in adrenal gland weight between male and female HD mice, although there was a clear and expected difference in WT mice with females showing significantly larger adrenal glands than males. Although the reason for this sex effect is unclear, it confirms that sex can be an important factor

and should be accounted for in HD neuroendocrine studies, as has been previously shown in stress-induced CORT release in R6/1 mice (Du *et al.*, 2012).

While CORT release and HPA-axis function have been assessed in multiple rodent models of HD, all have failed to recapitulate the basal elevation in CORT shown in human patients (Du *et al.*, 2012; Hult Lundh *et al.*, 2013). As this phenomena may be occurring during late stages of disease, and may show abnormal circadian patterns of release, further assessment of CORT in other mouse models at later time-points are warranted. Considering that the mechanism that underlies these changes in HPA-axis activity is poorly understood, particularly in human patients, the R6/2 mouse may provide insights. I found that male R6/2 mice show hypertrophy of the adrenal gland, consistent with a previous study showing adrenal hypertrophy and increased ACTH immune-reactivity in the pituitary gland (Bjorkqvist *et al.*, 2006a). While these changes may be directly causal to an elevation in CORT, it is also possible that these changes are simply a consequence of hyper-activation of the HPA-axis by upstream brain regions that regulate it. One candidate is the SCN, the circadian pacemaker in the brain. The SCN shows clear pathology in HD (Fahrenkrug *et al.*, 2007; Morton *et al.*, 2005; van Wamelen *et al.*, 2013), and regulates the circadian rhythm of HPA-axis activation which leads to a diurnal pattern of CORT release. Although speculative, it is possible that changes in the SCN could lead to overstimulation of the HPA-axis, leading to the increased blood levels of ACTH and adrenal hypertrophy shown in (male) R6/2 mice (Bjorkqvist *et al.*, 2006a). This is consistent with our data showing that elevated CORT co-occurs with disruption in the circadian pattern of release, and that it occurs at a later stage of disease when SCN and circadian abnormalities are more pronounced. This is also consistent with our stress-induced CORT data, which showed a hypoactive HPA-axis response to restraint in HD mice, further suggesting that the HPA-axis is not just simply overactive. However, further complicating the matter is that stress-induced activation of the HPA-axis is mediated by a variety of brain

regions, including the amygdala, limbic cortex, and hippocampus (Ulrich-Lai & Herman, 2009) – all of which show pathology in R6/2 mice. It is possible that pathology in these upstream regions may impair stress-induced HPA-axis activation, leading to a blunted CORT response.

Although numerous studies have shown alterations in cortisol in clinical HD, there is not a clear consensus in the field over the magnitude and timing of that change. Heuser (1991) was the first to show abnormal levels of CORT in HD, with symptomatic patients showing a two-fold increase in basal plasma levels relative to healthy controls. Subsequent studies also showed an elevation in plasma and urinary CORT (Aziz *et al.*, 2009; Bjorkqvist *et al.*, 2006a; Leblhuber *et al.*, 1995; Saleh *et al.*, 2009), ranging from a small 10% increase (Leblhuber *et al.*, 1995) to a 3-fold increase in late stage patients (Bjorkqvist *et al.*, 2006a). Bjorkqvist (2006a) showed a clear progressive phenotype of elevated urinary cortisol in a large clinical sample (n=68 for controls, n=82 for HD), with pre-symptomatic patients showing a mild decrease in CORT levels, clinical stage I/II patients showing no difference from controls, stage III patients showing a 2-fold increase, and stage IV patients with a 3-fold increase. Saleh et al. (2009) conducted the largest neuroendocrine study in HD to date and showed a 50% increase in serum cortisol levels in HD patients (n=217) relative to age and sex matched WT controls. This study included subjects from all clinical stages, but failed to detect any association between disease progression and the magnitude of the elevation of CORT. Aziz (2009) has run the most detailed analysis of basal HPA-axis activity in a clinical HD sample, collecting blood samples from patients over 24-hours in 10 minute intervals. As expected, healthy controls showed an elevation in plasma CORT in the early morning (starting at approximately 5am), which return to nadir levels by noon. HD patients showed an early rise in plasma CORT (approximately 1am) and a delayed return to basal levels (approximately 5pm). Accordingly, they found a significant 50% elevation in 24 hour area-under-the-curve cortisol in patients. The limitations to this study is that it was a very small sample of early stage HD patients

(n=8) and healthy controls (n=8). Although these early studies were largely consistent, more recent studies have failed to replicate these findings. Two recent studies have shown the same finding - a small increase in post-waking salivary cortisol in pre-symptomatic HD-mutation carriers, but not in symptomatic HD patients (Hubers *et al.*, 2015; van Duijn *et al.*, 2010). Another two studies have shown either no difference (Shirbin, Chua, Churchyard, Hannan*, et al.*, 2013) or a small decrease in cortisol in early symptomatic patients (Shirbin, Chua, Churchyard, Lowndes*, et al.*, 2013). One possible difference in methodology that may account for these inconsistent in findings is that the earlier studies measured blood levels of CORT, which seem to be more consistently elevated, while the studies showing null or small increases in cortisol rely on salivary measures of the hormone. However, it would be surprising that this would explain the differences, as salivary and blood levels of cortisol are typically in agreement (Vining *et al.*, 1983). Although purely speculative, perhaps salivary levels of cortisol aren't as indicative of plasma levels of the hormone in the clinical HD population due to pathophysiological mechanisms germane to the disease. Additionally, another recent study failed to show an elevation in plasma or urinary cortisol in a clinical HD population (Kalliolia *et al.*, 2014). One limitation in these studies is that they largely represent earlier stages in the progression of the disease – and perhaps aren't detecting hypercortisolinemia that may develop at later stages. Another limitation is that many of the patients are medicated in many of these studies, which also may influence cortisol (Saleh *et al.*, 2009). Hopefully future clinical studies will clarify these inconsistencies, and better take into account disease stage, 24-hour pattern of release, as well as methodology for cortisol measurement.

HD patients have a devastating course of disease and the dopamine antagonist Tetrabenazine, which reduces motor symptoms, is currently the only FDA-approved treatment. There are currently no treatments which slow the disease progression. Although helpful,

treatments for weight-loss are largely limited to increasing caloric intake through nutritional supplementation (Trejo *et al.*, 2005). The key findings here, that elevated CORT exacerbates the metabolic phenotype and hastens time to death in R6/2 mice, highlight that the HPA-axis may be a novel therapeutic target for HD. More specifically, these data suggest that normalizing CORT levels may be of therapeutic benefit in HD patients, potentially slowing weight loss, increasing BMI, and potentially slowing the course of disease. Ongoing studies in our laboratory are assessing whether lowering CORT to WT levels in HD mice can prevent or slow the development of the myriad motor, cognitive and metabolic phenotypes that are germane to HD.

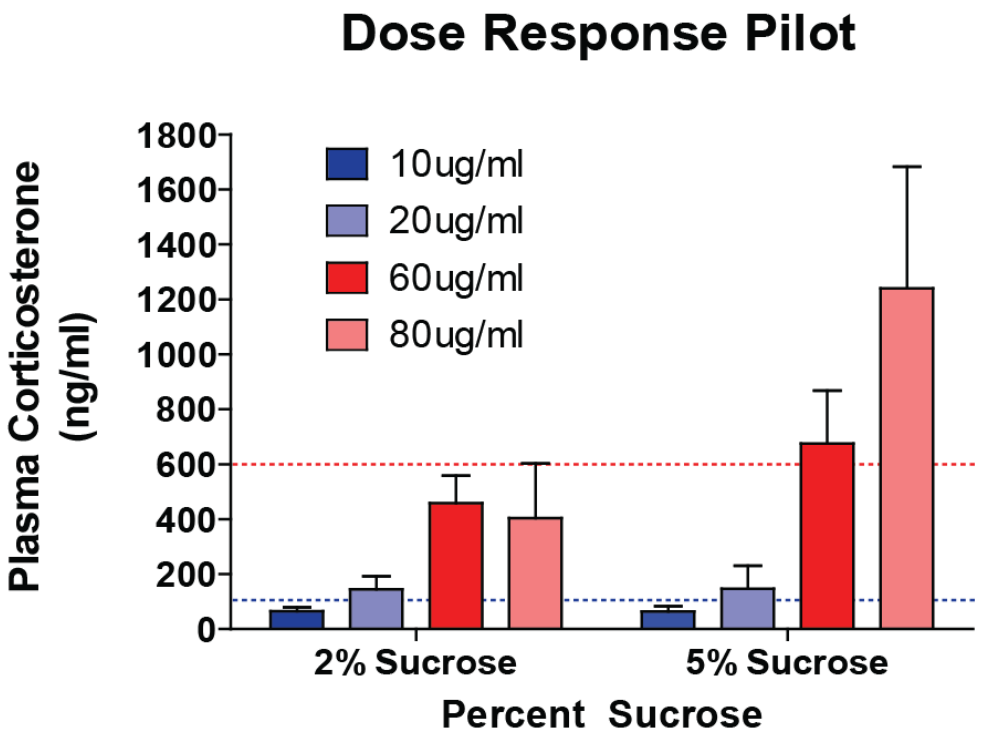

Supplemental Figure 2.1 - Dose Response Pilot. Mice were adrenalectomized and given one of 4 levels of CORT replacement (10ug/ml, 20ug/ml, 60ug/ml, and 80ug/ml). The goal of this study was to identify the CORT replacement doses that would reach the target plasma CORT levels – 100ng/ml for WT-levels (dotted blue line) and 600ng/ml for HD-levels (dotted red line). Replacement solutions were either supplemented with 2% or 5% sucrose, to increase palatability and thus increase solution intake and plasma CORT level. Replacement solution also contained 0.9% saline. Target WT-levels were achieved with 10µg/ml and HD-levels with 60µg/ml (both with 2% sucrose supplementation, which were the doses chosen for the larger adrenalectomy and CORT replacement study.

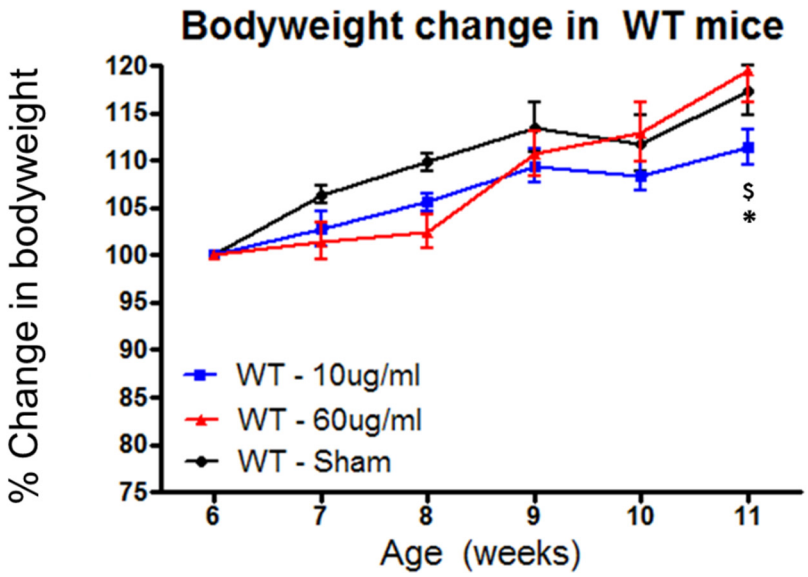

Supplemental Figure 2.2 – Body weight in wild-type mice. WT mice showed a consistent but small increase in bodyweight throughout the study, regardless of treatment. At the 11 week timepoint, mice on low-dose CORT showed a small but significant decrease in the amount of weight-gain relative to both the high dose CORT (* Tukey's post-hoc $p<.05$) and sham treated groups ($ Tukey's post-hoc $p<.05$).

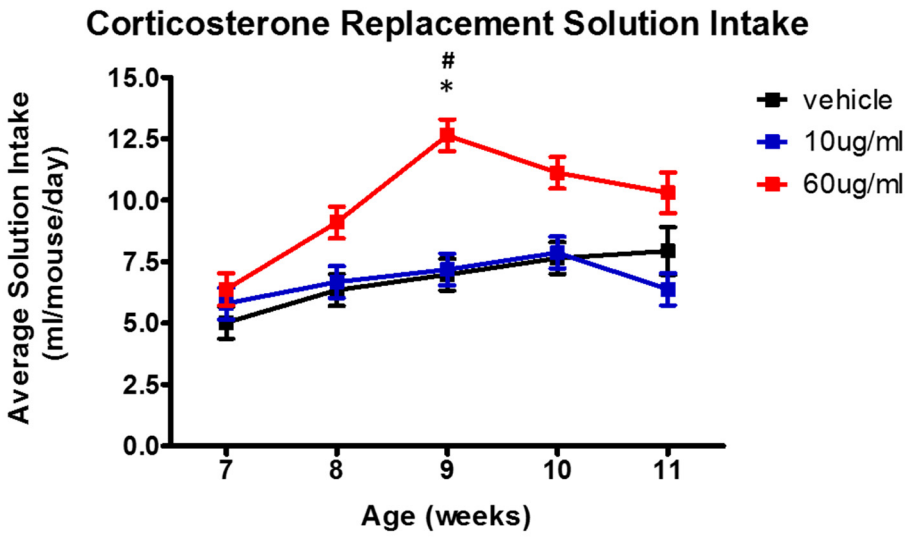

Supplemental Figure 2.3 – Corticosterone solution intake. Cage scores were taken daily for consumption of corticosterone solution, and averaged across the number of mice per cage. Weekly averages are presented here. There is a significant elevation of intake in the high dose (60ug/ml) group at 9 weeks of age, relative to the low dose (* Tukey's $p<.05$) for both and vehicle control groups (#Tukey's $p<.05$).

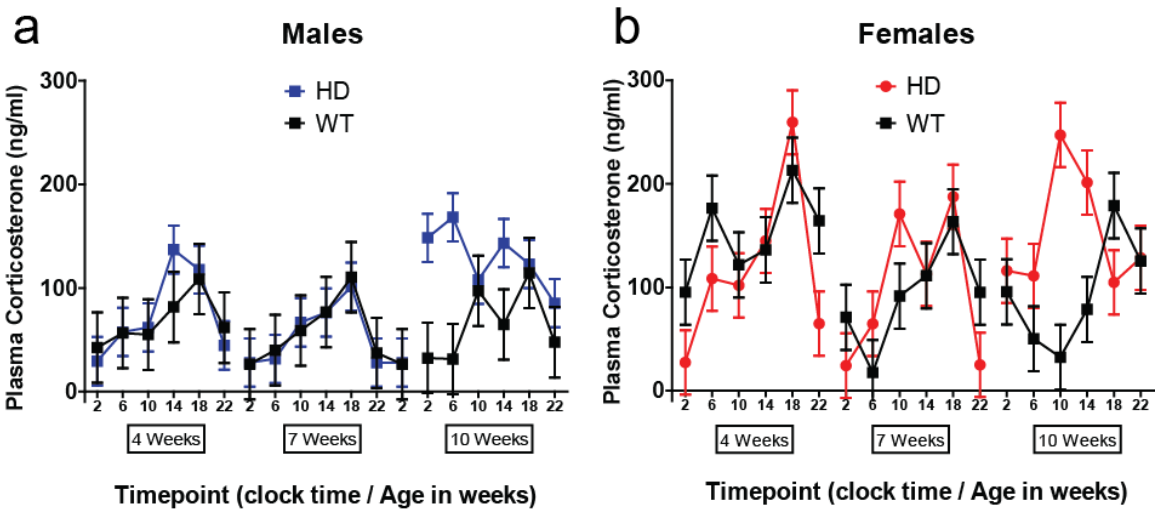

Supplemental Figure 2.4. - Circadian CORT release in males and females. Since there wasn't a statistically significant effect of sex (or its interactions) on plasma CORT levels in the circadian study, data were collapsed across sex for Fig 2. For qualitative purposes, circadian CORT profiles of (a) male and (b) female mice are presented here, separately.

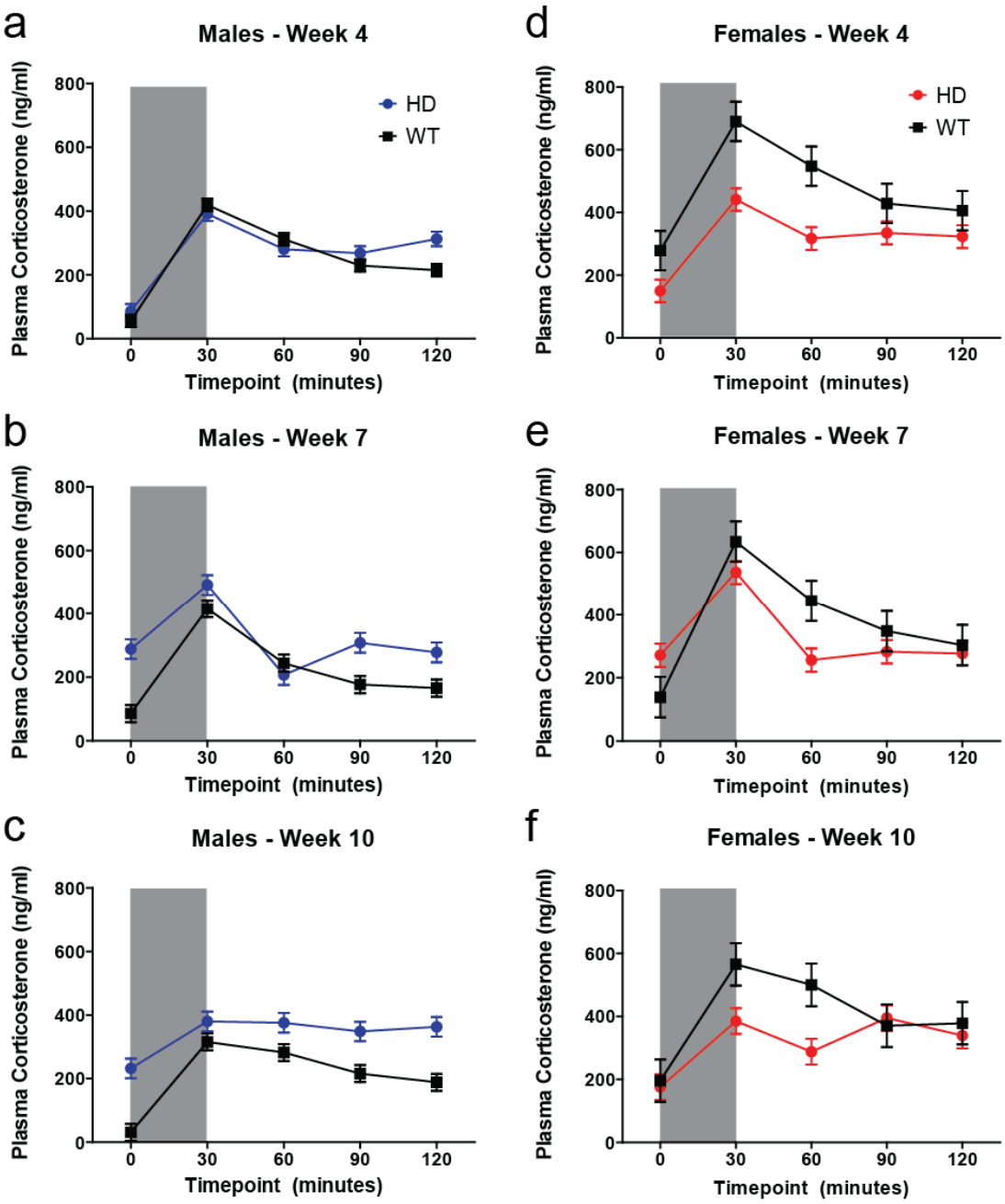

Supplemental Figure 2.5 - Stress induced CORT release at 4, 7, and 10 weeks of age. Since there wasn't a statistically significant effect of age (nor age*genotype) on stress induced CORT release in this study, data were collapsed across age for Fig 3. However, stress-induced CORT release profiles for male and female mice at 4, 7, and 10 weeks of age are also included here for qualitative purposes.

Chapter 3 – Normalizing Glucocorticoids Improves Metabolic and Neuropathological Symptoms in the R6/2 Transgenic Mouse Model of Huntington's disease

3.1 - Introduction

Glucocorticoids, which are chronically elevated in Huntington's disease (HD), have long been suspected as a contributor to the metabolic phenotype shown by patients (Aziz *et al.*, 2009; Bjorkqvist *et al.*, 2006a; Goodman *et al.*, 2008). This suspicion is logical, given that chronically elevated glucocorticoids lead to widespread metabolic dysfunction, including muscle wasting (Braun *et al.*, 2013; Grossberg *et al.*, 2010; Lee *et al.*, 2005), altered fat and protein metabolism (Lofberg *et al.*, 2002), insulin resistance (Black *et al.*, 1982), and osteoporosis (Moutsatsou *et al.*, 2012; Toth & Grossman, 2013) – all of which are symptoms of HD. However, while these findings from the Cushing's literature provide abundant circumstantial evidence for a role for glucocorticoids in HD symptomology, there has been little direct evidence to support this speculation. Data from the previous chapter provide some of the first direct evidence that elevated glucocorticoids do have a causal role in HD metabolic dysfunction. I confirmed that R6/2 mice show an elevation in circulating glucocorticoid levels and demonstrated that chronically elevated glucocorticoids exacerbate HD symptomology (Dufour & McBride, 2016) by leading to dramatic weight loss and significantly shortening lifespan (Dufour & McBride, 2016). Given the robust effects on weight loss in this previous experiment, I further characterized the effects of glucocorticoids on HD metabolism in a more comprehensive experiment presented here. In addition to playing a role in the HD metabolic phenotype, there is also abundant circumstantial evidence that elevated glucocorticoids may be exacerbating a variety of neuropathological changes that are inherent to HD, including regional reductions in brain volume (Andela *et al.*,

2013; Bourdeau *et al.*, 2002), reduced adult neurogenesis in the dentate gyrus (Brummelte & Galea, 2010; Cameron & Gould, 1994), and exacerbated mutant huntingtin inclusion body formation (Baglietto-Vargas *et al.*, 2013; Diamond *et al.*, 2000; Maheshwari *et al.*, 2014). Thus, in the experiments presented here in Chapter 3, I further assessed the role of glucocorticoids in the HD neuropathological and metabolic phenotypes, again utilizing the R6/2 HD transgenic mouse model.

Human HD patients show a variety of severe and progressive metabolic symptoms that include weight loss, muscle wasting, and insulin resistance (Aziz *et al.*, 2008; van der Burg *et al.*, 2009; van der Burg *et al.*, 2011). Calorimetry data suggest that patients are in a chronic catabolic state, and thus in negative energy balance (Goodman *et al.*, 2008). R6/2 transgenic mice recapitulate many of these human metabolic symptoms, with mice also showing progressive weight-loss, muscle wasting, and insulin resistance (Bjorkqvist *et al.*, 2005; Luthi-Carter *et al.*, 2002; van der Burg *et al.*, 2009). R6/2 mice are also in negative energy balance (Goodman *et al.*, 2008), with indirect calorimetry measures showing that this may be driven by a chronic increase in metabolic rate, as indicated by an increase in oxygen consumption (Bjorkqvist *et al.*, 2006b; Goodman *et al.*, 2008). In Cushing's disease, chronically elevated glucocorticoids lead to severe alterations in metabolism including weight loss, increased adiposity, muscle wasting, and insulin resistance (Braun *et al.*, 2013; Burt *et al.*, 2006; Grossberg *et al.*, 2010; Nieuwenhuizen & Rutters, 2008; Valassi *et al.*, 2012). Given that HD patients (and transgenic HD mice) simultaneously show a progressive increase in glucocorticoids along with a worsening metabolic profile, I postulated that this elevation may in fact be either mediating or contributing to the HD metabolic profile, similar to what is seen in Cushing's patients.

In addition to metabolic symptoms, there are abundant data that chronically elevated glucocorticoids in Cushing's disease can induce HD-like neuropathological changes. In Cushing's,

the chronic elevation of glucocorticoids similarly leads to whole brain atrophy (Bourdeau *et al.*, 2002), as well as regional reductions in cortical and hippocampal volume (Andela *et al.*, 2013; Lupien *et al.*, 1998), and a reduction in bi-caudate diameter (Bourdeau *et al.*, 2002). In human HD and in R6/2 HD mice there is striking reduction in whole brain and regional volume, with the striatum, cortex, and hippocampus being particularly affected (Kim *et al.*, 2014; Rosas *et al.*, 2003; Spargo *et al.*, 1993; Tabrizi *et al.*, 2009; Vonsattel *et al.*, 1985; Zhang *et al.*, 2010). While mutant huntingtin is likely the main driver of regional reductions in brain volume in HD, it is possible that chronically elevated glucocorticoids may be significantly exacerbating the phenotype.

R6/2 mice also show a progressive and robust reduction in dentate gyrus neurogenesis that onsets early in life, detectable from 3.5 weeks of age (Gil *et al.*, 2005). Dentate gyrus neurogenesis is known to be particularly sensitive to alterations in glucocorticoid levels, with high levels of corticosterone suppressing the proliferation of progenitor cells, and low levels stimulating proliferation (Wong & Herbert, 2004). R6/1 mice, another transgenic HD strain with similar genetics and slightly slower phenotypic progression to R6/2s, also show a significant reduction in dentate gyrus neurogenesis, which can be exacerbated by elevations in glucocorticoids (Mo, Pang*, et al.*, 2014). However, unlike R6/1 mice, R6/2 mice show a spontaneous and progressive elevation in glucocorticoid levels (see chapter 2) as a part of their HD phenotype, which could potentially exacerbate this HD related reduction in neurogenesis.

A hallmark of HD neuropathology is the formation of inclusion bodies, made up of aggregated mHTT protein (Landles *et al.*, 2010). There is evidence that glucocorticoid receptor signaling can have a potent effect on mHTT inclusion body formation – Diamond et al. (2000) showed that acute stimulation of mutant huntingtin expressing cells *in vitro* with dexamethasone, a potent glucocorticoid receptor agonist, causes mHTT protein to exist predominately in soluble form. Conversely, in cells that were not treated with dexamethasone, mHTT protein tended to be

in insoluble aggregated form (Diamond *et al.*, 2000). However, given that chronic elevations in glucocorticoids lead to robust downregulation of glucocorticoid receptors (Burnstein *et al.*, 1991), it is possible that chronically elevated corticosterone in R6/2 mice could paradoxically lead to an increase in inclusion formation. This also appears to be the case in Alzheimer's disease, another neurodegenerative disease associated with chronically elevated cortisol (Davis *et al.*, 1986; Swaab *et al.*, 1994) - elevated glucocorticoids in rodent models of Alzheimer's disease cause an increase in both amyloid beta plaques and Tau inclusion bodies (Green *et al.*, 2006), and blocking glucocorticoid receptors results in a reduction in both (Baglietto-Vargas *et al.*, 2013).

Thus, in the series of experiments presented in this chapter, I assessed the effects of glucocorticoids on HD metabolic and neuropathological symptoms, utilizing the same experimental approach as described in Chapter 2 (adrenalectomy with WT-level or HD-level corticosterone replacement, and sham surgery controls). Here, I tested the hypothesis that normalized glucocorticoids (low-dose / WT-level) would improve metabolic symptoms in R6/2 HD mice – that it would attenuate weight loss, increase food consumption, reduce VO_2 levels, and increase skeletal muscle and brain mass, which are likely associated with the chronically high metabolic state associated with the R6/2 phenotype. Additionally, I tested the hypothesis that normalized glucocorticoids would attenuate HD neuropathology that could possibly be affected by chronically elevated corticosterone – that it would increase regional brain volume and dentate gyrus neurogenesis towards wild-type levels and that it would reduce mHTT inclusion burden.

3.2 - Methods

Animals. All animals were group housed with littermates (3-5 mice per cage) under controlled conditions of temperature and light (12 hour light/dark cycle). Food (Laboratory Rodent Diet 5001, LabDiet, St. Louis, MO) and water were provided *ad libitum*. R6/2 mice (stock # 002810, carrying 160±5 cag repeats) were obtained from Jackson Laboratories (Bar Harbor, ME) and bred in the vivarium at the ONPRC. Wild-type males were mated with ovary transplanted wild-type females. Transgenic mice were genotyped using primers specific for the mutant human HTT transgene (forward primer 5' TCATCAGCTTTTCCAGGGTCGCCAT and reverse primer 5' CGCAGGCTAGGGCTGTCAATCATGCT), and age-matched wild-type littermates were used for the indicated experiments. Average CAG repeat length for the colony was assessed from a subset of animals by sequencing, with mice from the colony showing an average of 165 ± 5 (SD) CAG repeats (Laragen Sequencing and Genotyping, Los Angeles, CA). Body weights of all animals were recorded weekly. All experimental procedures were performed according to ONPRC and OHSU Institutional Animal Care and Use Committee.

Adrenalectomy Surgery. Mice were anesthetized with 3% isoflurane. A 2cm x 2cm square was shaved on their lower dorsal surface and an incision was made in the skin at the animal's dorsal midline (this opening was used for the removal of both adrenal glands). Next, a small (3-5mm) incision in the muscular wall was made, directly above the kidney. Small tweezers were used to grasp and gently remove the adrenal gland. This procedure was repeated for the animal's contralateral side (bilateral adrenalectomy). The muscle incisions were closed using absorbable suture and the dorsal skin was closed with wound clips.

Corticosterone Replacement. Corticosterone replacement was provided in the animals' drinking water, which was available ad-libitum. Corticosterone (Sigma, cat. #27840) was dissolved in a

small volume of ethanol (0.6%), and then added to dH_20. Since the aldosterone producing cells of the adrenal gland are lost to adrenalectomy, NaCl (0.9%) was also added to replace salt loss. Sucrose (2.0%) was also added to increase palatability of the solution. A dose of 10ug/ml corticosterone was used for the physiological/WT level replacement group and 35ug/ml of corticosterone was used for the high/HD level replacement group. Vehicle alone (2% sucrose, 0.9% NaCl, and 0.6% ethanol in dH_20) was given to the sham surgery animals.

Plasma Corticosterone Analysis. The tail clip method was utilized to collect blood for assessing peak blood corticosterone levels. The tip of the tail was clipped (0.5mm), and approximately 20ul of whole blood was collected from the tip and collected into heparinized capillary tubes, processed for plasma, and stored at -80°C until analysis. Handling of mice during tail-clip method blood collection was minimized, and typically lasted approximately 30 seconds. Blood was collected from all adrenalectomized mice on corticosterone replacement (10ug/ml and 35ug/ml) at 10 weeks of age at midnight, to better assess peak levels of corticosterone due to mainly dark-cycle intake of replacement solution. For sham WT mice, blood was collected at the start of the dark cycle (6pm) at which time these mice should show peak corticosterone levels. For sham HD mice, blood was collected at 10am, which should reflect peak corticosterone levels which is phase shifted forwarded (estimated peak time determined in previous experiment, see chapter 2). All plasma was assayed for corticosterone by the ONPRC Endocrine Technology CORE using an in-house radio-immuno assay.

Indirect Calorimetry. The comprehensive lab animal monitoring system (CLAMS Oxymax system, Columbus Instruments, Columbus, OH) was used to assess alterations in metabolic rate (indirect calorimetry) and food intake in subjects. Mice were measured at 5 and 10 weeks of age, and 24-hours of data were analyzed (6pm – 6pm). Mice were acclimated to the sealed chambers (3.5”) for 4 hours before the dark cycle (2pm-6pm), and these acclimation data were omitted from

analysis. As there are diurnal variations in indirect calorimetry measures, dark cycle and light cycle data were analyzed separately. Mice had ad lib access to food and water (water at 5 weeks of age, before surgery, and corticosterone replacement solution at 10 weeks) throughout their time in the chambers. Standard rodent chow was finely ground (required for accurate measurement of food intake) and placed in a specialized feeder at the base of the chambers, and food consumption was automatically measured by the CLAMS apparatus. Fluid intake was manually measured over the 24 hour period. Measures of oxygen intake (VO_2) and carbon dioxide production (VCO_2) were automatically collected by the software for each chamber every 18 minutes throughout the 24-hour period, and the respiratory exchange ratio (RER, Ratio VCO_2:VO_2) was automatically calculated by the software for each interval. There was a malfunction of the oxygen sensors during some of the indirect calorimetry runs (up to 8 mice are run at a time, 3 runs were affected, leading to exclusion of 21 mice), and thus a portion of the animals from this experiment were specifically excluded from the calorimetry analysis. Although the malfunction only affected a single timepoint for these animals, both timepoints were omitted to ensure that repeated measures were complete and reliable.

Necropsy. At 11 weeks of age, mice were deeply anesthetized with ketamine/xylazine and perfused with 15mLs of 0.9% saline. Brains and gastrocnemius muscle were carefully dissected and weighed. Brains were post-fixed in 4% paraformaldehyde for 24 hours, then stored in a 30% sucrose solution until they were sectioned.

Immunohistochemistry. Brains were cut into 40μm sections with a freezing sliding microtome and stored in cryoprotectant solution (30% sucrose, 30% ethylene glycol, in PBS) until stained. Serial sections from 48 mice (balanced for sex, genotype, and treatment) were stained using standard DAB immunohistochemistry using the following primary antibodies: 1) NeuN (1:750, Millipore ABN78) - a pan neuronal marker used here for volumetric analysis, 2) ki67 (1:150,

ThermoFisher MA5-14520) – a mitosis marker that is used to identify proliferating cells in the adult brain as a marker of neurogenesis, and 3) em48 (1:250, Millipore MAB5374) – an antibody that preferentially binds to aggregated mutant huntingtin protein. Sections were blocked (for endogenous peroxidases) in sodium-m-periodate for 20 minutes, then blocked (for non-specific antibody binding) in 5% goat serum for 1 hour, incubated in primary antibodies overnight (in 3% goat serum), washed and incubated in secondary antibody for 1 hour, amplified with VectaStain ABC kit, and developed with DAB (Nickel intensification was also used for the ki67 stain, to intensify the signal).

Neuropathology Quantification. NeuN stained sections were used to analyze regional volume of striatum, cortex, and hippocampus using the Cavalieri method in Microbrightfield Stereo Investigator software (MBF Bioscience, Milliston VT). The following parameters were used for the Cavalieri estimations from each region: 1) Striatum – 6 matched serial sections (every 12^{th} section, from +1.70 to -1.94) were assessed with a grid size of 75µm, 2) Cortex – 9 matched serial sections (every 12^{th} section, from +2.10 to -2.92) were assessed with a grid size of 150µm, and 3) Hippocampus – 5 matched serial sections (every 12^{th} section, from -1.46 to -3.88) were assessed with a grid size of 75µm. Parameters for analysis were optimized with pilots, aimed at minimizing Gunderson Coefficients of Error (m=0) to ≤0.100 (Average values: Striatum = 0.049, Cortex = 0.054, Hippocampus = 0.096). Ki67+ cells in the dentate gyrus were counted manually at 40x magnification in 5-6 serial sections (every 6^{th} section) from -1.58 to -2.80. Counts were taken for both hemispheres, for a total of 10-14 counts per mouse and averaged. Em48 stained sections were assessed for inclusion number and size using imageJ software (National Institutes of Health, Bethesda MD), following the method outlined in Gharami et al. (2008). Images were acquired at 100x in three serial sections, with an image taken from both the left and right hemispheres, for a total of 6 images per mouse for each region of interest: hippocampus (CA1 and dentate gyrus: -

1.70 to -3.16), hypothalamus (lateral hypothalamus: -0.82 to -2.18), striatum (dorsomedial: +0.86 to -0.46), and cortex (layer 5 motor cortex: +1.42 to +0.02). The acquired images were converted to 8-bit greyscale and the threshold was adjusted to a set level in each ROI to remove background staining. The number and size of EM48+ inclusion bodies were quantified using the particle analysis tool and averaged for each mouse across all 6 acquired images per ROI.

Statistical analysis. All statistical analyses were performed by using JMP Version 11 (SAS Institute Inc.). A repeated measures mixed-model analysis was used for all repeated measures (Dependent variables: bodyweight, VO_2, VCO_2, RER, food intake, and fluid intake; Independent variables: genotype, treatment, time-point). A two-way ANOVA was used to assess the effects of genotype and treatment group on: Organ mass (brain and gastrocnemius), Regional brain volume (striatum, cortex, hippocampus), and Neurogenesis. A one-way ANOVA was used to assess the effects of treatment on inclusion burden (inclusion size and number) across the 6 regions of interest (striatum, motor cortex, cingulate cortex, CA1 hippocampus, dentate gyrus, and lateral hypothalamus) in R6/2 mice. All analyses were carried out separately for males and females, as there were sexually dimorphic patterns of treatment effects. Pre-planned post-hoc contrasts were used to assess within genotype and within treatment pairwise comparisons in bodyweight at each time-point assessed. The alpha level for contrasts were Bonferroni adjusted (total of 48 comparisons - .05/48 = .0011) to avoid Type I error. Contrasts were utilized for the bodyweight analysis instead of Tukey's post-hoc comparisons to avoid Type II error (excessive alpha suppression) due to a high number of possible pairwise comparisons (435), most of which were not relevant to the hypotheses being tested. For all other analyses, Tukey's post-hoc comparisons were used if there was a significant fixed effect for the independent variables of interest. In all cases, a $p \leq 0.05$ was considered significant.

3.3 - Results

Timeline, experimental design, and rationale

In order to assess the role of glucocorticoids in HD metabolic symptomology and neuropathology, WT and R6/2 HD mice were adrenalectomized at 6 weeks of age, and treated with either low dose (10ug/ml, WT level, n=20-25 per genotype) or high dose (35ug/ml, HD level, n=17 per genotype) corticosterone replacement, provided in their drinking water (See **Fig. 3.1A** for experimental timeline). Another cohort of WT and HD mice were given sham surgeries, and provided with vehicle only (no corticosterone replacement) for their drinking water. Dosing was determined in pilot experiments, and adjusted from a previous study (Chapter 2, Dufour & McBride, 2016) to reduce the HD-level replacement to a dose that is closer to the levels of hypercortisolinemia normally seen in transgenic R6/2 mice (35ug/ml instead of 60mg/ml).

Plasma corticosterone levels

Blood was collected from subjects at 9.5 weeks of age to identify peak plasma corticosterone levels due to corticosterone treatment or due to endogenous circadian corticosterone release in sham surgery controls (**Fig. 3.1**), and analyzed in a subset of mice. Accordingly, blood was collected at midnight for adrenalectomized mice on corticosterone replacement (middle of dark cycle, when water intake is highest), 6pm for sham treated WT mice (start of the dark cycle, normal circadian peak time), and at 10am for sham treated R6/2 mice (peak time determined in previous experiment in Chapter 2, although perhaps not ideal). There was a trend for a sex effect ($F_{1,60}$ = 3.96, p=.0512), and thus the two sexes were analyzed independently for the final analysis. As expected, treatment affected plasma corticosterone levels in both males ($F_{1,30}$ = 17.16, p<.001) and females ($F_{1,30}$ = 5.32, p<.05). In males, Tukey's post-hoc comparisons indicate that high dose corticosterone replacement resulted in significantly elevated

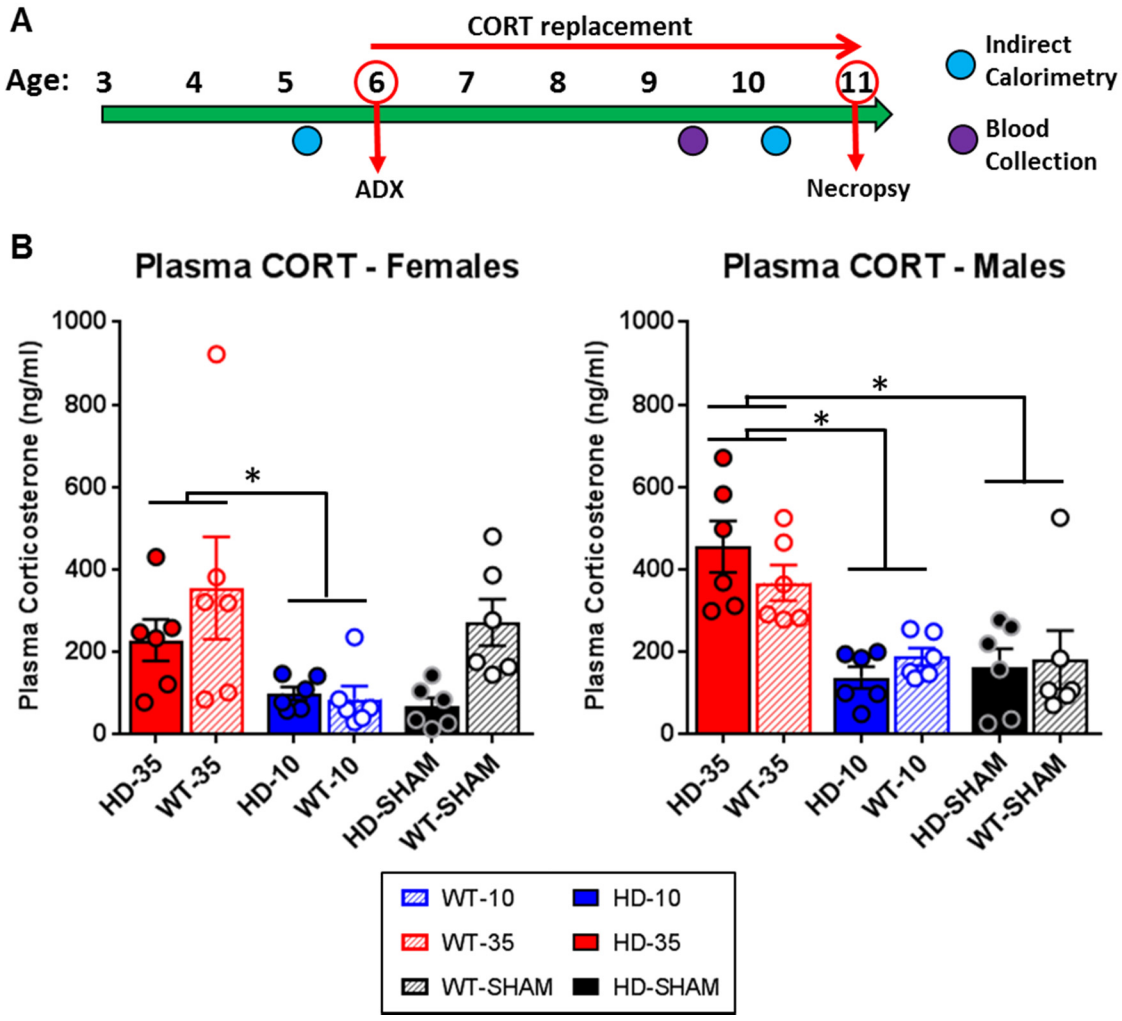

Figure 3.1 – Experimental timeline and plasma corticosterone levels. (A) Experimental timeline - WT and R6/2 HD mice underwent adrenalectomy surgery at 6 weeks of age and were given either low/WT dose corticosterone replacement (10ug/ml, blue) or high/HD dose corticosterone replacement (35ug/ml, red) in their drinking water from 6 to 11 weeks of age, at which time mice were sacrificed. A group of sham surgery controls were also included (black), and only received vehicle. All subjects were measured for indirect calorimetry at 5 and 10 weeks of age, body weight weekly, and blood was collected at 9.5 weeks of age for plasma corticosterone levels. (B) Plasma corticosterone analysis (N=36 per sex, 6 per genotype/treatment group) indicates that high dose treatment led (35ug/ml) to increased plasma levels in females relative to those on low dose treatment (10ug/ml), although they were not different from sham controls. For males, plasma levels from the high dose (35ug/ml) group were significantly higher than both those on low dose treatment (10ug/ml) and sham controls. Values represent Mean ± SE. *Indicate significant differences as indicated by Tukey's posthoc comparisons.

plasma corticosterone levels (WT: 367.5 ± 43.0 ng/ml, HD: 454.9 ± 62.4 ng/ml) relative to those on low dose replacement (WT: 187.6 ± 21.7 ng/ml, HD: 137.7 ± 25.9 ng/ml) and sham controls (WT: 181.4 ± 70.5 ng/ml, HD: 162.9 ± 44.8 ng/ml). For males, plasma corticosterone levels were not affected by genotype ($F_{1,30}$ = 0.03, p=.87) nor was there a treatment*genotype interaction ($F_{2,30}$ = 1.12, p=.34). In females, Tukey's post-hoc comparisons indicate that high dose corticosterone replacement resulted in significantly elevated plasma corticosterone levels (WT: 355.5 ± 135.9 ng/ml, HD: 228.9 ± 50.3 ng/ml) relative to those on low dose replacement (WT: 86.3 ± 31.0 ng/ml, HD: 100.1 ± 16.0 ng/ml), but were not different from sham controls (WT: 272.0 ± 68.4 ng/ml, HD: 68.5 ± 20.9 ng/ml). In females there was an effect of genotype ($F_{1,30}$ = 4.41, p<.05) on plasma corticosterone levels, which reflects an overall elevation in plasma corticosterone levels in WT females, regardless of treatment, but not a treatment*genotype interaction ($F_{1,30}$ = 1.60, p=.22). While the effect high dose versus low dose corticosterone replacement is clear, the data from the sham controls are less straight forward. The interpretation of these data is complicated by two factors: 1) There isn't an ideal time to measure plasma corticosterone levels in intact transgenic R6/2 mice, as there is circadian dysregulation and tremendous individual differences in terms of the time of peak corticosterone (See **Fig. 2.2**); and 2) There are plasma corticosterone values for two WT females and one WT males that are outside of the circadian range and in the stress-induced corticosterone range (>250 ng/ml - See **Supp. Figs. 2.4** and **2.5**).

Bodyweight analysis

I first tested the hypothesis that normalized glucocorticoid levels (10ug/ml - low dose WT-level treatment) would slow the progression of weight loss in R6/2 mice relative to those on high dose (35ug/ml – HD level) treatment and sham surgery controls. In a previous experiment (chapter 2), high dose corticosterone (60ug/ml) was associated with precipitous weight loss in transgenic R6/2 mice, although here a lower (35ug/ml) dose was used here for the high dose (HD

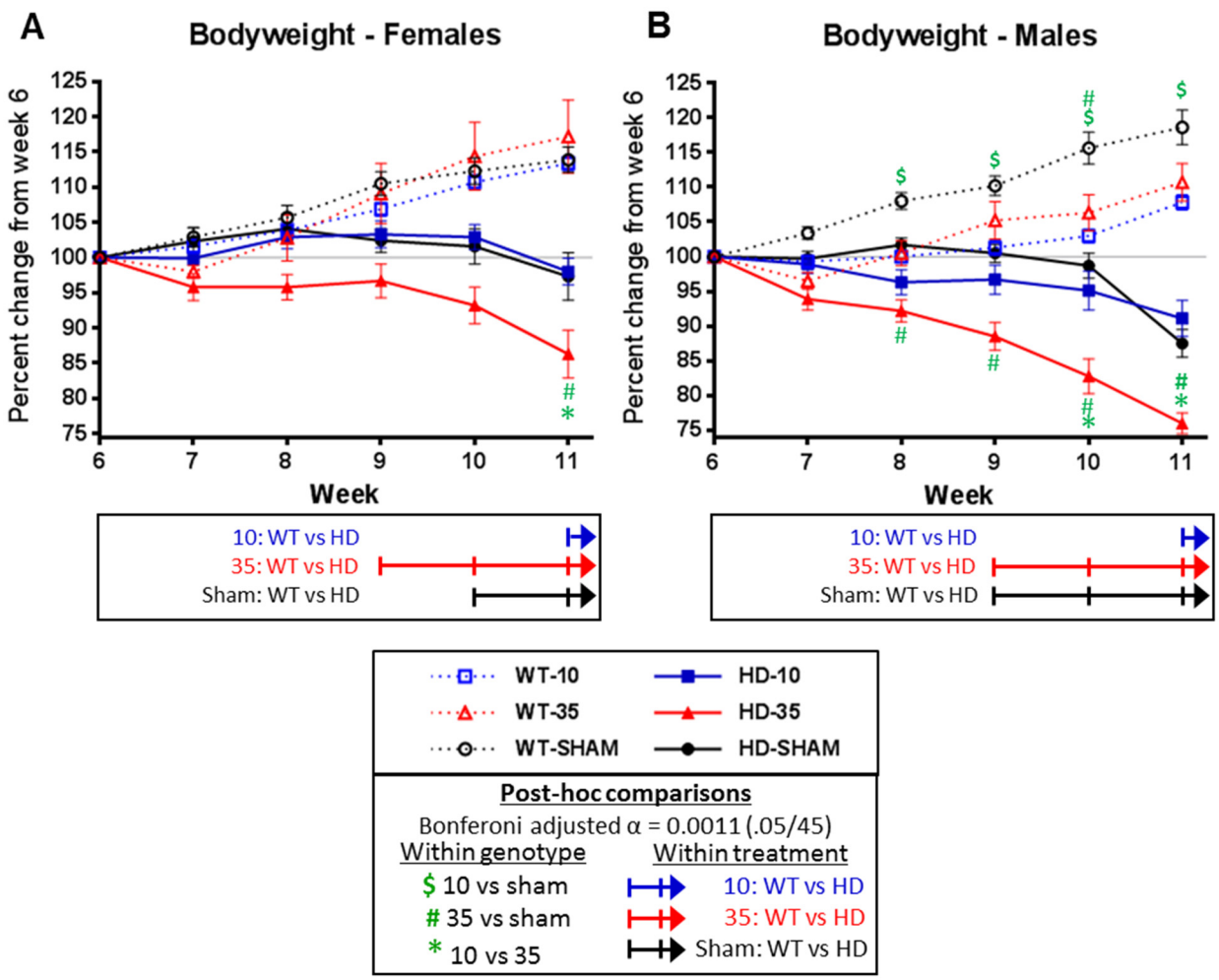

Figure 3.2 – Effect of glucocorticoid replacement on percent change in bodyweight. All WT mice gained weight following surgery/treatment at week 6, while HD mice lost weight, although the degree of weight loss varied according to treatment and genotype (Treatment*Genotype*Timepoint. Males: $p<.0001$; Females: $p<.005$). Within-genotype post-hoc comparisons (indicated by symbols in green: at top for wildtype, below for HD) indicate that HD males on high dose CORT (35ug/ml) show significantly more weight loss than HD sham males from weeks 8-11 and low dose (10ug/ml) HD males from weeks 10-11 (B). High dose HD females show significantly more weight loss at week 11 only, relative to the other treatments. Sham male WT mice showed increased weight gain relative to WT males on high dose (weeks 8-11) and low dose corticosterone treatment (week 10 only). Within treatment comparisons (e.g. low dose. WT vs HD) indicate that low dose CORT delayed weight loss in male R6/2 mice, which only becomes significant at 11 weeks of age (B, blue arrow), while sham (B, black arrow) and high dose (B, red arrow) treated males show significant weight loss from weeks 9-11. Low dose treatment also delays weight loss in HD females (A, blue arrow) to week 11, while weight loss begins at week 9 for high dose (A, red arrow) and week 10 for sham controls (A, black arrow). Alpha level was Bonferoni adjusted for 45 post-hoc comparisons (.05/45 = .0011 critical alpha). Overall N=52 for females (n= 7-11 per group) and N=60 for males (n=9-14 per group). Values represent Mean ± SE.

level) group, as it better matches the level of hypercortisolinemia normally seen in transgenic R6/2 mice. Change in bodyweight from 6 weeks of age, at which point mice underwent adrenalectomy or sham surgery, was calculated weekly until 11 weeks of age and analyzed using a 2-way repeated measures ANOVA. Pre-planned post-hoc orthogonal contrasts were used to make pairwise comparisons (both within treatment, and within genotype) and accordingly the alpha-level was Bonferoni adjusted to avoid type I error ($\alpha = .0011 = .05/45$ comparisons). As there are numerous sex effects across metabolic and neuropathological markers throughout these experiments, males and females were assessed separately for all analyses. There was a significant divergence in bodyweight change between genotypes (Females: Genotype*timepoint - $F_{4,192}=70.70$ $p<.0001$ / Males: Genotype*timepoint - $F_{4,220}=156.27$ $p<.0001$), with wild-type mice showing normal weight gain following surgery at 6 weeks, and transgenic mice showing a progressive decline in bodyweight (**Fig. 3.2**). Bodyweight was further influenced by an interaction of both treatment and genotype across the span of the experiment (Treatment*Genotype*Timepoint interaction) for both males ($F_{8,220}=7.54$ $p<.0001$) and females ($F_{8,192}=3.25$ $p<.005$). By the end of the experiment, at 11 weeks of age, all male transgenics had all lost significant weight relative to their 6 week baseline: 8.9% ± 2.6% for those on low dose corticosterone, 24.0% ± 1.5% for high dose, and 12.5% ± 2.0% for sham controls. As expected, wildtype males on all treatments gained weight relative to their 6 week baseline: an increase of 7.8% ± 1.1% for low dose, 10.7% ± 2.7% for high dose, and an 18.6% ± 2.5% for sham by week 11. For female transgenics, high dose corticosterone resulted in a loss of 13.7% ± 3.4% of bodyweight, while those on low dose (2.0% ± 1.9% loss) and sham controls (2.7% ± 1.8%loss) had only started to lose weight at this time-point. Treatment did not significantly affect bodyweight in wildtype females, with all treatment groups showing an increase ranging from 13.4% to 17.2%. Given that treatment affected bodyweight for the wildtype animals differently, both within-treatment post-

hoc comparisons (e.g. transgenic R6/2 on low dose compared with wildtype on low dose) and within-genotype post-hoc comparisons (e.g. low dose transgenics compared to high dose and sham treated transgenics) were utilized to better assess how treatment affected the R6/2 weight loss phenotype.

Within-treatment comparisons (**Fig. 3.2**, indicated by blue, red, and black arrows below the x-axis) illustrate the timepoint at which transgenic R6/2 mice show significant weight loss relative to WT control mice on the same treatment. This within-treatment comparison is important statistically, since treatment had subtle but significant effects on WT controls (described above), and thus should be accounted for when assessing the effect of treatment on the onset of the R6/2 weight-loss phenotype. These comparisons show that low dose corticosterone delayed the onset of weight loss in transgenic male and female R6/2 mice, which did not become significantly different from low-dose WT controls until 11 weeks (**Fig. 3.2A** and 3.**2B**, blue arrows, $p<.0011$). In contrast, male and female transgenic mice on high dose corticosterone showed significant weight loss earlier, starting at 9 weeks and continuing through week 11, relative to wild-type controls on the same treatment (High dose CORT, red arrows, $p<.0011$ for each of those 3 timepoints for both sexes). As expected, male R6/2 sham controls also showed significant weight loss relative to wild-type male sham controls from weeks 9 through 11 (black arrows, $p<.0011$ for all). There was a slight delay in female sham control, with transgenics showing significant weight loss in weeks 10 and 11 (black arrow, $p<.0011$), one week earlier than low dose transgenics and one week later than high dose transgenics.

Within-genotype post-hoc comparisons (**Fig. 3.2**, indicated by $,#,* in green, below data lines for transgenics, above data lines for wild-type mice) revealed that R6/2 mice on high dose corticosterone show significantly more weight loss, particularly in males, relative to low-dose treated and sham control R6/2 mice. This is consistent with the previous study (chapter 2), even

with the reduced dosing for the high corticosterone group (35ug/ml instead of 60ug/ml). For male transgenics, those on high dose corticosterone showed significantly more weight loss than sham controls from weeks 8-11 (# $p<.0011$) and low dose treated mice from weeks 10-11 (* $p<.0011$). High dose corticosterone also exacerbated weight loss in female transgenics, relative to those on low dose treatment (* $p<.0011$) and sham controls (# $p<.0011$), although this didn't become significant until the last time point at 11 weeks of age. Contrary to my hypothesis, within-genotype comparisons indicated that bodyweights were not significantly different between low-dose and sham control R6/2 mice, for either sex ($p>.0011$ for all timepoints).

Overall, within-treatment comparisons reveal that low dose treatment delays weight loss R6/2 mice, which accounts for how the same treatment affected matched WT mice controls. This may be in part accounted for the poorer recovery for adrenalectomized mice (low and high dose, WT and HD), who typically show more weight loss at week 7. Indeed, male wildtype sham mice did show increased weight gain compared to the two adrenalectomized groups. However, within-treatment comparisons suggest that the normalization of glucocorticoids did not delay the onset of weight-loss in R6/2 mice relative to sham controls, although it indicates that high dose treatment did result in dramatic weight-loss relative to the other two groups. Within-genotype comparisons also reveals that sham treated male HD mice lost weight earlier and more severely than females, which is expected for R6/2 mice (Hockly *et al.*, 2003), and that high dose corticosterone treatment here (35ug/ml) has a particularly strong effect on weight loss, even more severe than the endogenously high levels in sham control HD mice. As the within-genotype and within-treatment comparisons do not entirely agree, it is difficult to reconcile these two analyses. However, regardless of the type of posthoc analysis, it appears as though high dose CORT led to an exacerbation of the R6/2 weight loss phenotype much more robustly than low dose CORT may have attenuated it, relative to sham controls.

Indirect Calorimetry

To better assess the effect of glucocorticoid treatment on metabolism in R6/2 HD mice, 24-hour indirect calorimetry measures were taken from the subjects at 5 weeks of age (prior to surgery/treatment at week 6), and again at 10 weeks of age following 4 weeks of chronic treatment with corticosterone replacement (vehicle for sham controls). Gas exchange is measured with indirect calorimetry, including oxygen consumption (VO_2) and carbon dioxide production (VCO_2). From these values, the respiratory exchange ratio (RER) is calculated (Ratio of VCO_2:VO_2) for each individual, which indicates on a cellular level what nutrient source is preferentially used for fuel (Frayn, 1983). Mice were provided with ad-libitum food and water (water at baseline/5 weeks, corticosterone replacement solution or vehicle at 10 weeks of age), which was measured for the 24 hours of measurement. As indirect calorimetry measures shift between the light and dark cycles, these two 12 hour periods were analyzed separately, as well as the two sexes as there are sex differences in these measures. Previous studies with R6/2 mice have shown an increased in oxygen consumption relative to WT mice, an indicator of elevated metabolic rate (Goodman *et al.*, 2008; van der Burg *et al.*, 2008). Accordingly, here I tested the hypothesis that normalizing glucocorticoid levels would ameliorate the metabolic deficit shown by R6/2 mice, as measured by indirect calorimetry.

Genotype had a strong and consistent impact on all indirect calorimetry measures here, with R6/2 HD mice showing significantly elevated VO_2 and VCO_2 levels and a reduction in RER (Statistical tests outlined in **Table 3.1).** Although both VO_2 and VCO_2 levels are elevated, VO_2 is elevated to a larger degree than VCO_2 in R6/2 mice here, which is what drives the reduction in RER. Treatment also had strong impact on calorimetry measures in transgenic R6/2 male mice (Reflected by significant Treatment*Genoptype*Timepoint fixed effects for dark and light cycle

VO_2 and RER, and for light cycle VCO_2, $p<.05$ for all) with few significant effects on wildtype male mice or on females of either genotype.

Tukey's posthoc tests indicate that in male R6/2s, elevated (high dose, HD-level) corticosterone drives a strong and significant elevation in indirect calorimetry measures relative to baseline: a 15.6% increase in dark cycle VO_2 (15.6% increase over baseline, **Fig. 3.4A**), light cycle VO_2 (37.9%, **Fig. 3.4D**), and light cycle VCO_2 (33.6%, **Fig. 3.4E**). Similarly, sham male R6/2s also show a significant elevation over baseline in light cycle VO_2 (17.2%, **Fig. 3.4D**) and light cycle VCO_2 (12.4%, **Fig. 3.4E).** Normalizing glucocorticoids partially prevents these elevations in VO_2 and VCO_2 from baseline shown in sham and high dose males, as male R6/2 mice treated with low dose corticosterone do not show any significant changes from baseline in dark cycle VO_2 (3.4% decrease, **Fig. 3.4A**), light cycle VO_2 (10.8% increase, **Fig. 3.4B**), dark cycle VCO_2 (3.1% decrease, **Fig. 3.4D**), or light cycle VCO_2 (11.2% increase, **Fig. 3.4D**).

Normalizing glucocorticoids also prevents the reduction in the respiratory exchange ratio (RER) in males that is characteristic of R6/2 mice. RER reflects the preferential utilization of macronutrients in energy production, with a value of 1.00 reflecting exclusive utilization of carbohydrates, a value of 0.70 reflecting an exclusive utilization of fatty acids for energy, and intermediate values representing a mixture of both carbohydrates and fats (Frayn, 1983). R6/2 males on low dose treatment showed a non-significant 0.1% reduction in dark cycle RER (**Fig 3.4C**) and a non-significant 0.8% increase in light cycle RER (**Fig. 3.4F**), relative to baseline. Additionally, low dose treated R6/2 mice were not significantly different from low dose treated WT controls for either dark cycle RER (3.9% decrease, **Fig. 3.4C**) or light cycle RER (3.4% decrease, **Fig. 3.4F**). In contrast, male R6/2 mice on high dose corticosterone showed a significant 8.0% reduction in dark cycle RER (**Fig. 3.4C**) and a significant 6.2% reduction in light cycle RER (**Fig. 3.4F**), reflecting an

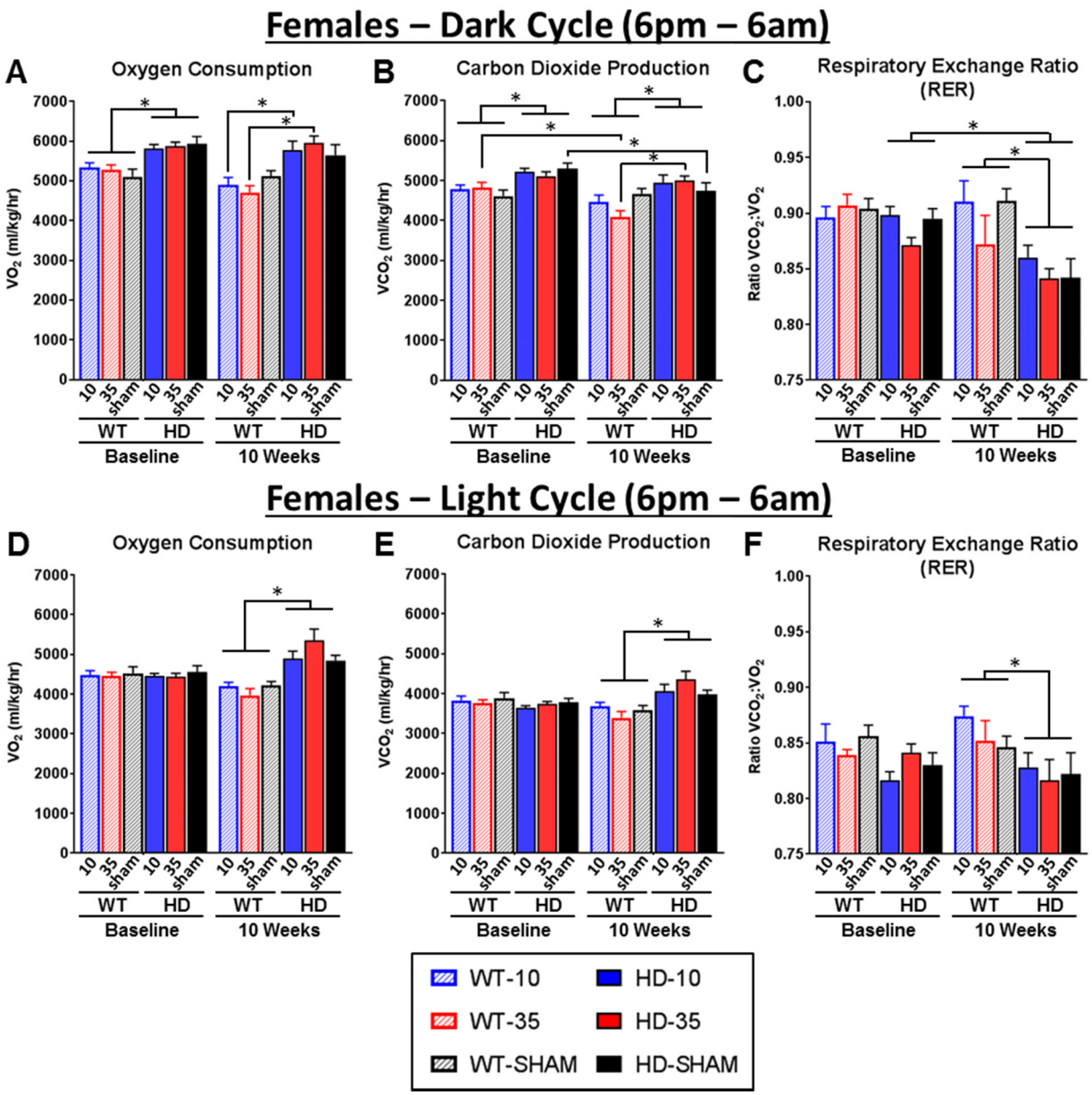

Figure 3.3 – Effect of glucocorticoid replacement on indirect calorimetry (CLAMS) in females. Mice were measured for indirect calorimetry at 5 weeks (baseline) and 10 weeks of age, following surgery and corticosterone treatment at 6 weeks of age. Unlike males (see figure 4), treatment effects were rare and small for female mice. R6/2 mice showed elevated night cycle VO_2 (A) and VCO_2 (B) (Treatment: $p<.05$), and also showed an elevation in light-cycle VO_2 (D) and VCO_2 (E) at 10 weeks (Genotype*timepoint: $p<.05$). Female R6/2 mice also showed a reduction in dark cycle RER at 10 weeks (C, Genotype*Timepoint: $p<.05$) and light cycle RER at baseline and 10 weeks (F, Genotype: $p<.05$). Both low dose and high dose treatment is associated with an increase in dark cycle VO_2 (*Tukey's posthoc), but not for sham R6/2 mice (A). High dose CORT (35ug/ml) is associated with a reduction in VCO_2 in WT females, while sham treatment is associated with a reduction in R6/2 females (B, *Tukey's posthocs). High dose CORT treated R6/2 females also showed an elevation in VCO_2 at 10 weeks, relative to WT females on the same treatment. Overall N=44, with n=7-9 per group. Values represent Mean ± SE. *Indicate significant differences as indicated by Tukey's posthoc comparisons.

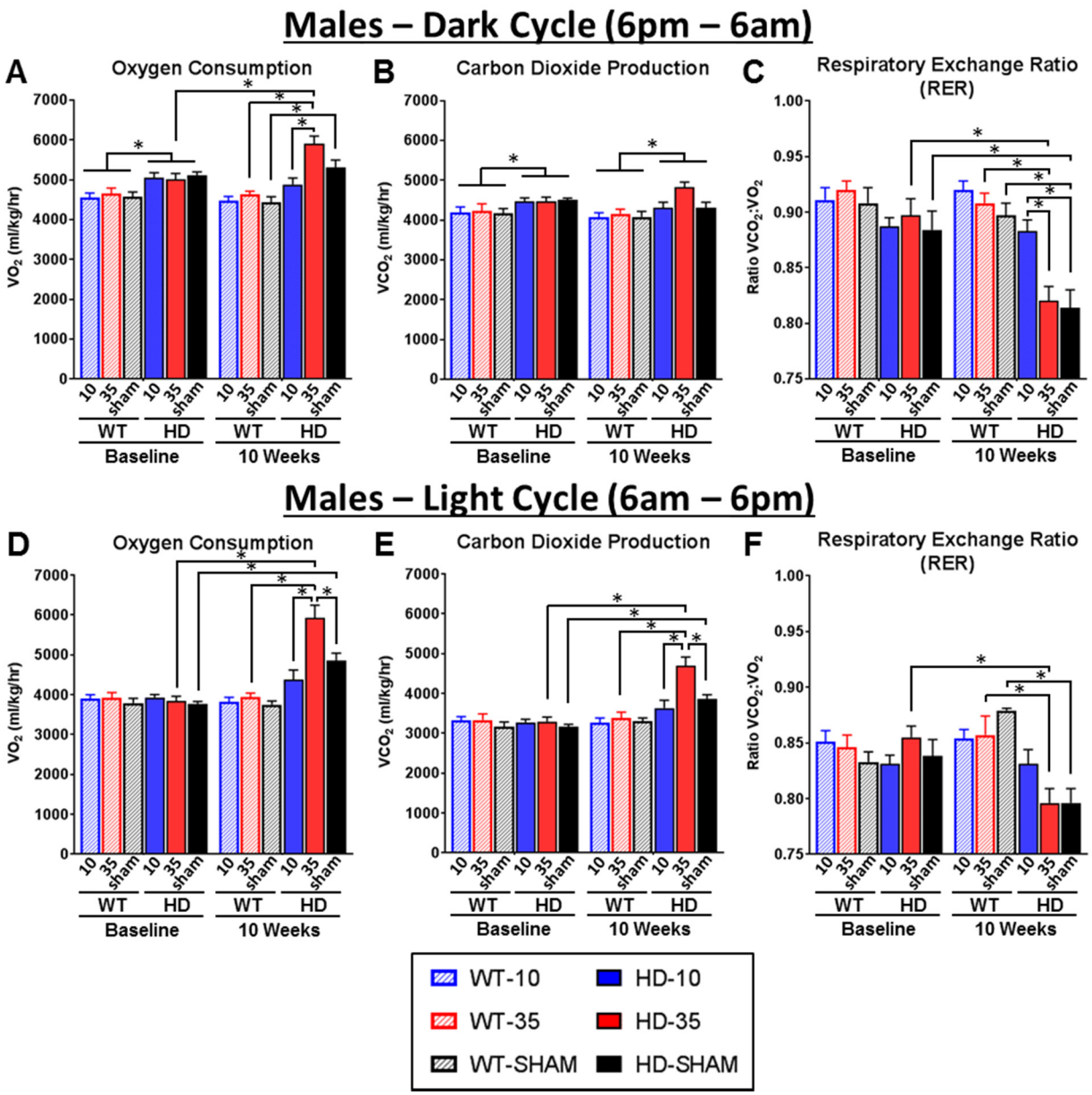

Figure 3.4 – Effect of glucocorticoid replacement on indirect calorimetry (CLAMS) in males. Mice were measured for indirect calorimetry at 5 weeks (baseline) and 10 weeks of age, following surgery and corticosterone treatment at 6 weeks of age. High dose corticosterone (35ug/ml) treatment resulted in a robust elevation in light (A) and dark cycle VO_2 (B), as well as light cycle VCO_2 (E) (Signficant Treatment*Genotype*Timepoint: p<.05 for all 3). Both dark cycle (C) and light cycle RER (F) was reduced in sham and high dose R6/2 mice following treatment at 10 weeks (Significant Treatment*Genotype*Timepoint, p<.05 for both), which was normalized by low dose (10ug/ml) corticosterone treatment. *Indicates significantly different Tukey's posthoc pairwise comparisons. Overall N=47 (n=7-9 per group). Values represent Mean ± SE. *Indicate significant differences as indicated by Tukey's posthoc comparisons.

increase in the utilization of fatty acids for energy relative to carbohydrates. Sham control male R6/2 mice showed a significant 9.3% reduction in dark cycle RER and a non-significant 5.6% reduction in light cycle RER, showing a similar preferential utilization of fatty acids. Additionally, male R6/2 mice on high dose treatment and sham controls were both significantly lower than wildtype controls on the same treatment for both dark cycle (7.4% decrease for high dose and 10.4% decrease for sham) and light cycle RER (5.8% decrease for high dose and 8.6% decrease for sham).

Although there were clear genotype effects in females, with transgenics showing increased VO_2 and VCO_2 and decreased RER, there was only a few small and inconsistent effects of treatment. This is reflected only in dark cycle VO_2 (Treatment*Genotype*Timepoint: $F_{2,38}$=4.64 $p<.05$) and dark cycle VCO_2 (Treatment*Genotype*Timepoint: $F_{2,39}$= 8.68 $p<.05$). Tukey's post-hoc comparisons indicate that for dark cycle VO_2, low dose and high dose corticosterone treated R6/2 females show a significant 17.7% and 26.5% elevation in dark cycle VO_2 at 10 weeks, respectively, relative to WT controls on the same treatment (**Fig. 3.3A**). Tukey's post-hoc comparisons indicate that R6/2 sham controls show a significant 4.8% reduction from baseline for dark cycle VCO_2 (**Fig. 3.3B**). R6/2 females on high dose corticosterone show 26.5% higher dark cycle VCO_2 levels relative to high dose WT at 10 weeks (**Fig 3.3B**). In spite of some of these small treatment induced differences in VO_2 and VCO_2 levels, the RER values for female transgenics were unaffected by treatment (**Fig. 3.3C and 3.3D**), suggesting similar patterns of micronutrient utilization for cellular metabolism.

Food and water intake

Food consumption and fluid intake (treatment or vehicle solution) was measured for all mice while in the CLAMS metabolic chambers. Measures reflect intake over a full 24 hour period,

after acclimation to the chambers. Although small reductions in food consumption in late stage R6/2 mice have been previously documented (van der Burg *et al.*, 2008), there was a much larger reduction in food intake detected here for both female (**Fig. 3.5A** - Genotype*Timepoint: $F_{1,39}$=34.85 p<.05) and male (**Fig. 3.5C** - Genotype*Timepoint: $F_{1,38}$=34.85 p<.0001) transgenic R6/2 mice at 10 weeks of age. There were no detectable differences in food intake between genotypes at baseline (Tukey's posthoc, *p*>.05 at 5 weeks), suggesting that late stage hypophagia may be a significant contributor to precipitous weight loss that occurs at end stages of disease in R6/2 mice.

While treatment did not significantly affect food consumption in females at either time point, there was a significant effect on male HD mice (Treatment*Genotype*Timepoint $F_{1,38}$=34.85 p<.05). Tukey's posthoc comparisons indicate that all groups of male HD mice showed a significant reduction in food intake relative to baseline (**Fig. 3.5C**): 27.5% for low dose (3.80 ± 0.17g baseline vs 2.76 ± 0.18g post), 58.5% for high dose (3.99 ± 0.48g vs 1.65 ± 0.37g), and 46.5% for sham controls (3.48 ± 0.29g vs 1.86 ± 0.28). However, Tukey's comparisons also indicate that the normalization of glucocorticoids led to slight attenuation of hypophagia in R6/2 males, as food intake levels at 10 weeks were not significantly different between male R6/2 and WT mice on low dose corticosterone, although sham and high dose treated R6/2 males were significantly different from WT controls.

As expected, there was a significant increase in fluid intake in both female (**Fig. 3.5B** - Genotype*Timepoint: $F_{1,39}$=8.38 p<.01) and male (**Fig. 3.5D** - Genotype*Timepoint: $F_{1,41}$=17.53 p<.001) R6/2 HD mice at the 10 week time point – a phenotype that had been previously characterized (Wood *et al.*, 2008). Treatment did not affect intake levels in any way (*p*>.05 for all), with all groups of HD mice showing a similar increase in consumption.

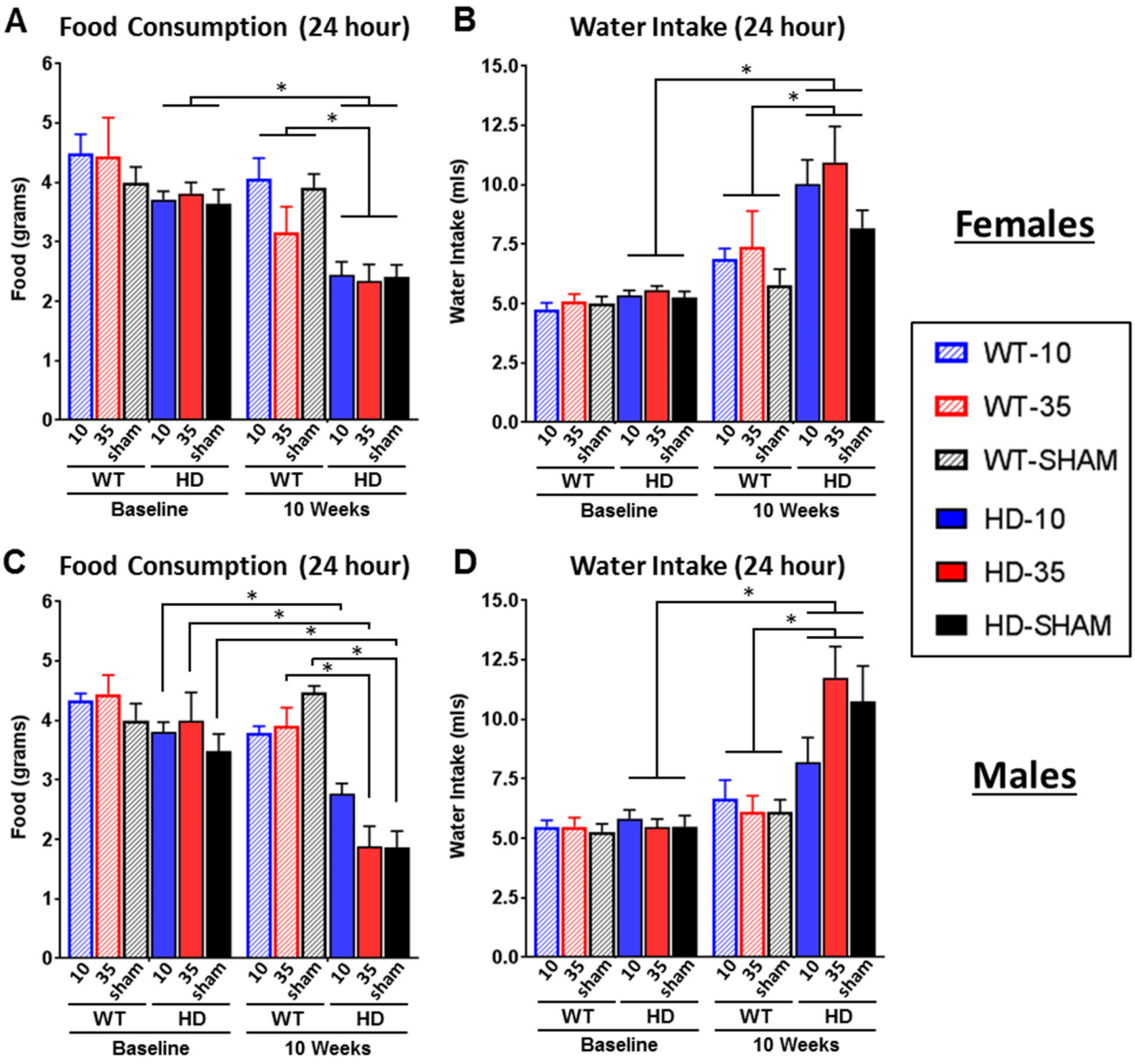

Figure 3.5 – Effect of glucocorticoid replacement on food and water intake. 24-hour food and water intake were measured in CLAMS metabolic chambers at 5 (baseline) and at 10 weeks of age, after adrenalectomy and corticosterone treatment (or sham surgery and vehicle) starting at 6 weeks of age. Female (A) and male (C) R6/2 mice showed a significant reduction in food intake at 10 weeks (Genotype*Timepoint: p<.05 for both males and females), although intake levels were not different at baseline (Tukey's p>.05). Although food intake was reduced for males on all treatments, low dose CORT (10ug/ml) attenuated the severity of hypophagia in R6/2 males. Female and male R6/2 mice also showed a significant increase in fluid intake (water at baseline, corticosterone or vehicle at 10 weeks) at 10 weeks (Genotype*Timepoint: p<.05 for both males and females). There was not an effect of treatment on fluid intake (Treatment and treatment*genotype: *p*>05 for both sexes). Overall N=44 (n= 7-8 per group) for females and N=47 for males (n=7-9 per group). Values represent Mean ± SE. *Indicate significant differences as indicated by Tukey's posthoc comparisons.

Organ weights

Both brain and skeletal muscle are known to be particularly sensitive to chronic alterations in glucocorticoid levels, with chronically elevated glucocorticoids associated with Cushing's like reductions in brain (Bourdeau *et al.*, 2002) and muscle mass (Braun *et al.*, 2013). Thus, to assess whether glucocorticoids contribute to overall reductions in brain and skeletal muscle mass that is characteristic of R6/2 HD mice, wet weight of both tissues were assessed during necropsy at 11 weeks of age. Here, I tested the hypotheses that normalizing glucocorticoid levels (HD mice on low/WT-dose) in R6/2 HD mice would reduce the loss of gastrocnemius skeletal muscle mass and brain mass.

Glucocorticoid levels significantly affected gastrocnemius mass (**Fig. 3.6**), although it did so differently in wild-type and transgenic R6/2 HD mice (Males - Treatment*Genoptype: $F_{2,54}$=3.83, p<.05, Females - Treatment*Genoptype: $F_{2,46}$=7.25, p<.01). As hypothesized, normalization of glucocorticoid levels significantly increased muscle mass in transgenic R6/2 mice, as indicated by Tukey's posthoc comparisons. In female R6/2 mice (**Fig. 3.6A**) low dose corticosterone treatment led to a significant 27.0% increase in muscle mass (72.2 ± 1.6mg) relative to those on high dose treatment (55.9 ± 2.4mg), and a non-significant 16.6% increase relative to sham controls (62.0 ± 2.5mg). In males, there was a significant 28.2% increase in gastrocnemius muscle mass in those on low dose corticosterone (76.7 ± 2.3mg) relative to those on high dose treatment (59.8 ± 3.5mg). Sham control R6/2 mice show an intermediate mass (66.4mg for males, 62.0mg for females), which were not significantly different from either treatment group. In contrast, high dose glucocorticoids resulted in a Cushing's like reduction in gastrocnemius muscle mass in both female (**Fig. 3.6A**) and male wild-type mice (**Fig. 3.6C**), with those on high dose corticosterone showing significantly reduced mass relative to those on low dose corticosterone and sham controls (Tukey's post-hoc comparisons). For males, this represents a 12.5% decrease

in muscle mass for mice on high dose treatment (107.9 ± 4.3mg) relative to those on low dose treatment (123.3 ± 2.6mg) and a 16.7% decrease relative to sham controls (129.6 ± 3.4mg). For females, this represents a 27.0% decrease for mice on high dose treatment (81.5 ± 2.9mg) relative to those on low dose treatment (111.3 ± 2.8mg) and a 23.1% decrease relative to sham controls (107.2 ± 3.0mg).

As with muscle mass, treatment affected brain mass in female WT and R6/2 mice differently (Treatment*Genoptype: $F_{2,46}$=4.65, p<.05). As hypothesized, normalization of glucocorticoids improved brain mass in R6/2 female mice (**Fig. 3.6B**), with those on low dose corticosterone showing a small but significant 7.0% increase in brain mass (412.4 ± 3.9mg), relative to those on high dose corticosterone (385.6 ± 5.7mg). Tukey's post-hoc comparisons also indicated that there was a Cushing's like reduction in brain mass in wild-type female mice on high dose corticosterone (438.9 ± 9.6mg), which were 9.7% smaller than those on low-dose corticosterone (485.9 ± 3.1mg) and 8.8% lower than sham controls (481.3 ± 5.6mg). Surprisingly, there was not a similar interaction of genotype and treatment in male R6/2 mice (**Fig. 3.6D**, Treatment*Genoptype: $F_{2,54}$=0.93, p=.40), although the transgenics did show a significantly reduced brain mass relative to wild-type mice (Genotype: $F_{1,54}$=3.32, p<.01), and a Cushing's like reduction in brain mass for both R6/2 and wild-type males on high dose corticosterone (Treatment: $F_{2,54}$=4.65, p<.05).

Although glucocorticoid normalization did not fully prevent a loss in brain and muscle mass to wild-type levels, these data provide preliminary evidence that elevated glucocorticoids exacerbate the phenotype, and that normalization of glucocorticoids could potentially attenuate the reduction in skeletal muscle and brain mass that is a characteristic symptom of the disease.

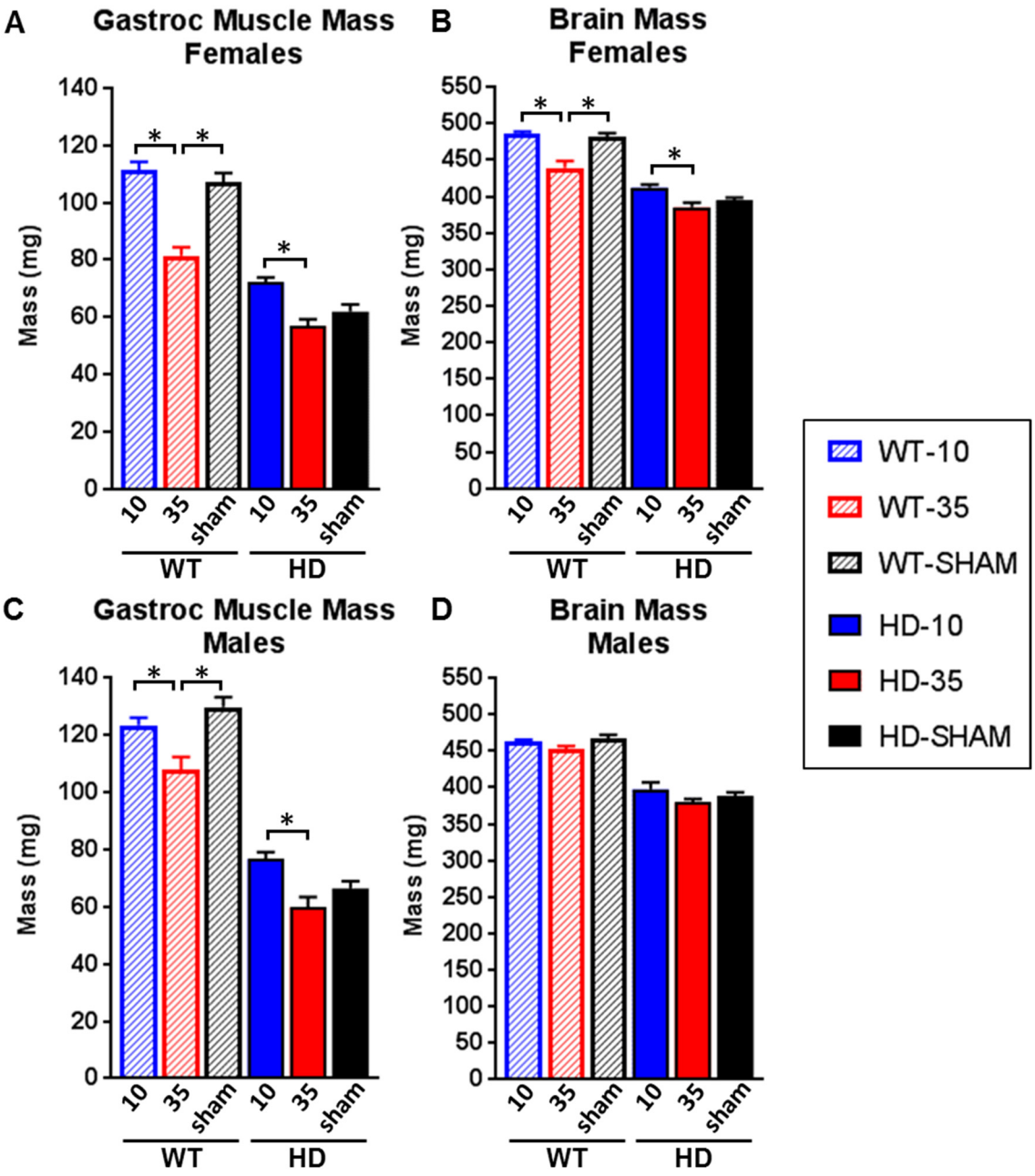

Figure 3.6 – Effect of glucocorticoid replacement on brain and muscle mass. High dose glucocorticoid treatment (35-ug/ml) resulted in a significant Cushing's like reduction in gastrocnemius muscle mass in WT females (A) and males (C), and in brains for WT females (B). Normalizing glucocorticoid levels in R6/2 mice resulted in a significant increase in gastrocnemius mass in females (A) and males (C), and brain mass in females (B). Significant Genotype*Treatment effect for female ($p<.01$) and male gastrocnemius muscle ($p<.05$), and female brain ($p<.05$) but not male brain mass ($p=.40$). Overall N=52 for females (n= 7-11 per group) and N=60 for males (n=9-14 per group). Values represent Mean ± SE. *Indicate significant differences as indicated by Tukey's posthoc comparisons.

Regional Brain volume

One hallmark neuropathological symptom of HD, present in both human patients and in the R6/2 mouse model, is regional brain atrophy. Cushing's patients also show whole brain and regional atrophy in many of the same areas, including the hippocampus and the striatum (Andela *et al.*, 2013; Bourdeau *et al.*, 2002; Lupien *et al.*, 1998). While mutant huntingtin is likely the main driver of regional reductions in brain volume for HD, it is possible that chronically elevated glucocorticoids are perhaps exacerbating this mHTT driven phenotype. Thus, I tested the hypothesis that normalizing glucocorticoid levels would attenuate reductions in regional brain volume that are characteristic of R6/2 mice.

As expected, both male and female R6/2 mice show reduced regional volume across all regions assessed ($p<.001$ for all) relative to WT mice (**Fig. 3.7**). Although there was no effect of treatment on striatal or hippocampal volume here ($p>.05$ for treatment and treatment*genotype for both regions, for males and females), there was an effect of treatment ($F_{2,18}=8.07$, $p<.005$) on cortical volume in females, with those on high dose corticosterone showing significantly reduced brain volume relative to those on low dose treatment, as assessed with Tukey's post-hoc comparisons. However, the effect on both genotypes were similar (No genotype*treatment interaction: $F_{2,18}=1.58$, $p=.23$) and thus elevated corticosterone induces a reduction in cortical volume regardless of genotype. As there was no difference between HD sham and low dose mice, normalizing glucocorticoids does not improve this phenotype beyond normal reduction in regional volume. For males, there was a trend for the effect of treatment ($F_{2,18}=2.97$, $p=.077$), likely reflecting a non-significant reduction for wild-type and transgenic mice on high dose corticosterone treatment. As with females, there was not a differential effect of treatment on cortical volume between genotypes for males (Treatment*genotype: $F_{2,18}=0.20$, $p=.82$).

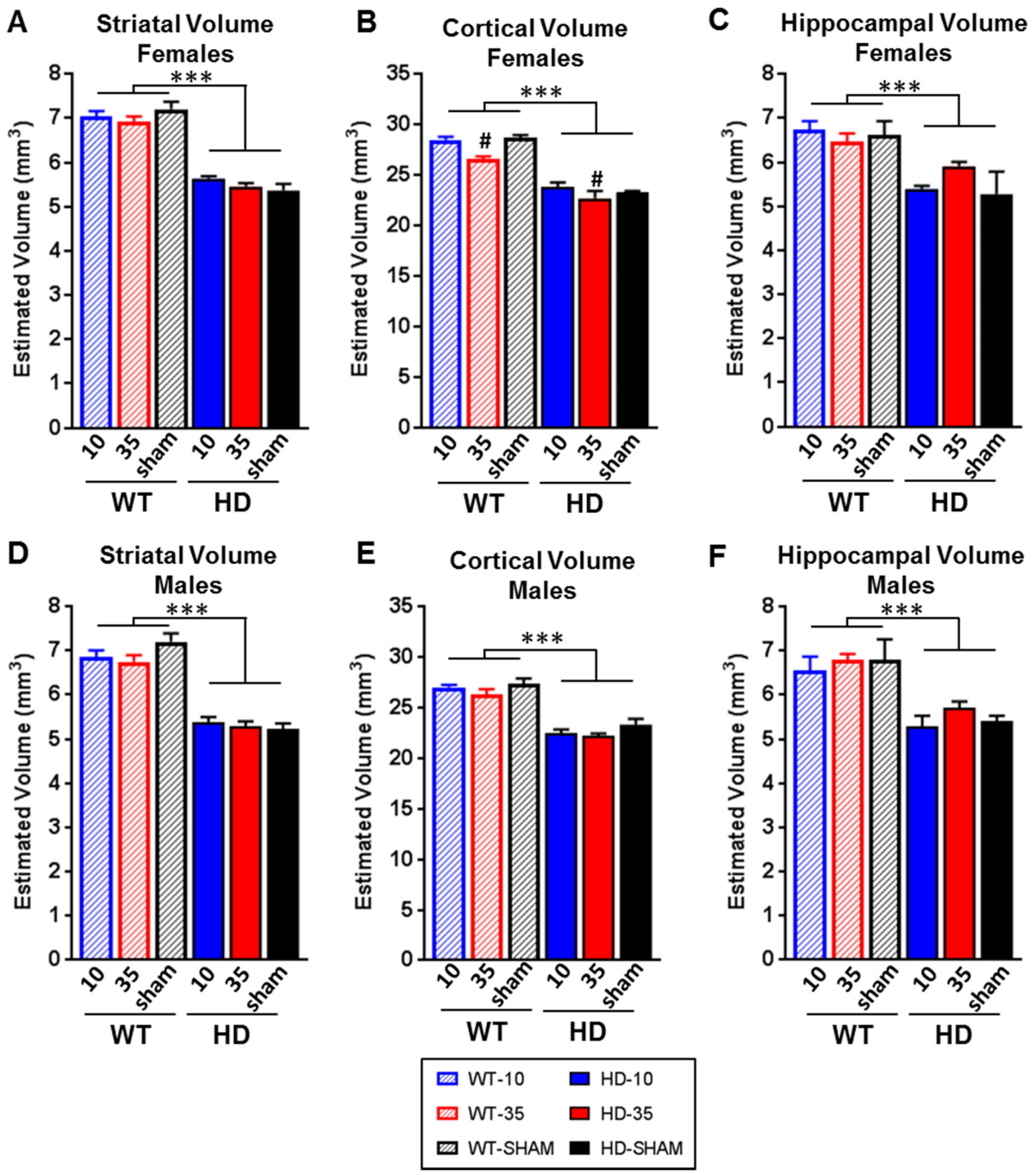

Figure 3.7 – Effect of glucocorticoid replacement on regional brain volume. Regional brain volume was estimated in the striatum (A, D), cortex (B,E), and hippocampus (C,F) using the Cavalieri stereological method on NeuN stained serial sections for wild-type and transgenic R6/2 mice treated with either high dose (35ug/ml) or low dose (10ug/ml) corticosterone, and sham surgery controls. Females are shown on the top panel (A-C), and males on the bottom (D-F). There was a significant*genoptype fixed effect in all regions (****p*<.001), with transgenic mice showing reduced regional brain volume relative to wild-types. There was also a treatment effect in the cortex for females (B, *p*<.01), with those on high dose replacement showing reduced cortical volume relative to those on low dose treatment and sham controls (# *p*<.05 Tukey's posthoc). Overall N=24 for each sex, n=4 per group. Values represent Mean ± SE.

Neurogenesis

Adult neurogenesis in the dentate gyrus is potently modulated by glucocorticoids, with high levels associated with reduced neurogenesis and low levels associated with increased neurogenesis (Wong & Herbert, 2004). R6/2 mice, which have elevations on glucocorticoids, also show reduced dentate gyrus neurogenesis (Gil *et al.*, 2005). Experimentally elevated levels of glucocorticoids further reduce neurogenesis in the related transgenic R6/1 HD mouse (Mo, Pang, *et al.*, 2014). Thus, in another experiment, I tested the hypothesis that normalizing glucocorticoid levels will improve neurogenesis in R6/2 mice, reflected by an increased number of proliferating ki67+ cells, a marker for neurogenesis, in the dentate gyrus. Thus, serial coronal tissue sections were stained for ki67 (**Fig. 3.8A-L**) and total counts of ki67+ cells in the hippocampus of each section were quantified and analyzed statistically.

As expected, R6/2 mice show a significant reduction in ki67+ cells in the dentate relative to WT mice (**Fig. 3.8M** and **Fig. 3.8N**, Genotype fixed effect, p<.0001 for males and females), replicating the phenotype shown previously (Gil *et al.*, 2005; Mo, Pang, *et al.*, 2014). Glucocorticoid treatment significantly affected the number of ki67+ cells in females (Treatment: $F_{2,18}$=5.62, p<.05), with those on high dose corticosterone showing significantly fewer ki67+ cells than those on low dose, regardless of genotype (Tukey's post-hoc). For male mice, although there was a clear effect of genotype on the number of ki67+ cells, there was no effect of treatment on either genotype (Treatment: $F_{2,18}$=0.05 p>.05, Treatment*Genotype: $F_{2,18}$=0.48 p>.05).

Although there wasn't a significant treatment*genotype interaction for females (Treatment*Genotype: $F_{2,18}$=2.05, p=.16), there appears to be a divergent pattern in how corticosterone treatment affected neurogenesis between genotypes. As the sample size is quite small here (n=4/group), this lack of significance may be related to insufficient power. In R6/2 females, mice on low dose corticosterone (20.3 ± 1.9 ki67+ cells/section) show a 64.7% increase

in the number of ki67+ cells relative to those on high dose (12.7 ± 1.9) and a 73.8% increase relative to sham controls (12.0 ± 1.2). The difference in the mean number of ki67+ cells in female R6/2 mice on high dose and sham controls is minimal, a differences of means of only 0.7 cells/section (a 5.9% increase for those on high dose corticosterone). This suggests that the difference in ki67+ cells between low dose and high dose reflects an increase in neurogenesis induced by the normalization of glucocorticoids. For wild-type females, those on high dose corticosterone (32.4 ± 1.6 ki67+ cells/section) showed a 22.7% reduction in ki67+ cells relative to those on low dose corticosterone (41.1 ± 3.9) and a 20.6% reduction relative to sham controls (40.8 ± 3.2). Average number of ki67+ cells were quite similar between the low dose group and sham controls in WT females, a difference of means of only 0.3 cells/section (a 0.7% increase in the low dose group relative to sham controls), suggesting that high dose corticosterone was sufficient to induce a Cushing's like reduction in neurogenesis in WT females.

As with brain mass taken at necropsy, females were uniquely sensitive to variations in glucocorticoid levels, while males were not affected here. While the genotype*treatment interaction fixed effect wasn't statistically significant, it appears as though high levels of glucocorticoids are resulting in a Cushing's like reduction in neurogenesis in WT females, and that normalization of glucocorticoids results in an increase in neurogenesis in HD females.

Em48+ inclusion bodies

Since there is evidence that acute glucocorticoid receptor signaling has a potent effect on whether mutant huntingtin exists in aggregate or soluble form in vitro (Diamond *et al.*, 2000), and worsens inclusion formation in other neurodegenerative disorders (Baglietto-Vargas *et al.*, 2013; Green *et al.*, 2006), I assessed the effect of different levels of glucocorticoids on inclusion burden in R6/2 mice in vivo. Thus, I tested the hypothesis that normalized glucocorticoid levels result in

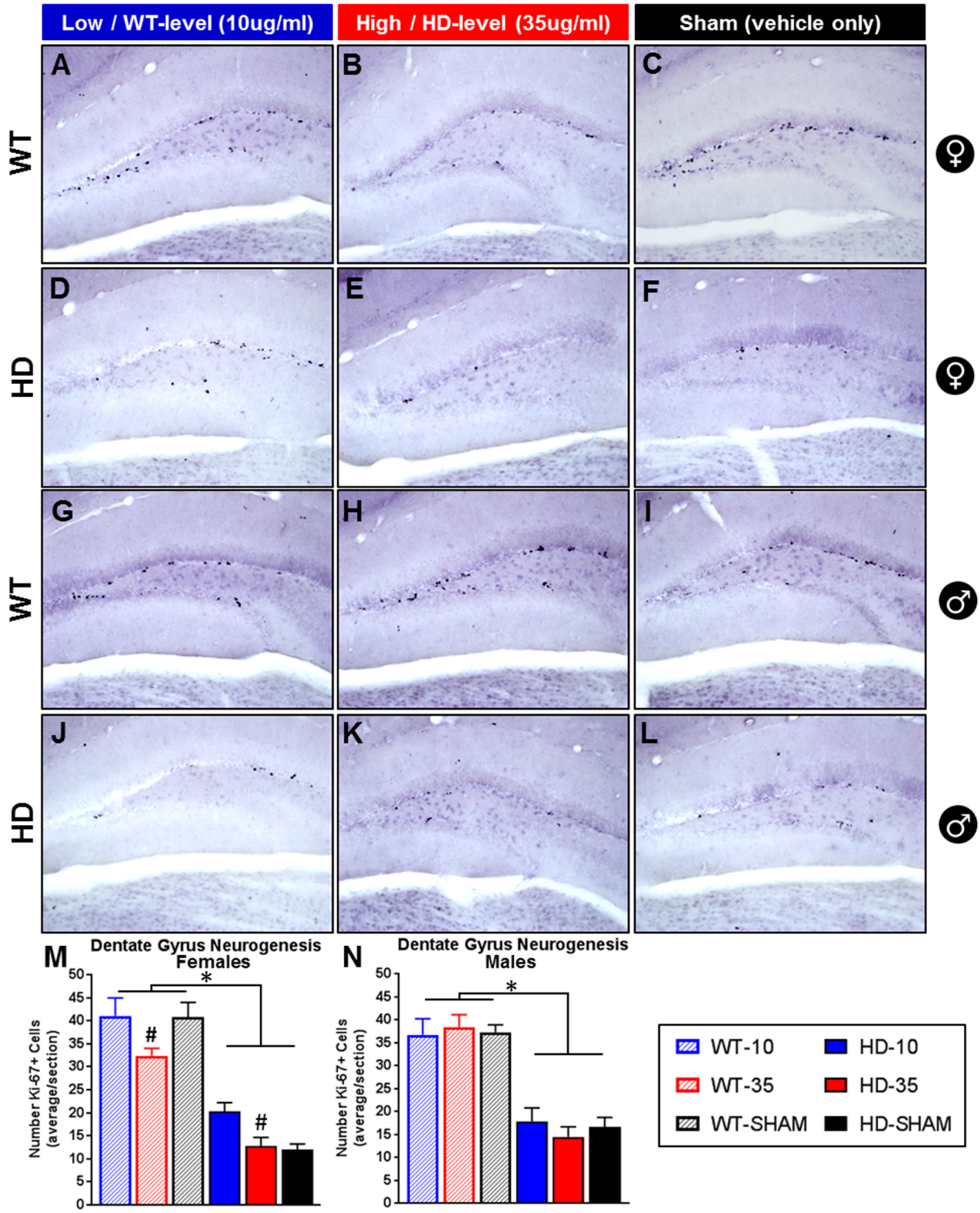

Figure 3.8 – Effect of glucocorticoid replacement on neurogenesis in the dentate gyrus. Representative images of Ki-67+ mitotic cells, a marker for neurogenesis, in the dentate gyrus of wild-type (females A-C, males G-I) and transgenic R6/2 mice (females D-F, males J-L). R6/2 mice show fewer ki67+ cells than WT (M,N - $p<.05$) and treatment with low dose CORT (10ug/ml) increases ki67+ cells in females relative to those on high dose (35ug/ml) (M, Treatment: $p<.05$, Tukey's posthoc 10 vs 35 #$p<.05$). Treatment had no effect on males ($p>.05$). N=24 for each sex, n=4 per group. Values represent Mean ± SE.

reduced inclusion burden, as measured by reduced inclusion number and/or size, in vivo. Sections from male and female R6/2 mice were stained with DAB immunohistochemistry with the em48 antibody, which is a specific marker for aggregated mutant huntingtin protein, and inclusion number and size was quantified systematically in ImageJ in a total of six brain regions. The striatum and cortex (motor and cingulate) were assessed as they are most severely affected in HD. The hippocampus (dentate gyrus and CA1 region) were also assessed, as they are both have high expression of glucocorticoid receptors and might be particularly affected by variations in glucocorticoid levels. The lateral hypothalamus was also assessed, to provide a preliminary analysis of whether the effects of glucocorticoids on metabolism and body weight could be explained, in part, by decreased neuropathology in this key metabolic regulatory region.

Again, as with neurogenesis and brain weight, there was a sexually dimorphic response to glucocorticoid treatment on em48+ inclusions in R6/2 mice. In females, normalization of glucocorticoid levels reduced em48+ inclusion burden resulting in a significant reduction in the number of inclusions in the striatum (**Fig. 3.9D**, Treatment: $F_{2,9}$=4.68, p<.05) and the dentate gyrus (**Fig. 3.9X**, Treatment: $F_{2,9}$=6.25, p<.05), and a significant reduction in inclusion size in motor cortex (**Fig. 3.9J**, Treatment: $F_{2,9}$=14.34, p<.01) and cingulate cortex (**Fig. 3.9O**, Treatment: $F_{2,9}$=5.68, p<.05). For females, there was no effect of treatment in either the CA1 region of the hippocampus, or in the lateral hypothalamus (p>.05 for both). Unexpectedly, there was no effect of treatment on inclusion burden (number or size) in male R6/2 mice in any region examined (p>.05 for all).

Tukey's posthoc tests indicated that in the striatum (**Fig. 3.9A-E**), normalized glucocorticoid levels was associated with a large and significant 54% reduction in inclusion number (5.5 ± 1.2) in female R6/2 mice relative to those on high dose replacement (12.0 ± 0.9), and a non-significant 50% reduction relative to sham controls (11.0 ± 2.3). In the dentate gyrus (**Fig. 3.9U-Y**), normalized glucocorticoid levels led to a large and significant 70% reduction in

inclusion number (11.0 ± 2.9) relative to those on high-dose treatment (36.8 ± 5.9), and a significant 72% reduction relative to sham controls (39.3 ± 8.6). In the motor cortex (**Fig. 3.9F-J**), females on low dose corticosterone showed a significant 24% reduction in inclusion size (3.00μm^2 ± 0.09) relative to those on high dose corticosterone (3.96μm^2 ± 0.21), and a significant 27% reduction relative to sham controls (4.11μm^2 ± 0.15). In the cingulate cortex (Fig 9K-O), females on low dose corticosterone showed a significant 21% reduction in inclusion size (2.28μm^2 ± 0.14) relative to high dose corticosterone (2.90μm^2 ± 0.14), and a non-significant 18% reduction relative to sham controls (2.79μm^2 ± 0.13).

Taken together, these data show that normalizing glucocorticoids has the ability to reduce inclusion burden in R6/2 mice, although the effect of treatment is strongly affected by sex (females were responsive to treatment while males were not) and varies dramatically by brain region.

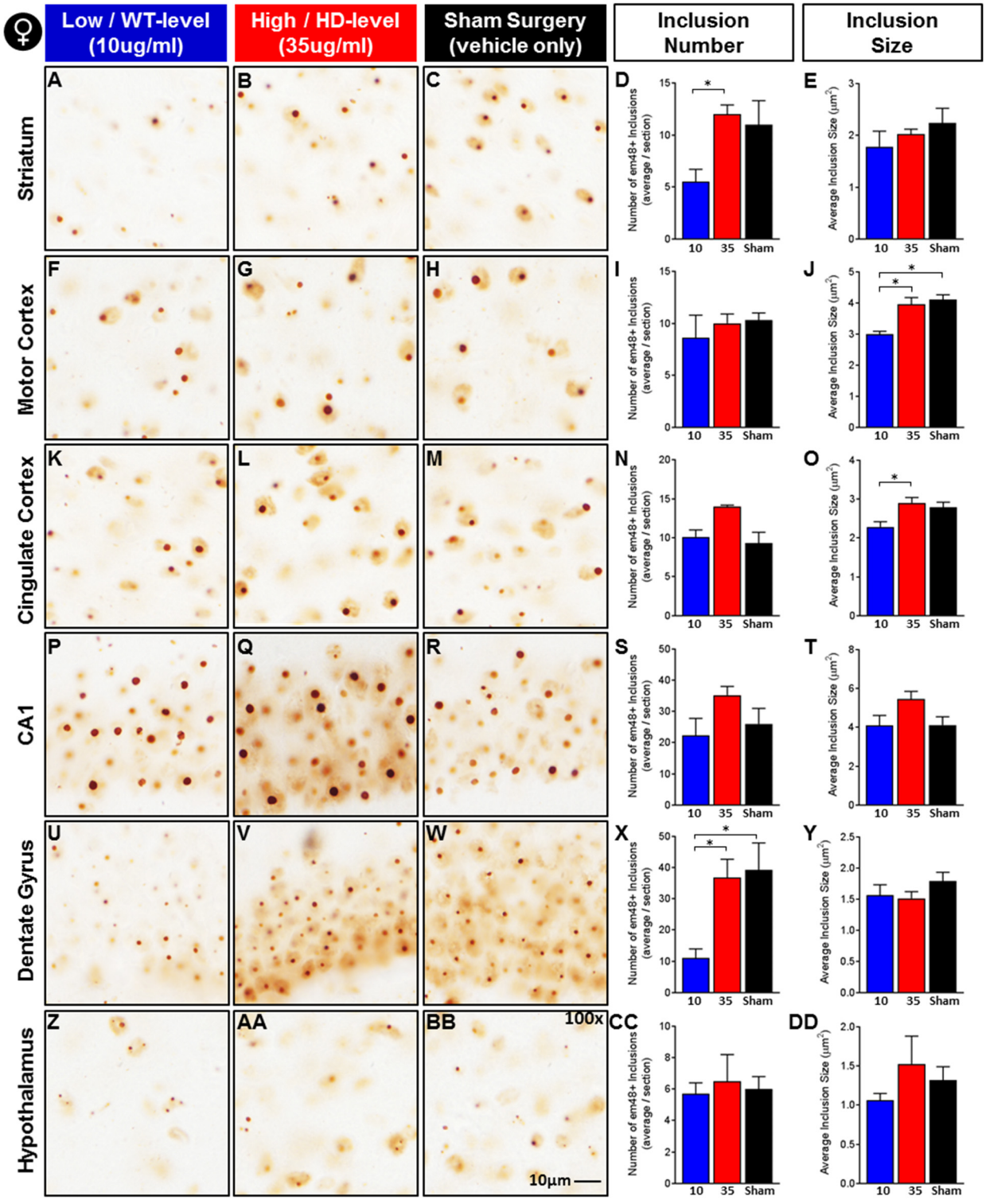

Figure 3.9 – Effect of glucocorticoid replacement on em48+ inclusion bodies in female R6/2 mice. Representative images from Striatum (A-C), Motor Cortex (F-H), Cingulate Cortex (K-M), Hippocampus (CA1: P-R and Dentate Gyrus: U-W), and Lateral Hypothalamus (Z-BB). Females on low dose CORT (10ug/ml) showed significantly fewer em48+ inclusions in the striatum (D) and dentate gyrus (X), and reduced inclusion size in the motor (J) and cingulate cortices (O) (Treatment: $p<.05$). Overall N=12, n=4 per group. Scale bar reflects 10µm. Values represent Mean ± SE. *Indicate significant differences as indicated by Tukey's posthoc comparisons.

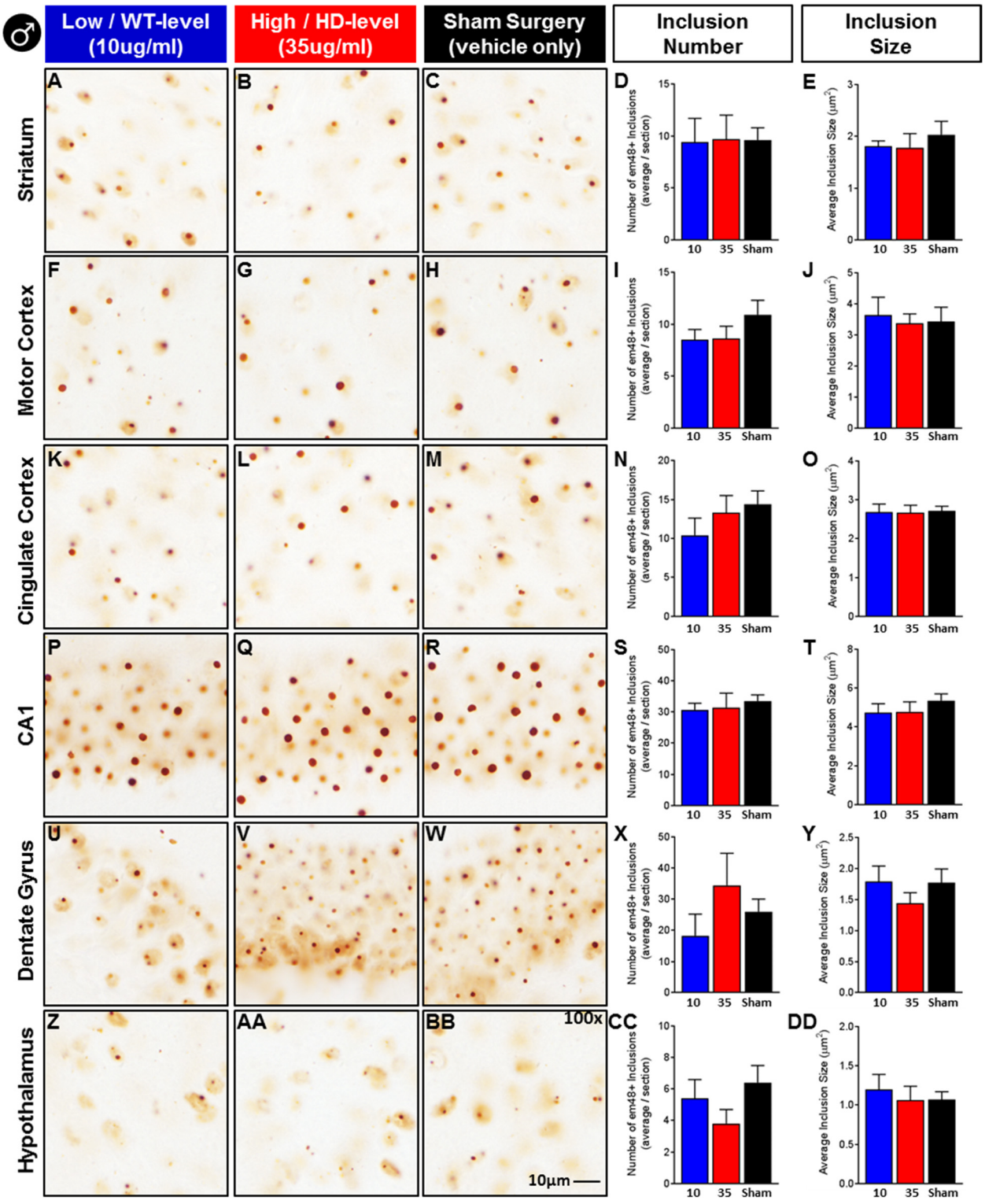

Figure 3.10 – Effect of glucocorticoid replacement on em48+ inclusion bodies in male R6/2 mice. Representative images from Striatum (A-C), Motor Cortex (F-H), Cingulate Cortex (K-M), Hippocampus (CA1: P-R and Dentate Gyrus: U-W), and Lateral Hypothalamus (Z-BB). For males, treatment did not significantly affect inclusion burden (number or size) in any region assessed (Treatment: $p>.05$ for all). Overall N=12, n=4 per group. Scale bar reflects 10µm. Values represent Mean ± SE. *Indicate significant differences as indicated by Tukey's posthoc comparisons.

Table 3.1 – Statistical Analyses, Effect of Genotype on Indirect Calorimetry Measures. Statistical analysis of genotype fixed-effects are presented here in this table (collapsed across treatment and timepoint) – to illustrate the robust genotype associated alterations in R6/2 mice of both sexes. % Change specifies the degree to which these measures are altered between the two genotypes.

Measure	Sex	Time	Figure	Fixed Effect	F-Value	P-value	WT mean	HD mean	% Change
VO_2	Female	night	4A	Genotype	38.94	<.0001	5062	5833	15.2%
VCO_2	Female	night	4B	Genotype	22.47	<.0001	4567	5054	10.7%
RER	Female	night	4C	Genotype	15.21	0.0004	0.901	0.868	-3.7%
VO_2	Female	day	4D	Genotype	20.38	<.0001	4310	4759	10.4%
VCO_2	Female	day	4E	Genotype	8.08	0.0072	3700	3927	6.2%
RER	Female	day	4F	Genotype	11.6	0.0016	0.855	0.826	-3.4%
VO_2	Male	night	5A	Genotype	43.92	<.0001	4545	5209	14.6%
VCO_2	Male	night	5B	Genotype	16.47	0.0002	4148	4479	8.0%
RER	Male	night	5C	Genotype	31.88	<.0001	0.911	0.864	-5.1%
VO_2	Male	day	5D	Genotype	39.37	<.0001	3845	4451	15.8%
VCO_2	Male	day	5E	Genotype	21.1	<.0001	3292	3652	10.9%
RER	Male	day	5F	Genotype	15.21	0.0003	0.854	0.824	-3.5%

Table 3.2 - Summary - Effect of Glucocorticoid Normalization on HD Symptomology

			Effect of WT-level CORT replacement in	
Measure	**Figure**	**R6/2 phenotype**	**Male R6/2**	**Female R6/2**
Bodyweight	3.2	weight loss	small increase	small increase
Calorimetry				
VO2	3.3 / 3.4	increased	decreased	none
VCO2	3.3 / 3.4	increased	decreased	none
RER	3.3 / 3.4	decreased	increased/rescued	none
Muscle Mass	3.6	decreased	increased	increased
Brain Mass	3.6	decreased	none	increased
Regional Brain Volume				
Striatum	3.7	decreased	none	none
Cortex	3.7	decreased	none	none
Hippocampus	3.7	decreased	none	none
Neurogenesis (ki67)	3.8	decreased	none	increased
Inclusion Burden				
Striatum	3.9/3.10	present	none	reduced number
Motor Cortex	3.9/3.10	present	none	reduced size
Cingulate Cortex	3.9/3.10	present	none	reduced size
CA1 - Hippocampus	3.9/3.10	present	none	none
DG - Hippocampus	3.9/3.10	present	none	reduced number
Hypothalamus	3.9/3.10	present	none	none

3.4 - Discussion

It has long been speculated that neuroendocrine changes may contribute the metabolic phenotype shown by HD patients – in particular, that chronically elevated glucocorticoids contribute to increased metabolism, weight loss, and muscle wasting (Aziz *et al.*, 2009; Bjorkqvist *et al.*, 2006a; Goodman *et al.*, 2008; Petersen & Bjorkqvist, 2006; Saleh *et al.*, 2009). There is also indirect evidence that suggests chronically elevated glucocorticoids could possibly exacerbate HD neuropathology, including regional changes in brain volume (Bourdeau *et al.*, 2002), reductions in neurogenesis (Brummelte & Galea, 2010; Cameron & Gould, 1994; McEwen, 1999), as well as mutant huntingtin protein aggregation (Diamond *et al.*, 2000; Labbadia *et al.*, 2011; Maheshwari *et al.*, 2014). In previous experiments (Chapter 2), I demonstrated that significant elevations in corticosterone do indeed impact the HD metabolic phenotype, by exacerbating weight-loss in the transgenic R6/2 HD mouse model. Here, in Chapter 3, I extended these findings and demonstrated that normalizing corticosterone to WT levels in R6/2 mice attenuates weight loss, muscle wasting, reductions in brain mass, inclusion body formation, and deficits in neurogenesis (Outlined in **Table 3.2**). Although treatment did not fully rescue any of these metabolic or neuropathological symptoms, these data provide proof of principle that normalizing glucocorticoid levels or blocking the glucocorticoid receptor could possibly attenuate symptomology in clinical HD cases. My data from Chapter 3 also further demonstrate that when glucocorticoids become elevated in HD mice, and likely HD patients, it further exacerbates the disease phenotype.

Progressive weight loss is a well-documented symptom of HD (Aziz *et al.*, 2008; Trejo *et al.*, 2004), which occurs simultaneously with a progressive increase in glucocorticoid levels (Bjorkqvist *et al.*, 2006a; Saleh *et al.*, 2009) and a chronic elevation of metabolic rate (Gaba *et al.*, 2005; Pratley *et al.*, 2000). All of these co-occurring symptoms are recapitulated in the R6/2 mouse model (Bjorkqvist *et al.*, 2006a; She *et al.*, 2011; van der Burg *et al.*, 2008), and the

relationship between glucocorticoids and specific metabolic abnormalities in HD are poorly characterized. In this study, the normalization of glucocorticoids resulted in a delay in weight-loss in both males and female R6/2 mice, as indicated by within treatment comparisons. This compliments my previous data whereby experimentally increased glucocorticoid levels were associated with precipitous weight loss (Dufour & McBride, 2016), and illustrates that while glucocorticoids are not solely responsible for the weight loss HD phenotype, they do contribute.

It is postulated that weight loss in HD is driven by a chronic elevation in whole organism metabolic rate (Gaba *et al.*, 2005; Pratley *et al.*, 2000), leading to a state of negative energy balance (Goodman *et al.*, 2008). R6/2 mice are in a state of elevated metabolism, as indicated by indirect calorimetry, with mice showing increased oxygen consumption (VO_2) (She *et al.*, 2011; van der Burg *et al.*, 2008). This increase in metabolic rate precedes the onset of weight loss, which is progressive and severe in R6/2 mice (She *et al.*, 2011; van der Burg *et al.*, 2008). I detected this elevation in VO_2 in both male and female R6/2 mice here, as early as 5 weeks of age (during the dark cycle). These data demonstrate, for the first time, that R6/2 mice also have an elevation in dark cycle VCO_2 production, which is present early on at 5 weeks of age. These patterns persist and worsen with time, with R6/2 mice showing even more significant elevations in VO_2 and VCO_2 at 10 weeks of age. While both were elevated in R6/2 mice here, VO_2 is more elevated than VCO_2, leading to a reduction in the respiratory exchange ratio (RER, ratio VCO_2:VO_2). RER is an indirect indicator of nutrient utilization, with higher values (near 1.00) reflecting preferential utilization of carbohydrates for cellular metabolism and lower values (near 0.70) reflecting preferential utilization of lipids. These calorimetry values are derived from biochemical expectations for the full metabolism of glucose (6 mol O_2 utilized and 6 mol CO_2 produced per glucose molecule, ratio = 1.0) and for fatty acids (78 mol O_2 utilized and 55 mol CO_2 produced per F.A. molecule, ratio = 0.70) (Frayn, 1983). They are 'indirect' in that this measure utilizes whole-animal oxygen intake

and carbon dioxide output as a proxy for the amount of overall O_2 reactants and CO_2 products utilized in the biochemical metabolism of different nutrients on a molecular level. Thus, this reduction in RER in R6/2 mice likely reflects a shift to increased utilization of fatty acids as a metabolic fuel source, rather than carbohydrates.

Treatment had a strong and consistent impact on indirect calorimetry measures in male R6/2 mice. Here, normalization of glucocorticoids (low-dose WT-level replacement) leads to a normalized metabolic rate, as indicated by improved measures of VO_2, VCO_2, and RER. In fact, R6/2 males on wild-type level corticosterone replacement showed a full rescue in their dark cycle RER values to wild-type levels (and a partial rescue for light cycle RER), demonstrating that the normalization of glucocorticoids has the ability to improve whole organism metabolic rate and nutrient utilization. Surprisingly, high dose corticosterone did not exacerbate metabolic rate in R6/2 females, and the normalization of glucocorticoids also failed to normalize any metabolic readout (VO_2, VCO_2, or RER) to WT levels. This was surprising, especially given that normalized glucocorticoid levels resulted in an attenuation in the weight loss phenotype in female R6/2 mice. This suggests that there might be another mechanism that is driving the weight loss improvement seen here, other than simply a normalization in metabolic rate. Wildtype mice of both sexes were also unresponsive to different glucocorticoid levels, with respect to indirect calorimetry. This is an intriguing finding, which illustrates that R6/2 male mice are uniquely sensitive to alterations in glucocorticoids, at least at the doses and time-points investigated here.

While chronically elevated glucocorticoids are known to be the key mediator of muscle wasting in a variety of conditions, including Cushing's syndrome and chemotherapy associated cachexia (Braun *et al.*, 2013; Grossberg *et al.*, 2010), it was previously unclear if this elevation in HD contributes to the muscle wasting phenotype. The data here show that it does contribute: the normalization of glucocorticoids in R6/2 mice significantly reduced muscle wasting in both sexes.

However, while there was significant improvement, muscle mass was only partially rescued in these mice, suggesting that chronically elevated glucocorticoids are only partial contributors to the HD cachexia phenotype. The lack of sexual dimorphism here is interesting, especially given the robust sexual dimorphism in the calorimetry measures. This emphasizes that muscle wasting in HD may not be simply due to chronic elevations in metabolic rate (e.g. leading to muscle breakdown for nutrient utilization), as it still occurs in male R6/2 mice when there calorimetry measures are fully normalized. Conversely, there was significant attenuation of muscle wasting in female R6/2 mice without any treatment induced improvement in calorimetry measures. Instead of elevated metabolism being the driver of cachexia, an alternative possibility is that mutant huntingtin toxicity within skeletal muscle itself could be a main driver of cachexia in HD, which is further exacerbated by chronically elevated glucocorticoid levels. Indeed, mutant huntingtin is expressed in skeletal muscle, which shows significant pathology itself, including the presence of inclusion bodies and increased markers of inflammation and apoptosis (Magnusson-Lind *et al.*, 2014; Moffitt *et al.*, 2009). Glucocorticoids are also known to be modulators of apoptosis pathways, with chronically high levels being associated with increased apoptosis in a variety of tissues including muscle, brain, and bone (Gruver-Yates & Cidlowski, 2013; Lee *et al.*, 2005; Moutsatsou *et al.*, 2012; Sapolsky *et al.*, 1985). Similarly, high doses of glucocorticoids are associated with an increase in protein breakdown and catabolism in skeletal muscle (Lofberg *et al.*, 2002). Thus, while not directly tested here, improvement in muscle mass here likely reflects the normalization of this hormonal factor, which worsens cachexia at high levels by further activating inflammatory and apoptotic pathways, and which are already activated by mutant huntingtin toxicity. It is possible that the resulting increase in skeletal muscle mass could alone explain the attenuation in weight loss shown here in male and female R6/2 mice, rather than a treatment induced improvement in metabolic rate.

One surprising finding from the calorimetry data is that R6/2 mice of both sexes here showed a dramatic decrease in food intake at 10 weeks of age. In previous studies, the R6/2 weight loss phenotype has been demonstrated to occur in spite of maintaining normal levels of food intake throughout disease progression (She *et al.*, 2011), or with a very slight hypophagia only at end stage (van der Burg *et al.*, 2008). It is not clear what is responsible for this discrepancy – it is possible that the mice had trouble obtaining and consuming food in the specialized feeders at the bottom of the calorimetry chambers, due to motor impairment. Indeed, R6/2 mice have previously been shown to have an increase in time spent feeding (van der Burg *et al.*, 2008), which suggests that they compensate for motor impairments in food consumption by spending more time consuming food, and thereby normalize the amount of calories consumed to wild-type levels. They have been shown to have a slight attenuation in caloric intake at very late stages (van der Burg *et al.*, 2008), which appears to be insufficient to mediate weight loss. If the hypophagia detected here represents particular difficulty eating in the chambers, rather than a generalized reduction in food intake, then hypophagia would be limited to only the 24 hours spent in the chambers, and would likely have little impact on overall bodyweight or metabolic readouts. However, if the R6/2mice here did show profound and chronic hypophagia, in contrast to previous studies, this could be a significant contributor to the overall metabolic findings. There was a small but significant treatment effect on food intake, with normalized glucocorticoids improving 24-hour food intake in male R6/2 mice. Again, if this treatment effect was consistent across the course of the experiment, it would possibly contribute to the attenuation of weight loss in males. However, treatment did not affect food intake in females, in spite of slowed weight-loss and improved skeletal muscle mass for the normalized glucocorticoid group. Accordingly, these treatment effects are likely not mediated by alterations in food intake, at least for female R6/2 mice.

In addition to improving some metabolic features in R6/2 mice, the normalization of glucocorticoids significantly improved neuropathological readouts, leading to a significant increase in brain mass, neurogenesis, and a decrease in mutant huntingtin inclusion burden in female R6/2 mice. However, as with the metabolic findings, none of these neuropathological symptoms were fully rescued, which again demonstrates that while elevated glucocorticoids exacerbate many HD symptoms they do not exclusively mediate them. Unexpectedly, neuropathological markers in male R6/2s were not affected by different levels of glucocorticoid replacement, although they were more sensitive to the effects of glucocorticoids on metabolism.

Brain atrophy was reduced in female R6/2 mice with normalized glucocorticoid levels here, and wild-type females on high dose corticosterone also showed a Cushing's like reduction in brain mass. Males of both genotypes were resistant to these effects on brain mass. Surprisingly, treatment had no effect on striatal and hippocampal brain volume in either sex, in spite of significant differences in female brain mass. There was a slight, but significant effect of treatment on cortical volume in females of both genotypes, with those on high/HD dose corticosterone showing reduced cortical volume relative to those on low/WT dose treatment. R6/2 mice, and human HD patients, show alterations in neuronal volume and cell loss in the brain (Stack *et al.*, 2005), which are both likely contributors to reductions in brain mass and regional brain volume. Glucocorticoids are known to be modulators of apoptosis pathways, with abnormally high levels being associated with increased apoptosis in brain (Gruver-Yates & Cidlowski, 2013; Sapolsky *et al.*, 1985; Sapolsky *et al.*, 1990). Although not directly measured here, it is likely that improvement in brain mass in female R6/2 mice reflects an attenuation glucocorticoid induced apoptosis. However, it is unclear why female R6/2 mice would be more sensitive than males to the therapeutic effects of normalized glucocorticoids on apoptosis and brain mass. Interestingly, wild-type females were also more sensitive to the effects of experimentally elevated glucocorticoids,

showing a Cushing's like reduction in brain mass and cortical volume, while wild-type males did not demonstrate such changes here.

The normalization of glucocorticoids also appears to improve levels of neurogenesis in the dentate gyrus of R6/2 females. Here, there was a significant effect of treatment for both wild-type and HD females, with those on low/WT dose showing increased neurogenesis relative to those on high dose corticosterone. Although the data did not indicate a treatment by genotype interaction, neurogenesis levels in sham controls suggest that the finding in R6/2 females represents a low/WT-dose induced improvement in neurogenesis (the mean number of ki67+ cells are increased relative to both high/HD dose treated mice and sham controls). Conversely, it appears that the difference between high and low dose treatment in wild-type females represents a Cushing's like reduction in neurogenesis (the mean number of ki67+ cells in the high/HD dose treated mice are lower than both the low/wt dose group and sham controls). The sample size is small here (n=4 per group), and insufficient power may account for the lack of significance for a more complex treatment*genoptype interaction. Thus, while this finding is preliminary and should be followed up in a larger cohort to confirm the finding statistically, it isn't surprising that a chronic elevation in glucocorticoids, which is associated with the HD phenotype, worsen neurogenesis in HD mice. The dentate gyrus has long been known to be particularly sensitive to chronic elevations in glucocorticoids, which suppresses differentiation of dentate gyrus progenitor cells (Brummelte & Galea, 2010; Cameron & Gould, 1994; Gould *et al.*, 1992) and also activates apoptosis in mature dentate gyrus neurons (Crochemore *et al.*, 2005; Lu *et al.*, 2003). It is surprising that neurogenesis was unaffected by glucocorticoids in both wild-type and R6/2 males here, as it was for brain mass and regional volume. However, when contrasted with the female findings of a treatment induced increase in neurogenesis, brain mass, and cortical volume, it emphasizes that female brains are uniquely sensitive to glucocorticoids across all measures, and

suggests that improvements in brain mass and cortical volume in female R6/2s may in part be mediated by improved neurogenesis and the migration and differentiation of progenitor cells to regions affected by disease. Again, while these improvements were significant, there was not full rescue of any of these measures, which confirms that elevated glucocorticoids are exacerbating this neuropathological phenotype, but not directly mediating any of them.

Normalizing glucocorticoid levels in female R6/2 mice here resulted in a marked reduction in inclusion number in the striatum and dentate gyrus, as well as reduction in inclusion size the motor and cingulate cortices. It is unclear why in certain brain regions there was a reduction in aggregate number, in others a reduction in aggregate size, and in others no effect of treatment whatsoever. While this may simply reflect region specific differences in glucocorticoid receptor expression, or in other molecular cofactors and targets of the activated receptor, further assessment of why these differences emerged are warranted. However, the key finding here of a treatment induced reduction in inclusion burden is consistent with the Alzheimer's disease (AD) literature, where chronically elevated glucocorticoids are associated with increased amyloid-beta and tau inclusion burden (Green *et al.*, 2006) and blocking glucocorticoid receptors attenuates inclusion burden in rodent models (Baglietto-Vargas *et al.*, 2013). There is also good evidence in that mHTT aggregation is particularly sensitive to glucocorticoids. Acute administration of dexamethasone (a potent glucocorticoid receptor agonist) on cultured cells expressing mutant huntingtin and glucocorticoid receptors (GRs) potently modulates inclusion burden: mHTT protein is predominately in soluble form when dexamethasone is present, and predominately in insoluble aggregate form when absent (Diamond *et al.*, 2000). While this in-vitro study provides a strong link between glucocorticoid signaling and mHTT aggregation, their findings represent the inverse of what was found here and in the AD literature. This discrepancy is probably best explained by the differences in administration here, as this study assessed the effects of chronic elevations of

corticosterone (and its normalization) on inclusion burden. Chronic elevations in glucocorticoids lead to a compensatory downregulation in GR mRNA and protein levels and a reduction in glucocorticoid binding (Burnstein *et al.*, 1991). It's possible that normalizing glucocorticoid levels here to a more typical physiological range could help to maintain GR signaling mediated suppression of aggregation (at peak levels), and that chronically high levels paradoxically impairs this process by attenuating GR signal transduction. Thus, although plasma levels of corticosterone are elevated, perhaps this elevation can no longer activate these downstream processes that suppress aggregation.

GR signaling could possibly affect mutant huntingtin (mHTT) aggregate formation by: 1) Reducing expression of mHTT protein resulting in slower/reduced aggregation of soluble mHTT, 2) Increasing degradation of aggregated and/or soluble mHTT, and/or 3) Impairing the aggregation process itself. Activation of glucocorticoid receptors (GRs) activates two separate molecular pathways that could independently achieve these changes in protein homeostasis. When not bound to ligand (cortisol in humans, corticosterone in rodents, or dexamethasone in pharmacological studies), GRs are bound to heat shock proteins (Hsp70 and Hsp90) which maintain the GR in an open conformational state whereby the ligand binding domain is accessible to glucocorticoids (Pratt, 1993). When ligand binds to the GR, the activated GR-ligand complex will form homodimers and translocate to the nucleus, where they further bind either co-activator or co-repressor complexes resulting in corresponding transcriptional changes in genes that contain GR binding domains (Weikum *et al.*, 2017). Wild-type Huntingtin gene expression does not appear to be altered by GR mediated transcriptional changes (Reddy *et al.*, 2009), thus reduced inclusion burden is not mediated by a downregulation in mHTT protein levels, and is instead likely mediated by indirect GR-mediated effects on protein turnover and/or aggregation processes themselves. GR signaling does result in the activation of the Heat Shock response,

including an upregulation in Heat Shock Factor 1 (HSF1) and Hsp70 (Maheshwari *et al.*, 2014; Sun *et al.*, 2000), which would have the ability to alter mHTT aggregation. Heat shock chaperones regulate protein folding, aggregation, ubiquitination, and degradation by the proteasome in healthy cells (Luo *et al.*, 2010; Pratt, 1993; Wacker *et al.*, 2009), and are known to influence the formation of protein aggregates in a variety of neurodegenerative diseases including HD, Parkinson's disease (Luk *et al.*, 2008), and Alzheimer's disease (Evans *et al.*, 2006). Hsp70 and Hsp90 have antagonistic influences on aggregation in neurodegenerative disease: Hsp70 activity is associated with reduced protein aggregation and toxicity, while Hsp90 tends to stabilize toxic aggregates in their misfolded conformation and block their degradation (Luo *et al.*, 2010; Wacker *et al.*, 2009).

Interestingly, experimental manipulation of heat shock proteins in R6/2 mice directly affects inclusion burden - Hsp70 knockout in R6/2 mice increases the size of cortical aggregates (Wacker *et al.*, 2009) while overexpression of Hsp70 leads to a delay in inclusion formation and increases solubility of aggregates in slice culture (Hay *et al.*, 2004), although it does not seem to affect inclusion formation in vivo (Hansson *et al.*, 2003; Hay *et al.*, 2004). The possibility that glucocorticoid signaling may affect this process is intriguing, as glucocorticoids are likely omitted in the in-vitro preparations here but present in vivo. Chronic pharmacological inhibition of Hsp90 resulted in a significant reduction in aggregates in cortex, hippocampus, brain stem, and muscle in R6/2 mice at 9 weeks of age; this reduction was transient though and was no longer detectible at 14 weeks of age (Labbadia *et al.*, 2011). Chronic Hsp90 inhibition also resulted in a small transient increase in soluble mHTT protein in cortex at 9 weeks of age, which was no longer detectable at 14 weeks (Labbadia *et al.*, 2011). Interestingly, pharmacological inhibition of Hsp90 results in a heat shock response (HSR), including a dramatic upregulation in Hsp70 expression in wildtype mice. R6/2 mice show a similar pharmacologically induced increase in Hsp70 at early

ages, but lose this responsiveness to Hsp90 inhibition as the disease progresses, starting at 8 weeks of age (Labbadia *et al.*, 2011). It's also interesting that R6/2 mice show a 50% downregulation in Hsp70 as a part of their phenotype, roughly starting at 8 weeks of age (Hay *et al.*, 2004). It is unclear how expression and activation of these heat shock proteins are affected by the chronic elevation in corticosterone that is a part of the R6/2 phenotype, beginning between weeks 7-10 (Dufour & McBride, 2016), especially as it likely results in a downregulation of GR expression and reactivity (Burnstein *et al.*, 1991). Perhaps normalizing glucocorticoid levels helps to retain normal GR receptor function, including its activation of HSP70, which clearly has anti-aggregation properties. Conversely, it is not clear how Hsp70 downregulation in R6/2 mice may impact GR activation, as this chaperone is required for GRs to be in a conformational state in which glucocorticoids can activate them. It is quite striking that silencing Hsp70 in R6/2 mice resulted in shortened survival time and increased weight loss (Wacker *et al.*, 2009), similar to my previous findings on the effects of high dose corticosterone (Dufour & McBride, 2016).

The relationship between glucocorticoid receptor signaling, heat shock response, and inclusion formation is incredibly complex, as outlined above. A set of experiments from Maheshwari *et al.* (2014) deserve particular attention, in that they provide further insight into the complex relationships between these three factors, although their findings are hard to reconcile with those presented here and in Chapter 2. In this experiment, intact R6/2 and wild-type mice were given daily injections of dexamethasone, a potent and highly specific GR agonist, or vehicle from 5-8 weeks of age. The authors found that chronic dexamethasone treatment induced a heat-shock response (increased Hsp70 and HSF1), reduced ubiquitin-positive aggregates and improved motor symptoms at the 8 week timepoint, although it failed to attenuate weight-loss or increase lifespan (Maheshwari *et al.*, 2014). In contrast, data from Chapter 2 show that high levels of glucocorticoids levels potently exacerbate weight loss and shorten lifespan in R6/2 mice (Dufour

& McBride, 2016). Also, data from this chapter show that normalizing glucocorticoids to wild-type levels induces a potent, although region specific, reduction in inclusion burden (e.g. 70% reduction in inclusion number in the dentate gyrus) at later stages of disease progression. There are three key differences in experimental design that make these divergent findings difficult to reconcile. First – only a single dose of dexamethasone was used by Maheshwari *et al*. (2014), and it is unclear if this dose represents an increase or decrease in glucocorticoid signaling relative to the R6/2 phenotype. The second difference is in the pharmacological properties of ligand: dexamethasone is a synthetic and highly selective GR agonist while the endogenous ligand (cortisol or corticosterone) is much more promiscuous and achieves some of if its effects by signaling at the mineralocorticoid receptor. This may lead to functional differences in the effect of ligand, for example corticosterone can modulate cell proliferation and differentiation of progenitors in the dentate gyrus, while dexamethasone only modulates proliferation and fails to affect differentiation (Yu *et al.*, 2004). The third key difference is in timeframe – the endpoint in the dexamethasone study was 8 weeks of age, while the endpoint here was at 11 weeks, which represents a later stage of disease. If dexamethasone treatment represents an increase in GR signaling relative to basal R6/2 conditions, it is possible that short term high dose GR activation (3 weeks, by dexamethasone) results in reduced aggregation, while longer term GR activation (5 weeks, by spontaneous R6/2 and experimentally elevated corticosterone, here) worsens aggregation, possibly through GR receptor downregulation.

Together, the data from the studies presented here in Chapter 3, further demonstrate that the elevated glucocorticoid phenotype of HD does indeed exacerbate other HD symptomology, including metabolic and neuropathological abnormalities. However, there was an unexpected and robust sexually dimorphic response to treatment, with normalized corticosterone improving in-vivo metabolic readouts predominately in male R6/2 mice and post-

mortem neuropathology exclusively in female R6/2 mice. However, some metabolic effects of treatment were shared by both sexes, including a therapeutically induced attenuation in weight loss and improvement in skeletal muscle mass. Regardless, it is not immediately clear why this sexual dimorphic response occurred. One possibility is that male R6/2 mice show a slightly faster disease progression, losing weight and dying about a week earlier than females on average (Cummings *et al.*, 2012; Wood *et al.*, 2010). Since the majority of the post-treatment measures were taken at a single timepoint (muscle mass, brain mass, and neuropathology were assessed at week 11 and calorimetry at 10 weeks of age) the findings represent the cumulative changes induced by treatment at only that point in time. It is possible that the male R6/2 mice were already entering late stage phenotype with a profound metabolic symptoms at 10 weeks of age, while female R6/2s had only more subtle alterations in metabolism. It is possible that instead of affecting calorimetry measures directly, perhaps normalized glucocorticoid treatment had a direct effect on end-stage symptom progression broadly, but not necessarily on calorimetry directly. Similarly, neuropathological readouts are perhaps attenuated by low dose corticosterone earlier in disease progression, and female specific improvements in neuropathology simply reflect the stage of progression at 11 weeks of age. Indeed, manipulations in HSP proteins have clear effects on inclusion formation during mid-stage disease progression, but by end stages these effects are lost (Labbadia *et al.*, 2011). It is possible that normalized glucocorticoid treatment induced similar reductions in mHTT aggregation in males earlier in the experiment, but that they were no longer effective by 11 weeks of age. However, another possible explanation for the sexual dimorphic response is simply differences in HD pathology that are specific to each sex. For example, male R6/2 mice (and human patients) show dramatic atrophy of the testes during end stages of disease and a concomitant reduction in circulating testosterone levels (Papalexi *et al.*, 2005; Saleh *et al.*, 2009; Van Raamsdonk *et al.*, 2007), which would likely impact metabolism and muscle

homeostasis (Herbst & Bhasin, 2004). Female reproductive hormones are less impacted by mHTT toxicity (Saleh *et al.*, 2009), and could possibly offer neuroprotective effects for females (Tunez *et al.*, 2006).

While the findings here raise many further questions about mechanisms of action, as well as why there is such hetergeneity in treatment response (e.g. sex effects, region specific effects on inclusions), they also confirm and extend previous findings (Dufour & McBride, 2016), and further demonstrate that elevated glucocorticoids do in fact contribute to HD symptomology. The ability to attenuate HD symptoms through normalization of glucocorticoid levels, as demonstrated here, also demonstrates that improving glucocorticoid homeostasis could provide therapeutic benefit for HD patients. This finding may be extremely important for individuals showing particularly high levels of cortisol, which have been shown to more dramatically worsen symptoms (Dufour & McBride, 2016).

Chapter 4: Assessing the Role of the Anterior Cingulate Cortex in Huntington's Disease Mood Symptoms

4.1 - Introduction

Psychiatric symptoms are prevalent in Huntington's disease (HD), including high rates of depression and anxiety (Anderson & Marder, 2001; Levy *et al.*, 1998; Pflanz *et al.*, 1991), which have a particularly negative impact on quality of life for patients (Anderson & Marder, 2001; Ho *et al.*, 2009). These symptoms typically appear in the prodromal premanifest stage, before the onset of full disease including the characteristic motor phenotype (Anderson & Marder, 2001; Julien *et al.*, 2007). In contrast to HD motor symptoms, which have long been known to be mediated by severe degeneration of the striatum and motor cortex (Albin *et al.*, 1992; Deng *et al.*, 2004; Galvan *et al.*, 2012; Thu *et al.*, 2010; Vonsattel *et al.*, 1985), the mechanisms that underlie mood symptoms in HD are poorly understood. It is unclear if severe pathology in a single brain region is responsible, or if it results from simultaneous pathology across a variety of brain regions. Indeed, many limbic brain regions associated with depression and anxiety are affected in HD, including the hippocampus, hypothalamus, cortex, and brainstem monoamine systems (Bedard *et al.*, 2011; Gabery *et al.*, 2010; Ransome *et al.*, 2012; Zweig *et al.*, 1992).

Recent evidence from human clinical imaging and neuropathological studies implicate a particular limbic region of cortex, the anterior cingulate cortex (ACC), as a possible substrate for HD mood symptoms. ACC volume is inversely correlated with mood symptom severity in HD patients (Hobbs *et al.*, 2011). Diffusion tensor imaging has also shown reduced fractional anisotropy in the ACC of HD patients with mood symptoms, indicative of microstructural abnormalities in this region (Sprengelmeyer *et al.*, 2014). Some of these changes seem to be associated with mood symptoms generally, as non-HD patients with unipolar and bipolar

depression show reduced grey matter volume and decreased activity in the ACC (Drevets *et al.*, 1997; Drevets *et al.*, 2008), and those with generalized anxiety disorder also show reduced ACC activation in response to emotional conflict (Etkin *et al.*, 2010). Thus, this relationship between mood symptoms and ACC dysfunction is correlational, as indicated by imaging studies in both HD and non-HD populations. However, postmortem neuropathological studies from HD cases provide evidence of a more causal link. While postmortem tissue from HD patients typically shows widespread degeneration of the cerebral cortex, the pattern of cortical degeneration is idiosyncratic to patients in a way that parallels HD symptomology. HD patients with mood symptoms show a dramatic loss of pyramidal cells and GABAergic interneurons in the ACC, while those without mood symptoms do not show cell loss in the ACC (Kim *et al.*, 2014; Thu *et al.*, 2010). Conversely, HD patients with predominant motor symptoms (but no mood symptomology) show dramatic loss of pyramidal cells in the motor cortex (MC), while for those with mood symptoms (but no motor symptomology) the motor cortex is spared (Kim *et al.*, 2014; Thu *et al.*, 2010). These data suggest that the impairments in the ACC, shown by clinical HD patients with mood symptoms, is likely mediated by progressive degeneration of that region. However, there are two important limitations to these data: 1) The neuropathological data are still correlational (taken at a single time-point – death) and cannot independently show causation and 2) This finding does not rule out involvement of other brain regions in HD mood symptoms, as other regions were not assessed. Due to these limitations that are inherent to human studies, controlled experiments using an HD animal model could help to answer the questions raised by these clinical findings: 1) Is ACC pathology causal to HD mood symptoms, or is it simply correlated?, and 2) Does dysfunction in other limbic brain regions also contribute to HD mood symptoms?

Thus, in the experiments presented here, I utilized the BACHD transgenic mouse model of HD to better understand the role of mutant huntingtin toxicity in the ACC in HD mood

symptoms. The BACHD transgenic mouse model carries a full length human mutant huntingtin transgene with 97 CAG repeats (Gray *et al.*, 2008). It is a unique HD rodent model in that exon 1 of the mutant huntingtin transgene, which contains the CAG repeat region that confers toxicity, is flanked by loxP sites (Choudhury *et al.*, 2016) which enable the transgene to be excised in vivo by the enzyme Cre-recombinase (Sauer, 1998). By delivering viral vectors that carry a Cre-recombinase gene, which achieve Cre-recombinase expression in the target brain region or tissue, it is possible to achieve targeted silencing of the disease causing transgene through Cre-mediated excision (Gaveriaux-Ruff & Kieffer, 2007; Sauer, 1998). BACHD mice were also chosen for these experiments because they show robust depressive- and anxiety-like behavior, including increased behavioral despair (increased immobility in the forced swim test), anhedonia (reduced sucrose preference), and increased time in the dark in the light-dark anxiety task (Hult Lundh *et al.*, 2013; Menalled *et al.*, 2009; Wang *et al.*, 2014). Wang and colleagues (2014) showed that silencing mHTT in the whole cerebral cortex in BACHD mice fully ameliorates depressive- and anxiety- like behavior, while striatal mHTT silencing does not improve these symptoms (Wang *et al.*, 2014). While mood symptoms in BACHD mice may be mediated by widespread cortical pathology, it is also possible that pathology in a particular sub-region of cortex was responsible for the amelioration of mood symptoms. Given the robust link between ACC pathology specifically and HD mood symptoms in human studies, it is possible that ACC pathology is solely responsible for HD mood symptoms, and that silencing mHTT in the ACC of BACHD would be sufficient to improve mood symptomology.

Thus, in this chapter, I tested the hypothesis that HD mood symptoms are specifically mediated by Anterior Cingulate dysfunction in the BACHD mouse model. The main goal of this study was to demonstrate that a relationship between ACC pathology and HD mood symptoms is not only correlational, but that it is in fact causal. By doing so, it would identify the ACC as a novel

target for therapeutic intervention in HD, potentially for RNAi therapies. It would also validate the BACHD model as a tool to better understand how the ACC pathology mediates mood symptoms, how this pathology develops, and potentially to identify why some HD patients develop these symptoms and others do not.

4.2 - Methods

Animals. All mice on study were pair housed with littermates (same sex and genotype) under controlled conditions of temperature and light (12 hour light/dark cycle). Food and water were provided *ad libitum*. BACHD mice (stock # 008197) were obtained from Jackson Laboratories (Bar Harbor, ME) and bred in the vivarium at the ONPRC. Transgenic mice were genotyped using primers specific for the mutant human HTT transgene (forward primer 3'-TGTGATTAATTTGGTTGTCAAGTTTT-5' and reverse primer REV 3'-AGCTGGAAACATCACCTACATAGACT-5'). Body weights of all animals were recorded weekly. All experimental procedures were performed according to ONPRC and OHSU Institutional Animal Care and Use Committee.

AAV Vectors. AAV2/1 vectors were utilized in this study, carrying either a gene for Green Fluorescent Protein (eGFP) only or a gene for Cre-Recombinase and eGFP, separated by an IRES sequence. Expression of both control (AAV2/1-eGFP) and treatment (AAV2/1-CreIRESeGFP) vectors were driven by a Cytomegalovirus promoter (CVM). Vectors were generated by the Gene Transfer Vector Core at the University of Iowa at a titer of 1.07E13 for the AAV2/1-CreIRESeGFP prep and 3.04E12for the AAV2/1-eGFP prep.

Surgery. Mice were anesthetized with ketamine/xylazine and placed into a stereotaxic frame (Kopf, Tujunga, CA). An incision was made in the scalp, followed by four craniotomies. Mice received four 1.00µl injections of either AAV-eGFP or AAV-CreIRESeGFP at a titer of 3.00e12 at the following coordinates: Left Rostral (+1.70 A/P, +0.30 M/L, -1.50 D/V), Left Caudal (+0.40 A/P, +0.30 M/L, -1.00 D/V), Right Rostral (+1.70 A/P, -0.30 M/L, -1.50 D/V), and Right Caudal (+0.40 A/P, -0.30 M/L, -1.00 D/V). Vector was infused at each injection site over 5 minutes (0.2µl/min

rate) using a Hamilton 700 series syringe and a 33 gauge needle. The needle was left in place for an additional 5 minutes following each infusion to allow for undisturbed spread of vector.

Light Dark Box. This procedure was performed in the open field chambers described in Chapter 2 (Dufour & McBride, 2016). An opaque perspex insert was placed into the open field chamber (40.64 x 40.64 cm), which is half the size of the overall chamber (40.64 x 20.32 cm). This opaque insert makes half of the open field chamber dark and also contains an opening that allows the mouse free access to both sides (dark and open) of the chamber. The open side of the chamber is illuminated with a 900 lux led light panel. Mice were assessed for time spent in the dark side of the chamber over a 10 minute period at 6, 11, and 15 weeks of age. The first 5 minutes of the test were used for analysis. Mice were habituated for this procedure with two 15 minute sessions at 4 weeks of age.

Sucrose Preference. At 5, 10, and 14 weeks of age, mice were given four days of access to two water bottles that contained either water or 2% sucrose solution. The bottles were rotated between sides every 24 hours at which point the bottles were weighed to assess consumption of each solution. Testing was immediately preceded by 72 hours of habituation to two bottles of water at each age.

Forced Swim Test. At 15.5 weeks of age, mice were placed into a plastic cylinder (25cm tall, 20cm in diameter) that was filled halfway with 24°C water for the forced swim test. Mice were in the water for a total of 6 minutes, and were video recorded. The amount of time spent swimming, floating, and climbing was measured and quantified using The Observer software (Noldus, Wageningen, the Netherlands).

Necropsy. At 15.5 weeks of age, after the Forced Swim Test, mice were deeply anesthetized with ketamine/xylazine and perfused with 15mLs of 0.9% saline. Brains were dissected from half of the

subjects for immunohistochemistry – following dissection, they were post-fixed in 4% paraformaldehyde for 24 hours and then stored in a 30% sucrose solution until they were sectioned. For the other half of the subjects, brains removed and immediately placed into ice-cold 0.9% saline and cut into 1mm slabs using a brain matrix. Each slab was imaged under a fluorescence microscope to confirm vector expression (as indicated by eGFP fluorescence) and subsequently the surgically targeted area (pre-limbic, infra-limbic, and cingulate cortices) was micro-dissected, frozen on dry ice, and then stored at -80°C until analysis. Animals showing transduction of less than 50% of the region of interest were excluded from the Forced Swim Test and Light-Dark box analyses (3 animals were removed for this reason – 1 Male-HD-Cre, 1 Female-HD-Cre, and 1 Male-HD-GFP). Cage scores were used for the sucrose preference test – transduction scores were averaged across both mice for each cage, and any cage with an average of less than 50% transduction would be removed (none met this criteria).

Immunofluorescence. Brains were cut into 40μm sections with a freezing sliding microtome and stored in cryoprotectant solution (30% sucrose, 30% ethylene glycol, in PBS) until stained. Serial sections from 40 mice (balanced for sex, genotype, and treatment) were stained for Immunofluoresence using antibodies against eGFP (rabbit, 1:1000, A6455 Invitrogen) – and Cre-recombinase (mouse, 1:500, Millipore MAB3120). Sections were blocked (for non-specific antibody binding) in 5% goat serum for 1 hour, incubated in primary antibodies overnight (in 3% goat serum), washed and incubated in fluorescent secondary antibody for 1 hour (AlexaFluor 488 goat-anti-rabbit for GFP and AlexaFluor 568 goat-anti-mouse for Cre, Invitrogen). Sections were counterstained with Hoechst at a concentration of 1:10,000 in water for 1 minute, mounted onto glass slides and coverslipped for downstream microscsopic analysis.

Quantitiative real-time PCR. RNA was isolated from ACC samples using an AllPrep® DNA/RNA/Protein Mini Kit (Qiagen, Hilden, Germany) and was reverse transcribed with random primers and Multiscribe reverse transcriptase (Thermo Fisher Scientific, Waltham, MA). Relative human mHTT mRNA expression was assessed via qPCR. A TaqMan primer-probe set spanning the exon1/exon2 boundary of human mHTT mRNA (Assay ID: Hs00918134_m1, Thermo Fisher Scientific, Waltham, MA) was utilized to assess alterations in expression utilizing a TaqMan Gene Expression Assay. Relative gene expression was determined by using the $\Delta\Delta C_T$ method, normalizing to ATPB5 mRNA levels (TaqMan Assay ID: Mm00443967_g1, Thermo Fisher Scientific, Waltham, MA).

Statistical Analysis. All statistical analyses were performed by using JMP Version 13 (SAS Institute Inc.). A repeated measures mixed-model was used for all repeated measures (dependent variables: Percent time in the dark (light dark test), Number of light dark transitions (light dark test), Percent preference for sucrose (sucrose preference test); independent variables: genotype, sex, treatment, and time-point/age). For both the sucrose preference test and light dark test analyses there was a significant effect of sex, and thus the analyses were re-run separately for each sex. A three-way ANOVA was used to assess the effects of genotype, sex, and treatment group on immobility in the forced swim test. For all other analyses, Tukey's post-hoc comparisons were performed when statistically significant (and trending) fixed effects were detected ($p < 0.10$).

4.3 - Results

In order to assess the role of mutant huntingtin pathology in the anterior cingulate cortex (ACC) on HD mood symptoms, wildtype and transgenic BACHD mice (which carry a floxed copy of the human mutant huntingtin gene) were stereotaxically injected into the ACC at 6 weeks of age with an AAV1 vector expressing either the Cre-recombinase gene with an enhanced GFP (eGFP) reporter gene (AAV1-Cre-GFP, **Fig. 4.1B**) or an eGFP reporter gene alone (AAV1-eGFP, **Fig. 4.1C**), driven by a cytomegalovirus (CMV) promoter. The targeted region included the rodent infralimbic, prelimbic, and cingulate cortices, which together are considered to constitute a homologous structure to the human anterior cingulate cortex (Vogt & Paxinos, 2014). Animals were assessed for a variety of depressive- and anxiety-like behaviors associated with the HD phenotype at baseline, prior to surgery, and at different timepoints post-surgery depending on the particular assay. An overview of the experimental timeline is outlined in **Figure 4.1A**. Transduction patterns, as indicated by both eGFP and Cre expression, are demonstrated in **Figure 4.2**. Injections of both vector preps resulted in widespread transduction throughout the rostral-caudal extent of the targeted cingulate cortex. The ACC was microdissected in a subset of BACHD mice at necropsy for to estimate the level of treatment-induced silencing of mHTT expression via qPCR. AAV1-Cre treated mice showed a significant 70% reduction in ACC mHTT mRNA (Treatment: $F_{1,8}$= 101.57, p<.001) relative to those treated with AAV1-GFP (**Fig. 4.3**). Subjects treated with either AAV1-Cre or AAV1-GFP were measured for: 1) anxiety-like behavior using the light-dark box anxiety test, 2) anhedonia, a depressive-like behavior, using the sucrose preference test, and 3) behavioral despair, a depressive-like behavior, using the forced swim test.

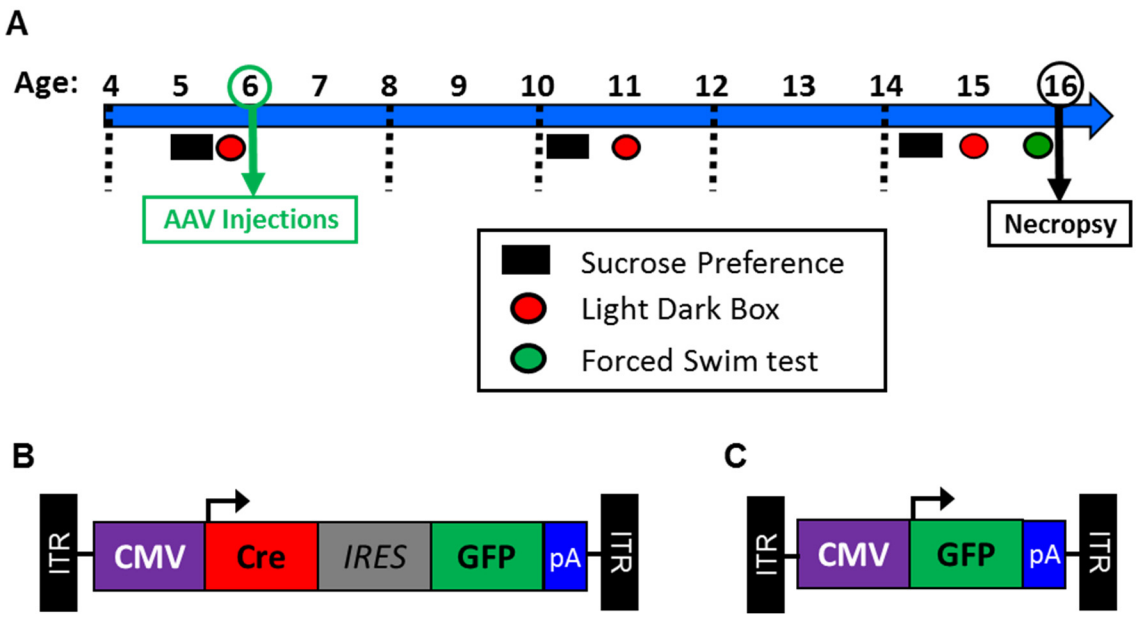

Figure 4.1 – Experimental Timeline and AAV constructs. (A) BACHD and WT Mice were stereotaxically injected with AAV2/1 vectors, carrying either a (B) CMV-Cre-GFP or a (C) CMV-GFP construct, into the anterior cingulate cortex at 6 weeks of age. Cre expression in BACHD mice selectively inactivates the floxed mutant huntingtin (*mHTT*) transgene in transduced cells in the anterior cingulate cortex. Subjects were measured for depressive- and anxiety-like behavior. The sucrose preference test was used to measure anhedonia at baseline (5 weeks of age), and again at 10 and 14 weeks of age. The forced swim test was used to measure behavioral despair at a single timepoint (16 weeks of age), before necropsy. The light-dark test was used to assess anxiety like behavior at baseline (6 weeks of age, before surgery), and again at 11 and 15 weeks of age. Mice were euthanized at 16 weeks of age and tissue was collected for either molecular analysis or histology. Overall N=78 (20 WT-Cre, 20 HD-Cre, 20 WT-GFP, 18 HD-GFP).

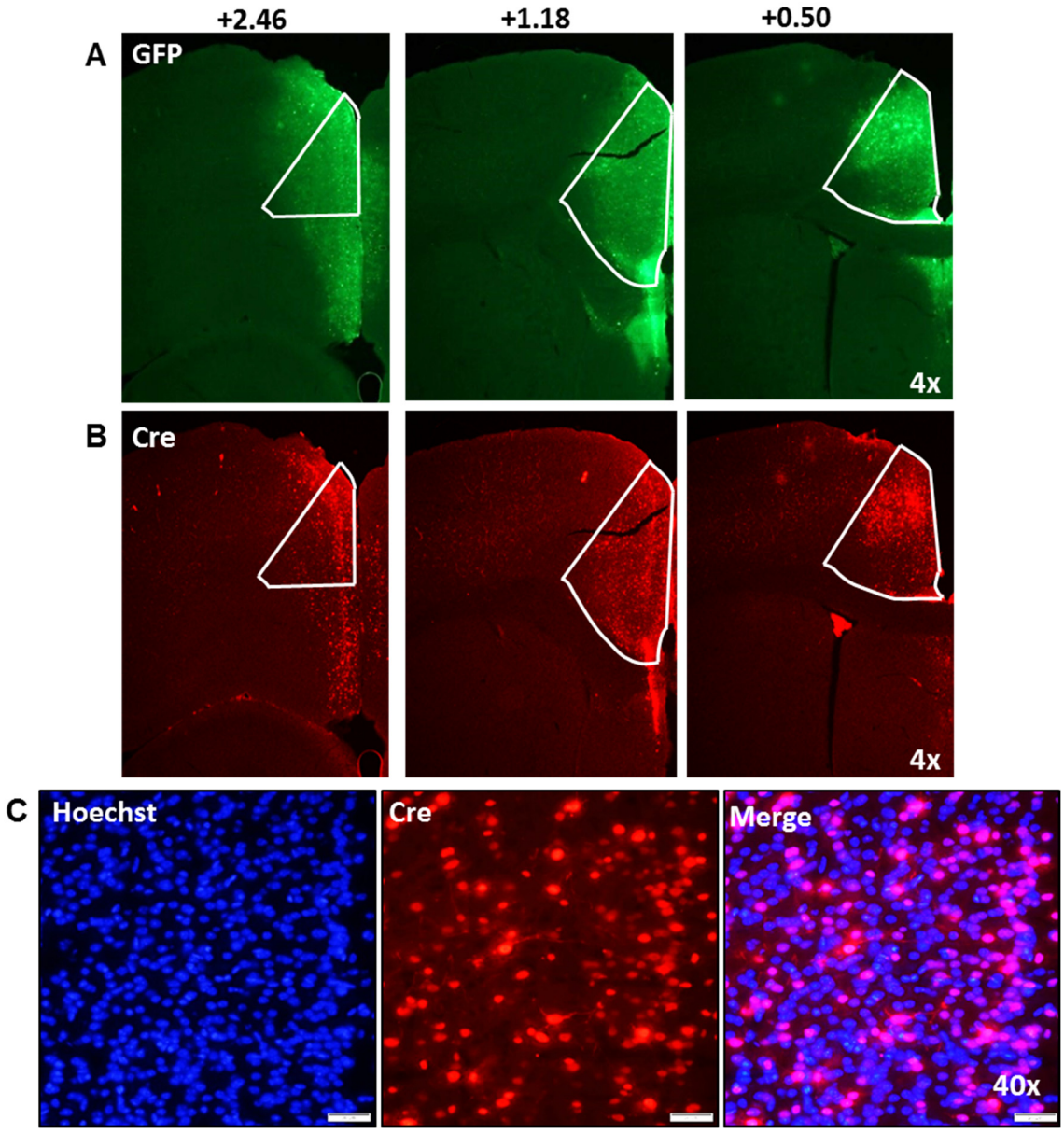

Figure 4.2 – AAV1-Cre-GFP expression. Stereotaxic infusion of AAV-Cre-Ires-GFP into the anterior cingulate cortex (outlined in white) leads to robust expression of (A) GFP and (B) Cre Recombinase throughout the rostral caudal extent of the structure. Stereotaxic A/P coordinates from bregma shown at top. (C) High magnification images (40x) indicate widespread expression of Cre-recombinase in the neurons of the anterior cingulate that co-localizes with the nucleus, as indicated by blue Hoechst stain.

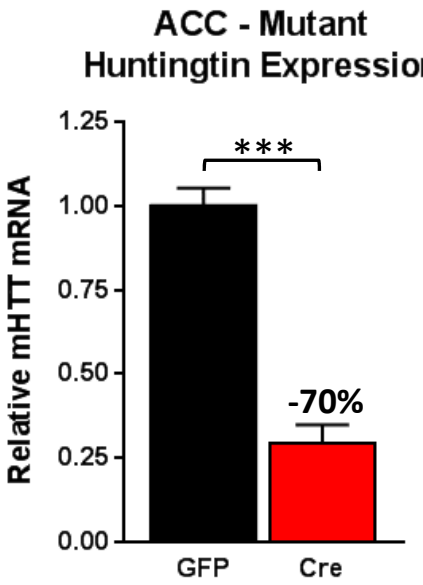

Figure 4.3 – mHTT expression levels. The ACC was microdissected at necropsy from a subset of BACHD mice (N=12) for molecular analysis. AAV1-Cre treated BACHD mice (n=6) showed a significant 70% reduction in mHTT mRNA (p<.001) relative to AAV1-GFP treated BACHD mice (n=6). Values represent Mean ± SE.

Light Dark Box Anxiety Test

Subjects were measured in the light-dark task to assess the effects of mHTT inactivation in the ACC on anxiety-like behavior in BACHD mice. Increased time in the dark is indicative of increased anxiety-like behavior, and here transgenic BACHD mice spent 9.7% more time in the dark (**Fig. 4.4A-B**) than wild-type controls (Genotype: Females $F_{1,70}$ = 16.90 p<.001; Males $F_{1,67}$ = 5.28 p<.05) consistent with previous studies (Hult Lundh *et al.*, 2013; Menalled *et al.*, 2009). Reduced number of transitions between the light and dark compartment is also used as a secondary measure of anxiety-like behavior in this task. BACHD mice also showed reduced light-dark transitions (**Fig. 4.4C-D**) relative to WT controls (Genotype: Females $F_{1,70}$ = 8.34 p<.01; Males $F_{1,67}$ = 9.40 p<.01). Over the course of the experiment, there was a significant improvement in light-dark task behavioral readouts, with an overall reduction in percent time in the dark (Timepoint: Females $F_{2,58}$ = 12.45 p<.001; Males $F_{2,66}$ = 25.29 p<.001) and increase in light-dark transitions (Timepoint: Females $F_{2,58}$ = 7.17 p<.01; Males $F_{2,66}$ = 13.12 p<.001) across both genotypes.

AAV1-Cre treatment did not significantly affect percent time in the dark in subjects (Treatment: Females $F_{1,70}$ = 0.20 p=0.66; Males $F_{1,67}$ = 0.25 p<.62) nor did it affect light-dark transitions (Treatment: Females $F_{1,70}$ = 0.06 p=0.81; Males $F_{1,67}$ = 0.06 p<.81). As AAV1-Cre injections were hypothesized to reduce anxiety-like behavior by silencing expression of the mHTT transgene specifically in BACHD transgenic mice, assessing the interaction of AAV1 treatment with genotype was of particular interest. However, there was no evidence that AAV1-Cre injection selectively reduced anxiety-like behavior in BACHD mice, as there was not a significant genotype*treatment, or genotype*treatment*timepoint interaction for either percent time in the dark, or on light-dark transitions (p>.05 for all).

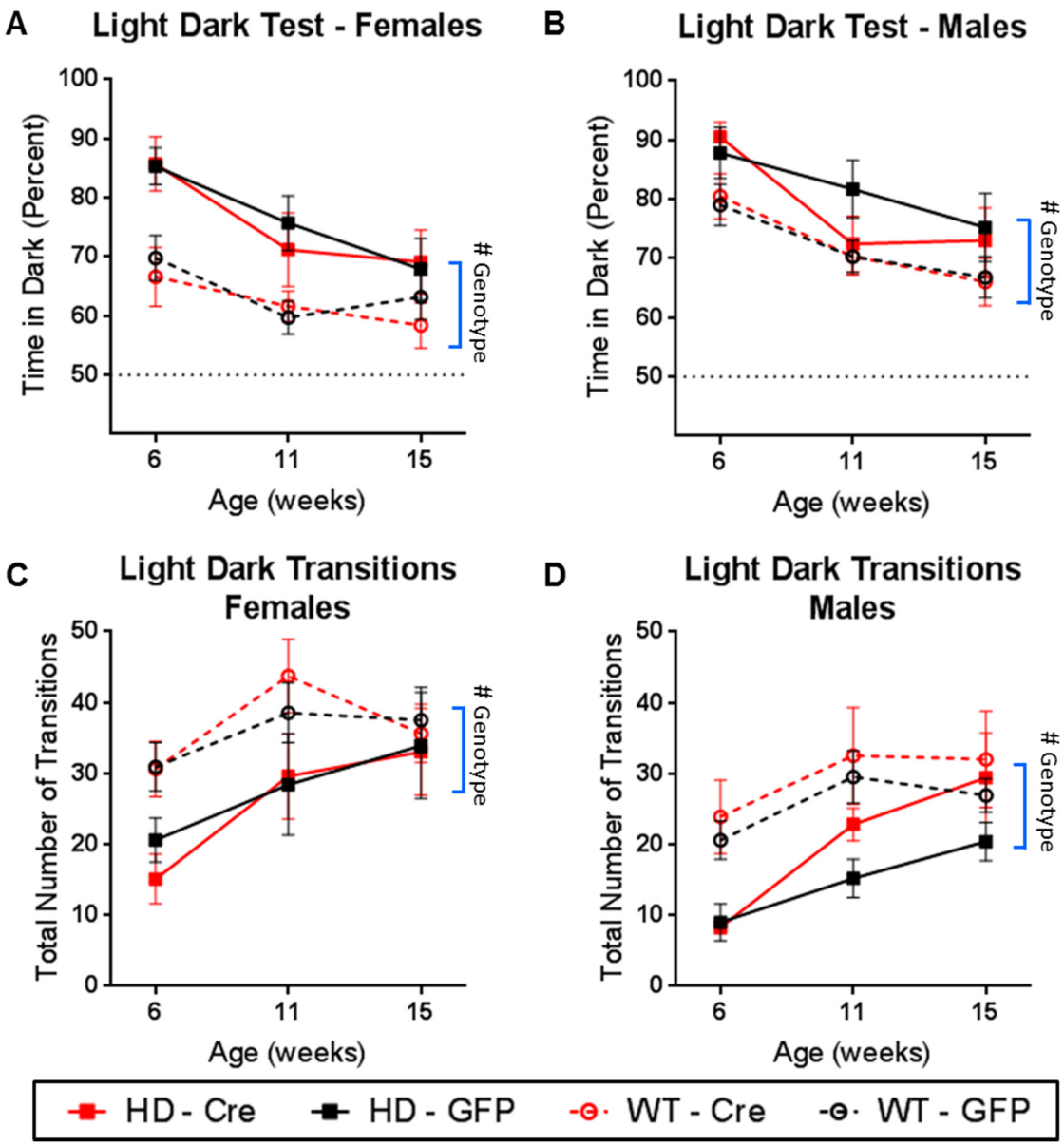

Figure 4.4 – Light Dark Test. BACHD transgenic HD mice were tested for the effect of intra-cingulate AAV1-Cre treatment on anxiety-like behavior in the Light Dark Test. Female (A,C) and male transgenic BACHD (B,D) mice spend more time in the dark than WT mice and show a reduced number of transitions between compartments (Genotype: $p<.05$ for all A-D, Indicated by bars with **# genotype**), both indicative of increased anxiety. Treatment with AAV1-Cre did not affect any light dark measures relative to AAV1-GFP treated controls, regardless of genotype ($p>.05$ for all effects of treatment and its interactions). There was a progressive reduction of anxiety-like behavior for all mice across both measures (Timepoint $p<.05$ for all, A-D) in WT and HD mice, likely reflecting habituation to the task. Values represent Mean ± SE. N=37M and N=33F.

Sucrose Preference Test

To assess the effects of mHTT inactivation in the anterior cingulate on anhedonia, a type of depressive-like behavior, mice were assessed with the sucrose preference test. Previous studies have indicated that BACHD mice show decreased preference for drinking a sucrose solution, relative to water solution, in this two bottle choice task (Hult Lundh *et al.*, 2013). There was no effect of AAV1-Cre treatment on sucrose preference here (p>.05 for treatment and all of its interactions). However, only a small deficit in sucrose preference was detected in female BACHD mice (Genotype: $F_{1,41}$ = 4.93, *p*<.05) here, relative to WT controls (**Fig. 4.5B**). Male BACHD mice did not show any deficit here (Genotype: $F_{1,42}$ = 0.94, *p*=.34) relative to WT controls (**Fig. 4.5A**). BACHD females showed a 5.3% reduction in sucrose preference (77.1% ± 2.4 for HD, 82.4% ± 1.1 for WT) at baseline, a 3.5% reduction at 10 weeks of age (80.9% ± 2.4 for HD, 84.4% ± 1.2 for WT), and a negligible 0.7% increase over WT females at 14 weeks of age (86.0% ± 2.4 for HD, 85.3% ± 1.2 for WT). Regardless of genotype of treatment, females also showed a significant increase in sucrose preference over time (Timepoint: $F_{2,28}$ = 6.33, *p*<.01). In contrast, there were no group differences in this measure, not only with respect to genotype, but also with respect to treatment and timepoint (*p*>.05 for all). Also, there was no detectible effect of AAV1-Cre treatment on sucrose preference in any cohorts here (*p*>.05 for treatment and all of its interactions in both males and females). However, given that the typical sucrose preference seen by others was not detected here in BACHD males at all, and only to a small degree in BACHD females, it is impossible to properly assess whether or not selective inactivation of mHTT in the cingulate could lead to a reduction in anhedonia.

Interestingly, although there was no difference in sucrose preference in males and a slight decrease in females, overall sucrose intake in transgenic BACHD mice was significantly elevated relative to WT mice in both sexes (**Supp. Fig 4.1A and 4.1D**, Genotype: Females $F_{1,41}$ = 5.74 p<.05;

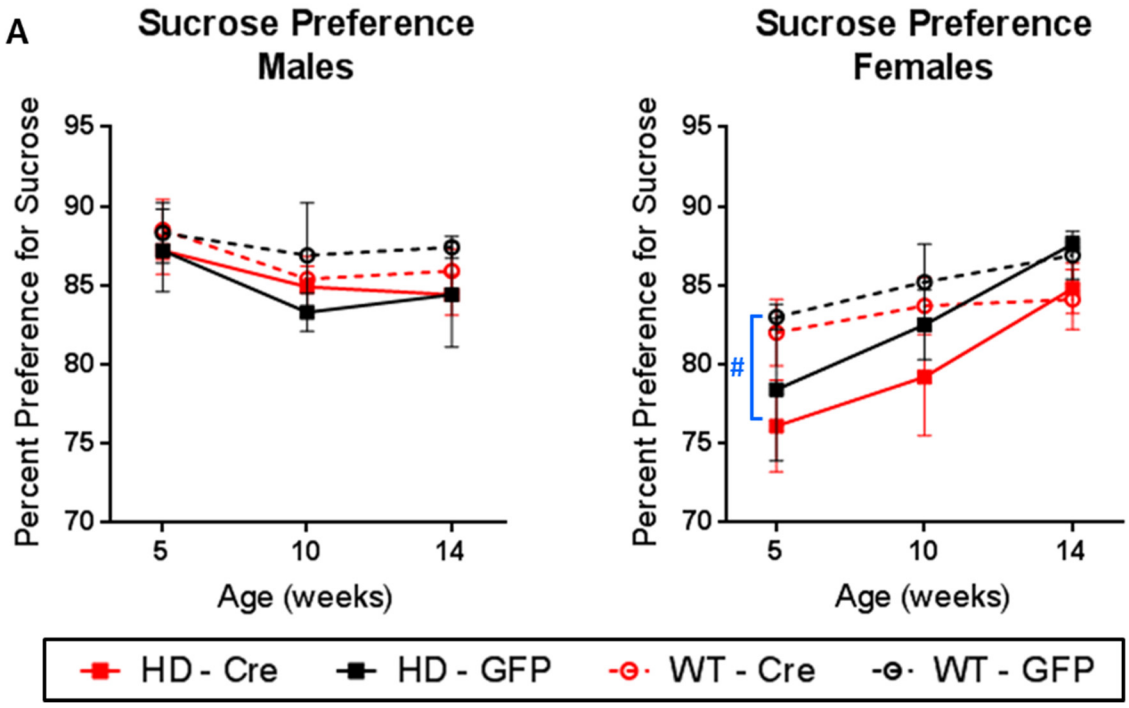

Figure 4.5 – Sucrose Preference Test. Mice were tested for the effect of intra-cingulate AAV1-Cre treatment on anhedonia, a depressive-like behavior, with the Sucrose Preference Test. In males (A), there was no difference between groups with respect to treatment, genotype, or timepoint (p>.05 for all). In females (B), BACHD mice showed a small but significant overall reduction in sucrose preference (Genotype: *p*<.05, indicated by **#**) relative to WT mice. As with males, there was no effect of treatment (p>.05), although females did show an overall age related increase in sucrose preference (Timepoint: *p*<.01), regardless of genotype. Cage scores from pair housed mice used here. Values here represent Mean ± SE. N=19 male cages and N=17 female cages.

Males $F_{1,37}$ = 13.77 p<.001). More specifically, BACHD females consumed 14% more sucrose solution (23.7 ± 0.8mls) than did WT females (20.9 ± 0.9mls) and BACHD males consumed 19% more (26.8 ± 1.1mls) than WT males (22.5 ± 1.2mls). Unlike other rodent HD models, BACHD mice show a paradoxical obesity phenotype (in contrast to the weight loss phenotype shown by patients and other rodent models) which is driven by an overall increase in spontaneous caloric intake (Hult *et al.*, 2011; Kudwa *et al.*, 2013), which could potentially be driving this increase in sucrose consumption shown here. BACHD mice also consumed significantly more water than WT mice (**Supp. Figs. 4.1B and 4.1E**, Genotype: Females $F_{1,41}$ = 18.20 p<.001; Males $F_{1,37}$ = 9.18 p<.01). This was a larger percent increase than for sucrose, with BACHD females consuming 39% more water (5.4 ± 0.3mls) than WT females (3.9 ± 0.2mls) and BACHD males consuming 39% more (4.6 ± 0.4mls) than WT males (3.3 ± 0.2mls). This is consistent with other transgenic HD lines which have been shown to have increased water intake as a part of their phenotype (Wood *et al.*, 2008). Since the increase in water intake is larger magnitude than the increase in sucrose intake in BACHD, it is likely that any detected deficits in sucrose preference in BACHD mice may simply reflect increased water consumption instead of decreased sucrose consumption (**Supp. Fig 4.1C and 4.1F**), as sucrose consumption here is actually increased in BACHD mice, which would negatively impact the validity of the test as an indicator of anhedonia.

Forced Swim Test

To assess the effects of AAV1-Cre mediated mHTT silencing in the anterior cingulate on behavioral despair, another type of depressive-like behavior, mice were assessed for immobility time in the forced swim test. Mice were placed in an inescapable cylinder filled half-way with water, and time spent swimming or floating was quantified over four minutes, after 2 minutes of habituation. Increased time immobile represents increased levels of behavioral despair. As has been shown previously (Hult Lundh *et al.*, 2013; Wang *et al.*, 2014), HD mice spent significantly

more time immobile than wild-type mice (Genotype: $F_{1,66} = 13.54$, $p<.001$) (**Fig. 4.6**). Sex did affect time immobile ($p>.05$ for Sex and all of its interactions). This was slightly more than a two-fold elevation, with HD mice showing 46.5 ± 6.5 seconds of immobility while WT mice were immobile for 21.9 ± 3.8 seconds. Treatment also affected performance in this task (Treatment: $F_{1,66} = 9.50$, $p<.01$) – AAV1-Cre treated mice showed significantly lower immobility time (23.6 ± 3.9 seconds) relative to AAV-GFP treated controls (43.4 ± 6.4 seconds). Given that AAV-Cre treatment should have a specific genetic effect in BACHD transgenic mice, by inactivating the mHTT transgene, it was of particular interest to assess whether there was a significant interaction between treatment and genotype, and reason to believe that there would be a differential response to AAV-Cre treatment between the two genotypes. There was a trend for an interaction (Treatment*Genotype: $F_{1,66} = 3.69$, p=.0591), with Cre-HD mice showing a 53% reduction in immobility time (29.8 ± 6.6 seconds) relative to AAV1-GFP treated HD mice (63.2 ± 10.0 seconds). WT mice showed even lower immobility times, with AAV1-Cre treated mice spending 18.1 ± 4.8 seconds immobile and AAV-GFP treated mice spending 25.8 ± 5.7 seconds immobile. Given that the a-priori hypothesis for this experiment was that AAV1-Cre treatment would selectively improve/normalize forced swim test performance in BACHD mice, but not WT mice, a Tukey's posthoc comparison was run to compare differences in subgroups following the trending finding of a Treatment*Genotype interaction. Tukey's comparisons indicate that AAV1-Cre treated BACHD mice have 'significantly' reduced immobility time relative to AAV1-GFP treated BACHD mice, but are not significantly different from WT mice on either treatment. Tukey's comparisons also indicated that AAV1-Cre and AAV1-GFP treated WT mice were not different from each other.

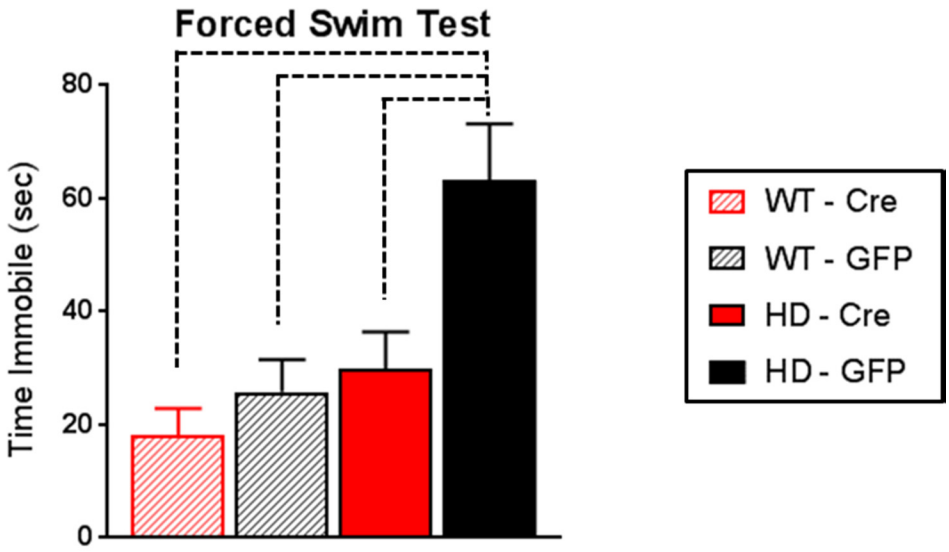

Figure 4.6 – Forced Swim Test. Mice were tested for the effect of intra-cingulate AAV1-Cre treatment on behavioral despair, a depressive-like behavior, in the Forced Swim Test. HD mice showed increased behavioral despair, relative to WT mice, as indicated by increased time immobile (Genotype - p<.001). AAV1-Cre treatment resulted in a reduction in immobility time relative to AAV-GFP treated mice (Treatment - *p*<.01). There was also a statistical trend for a Treatment*Genotype interaction (*p*=.059), and Tukey's posthoc comparisons indicate (dotted lines) that AAV1-Cre treated transgenic BACHD mice show a reduction in immobility time relative to AAV1-GFP treated transgenics, but are not different from WT mice receiving either AAV1-Cre or AAV1-GFP injections. Data is collapsed across sex, as there was no effect of sex or its interactions on immobility (*p*>.05). Values here represent Mean ± SE. N=37M and N=33F.

4.4 - Discussion

Of the four domains of Huntington's disease (HD) symptomology (motor, cognitive, mood, and metabolism), psychiatric symptoms have the most deleterious impact on quality of life for patients (Anderson & Marder, 2001; Ho *et al.*, 2009). Thus, it is striking that the neurobiological mechanisms that underlie this symptomology are the most poorly understood. However, there is recent human clinical (Hobbs *et al.*, 2011; Sprengelmeyer *et al.*, 2014) and neuropathological data (Kim *et al.*, 2014; Thu *et al.*, 2010) which suggest that pathology in the anterior cingulate cortex (ACC) may contribute to HD mood symptoms. One limitation to these human data is that it is correlational in nature - while it establishes a relationship between the anterior cingulate and HD mood symptoms, it does not demonstrate that pathology in this structure is causal to these symptoms. Thus, here in Chapter 4, I further assessed whether or not ACC pathology in HD is causal to HD mood symptoms by utilizing an animal model which enables this type of controlled experiment. I also further characterized which specific subtypes of mood symptoms may be associated with ACC pathology (i.e. is it associated with particular types of depressive symptoms, such as anhedonia, or with depressive and/or anxiety symptoms broadly). Thus, I tested the hypothesis that inactivation of the mutant Huntingtin (mHTT) transgene in the ACC, utilizing a molecular genetic approach (AAV1-Cre injections), would ameliorate depressive- and anxiety-like behavior in the transgenic BACHD mouse model, which carry a floxed mHTT transgene that can be excised by Cre recombinase (Gray *et al.*, 2008; Wang *et al.*, 2014). These data from this study provide preliminary evidence that mHTT pathology in the cingulate contributes is indeed causal to particular components of HD mood symptomology – that it contributes to behavioral despair, a type of depressive-like behavior, but that it does not contribute to anxiety-like symptomology. Anhedonia, another type of depressive-like behavior was also assessed here, but the effect of

mHTT inactivation in the ACC on this symptomology is inconclusive, as the BACHD model did not demonstrate a clear and robust phenotype in this study.

Behavioral despair, as reflected by increased immobility in the forced swim test, is a behavioral indicator of depressive-like symptomology in animal models and is the standard tool for screening novel anti-depressant medications (Lopez-Rubalcava & Lucki, 2000; Porsolt, Bertin*, et al.*, 1977; Porsolt, Le Pichon*, et al.*, 1977). BACHD mice have well documented deficits in the forced swim test, showing roughly a 3-fold elevation in immobility time (Hult Lundh *et al.*, 2013; Wang *et al.*, 2014) and BACHD mice in this study robustly demonstrated this phenotype (**Fig. 4.6**). Although preliminary (it is only a statistical trend, p=.059), AAV1-Cre mediated inactivation of mHTT in the ACC led to a reduction in immobility time in BACHD mice. Tukey's post-hoc comparisons demonstrate that AAV1-Cre treated BACHD mice showed reduced immobility relative to AAV1-GFP treated BACHD controls, and that their level of immobility was not different from WT mice treated with either AAV-Cre or AAV-GFP (**Fig 4.6**). Rodent studies have previously implicated the ACC in behavioral despair: lesion studies show that damage in the ACC in rats (specifically in the ventral infralimbic and prelimbic cortices, homologous the human subgenual ACC) leads to increased immobility in the forced swim test (Chang *et al.*, 2014). Thus, it is logical that mHTT pathology in the ACC would lead to a behavioral despair phenotype, and that reducing mHTT toxicity in this region alone could normalize this behavior towards WT levels. However, although this is a preliminary finding (as the fixed effect is only a statistical trend), if replicated and confirmed statistically, it would extend the human clinical findings and demonstrate that ACC pathology directly contributes to HD mood symptomology and that it is not only circumstantially correlated with it.

The premise of the experimental design here is that that there should be a particular biological interaction between genotype and treatment in this experiment, with AAV1-Cre

treatment leading to a reduction in mHTT expression in the ACC in transgenic BACHD mice, but have negligible effects in WT mice which do not carry a floxed gene. Thus, it was surprising that in the forced swim test here, that there was a significant statistical effect of AAV-Cre treatment on forced swim test performance, regardless of genotype. Mean immobility times were indeed reduced in mice of both genotypes treated with AAV-Cre, although by a much larger magnitude in BACHD mice (reduced by 29.5 seconds) than in WT mice (reduced by 5.8 seconds). However, the Tukey's posthoc comparisons from the genotype*treatment trend suggest that the robust effect of AAV-Cre treatment in BACHD mice may be driving the statistical finding of an overall treatment associated reduction in immobility.

Anhedonia, a lack of pleasure or interest in things that an individual typically finds pleasurable, is one of the core features of clinical depression (American Psychiatric Association, 2013). In order to further assess the effects of mHTT inactivation in the ACC on HD mood symptoms, mice were also assessed in the sucrose preference test, a measure of anhedonia used in rodent models. Robust sucrose preference deficits have been consistently demonstrated in a variety of transgenic HD mouse models (Pla *et al.*, 2014; Pouladi *et al.*, 2009; Renoir *et al.*, 2011), including the BACHD model, although this was only demonstrated in a single study (Hult Lundh *et al.*, 2013). However, here there was only a small and transient deficit in sucrose preference detected in female BACHD mice, which attenuated over the course of the experiment (**Fig. 4.5**). This improvement in phenotype occurred in both AAV1-Cre and AAV1-GFP treated female mice, and thus was not due to treatment. Male BACHD mice showed no deficit whatsoever. Given the lack of a phenotype in males, and the small transient deficit in females, this test did not serve as a good indicator of depressive-like behavior in this study, and thus, unfortunately wasn't a suitable test for the ability of mHTT inactivation in the ACC to improve HD mood symptoms.

It is unclear why these data disagree with the previously published sucrose preference findings from Hult Lundh *et al.* (2013). It also unclear which study better indicates the actual phenotype of BACHD mice. The parameters were similar for both experiments, including a sustained habituation to two bottles of water before the subjects were presented with the actual test with one bottle of sucrose and one bottle of water. Mice were housed in same sex and same genotype pairs in both studies. Preference data were averaged over two days here, while it was averaged over 3 days by Hult Lundh *et al.* (2013). While a slight difference in duration is unlikely to have impacted the findings, there were three other differences in experimental design that more plausibly could have impacted the outcome. First - a 2% sucrose solution was used in the test here, while a 1% solution was used in the Hult Lundh *et al.* (2013) study. Perhaps BACHD mice habituate to a higher percentage of sucrose, or find more nutritional value with the higher caloric qualities of the 2% solution. Second - bottles were alternated between left and right positions in the cage in this study between day 1 and 2 of testing, to avoid any potential confound of side-bias, but not alternated in the Hult Lundh *et al.* (2013) study. It is possible that BACHD mice showed more side bias coinciding with the water bottle position in the Hult Lundh *et al.* (2013) study, which inadvertently skewed the data to suppress values for sucrose intake/preference. Third, data from singly housed mice were included in the Hult Lundh *et al.* (2013) study, which was due to male mice being separated due to aggression. Transgenic male BACHD mice are particularly aggressive and often must be housed in isolation in our colony due to fighting and severe wounding of cage mates (personal observation). In this study, all included mice were pair housed throughout the entirety of the study. This is an important difference, as isolation housing will induce depressive-like behavior, including increased immobility in the forced swim test and reduced sucrose preference (Takatsu-Coleman *et al.*, 2013). It is possible that the deficits in

sucrose preference in the Hult Lundh *et al.* (2013) study resulted from isolation induced anhedonia, which would likely be limited to the very aggressive transgenic male BACHD mice.

Regardless of whether or not sucrose preference deficits are a true and replicable phenotype in BACHD mice, they likely have poor validity as an indicator of anhedonia in this transgenic model, and thus of depressive-like behavior generally. The rationale for this claim is outlined in **Supplemental Figure 4.1**, which demonstrates that BACHD mice showed increased fluid intake, including a large increase water consumption and a smaller increase in 2% sucrose consumption in this study. Thus, it is entirely possible that a sucrose preference deficit could be driven by the dramatic increase in water intake, instead of a decreased interest or pleasure in sucrose (e.g. anhedonia) as this measure is intended to indicate. In fact, female BACHD mice here that showed a mild deficit in sucrose preference actually had an increase in total sucrose consumption relative to WT females. Furthermore, BACHD mice show a paradoxical obesity phenotype (Hult *et al.*, 2011), in contrast to the weight-loss phenotype shown in human HD patients (Aziz *et al.*, 2008; Djousse *et al.*, 2002; Trejo *et al.*, 2004) and most other transgenic HD mouse models (Goodman *et al.*, 2008; van der Burg *et al.*, 2008). BACHD mice have a voluntary increase in caloric intake as a part of their phenotype (Hult *et al.*, 2011), and food restriction normalizes their weights close to wild-type levels (although not completely – other metabolic abnormalities also contribute) (Kudwa *et al.*, 2013). It is hard to distinguish between the animals motivation for caloric intake, which is likely elevated in BACHD mice, with the hedonic properties of a 2% sucrose solution to these mice. This confound in nutritional/hedonic motivation, in addition to increased water intake as a part of their phenotype, likely renders the sucrose preference test as an unreliable measure for anhedonia in this particular HD model.

Increases in anxiety-like behavior are a robust and consistent finding in BACHD mice and unlike sucrose preference measures, these findings have been replicated many times (Hult Lundh

et al., 2013; Menalled *et al.*, 2009; Soylu-Kucharz *et al.*, 2016; Wang *et al.*, 2014). Consistent with these studies, performance in the light dark test in this experiment indicated a robust anxiety-like phenotype in BACHD mice. However, this phenotype was not impacted by AAV1-Cre treatment, suggesting that mHTT pathology in the ACC of BACHD mice is not solely responsible for anxiety-like behavior. Thus, these findings do not support my original hypothesis that mHTT inactivation in the ACC would reduce anxiety-like behavior in a transgenic mouse model of HD. The most parsimonious explanation for this discrepancy is that anxiety symptoms in BACHD mice are not due to mHTT toxicity in the ACC, but are instead driven by toxicity in another brain region (or in multiple other brain regions). For instance, it is possible that the anxiety phenotype is driven by simultaneous mHTT induced alterations in monoamine circuitry to the ACC, and that silencing mHTT expression in the entire circuit would be essential to ameliorate the phenotype. There is pathology in human HD in both the amygdala (Kipps *et al.*, 2007; Mason *et al.*, 2015) and the locus coeruleus (Zweig *et al.*, 1992), and both regions are implicated in anxiety disorders (Ressler & Nemeroff, 2000; Shin & Liberzon, 2010). Another possible locus is the orbitofrontal cortex, which is altered in human obsessive compulsive disorder (Chamberlain *et al.*, 2008; Graybiel & Rauch, 2000) and other anxiety disorders (Milad & Rauch, 2007; Ressler & Nemeroff, 2000) as well as in HD (Feigin *et al.*, 2006; Ille *et al.*, 2011). As mentioned previously, Wang and colleagues (2014) found that widespread silencing of mHTT throughout the cortex fully rescued anxiety-like behavior in BACHD mice, which suggests that perhaps another cortical region is responsible for this symptomology. Given this finding, as well as the data from this study excluding the ACC, the OFC would be a good candidate as the putative substrate for anxiety symptoms in BACHD mice, which could be assessed in future studies. However, there is a limitation to the Wang *et al.* (2014) study - while the authors claimed that the Emx1-Cre line that they crossed with BACHD mice resulted in selective cortical silencing, the Emx1 promoter also drives significant Cre expression in

the septum, amygdala, and hippocampus (Gorski *et al.*, 2002), all of which are implicated in anxiety symptoms (Parfitt *et al.*, 2017; Shin & Liberzon, 2010). Thus, it is possible that Emx1-Cre mediated mHTT silencing in one of these other regions was responsible for an improvement in anxiety-like behavior in the Wang *et al.* (2014) study. Another possible scenario that would explain these findings is that perhaps mHTT pathology in the ACC does mediate an anxiety phenotype, but that there was simply an insufficient level of mHTT silencing in the ACC here to result in a significant improvement in this symptom. However, given that there was a robust 70% reduction in mHTT mRNA levels, it is unlikely (but not impossible) that this was insufficient to rescue this phenotype.

The overall findings from this study provide preliminary evidence that mHTT toxicity in the ACC contributes to some depressive symptomology (behavioral despair) in HD, but not anxiety. One important aspect of this finding is that it extends the correlational human clinical and neuropathological HD findings, and demonstrates that there is a causal relationship between ACC pathology and depressive symptomology. Furthermore, these data help to refine the interpretation of these clinical studies, which typically compared populations of HD patients with or without mood symptomology, without distinguishing between anxiety and depressive symptoms. Given that depressive- and anxiety symptoms are incredibly comorbid in psychiatric populations, it is hard to distinguish these two types of symptoms in clinical populations. The results of this study suggest that while ACC pathology is correlated with a particular type of depressive symptomology (behavioral despair) since it is causal to such symptoms, it is only circumstantially correlated with anxiety symptomology. Another application of the findings here is that it validates the BACHD model as a tool to further assess the mechanisms of ACC pathology in HD depressive symptomology. For instance, this allows the further studies in BACHD to identify which subpopulations of ACC neurons are affected, how they are affected (e.g. alterations in

electrical properties, firing rates, and/or transcription), and why they are affected in some individuals but not others leading to symptom heterogeneity. The most exciting application of this finding is that it identifies the ACC as a novel point of therapeutic intervention to improve depressive symptomology in HD patients. This is important as gene silencing therapies, such as RNA interference therapeutics (Dufour *et al.*, 2014; Harper *et al.*, 2005; Kordasiewicz *et al.*, 2012; McBride *et al.*, 2008; McBride *et al.*, 2011; Stanek *et al.*, 2014), are moving into clinical trials (Wild & Tabrizi, 2017). Ideally, this finding will emphasize that the ACC is an important target for such therapies and should be incorporated into this therapeutic approach to offer a more comprehensive improvement in HD clinical symptomology.

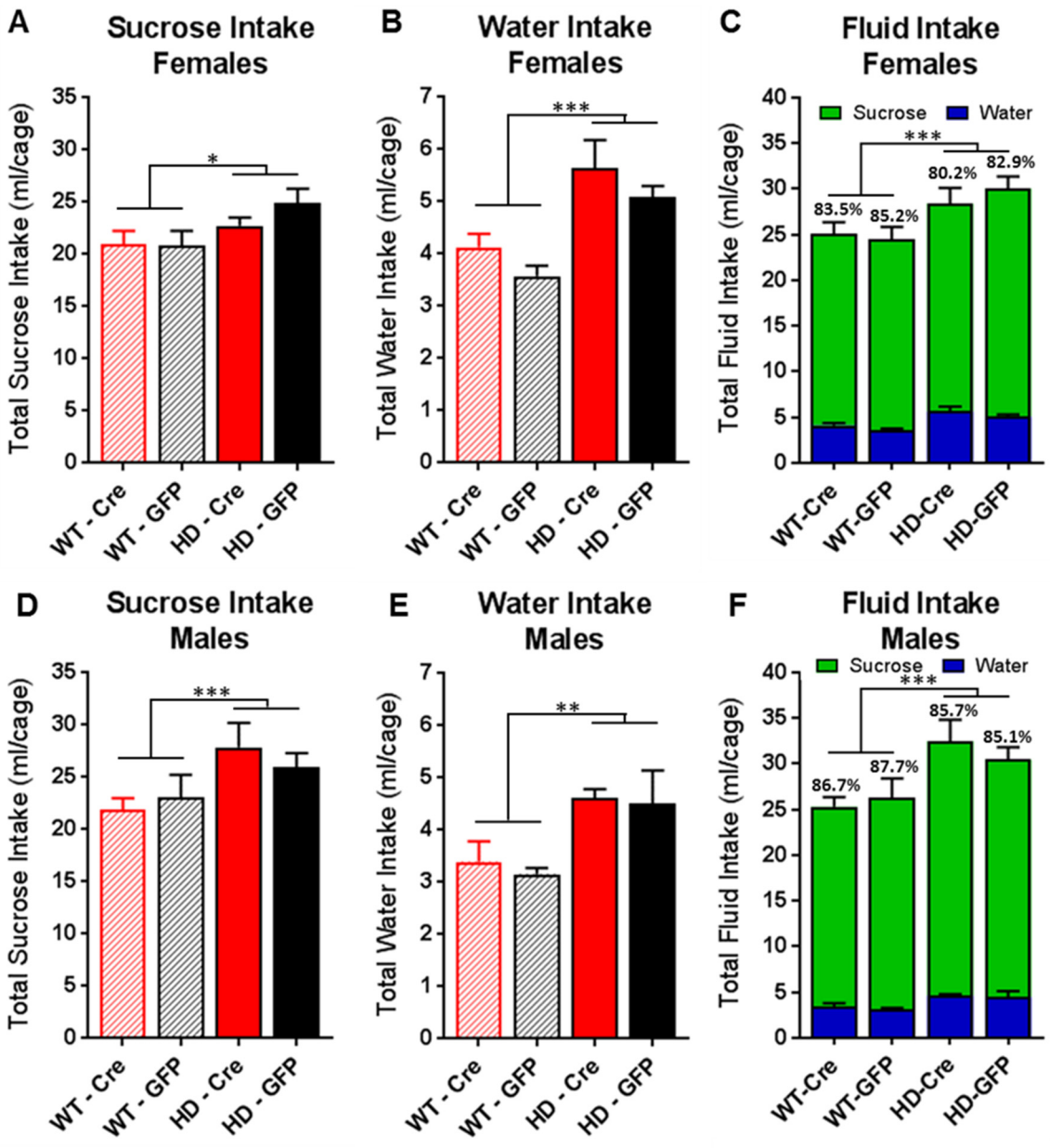

Supplemental Figure 4.1 – Sucrose Preference Fluid Intake. Total intake of sucrose, water and overall fluid was quantified from the sucrose preference test over 48 hours, for each cage. Mice were pair-housed (same sex, genotype, treatment in each cage) to avoid an isolation-induced reduction in sucrose preference. Although there were only significant differences in sucrose preference in female BACHD cages, relative to female WT cages, both male and female BACHD mice showed increased sucrose intake (A,D – Genotype $p<.05$) as well as increased water intake (B,E – Genotype $p<.05$) relative to WT mice. Accordingly, they also showed increases in overall fluid intake (C,F – Genotype $p<.05$). Data are collapsed across timepoint. Values represent Mean ± SE. In C and F, values above bars indicate sucrose percent preference. N=19 male cages and N=17 female cages. *P*-values for genotype fixed effects are indicated by *$p<.05$, **$p<.01$, ***$p<.001$

Chapter 5 – Discussion

The prognosis for patients with Huntington's disease (HD) is incredibly poor. This genetic neurological disorder onsets in midlife, causing a wide spectrum of severe and debilitating symptoms, progresses over 10-15 years, and always leads to death (Ross *et al.*, 2014). There are no currently approved therapeutics that can delay the onset or slow the progression of the disease in any way (Ross *et al.*, 2014; Travessa *et al.*, 2017; Wild & Tabrizi, 2017). Thus, there is tremendous need to discover new therapeutic approaches that can slow or halt disease progression and thereby improve quality of life for patients. Inherent to this goal is to develop a better understanding of how mutant huntingtin toxicity leads to pathology, and thus generates the clinical symptom profile of the disease. By better understanding these processes, novel points of therapeutic intervention can be identified and targeted with novel experimental treatments. The overarching goal of the studies presented here was to characterize two novel therapeutic approaches for Huntington's disease, targeting two separate disease pathways.

In the first set of experiments (Chapters 2 and 3) I assessed whether elevated glucocorticoid levels, itself a symptom of HD, contributed to the progression of HD symptoms. In the first subset of these experiments, presented in Chapter 2, I was able to confirm that the R6/2 mouse model does show elevated corticosterone levels, that the pattern of release is dysregulated, and that elevated corticosterone leads to severe weight loss and a significantly shorter latency to death. In a second set of experiments, presented in Chapter 3, I demonstrated that the converse is also true – that normalizing (i.e. lowering) glucocorticoids to wildtype levels in R6/2 HD mice significantly improves HD metabolic and HD neuropathological symptoms. In the final set of experiments, presented in Chapter 4, I assessed whether mHTT pathology in the

anterior cingulate cortex contributes to HD mood symptoms in the BACHD mouse model. From this investigation, I was able to demonstrate that silencing mHTT expression in the ACC improves depressive symptomology, but not anxiety symptoms, suggesting that huntingtin lowering therapies that target the ACC could be beneficial in improving depressive symptomology in patients.

5.1 - Glucocorticoids and HD Symptomology: Summary and Therapeutic Applications

It has long been known that glucocorticoid levels are elevated in HD patients (Bjorkqvist *et al.*, 2006a; Heuser *et al.*, 1991; Saleh *et al.*, 2009; Shirbin, Chua, Churchyard, Hannan*, et al.*, 2013), and it has long been speculated that this elevation contributes to HD symptomology (Petersen & Bjorkqvist, 2006; Saleh *et al.*, 2009; Shirbin, Chua, Churchyard, Hannan*, et al.*, 2013). However, evidence of a direct causal relationship between hypercortisolinemia and HD symptomology was previously lacking. There are a handful of human clinical studies that have demonstrated an inverse correlation between plasma cortisol levels and HD cognitive (Shirbin, Chua, Churchyard, Hannan*, et al.*, 2013) and metabolic symptoms (Saleh *et al.*, 2009), as well as a handful of studies in transgenic mouse models showing that experimental elevations in corticosterone can also worsen HD cognitive and metabolic symptomology (Mo, Pang*, et al.*, 2014; Mo *et al.*, 2013). However, it was previously unclear if chronically elevated glucocorticoids, within the range commonly experienced by HD models and in patients, directly contributes to symptoms. To address this question, I manipulated the levels of circulating glucocorticoid levels in the R6/2 HD mouse model by performing adrenalectomies and providing subjects with differing levels of corticosterone replacement (a normal WT level of CORT replacement and high-dose HD-level CORT replacement). Through these experiments, reported in Chapters 2 and 3 of this dissertation, I was able to demonstrate that chronically elevated glucocorticoid levels do in fact worsen HD

symptomology, and that normalizing glucocorticoids to WT levels can attenuate some HD symptoms.

While adrenalectomy with cortisol replacement is not a practical or ideal therapeutic approach for human disease, reducing the deleterious consequences of chronic hypercortisolinemia by blocking glucocorticoid receptors is a more plausible strategy. Mifepristone, a glucocorticoid receptor (GR) antagonist, is an existing FDA-approved therapeutic that is clinically used to treat Cushing's disease symptoms (Fleseriu *et al.*, 2012; Morgan & Laufgraben, 2013). It is possible that mifepristone could also show efficacy in clinical populations for treating HD symptoms that are associated with chronically elevated cortisol. The findings from Chapters 2 and 3 illustrate the some of the possible benefits that mifepristone could provide for HD patients.

In Chapter 2 I demonstrated that exceedingly high levels of glucocorticoids interact with the HD phenotype, significantly exacerbating weight loss and further shortening the lifespan of R6/2 mice. WT mice did not lose weight, nor did they have a shortened lifespan within the age range investigated, demonstrating that these effects represent an interaction of glucocorticoid treatment with the HD genotype. The survivorship data are particularly interesting as they suggest that blocking GR signaling could possibly extend lifespan for patients. This would be one of the most beneficial possible outcomes of mifepristone therapy, as there are currently no medications that can extend lifespan in HD (Ross *et al.*, 2014; Ross & Tabrizi, 2011; Wild & Tabrizi, 2017). However, as the high dose (HD-level) CORT replacement was exceedingly high in the Chapter 2 experiment, this hastened time to death may only associated with exceedingly high levels of glucocorticoids that are outside of the typical HD physiological range. However, it would still be of interest as an outcome measure if mifepristone is investigated clinically as an HD therapeutic.

In the Chapter 3 experiments, I refined the dose of the HD-level (high dose) CORT replacement to a more physiologically relevant level, based on a circadian analysis of glucocorticoid levels in R6/2 mice which is outlined in Chapter 2. While the HD-level dose was now closer to the typical physiological HD range, it still resulted in further worsening of the R6/2 weight loss phenotype like it did in Chapter 2. This demonstrates that the HD weight loss phenotype is particularly sensitive to elevations in glucocorticoids and that blocking GRs with mifepristone could possibly attenuate weight loss symptomology in HD patients. Furthermore, normalized glucocorticoid levels (WT-level replacement) in R6/2 male mice led to a significant improvement in indirect calorimetry readouts, demonstrating that the elevated metabolic rate shown by R6/2 mice (Bjorkqvist *et al.*, 2006a; Goodman *et al.*, 2008) is exacerbated by elevated glucocorticoids and rescued by its normalization. It is interesting that elevated glucocorticoids did not affect metabolic rate in WT mice, again demonstrating that there was a specific interaction of glucocorticoids with the HD phenotype. Brain atrophy and skeletal muscle wasting are two well characterized phenotypes in clinical HD (Kosinski *et al.*, 2007; Rosas *et al.*, 2003; Tabrizi *et al.*, 2009; Trejo *et al.*, 2004; Vonsattel *et al.*, 1985) that are replicated by the R6/2 mouse model (Chaturvedi *et al.*, 2009; Ribchester *et al.*, 2004; Strand *et al.*, 2005; Zhang *et al.*, 2010). Normalized glucocorticoid levels attenuated brain atrophy in females and skeletal muscle wasting in both male and female R6/2 mice, suggesting that mifepristone could possibly attenuate these symptoms in human patients. It is interesting that females were specifically responsive to glucocorticoids with respect to brain mass, as normalized glucocorticoids also led to a female-specific improvement in HD neuropathology. In particular, the normalization of glucocorticoid levels resulted in a 50-70% reduction in the number of inclusions in the striatum and dentate gyrus as well as a 20-27% reduction in inclusion size in the cingulate and motor cortices. Low dose (WT-level) glucocorticoid replacement was also associated with an increase in dentate gyrus

neurogenesis in females, which is impaired in R6/2 mice. This provides preliminary evidence that mifepristone could possibly slow the clinical progression of HD neuropathology, which could have a widespread impact on symptomology and/or the rate of disease progression.

While the normalization of glucocorticoids in these experiments led to an attenuation in a variety of HD symptoms, treatment did not achieve full rescue of any particular symptom measured, with the single exception of the respiratory exchange ratio (RER) deficit in male R6/2 mice. It appears as though the majority of the symptomology assessed here is largely due to the direct effects of mHTT toxicity in the brain or the peripheral tissues themselves, and that chronically elevated glucocorticoids further exacerbates this type of symptomology in-vivo. Skeletal muscle is a good example – mHTT is expressed in this tissue, directly leading to inclusion formation, transcriptional alterations, oxidative stress, intra-cellular metabolic impairment, and cell death (Chaturvedi *et al.*, 2009; Moffitt *et al.*, 2009; Strand *et al.*, 2005). Chronically elevated glucocorticoids maintain an organism in a chronic catabolic state (directly mediated by the transcriptional effects of GR signaling) whereby there is widespread breakdown of protein to liberate amino acids for gluconeogenesis (Lofberg *et al.*, 2002; Sapolsky *et al.*, 2000; Weinstein *et al.*, 1995), eventually leading to skeletal muscle wasting and cell death (Grossberg *et al.*, 2010; Lee *et al.*, 2005; Lofberg *et al.*, 2002). Thus, while mHTT toxicity is likely sufficient to bring about muscle pathology, including muscle wasting and cell death, the overall clinical symptomology is likely enhanced by the synergistic effects of chronically elevated glucocorticoids. Accordingly, while mifepristone could possibly reduce HD symptom severity, or possibly slow symptom progression, it is unlikely that it could fully remedy any particular symptom domain. While the data from these adrenalectomy experiments provide proof of concept that glucocorticoids worsen HD symptoms, and conversely that the normalization of glucocorticoid levels can attenuate symptoms, it is hard to directly translate the magnitude of improvement in mice here

with how well mifepristone could improve symptoms clinically in human HD patients. It is possible that human patients could show more robust improvement than did R6/2 mice here, as R6/2 mice show a particularly aggressive phenotype that leads to robust symptomology and death over 12-14 weeks (Mangiarini *et al.*, 1996; Menalled *et al.*, 2009). While human patients also show robust symptomology and premature death, the process is much more protracted (progressing over 15 years after decades of being latent) and thus there may be a larger therapeutic window whereby glucocorticoid treatment could ameliorate symptoms. Conversely, it also possible that human patients would be less responsive to treatment than were R6/2 mice. This has been the case for many experimental drugs that showed efficacy in reducing symptoms in rodent HD models but ultimately failed in clinical trials (McColgan & Tabrizi, 2017; Rodrigues & Wild, 2017; Stack & Ferrante, 2007; Travessa *et al.*, 2017). However, this is all an empirical question, which can really only be clarified by testing the efficacy of mifepristone in treating HD symptoms in a clinical population.

Due to limitations in the R6/2 model, the role of chronically elevated glucocorticoids in HD psychiatric and cognitive symptoms were not investigated here. As chronically elevated glucocorticoids are sufficient to cause both psychiatric (particularly mood) and cognitive symptoms (Starkman *et al.*, 1981), it remains an outstanding question as to whether or not normalizing glucocorticoids could ameliorate these symptoms that also occur in HD. The R6/2 model is the only known animal model of HD hypercortisolinemia (Bjorkqvist *et al.*, 2006a), and thus was chosen for these studies as it would enable the assessment of normalizing glucocorticoid levels on HD symptoms. These mice only show a transient increase in depressive-like behavior early in the course of disease (Ciamei *et al.*, 2015), before the age of onset of elevated glucocorticoid levels. Additionally, R6/2 mice show a paradoxical reduction in anxiety-like behavior during symptom progression (Bissonnette *et al.*, 2013; Domenici *et al.*, 2007), in contrast

to the increased levels of anxiety shown by patients (Anderson & Marder, 2001) and other rodent models (Hult Lundh *et al.*, 2013; Wang *et al.*, 2014). Accordingly, these mood phenotypes in R6/2 mice show poor construct and predictive validity for the potential effects of the normalization of glucocorticoids in human HD, and were thus not investigated here. While R6/2 mice have been shown to have cognitive deficits reminiscent of human HD, including deficits in executive function, cognitive assessments have largely been assessed in swim tests (e.g. swim tank t-maze and morris water maze) in spite of the progressive motor symptoms shown in these mice (Lione *et al.*, 1999; Wood *et al.*, 2010). To assess cognition with non-swimming based cognitive tasks, R6/2 mice must be significantly food restricted (Lione *et al.*, 1999; Oakeshott *et al.*, 2011). As food restriction would have likely impacted the metabolic phenotype of these mice, cognitive measures were omitted from the studies described in this dissertation. Accordingly, it remains an open question as to whether or not the normalization of glucocorticoids could improve cognitive symptoms in HD, and to what degree they could improve it. However, there are correlational clinical data that suggest that elevated glucocorticoids worsen cognitive symptoms in HD (Shirbin, Chua, Churchyard, Hannan*, et al.*, 2013), and thus it would be interesting to assess the effect of mifepristone on both cognitive and mood symptoms in a clinical HD population.

Although mifepristone has shown to be safe and effective in a non-HD population (Cushing's patients) (Fleseriu *et al.*, 2012; Morgan & Laufgraben, 2013), it will be important to assess whether or not HD patients may be more negatively impacted by the side-effects of the medication. This is particularly important as the drug not only has potent glucocorticoid receptor antagonist properties, it is also a potent progesterone receptor antagonist (Morgan & Laufgraben, 2013). Another complication is that mifepristone is metabolized by Cytochrome P3A and thus has pharmacokinetic interactions with a variety of other drugs metabolized by this route (Morgan & Laufgraben, 2013), which could be complicated by the use of other off-label pharmacotherapies

in HD patients. Thus, it will be important to assess both safety, as well as efficacy, in a clinical HD population to truly know whether or not mifepristone is a plausible therapeutic approach to treat some of the symptoms of HD, and possibly slow disease progression.

5.2 - The ACC and HD Mood Symptoms: Summary and Therapeutic Applications

RNA-interference therapeutics are a promising approach for treating HD, whereby molecular tools (i.e. antisense oligonucleotides, microRNAs) are used to silence the disease-causing mutant huntingtin gene, and thereby stop the pathological process before it has caused widespread tissue damage and global symptomology (Harper *et al.*, 2005; Kordasiewicz *et al.*, 2012; Wild & Tabrizi, 2017). For instance, Harper *et al.* (2005) demonstrated that intra-striatal AAV delivery of an RNAi therapeutic that targets the mHTT gene results in a 50% reduction in mHTT mRNA levels, reduces HD neuropathology, and rescues HD motor symptoms in the N171-82Q HD mouse model. Due to the success of this and similar studies in rodent models and safety in non-human primates (e.g. Boudreau *et al.*, 2009; Franich *et al.*, 2008; Grondin *et al.*, 2012; McBride *et al.*, 2011; Stanek *et al.*, 2014), there is particular interest in adapting this intra-striatal AAV-RNAi therapeutic approach to treat HD motor symptoms in human patients (Wild & Tabrizi, 2017).

However, while intra-striatal AAV-RNAi therapeutics are a logical approach to treat HD motor symptoms, and possibly offer some improvement for cognitive symptoms, it is less likely to treat to other HD symptom domains. Using AAV-RNAi to targeting the neural substrates that mediate other HD symptom domains remain a challenge. This is due in part to the limitations in surgical delivery of AAV-RNAi therapies; for instance, targeting whole cerebral cortex might be necessary for improving widespread cognitive function for HD patients, although it is difficult to target such a large brain region using a traditional viral based strategy. The other difficulty is that the neural substrates that mediate many non-motor HD symptoms remain unclear. This is

particularly true for psychiatric symptoms in HD, which are poorly understood with respect to how neuropathology within a particular brain region (or regions) may underlie them. Accordingly, I wished to further clarify which neural substrate(s) could possibly be contributing to HD psychiatric symptoms, with a particular interest in mood symptomology, which is particularly prevalent and deleterious for HD patients (Anderson & Marder, 2001; Ho *et al.*, 2009). The overarching goal of this line of investigation was to identify a potential target for RNAi therapeutics that would lead to improvement in HD mood symptoms.

There are numerous limbic brain regions affected in HD that could potentially contribute to mood symptoms such as the cortex, amygdala, hippocampus, and brainstem monoamine systems (Bedard *et al.*, 2011; Ransome *et al.*, 2012; Rosas *et al.*, 2008; Zweig *et al.*, 1992). However, there is human clinical imaging (Hobbs *et al.*, 2011; Sprengelmeyer *et al.*, 2014) and neuropathological data (Kim *et al.*, 2014; Thu *et al.*, 2010) that demonstrate a correlation between abnormalities in the anterior cingulate cortex and clinical HD mood symptoms. As these data are correlational, it is unclear whether or not mHTT induced pathology in this region is driving HD mood symptoms, and thus would serve as a suitable target for RNAi therapeutics. Accordingly, in Chapter 4, I assessed the role of the anterior cingulate cortex in HD mood symptoms in the BACHD mouse model of HD to further characterize whether this brain region would be a suitable target to treat HD mood symptoms. The mutant huntingtin transgene in BACHD mice is floxed (exon 1 bearing the CAG repeat expansion is flanked by lox-p sites), enabling the inactivation of the transgene with Cre-recombinase. A Cre-recombinase approach was chosen instead of a miRNA based RNAi approach as Cre-based silencing should be more efficient (theoretically Cre will achieving 100% silencing in transduced cells by excising the transgene instead of partial silencing expected from mRNA degradation by an RNAi construct). These mice also show robust HD mood symptomology, including depressive- and anxiety-like behavior (Hult Lundh *et al.*, 2013; Menalled

et al., 2009; Wang *et al.*, 2014). Thus, BACHD and WT mice were injected with AAV1 vectors expressing either the Cre-recombinase gene and an eGFP reporter, or an eGFP reporter alone, and assessed for the effects of mHTT inactivation in the ACC on mood symptomology (depressive- and anxiety-like behavior).

Silencing mHTT expression in the ACC did result in improvement in some HD mood symptoms in BACHD mice. In particular, AAV1-Cre treatment in the ACC in BACHD mice led to a reduction in immobility time in the forced swim test, an indicator of behavioral despair (a type of depressive-like behavior). AAV1-Cre treatment in the ACC in BACHD mice did not affect their anxiety phenotype, as transgenic mice on either treatment (AAV1-Cre or AAV1-eGFP) showed a similar elevation in time spent in the dark in the light-dark task. Anhedonia, a depressive-like behavior, was also assessed in these subjects with the sucrose preference test. While female BACHD mice showed a small and transient deficit in sucrose preference at early ages, male BACHD mice did not show a deficit. Due to both factors, as well as some limitations in model validity inherent to BACHD mice with respect to this test (e.g. increased water and sucrose intake as a part of their phenotype), the role of HD pathology in the ACC on the hedonic aspects of mood symptomology remains unclear. Together, these data indicate that mHTT pathology in the ACC is causal to some HD depressive symptomology while it does not appear to mediate anxiety symptomology. This provides preliminary evidence that the ACC may be a suitable target for RNAi gene therapy in HD to treat depressive-symptoms. The substrate for anxiety symptoms remains unclear and the assessment of mHTT toxicity in other brain regions on this type of symptomology will hopefully be addressed in future studies to enable its integration into a more comprehensive RNAi therapeutic approach.

5.3 - The Current Status of HD Therapeutics

Currently there are no medications that can slow the progression of Huntington's disease (Ross & Tabrizi, 2011; Travessa *et al.*, 2017). There are only two FDA-approved medications for the treatment of HD symptoms - Tetrabenazine (Huntington Study Group, 2006; Yero & Rey, 2008) and Deutetrabenazine (Huntington Study Group *et al.*, 2016), which can reduce chorea symptoms in patients. Otherwise, specific HD symptoms are typically treated with off-label pharmacotherapies and other types of non-pharmacological management (e.g. high calorie nutritional therapy for weight loss) (Anderson & Marder, 2001; Shoulson & Fahn, 1979; Trejo *et al.*, 2005). While the development of novel therapeutics is of tremendous interest to the field, it has been challenging to successfully identify efficacious therapies for patients (Rodrigues & Wild, 2017; Travessa *et al.*, 2017). Many experimental drugs have been identified that are robustly efficacious in treating HD neuropathological process and symptomology in animal models of the disease, including coenzyme-Q10 and creatine antioxidant therapies (Andreassen *et al.*, 2001; Beal *et al.*, 1994; Ferrante *et al.*, 2002; Ferrante *et al.*, 2000; Schilling *et al.*, 2001; Stack *et al.*, 2006), phosphodiesterase 10A inhibitors (Giampa *et al.*, 2009), minocycline (Chen *et al.*, 2000; Stack *et al.*, 2006), and pridopidine (Squitieri *et al.*, 2015). However, every one of these treatments ultimately failed in clinical trials, largely due to a lack of efficacy (Hersch *et al.*, 2017; Huntington Study Group, 2010; McColgan & Tabrizi, 2017; McGarry, Kieburtz*, et al.*, 2017; McGarry, McDermott*, et al.*, 2017; Rodrigues & Wild, 2017; Travessa *et al.*, 2017). While there are still other pharmacotherapies currently in clinical trials for the treatment of HD (Rodrigues & Wild, 2017), it is unclear if any will provide benefit to patients. This is likely due to the widespread nature and severe toxicity associated with mutant huntingtin protein. While a variety of drugs have been demonstrated to attenuate some of the downstream deleterious consequences of mHTT toxicity

on cell, molecular, and systems-level physiology, it appears as though this toxicity is difficult to overcome in clinically significant levels through pharmacotherapies alone.

Although traditional pharmaceutical development for HD therapies has been largely disappointing, there has recently been a dramatic change in the development of novel therapeutics for HD. This due to the maturation of molecular therapies, such as RNA interference, which directly reduce expression of mHTT and thus prevent the ability for mHTT to manifest its toxicity (Harper *et al.*, 2005; Kordasiewicz *et al.*, 2012). By silencing the HD gene, these therapeutics have the ability to block the onset of overt pathology and clinical symptomology (Harper *et al.*, 2005). These types of therapeutics have shown robust efficacy in HD animal models for over 10 years (Boudreau & Davidson, 2010; Boudreau *et al.*, 2009; Grondin *et al.*, 2012; Harper *et al.*, 2005; Kordasiewicz *et al.*, 2012; McBride *et al.*, 2011; Stanek *et al.*, 2014), and the first clinical RNAi therapeutic for HD (IONIS-HTT_{RX}) is currently under FDA investigation as an investigational new drug (Rodrigues & Wild, 2017; Wild & Tabrizi, 2017). IONIS-HTT_{RX} is an antisense oligonucleotide (ASO) that targets HTT mRNA, which is infused intrathecally, to hopefully achieve widespread CNS silencing of mHTT expression in patients. It has completed phases I and IIa, has shown to be safe and well tolerated, and is currently moving into phase IIb for larger trials to assess efficacy and to further assess safety. While the progress of the IONIS-HTT_{RX} trial is incredibly promising, there are also other RNAi and gene-modifying therapeutic approaches that are moving towards clinical trials (Wild & Tabrizi, 2017), including miRNA-based intra-striatal AAV-RNAi gene therapy (Grondin *et al.*, 2012; McBride *et al.*, 2011; Samaranch *et al.*, 2017), AAV-delivered zinc-finger transcriptional repressors (Agustin-Pavon *et al.*, 2016; Garriga-Canut *et al.*, 2012), and AAV-delivered Crispr-Cas9 gene editing to reduce the number of CAG repeats in the *mHTT* gene (Monteys *et al.*, 2017; Shin *et al.*, 2016).

While these experimental therapeutics are exciting and promising, there are limitations and challenges in their development relating to their safety and efficacy. For RNAi therapeutics, including ASOs and miRNA based therapies, most experimental constructs will silence both the wild-type as well as the mutant huntingtin alleles (Wild & Tabrizi, 2017), as it is difficult to differentiate between these sequences using short antisense sequences. While partial silencing of wild-type HTT has been shown to be safe and tolerable in rodents (Boudreau *et al.*, 2009; Drouet *et al.*, 2009) and rhesus macaques (McBride *et al.*, 2011), it is not ideal and could potentially affect the ability to dose these RNAi therapeutics adequately. Another challenge is that unlike a traditional pharmacotherapy, AAV-based gene therapies are irreversible and thus would be problematic if they result in toxicity. However, while ASOs would likely avoid these complications associated with viral vectors – they have their own limitations. It remains to be determined whether intrathecal delivery of ASOs will achieve widespread reductions in HTT mRNA throughout the CNS; in larger animal models they tend to penetrate into the cortex well but fail to penetrate into subcortical structures such as the striatum (Kordasiewicz *et al.*, 2012).

Optimizing these therapies so that they can provide widespread symptom relief for HD patients will require a comprehensive understanding of how mHTT toxicity in particular brain regions and peripheral tissues lead to the development of particular clinical symptoms. Doing so will enable researchers and clinicians to choose an ideal type of molecular tool (i.e. RNAi, ASOs, zinc-finger nucleases) and an appropriate route of surgical delivery (i.e. intrathecal ASOs, intracranial delivery of AAV-RNAi, etc.) that will target the particularly affected tissues that lead to clinical symptomology. For instance, while intra-striatal AAV-RNAi would likely lead to robust improvement in motor symptoms, and possibly some improvement in cognitive symptoms, it would be unlikely to improve psychiatric and metabolic symptoms of the disease in any meaningful way. As a comprehensive understanding for the biological basis of many non-motor

HD symptoms is lacking, it remains unclear which regions of the brain and periphery will need to be targeted, in addition to the striatum.

For these reasons, I wished to focus the studies of this dissertation on the characterization two different systems in HD that may be driving clinical symptomology, with the overarching goal to identify whether they would serve as novel points for therapeutic intervention in HD. Accordingly, I assessed the role of glucocorticoids and the anterior cingulate cortex in the progression of HD metabolic, neuropathological, and psychiatric symptomology. In Chapters 2 and 3, I was able to show that glucocorticoid dysregulation in HD exacerbates both metabolic and neuropathological symptoms, although it does not appear to drive any particular symptom alone. These findings may inform the development of novel therapeutics in two ways. First, it demonstrates that hypercortisolinemia in HD is one symptom that should ultimately be addressed as a part of a comprehensive gene therapy strategy in HD. It also highlights that mHTT toxicity in the periphery likely contributes to the overall clinical profile of HD, and accordingly should be addressed by these novel therapeutic approaches. Further refinement and optimization of molecular therapies for HD so that they can provide comprehensive silencing of mHTT throughout the whole organism will take many years, if not decades. Accordingly, the second way in which these glucocorticoid experiments informs the development of novel therapeutics, is that it indicates that mifepristone could possibly provide symptom relief for patients in the short term. As this drug is already FDA-approved, this is something that could be tested immediately to help slow the progression of HD symptoms. In Chapter 4 I was able to show that mHTT pathology in the anterior cingulate cortex directly contributes to the progression of HD depressive symptomology, but not anxiety symptomology. The relevance of this finding to current molecular therapeutic strategies is more straightforward than for the glucocorticoids studies: it emphasizes that the ACC will be an important brain region to target in order to improve mood symptoms for

HD patients. It will be important to further identify which other brain regions are implicated in anxiety and other psychiatric symptoms, so that they can also be targeted and hopefully be incorporated into a comprehensive gene therapy strategy that successfully ameliorates all four HD symptom domains.

References

ACMG/ASHG. (1998). ACMG/ASHG statement. Laboratory guidelines for Huntington disease genetic testing. The American College of Medical Genetics/American Society of Human Genetics Huntington Disease Genetic Testing Working Group. *Am J Hum Genet, 62*(5), 1243-1247.

Adams, C. M. (2007). Role of the transcription factor ATF4 in the anabolic actions of insulin and the anti-anabolic actions of glucocorticoids. *J Biol Chem, 282*(23), 16744-16753. doi: 10.1074/jbc.M610510200

Agustin-Pavon, C., Mielcarek, M., Garriga-Canut, M., & Isalan, M. (2016). Deimmunization for gene therapy: host matching of synthetic zinc finger constructs enables long-term mutant Huntingtin repression in mice. *Mol Neurodegener, 11*(1), 64. doi: 10.1186/s13024-016-0128-x

Albin, R. L., Reiner, A., Anderson, K. D., Dure, L. S. t., Handelin, B., Balfour, R., . . . Young, A. B. (1992). Preferential loss of striato-external pallidal projection neurons in presymptomatic Huntington's disease. *Ann Neurol, 31*(4), 425-430. doi: 10.1002/ana.410310412

American Psychiatric Association. (2013). *Diagnostic and statistical manual of mental disorders : DSM-5 (5th ed.)*. Arlington, VA: American Psychiatric Publishing.

Andela, C. D., van der Werff, S. J., Pannekoek, J. N., van den Berg, S. M., Meijer, O. C., van Buchem, M. A., . . . Pereira, A. M. (2013). Smaller grey matter volumes in the anterior cingulate cortex and greater cerebellar volumes in patients with long-term remission of Cushing's disease: a case-control study. *Eur J Endocrinol, 169*(6), 811-819. doi: 10.1530/EJE-13-0471

Anderson, K. E., & Marder, K. S. (2001). An overview of psychiatric symptoms in Huntington's disease. *Curr.Psychiatry Rep., 3*(5), 379-388.

Andre, V. M., Cepeda, C., & Levine, M. S. (2010). Dopamine and glutamate in Huntington's disease: A balancing act. *CNS.Neurosci.Ther., 16*(3), 163-178.

Andreassen, O. A., Dedeoglu, A., Ferrante, R. J., Jenkins, B. G., Ferrante, K. L., Thomas, M., . . . Beal, M. F. (2001). Creatine increase survival and delays motor symptoms in a transgenic animal model of Huntington's disease. *Neurobiol.Dis., 8*(3), 479-491.

Andrew, S. E., Goldberg, Y. P., Kremer, B., Telenius, H., Theilmann, J., Adam, S., . . . et al. (1993). The relationship between trinucleotide (CAG) repeat length and clinical features of Huntington's disease. *Nat Genet, 4*(4), 398-403. doi: 10.1038/ng0893-398

Andrich, J., Schmitz, T., Saft, C., Postert, T., Kraus, P., Epplen, J. T., . . . Agelink, M. W. (2002). Autonomic nervous system function in Huntington's disease. *J Neurol Neurosurg Psychiatry, 72*(6), 726-731.

Arrasate, M., Mitra, S., Schweitzer, E. S., Segal, M. R., & Finkbeiner, S. (2004). Inclusion body formation reduces levels of mutant huntingtin and the risk of neuronal death. *Nature, 431*(7010), 805-810. doi: 10.1038/nature02998

Arriza, J. L., Simerly, R. B., Swanson, L. W., & Evans, R. M. (1988). The neuronal mineralocorticoid receptor as a mediator of glucocorticoid response. *Neuron, 1*(9), 887-900.

Aziz, N. A., Anguelova, G. V., Marinus, J., van Dijk, J. G., & Roos, R. A. (2010). Autonomic symptoms in patients and pre-manifest mutation carriers of Huntington's disease. *Eur J Neurol, 17*(8), 1068-1074. doi: 10.1111/j.1468-1331.2010.02973.x

Aziz, N. A., Pijl, H., Frolich, M., van der Graaf, A. W., Roelfsema, F., & Roos, R. A. (2009). Increased hypothalamic-pituitary-adrenal axis activity in Huntington's disease. *J.Clin.Endocrinol.Metab, 94*(4), 1223-1228.

Aziz, N. A., Roos, R. A., Gusella, J. F., Lee, J. M., & MacDonald, M. E. (2012). CAG repeat expansion in Huntington disease determines age at onset in a fully dominant fashion. *Neurology, 79*(9), 952-953.

Aziz, N. A., van der Burg, J. M., Landwehrmeyer, G. B., Brundin, P., Stijnen, T., & Roos, R. A. (2008). Weight loss in Huntington disease increases with higher CAG repeat number. *Neurology, 71*(19), 1506-1513.

Baglietto-Vargas, D., Medeiros, R., Martinez-Coria, H., LaFerla, F. M., & Green, K. N. (2013). Mifepristone alters amyloid precursor protein processing to preclude amyloid beta and also reduces tau pathology. *Biol Psychiatry, 74*(5), 357-366. doi: 10.1016/j.biopsych.2012.12.003

Bale, T. L., Picetti, R., Contarino, A., Koob, G. F., Vale, W. W., & Lee, K. F. (2002). Mice deficient for both corticotropin-releasing factor receptor 1 (CRFR1) and CRFR2 have an impaired stress response and display sexually dichotomous anxiety-like behavior. *J Neurosci, 22*(1), 193-199.

Bamford, K. A., Caine, E. D., Kido, D. K., Cox, C., & Shoulson, I. (1995). A prospective evaluation of cognitive decline in early Huntington's disease: functional and radiographic correlates. *Neurology, 45*(10), 1867-1873.

Bar, K. J., Boettger, M. K., Andrich, J., Epplen, J. T., Fischer, F., Cordes, J., . . . Agelink, M. W. (2008). Cardiovagal modulation upon postural change is altered in Huntington's disease. *Eur J Neurol, 15*(8), 869-871. doi: 10.1111/j.1468-1331.2008.02173.x

Barahona, M. J., Sucunza, N., Resmini, E., Fernandez-Real, J. M., Ricart, W., Moreno-Navarrete, J. M., . . . Webb, S. M. (2009). Persistent body fat mass and inflammatory marker increases after long-term cure of Cushing's syndrome. *J Clin Endocrinol Metab, 94*(9), 3365-3371. doi: 10.1210/jc.2009-0766

Bass, J., & Takahashi, J. S. (2010). Circadian integration of metabolism and energetics. *Science, 330*(6009), 1349-1354. doi: 10.1126/science.1195027

Beal, M. F., Henshaw, D. R., Jenkins, B. G., Rosen, B. R., & Schulz, J. B. (1994). Coenzyme Q10 and nicotinamide block striatal lesions produced by the mitochondrial toxin malonate. *Ann Neurol., 36*(6), 882-888.

Bedard, C., Wallman, M. J., Pourcher, E., Gould, P. V., Parent, A., & Parent, M. (2011). Serotonin and dopamine striatal innervation in Parkinson's disease and Huntington's chorea. *Parkinsonism.Relat Disord.*

Bence, N. F., Sampat, R. M., & Kopito, R. R. (2001). Impairment of the ubiquitin-proteasome system by protein aggregation. *Science, 292*(5521), 1552-1555. doi: 10.1126/science.292.5521.1552

Benchoua, A., Trioulier, Y., Zala, D., Gaillard, M. C., Lefort, N., Dufour, N., . . . Brouillet, E. (2006). Involvement of mitochondrial complex II defects in neuronal death produced by N-terminus fragment of mutated huntingtin. *Mol Biol Cell, 17*(4), 1652-1663. doi: 10.1091/mbc.E05-07-0607

Benn, C. L., Sun, T., Sadri-Vakili, G., McFarland, K. N., DiRocco, D. P., Yohrling, G. J., . . . Cha, J. H. (2008). Huntingtin modulates transcription, occupies gene promoters in vivo, and binds directly to DNA in a polyglutamine-dependent manner. *J Neurosci, 28*(42), 10720-10733.

Berardelli, A., Noth, J., Thompson, P. D., Bollen, E. L., Curra, A., Deuschl, G., . . . Roos, R. A. (1999). Pathophysiology of chorea and bradykinesia in Huntington's disease. *Mov Disord, 14*(3), 398-403.

Bielohuby, M., Herbach, N., Wanke, R., Maser-Gluth, C., Beuschlein, F., Wolf, E., & Hoeflich, A. (2007). Growth analysis of the mouse adrenal gland from weaning to adulthood: time-

and gender-dependent alterations of cell size and number in the cortical compartment. *Am.J.Physiol Endocrinol.Metab, 293*(1), E139-E146.

Bissonnette, S., Vaillancourt, M., Hebert, S. S., Drolet, G., & Samadi, P. (2013). Striatal pre-enkephalin overexpression improves Huntington's disease symptoms in the R6/2 mouse model of Huntington's disease. *PLoS One, 8*(9), e75099. doi: 10.1371/journal.pone.0075099

Bjorkqvist, M., Fex, M., Renstrom, E., Wierup, N., Petersen, A., Gil, J., . . . Mulder, H. (2005). The R6/2 transgenic mouse model of Huntington's disease develops diabetes due to deficient beta-cell mass and exocytosis. *Hum.Mol.Genet., 14*(5), 565-574.

Bjorkqvist, M., Petersen, A., Bacos, K., Isaacs, J., Norlen, P., Gil, J., . . . Mulder, H. (2006a). Progressive alterations in the hypothalamic-pituitary-adrenal axis in the R6/2 transgenic mouse model of Huntington's disease. *Hum.Mol.Genet., 15*(10), 1713-1721.

Bjorkqvist, M., Petersen, A., Bacos, K., Isaacs, J., Norlen, P., Gil, J., . . . Mulder, H. (2006b). Progressive alterations in the hypothalamic-pituitary-adrenal axis in the R6/2 transgenic mouse model of Huntington's disease. *Hum Mol Genet, 15*(10), 1713-1721. doi: 10.1093/hmg/ddl094

Black, P. R., Brooks, D. C., Bessey, P. Q., Wolfe, R. R., & Wilmore, D. W. (1982). Mechanisms of insulin resistance following injury. *Ann Surg, 196*(4), 420-435.

Boden, G., Ruiz, J., Urbain, J. L., & Chen, X. (1996). Evidence for a circadian rhythm of insulin secretion. *Am J Physiol, 271*(2 Pt 1), E246-252.

Boudreau, R. L., & Davidson, B. L. (2010). RNAi therapeutics for CNS disorders. *Brain Res., 1338*, 112-121.

Boudreau, R. L., McBride, J. L., Martins, I., Shen, S., Xing, Y., Carter, B. J., & Davidson, B. L. (2009). Nonallele-specific silencing of mutant and wild-type huntingtin demonstrates therapeutic efficacy in Huntington's disease mice. *Mol.Ther., 17*(6), 1053-1063.

Bourdeau, I., Bard, C., Forget, H., Boulanger, Y., Cohen, H., & Lacroix, A. (2005). Cognitive function and cerebral assessment in patients who have Cushing's syndrome. *Endocrinol.Metab Clin.North Am., 34*(2), 357-369, ix.

Bourdeau, I., Bard, C., Noel, B., Leclerc, I., Cordeau, M. P., Belair, M., . . . Lacroix, A. (2002). Loss of brain volume in endogenous Cushing's syndrome and its reversibility after correction of hypercortisolism. *J.Clin.Endocrinol.Metab, 87*(5), 1949-1954.

Bradford, J., Shin, J. Y., Roberts, M., Wang, C. E., Sheng, G., Li, S., & Li, X. J. (2010). Mutant huntingtin in glial cells exacerbates neurological symptoms of Huntington disease mice. *J Biol.Chem., 285*(14), 10653-10661.

Bradford, J. W., Li, S., & Li, X. J. (2010). Polyglutamine toxicity in non-neuronal cells. *Cell Res, 20*(4), 400-407. doi: 10.1038/cr.2010.32

Braun, T. P., Grossberg, A. J., Krasnow, S. M., Levasseur, P. R., Szumowski, M., Zhu, X. X., . . . Marks, D. L. (2013). Cancer- and endotoxin-induced cachexia require intact glucocorticoid signaling in skeletal muscle. *FASEB J, 27*(9), 3572-3582. doi: 10.1096/fj.13-230375

Brummelte, S., & Galea, L. A. (2010). Chronic high corticosterone reduces neurogenesis in the dentate gyrus of adult male and female rats. *Neuroscience, 168*(3), 680-690. doi: 10.1016/j.neuroscience.2010.04.023

Buisson, A., Callebert, J., Mathieu, E., Plotkine, M., & Boulu, R. G. (1992). Striatal protection induced by lesioning the substantia nigra of rats subjected to focal ischemia. *J Neurochem, 59*(3), 1153-1157.

Burnstein, K. L., Bellingham, D. L., Jewell, C. M., Powell-Oliver, F. E., & Cidlowski, J. A. (1991). Autoregulation of glucocorticoid receptor gene expression. *Steroids, 56*(2), 52-58.

Burt, M. G., Gibney, J., & Ho, K. K. (2006). Characterization of the metabolic phenotypes of Cushing's syndrome and growth hormone deficiency: a study of body composition and energy metabolism. *Clin Endocrinol (Oxf), 64*(4), 436-443. doi: 10.1111/j.1365-2265.2006.02488.x

Cameron, H. A., & Gould, E. (1994). Adult neurogenesis is regulated by adrenal steroids in the dentate gyrus. *Neuroscience, 61*(2), 203-209.

Canals, J. M., Pineda, J. R., Torres-Peraza, J. F., Bosch, M., Martin-Ibanez, R., Munoz, M. T., . . . Alberch, J. (2004). Brain-derived neurotrophic factor regulates the onset and severity of motor dysfunction associated with enkephalinergic neuronal degeneration in Huntington's disease. *J Neurosci, 24*(35), 7727-7739. doi: 10.1523/JNEUROSCI.1197-04.2004

Cattaneo, E., Zuccato, C., & Tartari, M. (2005). Normal huntingtin function: an alternative approach to Huntington's disease. *Nat Rev Neurosci, 6*(12), 919-930. doi: 10.1038/nrn1806

Caviston, J. P., & Holzbaur, E. L. (2009). Huntingtin as an essential integrator of intracellular vesicular trafficking. *Trends Cell Biol, 19*(4), 147-155. doi: 10.1016/j.tcb.2009.01.005

Caviston, J. P., Ross, J. L., Antony, S. M., Tokito, M., & Holzbaur, E. L. (2007). Huntingtin facilitates dynein/dynactin-mediated vesicle transport. *Proc Natl Acad Sci U S A, 104*(24), 10045-10050. doi: 10.1073/pnas.0610628104

Cepeda, C., Cummings, D. M., Andre, V. M., Holley, S. M., & Levine, M. S. (2010). Genetic mouse models of Huntington's disease: focus on electrophysiological mechanisms. *ASN Neuro, 2*(2), e00033. doi: 10.1042/AN20090058

Cepeda, C., Murphy, K. P., Parent, M., & Levine, M. S. (2014). The role of dopamine in Huntington's disease. *Prog.Brain Res., 211*, 235-254.

Chamberlain, S. R., Menzies, L., Hampshire, A., Suckling, J., Fineberg, N. A., del Campo, N., . . . Sahakian, B. J. (2008). Orbitofrontal dysfunction in patients with obsessive-compulsive disorder and their unaffected relatives. *Science, 321*(5887), 421-422. doi: 10.1126/science.1154433

Chan, A. W., Jiang, J., Chen, Y., Li, C., Prucha, M. S., Hu, Y., . . . Bachevalier, J. (2015). Progressive cognitive deficit, motor impairment and striatal pathology in a transgenic Huntington disease monkey model from infancy to adulthood. *PLoS.One., 10*(5), e0122335.

Chang, C. H., Chen, M. C., Qiu, M. H., & Lu, J. (2014). Ventromedial prefrontal cortex regulates depressive-like behavior and rapid eye movement sleep in the rat. *Neuropharmacology, 86*, 125-132. doi: 10.1016/j.neuropharm.2014.07.005

Chang, R., Liu, X., Li, S., & Li, X. J. (2015). Transgenic animal models for study of the pathogenesis of Huntington's disease and therapy. *Drug Des Devel Ther, 9*, 2179-2188. doi: 10.2147/DDDT.S58470

Chaturvedi, R. K., Adhihetty, P., Shukla, S., Hennessy, T., Calingasan, N., Yang, L., . . . Beal, M. F. (2009). Impaired PGC-1alpha function in muscle in Huntington's disease. *Hum.Mol.Genet., 18*(16), 3048-3065.

Chen, M., Ona, V. O., Li, M., Ferrante, R. J., Fink, K. B., Zhu, S., . . . Friedlander, R. M. (2000). Minocycline inhibits caspase-1 and caspase-3 expression and delays mortality in a transgenic mouse model of Huntington disease. *Nat Med, 6*(7), 797-801. doi: 10.1038/77528

Choudhury, S. R., Harris, A. F., Cabral, D. J., Keeler, A. M., Sapp, E., Ferreira, J. S., . . . Sena-Esteves, M. (2016). Widespread Central Nervous System Gene Transfer and Silencing After Systemic Delivery of Novel AAV-AS Vector. *Mol Ther, 24*(4), 726-735. doi: 10.1038/mt.2015.231

Ciamei, A., Detloff, P. J., & Morton, A. J. (2015). Progression of behavioural despair in R6/2 and Hdh knock-in mouse models recapitulates depression in Huntington's disease. *Behav Brain Res, 291*, 140-146. doi: 10.1016/j.bbr.2015.05.010

Cowan, C. M., & Raymond, L. A. (2006). Selective neuronal degeneration in Huntington's disease. *Curr Top Dev Biol, 75*, 25-71. doi: 10.1016/S0070-2153(06)75002-5

Crochemore, C., Lu, J., Wu, Y., Liposits, Z., Sousa, N., Holsboer, F., & Almeida, O. F. (2005). Direct targeting of hippocampal neurons for apoptosis by glucocorticoids is reversible by mineralocorticoid receptor activation. *Mol Psychiatry, 10*(8), 790-798. doi: 10.1038/sj.mp.4001679

Cui, L., Jeong, H., Borovecki, F., Parkhurst, C. N., Tanese, N., & Krainc, D. (2006). Transcriptional repression of PGC-1alpha by mutant huntingtin leads to mitochondrial dysfunction and neurodegeneration. *Cell, 127*(1), 59-69. doi: 10.1016/j.cell.2006.09.015

Cummings, D. M., Alaghband, Y., Hickey, M. A., Joshi, P. R., Hong, S. C., Zhu, C., . . . Levine, M. S. (2012). A critical window of CAG repeat-length correlates with phenotype severity in the R6/2 mouse model of Huntington's disease. *J Neurophysiol, 107*(2), 677-691. doi: 10.1152/jn.00762.2011

Cummings, D. M., Andre, V. M., Uzgil, B. O., Gee, S. M., Fisher, Y. E., Cepeda, C., & Levine, M. S. (2009). Alterations in cortical excitation and inhibition in genetic mouse models of Huntington's disease. *J Neurosci, 29*(33), 10371-10386. doi: 10.1523/JNEUROSCI.1592-09.2009

Dallman, M. F., Akana, S. F., Scribner, K. A., Bradbury, M. J., Walker, C. D., Strack, A. M., & Cascio, C. S. (1992). Stress, feedback and facilitation in the hypothalamo-pituitary-adrenal axis. *J Neuroendocrinol, 4*(5), 517-526. doi: 10.1111/j.1365-2826.1992.tb00200.x

Dallman, M. F., & Jones, M. T. (1973). Corticosteroid feedback control of ACTH secretion: effect of stress-induced corticosterone ssecretion on subsequent stress responses in the rat. *Endocrinology, 92*(5), 1367-1375. doi: 10.1210/endo-92-5-1367

Damiano, M., Galvan, L., Deglon, N., & Brouillet, E. (2010). Mitochondria in Huntington's disease. *Biochim Biophys Acta, 1802*(1), 52-61. doi: 10.1016/j.bbadis.2009.07.012

Davis, K. L., Davis, B. M., Greenwald, B. S., Mohs, R. C., Mathe, A. A., Johns, C. A., & Horvath, T. B. (1986). Cortisol and Alzheimer's disease, I: Basal studies. *Am J Psychiatry, 143*(3), 300-305. doi: 10.1176/ajp.143.3.300

de Almeida, L. P., Ross, C. A., Zala, D., Aebischer, P., & Deglon, N. (2002). Lentiviral-mediated delivery of mutant huntingtin in the striatum of rats induces a selective neuropathology modulated by polyglutamine repeat size, huntingtin expression levels, and protein length. *J Neurosci, 22*(9), 3473-3483. doi: 20026337

Deng, Y. P., Albin, R. L., Penney, J. B., Young, A. B., Anderson, K. D., & Reiner, A. (2004). Differential loss of striatal projection systems in Huntington's disease: a quantitative immunohistochemical study. *J Chem Neuroanat, 27*(3), 143-164. doi: 10.1016/j.jchemneu.2004.02.005

Desplats, P. A., Kass, K. E., Gilmartin, T., Stanwood, G. D., Woodward, E. L., Head, S. R., . . . Thomas, E. A. (2006). Selective deficits in the expression of striatal-enriched mRNAs in Huntington's disease. *J Neurochem, 96*(3), 743-757. doi: 10.1111/j.1471-4159.2005.03588.x

Diamond, M. I., Robinson, M. R., & Yamamoto, K. R. (2000). Regulation of expanded polyglutamine protein aggregation and nuclear localization by the glucocorticoid receptor. *Proc Natl Acad Sci U S A, 97*(2), 657-661.

Djousse, L., Knowlton, B., Cupples, L. A., Marder, K., Shoulson, I., & Myers, R. H. (2002). Weight loss in early stage of Huntington's disease. *Neurology, 59*(9), 1325-1330.

Domenici, M. R., Scattoni, M. L., Martire, A., Lastoria, G., Potenza, R. L., Borioni, A., . . . Popoli, P. (2007). Behavioral and electrophysiological effects of the adenosine A2A receptor antagonist SCH 58261 in R6/2 Huntington's disease mice. *Neurobiol Dis, 28*(2), 197-205. doi: 10.1016/j.nbd.2007.07.009

Drevets, W. C., Ongur, D., & Price, J. L. (1998). Reduced glucose metabolism in the subgenual prefrontal cortex in unipolar depression. *Mol Psychiatry, 3*(3), 190-191.

Drevets, W. C., Price, J. L., Simpson, J. R., Jr., Todd, R. D., Reich, T., Vannier, M., & Raichle, M. E. (1997). Subgenual prefrontal cortex abnormalities in mood disorders. *Nature, 386*(6627), 824-827. doi: 10.1038/386824a0

Drevets, W. C., Savitz, J., & Trimble, M. (2008). The subgenual anterior cingulate cortex in mood disorders. *CNS Spectr, 13*(8), 663-681.

Drouet, V., Perrin, V., Hassig, R., Dufour, N., Auregan, G., Alves, S., . . . Deglon, N. (2009). Sustained effects of nonallele-specific Huntingtin silencing. *Ann Neurol, 65*(3), 276-285. doi: 10.1002/ana.21569

Du, X., Leang, L., Mustafa, T., Renoir, T., Pang, T. Y., & Hannan, A. J. (2012). Environmental enrichment rescues female-specific hyperactivity of the hypothalamic-pituitary-adrenal axis in a model of Huntington's disease. *Transl.Psychiatry, 2*, e133.

Duff, K., Paulsen, J. S., Beglinger, L. J., Langbehn, D. R., Stout, J. C., & Predict, H. D. I. o. t. H. S. G. (2007). Psychiatric symptoms in Huntington's disease before diagnosis: the predict-HD study. *Biol Psychiatry, 62*(12), 1341-1346. doi: 10.1016/j.biopsych.2006.11.034

Dufour, B. D., & McBride, J. L. (2016). Corticosterone dysregulation exacerbates disease progression in the R6/2 transgenic mouse model of Huntington's disease. *Exp Neurol, 283*(Pt A), 308-317. doi: 10.1016/j.expneurol.2016.06.028

Dufour, B. D., Smith, C. A., Clark, R. L., Walker, T. R., & McBride, J. L. (2014). Intrajugular vein delivery of AAV9-RNAi prevents neuropathological changes and weight loss in Huntington's disease mice. *Mol Ther, 22*(4), 797-810. doi: 10.1038/mt.2013.289

Dumas, E. M., van den Bogaard, S. J., Middelkoop, H. A., & Roos, R. A. (2013). A review of cognition in Huntington's disease. *Front Biosci (Schol Ed), 5*, 1-18.

Ehrlich, M. E. (2012). Huntington's disease and the striatal medium spiny neuron: cell-autonomous and non-cell-autonomous mechanisms of disease. *Neurotherapeutics, 9*(2), 270-284. doi: 10.1007/s13311-012-0112-2

Elenkov, I. J., & Chrousos, G. P. (2002). Stress hormones, proinflammatory and antiinflammatory cytokines, and autoimmunity. *Ann N Y Acad Sci, 966*, 290-303.

Elliott, R. (2003). Executive functions and their disorders. *Br Med Bull, 65*, 49-59.

Engeland, W. C., & Arnhold, M. M. (2005). Neural circuitry in the regulation of adrenal corticosterone rhythmicity. *Endocrine, 28*(3), 325-332. doi: 10.1385/ENDO:28:3:325

Epping, E. A., Mills, J. A., Beglinger, L. J., Fiedorowicz, J. G., Craufurd, D., Smith, M. M., . . . Paulsen, J. S. (2013). Characterization of depression in prodromal Huntington disease in the neurobiological predictors of HD (PREDICT-HD) study. *J.Psychiatr.Res., 47*(10), 1423-1431.

Epping, E. A., & Paulsen, J. S. (2011). Depression in the early stages of Huntington disease. *Neurodegener Dis Manag, 1*(5), 407-414. doi: 10.2217/nmt.11.45

Etkin, A., Prater, K. E., Hoeft, F., Menon, V., & Schatzberg, A. F. (2010). Failure of anterior cingulate activation and connectivity with the amygdala during implicit regulation of emotional processing in generalized anxiety disorder. *Am J Psychiatry, 167*(5), 545-554. doi: 10.1176/appi.ajp.2009.09070931

Evans, C. G., Wisen, S., & Gestwicki, J. E. (2006). Heat shock proteins 70 and 90 inhibit early stages of amyloid beta-(1-42) aggregation in vitro. *J Biol Chem, 281*(44), 33182-33191. doi: 10.1074/jbc.M606192200

Exton, J. H. (1979). Regulation of gluconeogenesis by glucocorticoids. *Monogr Endocrinol, 12*, 535-546.

Fahrenkrug, J., Popovic, N., Georg, B., Brundin, P., & Hannibal, J. (2007). Decreased VIP and VPAC2 receptor expression in the biological clock of the R6/2 Huntington's disease mouse. *J.Mol.Neurosci., 31*(2), 139-148.

Farrer, L. A. (1986). Suicide and attempted suicide in Huntington disease: implications for preclinical testing of persons at risk. *Am.J.Med.Genet., 24*(2), 305-311.

Farrer, L. A., & Yu, P. L. (1985). Anthropometric discrimination among affected, at-risk, and not-at-risk individuals in families with Huntington disease. *Am.J.Med.Genet., 21*(2), 307-316.

Feigin, A., Ghilardi, M. F., Huang, C., Ma, Y., Carbon, M., Guttman, M., . . . Eidelberg, D. (2006). Preclinical Huntington's disease: compensatory brain responses during learning. *Ann Neurol, 59*(1), 53-59. doi: 10.1002/ana.20684

Ferrante, R. J., Andreassen, O. A., Dedeoglu, A., Ferrante, K. L., Jenkins, B. G., Hersch, S. M., & Beal, M. F. (2002). Therapeutic effects of coenzyme Q10 and remacemide in transgenic mouse models of Huntington's disease. *J Neurosci, 22*(5), 1592-1599.

Ferrante, R. J., Andreassen, O. A., Jenkins, B. G., Dedeoglu, A., Kuemmerle, S., Kubilus, J. K., . . . Beal, M. F. (2000). Neuroprotective effects of creatine in a transgenic mouse model of Huntington's disease. *J Neurosci, 20*(12), 4389-4397.

File, S. E., Mahal, A., Mangiarini, L., & Bates, G. P. (1998). Striking changes in anxiety in Huntington's disease transgenic mice. *Brain Res, 805*(1-2), 234-240.

Fleseriu, M., Biller, B. M., Findling, J. W., Molitch, M. E., Schteingart, D. E., Gross, C., & Investigators, S. S. (2012). Mifepristone, a glucocorticoid receptor antagonist, produces clinical and metabolic benefits in patients with Cushing's syndrome. *J Clin Endocrinol Metab, 97*(6), 2039-2049. doi: 10.1210/jc.2011-3350

Franchimont, D. (2004). Overview of the actions of glucocorticoids on the immune response: a good model to characterize new pathways of immunosuppression for new treatment strategies. *Ann N Y Acad Sci, 1024*, 124-137. doi: 10.1196/annals.1321.009

Franich, N. R., Fitzsimons, H. L., Fong, D. M., Klugmann, M., During, M. J., & Young, D. (2008). AAV vector-mediated RNAi of mutant huntingtin expression is neuroprotective in a novel genetic rat model of Huntington's disease. *Mol Ther, 16*(5), 947-956. doi: 10.1038/mt.2008.50

Frayn, K. N. (1983). Calculation of substrate oxidation rates in vivo from gaseous exchange. *J Appl Physiol Respir Environ Exerc Physiol, 55*(2), 628-634.

Fu, Y., Wu, P., Pan, Y., Sun, X., Yang, H., Difiglia, M., & Lu, B. (2017). A toxic mutant huntingtin species is resistant to selective autophagy. *Nat Chem Biol, 13*(11), 1152-1154. doi: 10.1038/nchembio.2461

Gaba, A. M., Zhang, K., Marder, K., Moskowitz, C. B., Werner, P., & Boozer, C. N. (2005). Energy balance in early-stage Huntington disease. *Am J Clin Nutr, 81*(6), 1335-1341.

Gabery, S., Murphy, K., Schultz, K., Loy, C. T., McCusker, E., Kirik, D., . . . Petersen, A. (2010). Changes in key hypothalamic neuropeptide populations in Huntington disease revealed by neuropathological analyses. *Acta Neuropathol, 120*(6), 777-788. doi: 10.1007/s00401-010-0742-6

Galvan, L., Andre, V. M., Wang, E. A., Cepeda, C., & Levine, M. S. (2012). Functional Differences Between Direct and Indirect Striatal Output Pathways in Huntington's Disease. *J Huntingtons Dis, 1*(1), 17-25. doi: 10.3233/JHD-2012-120009

Garrett, M. C., & Soares-da-Silva, P. (1992). Increased cerebrospinal fluid dopamine and 3,4-dihydroxyphenylacetic acid levels in Huntington's disease: evidence for an overactive dopaminergic brain transmission. *J Neurochem, 58*(1), 101-106.

Garriga-Canut, M., Agustin-Pavon, C., Herrmann, F., Sanchez, A., Dierssen, M., Fillat, C., & Isalan, M. (2012). Synthetic zinc finger repressors reduce mutant huntingtin expression in the brain of R6/2 mice. *Proc Natl Acad Sci U S A, 109*(45), E3136-3145. doi: 10.1073/pnas.1206506109

Garside, S., Furtado, J. C., & Mazurek, M. F. (1996). Dopamine-glutamate interactions in the striatum: behaviourally relevant modification of excitotoxicity by dopamine receptor-mediated mechanisms. *Neuroscience, 75*(4), 1065-1074.

Gaveriaux-Ruff, C., & Kieffer, B. L. (2007). Conditional gene targeting in the mouse nervous system: Insights into brain function and diseases. *Pharmacol Ther, 113*(3), 619-634. doi: 10.1016/j.pharmthera.2006.12.003

Gharami, K., Xie, Y., An, J. J., Tonegawa, S., & Xu, B. (2008). Brain-derived neurotrophic factor over-expression in the forebrain ameliorates Huntington's disease phenotypes in mice. *J Neurochem, 105*(2), 369-379. doi: 10.1111/j.1471-4159.2007.05137.x

Giampa, C., Patassini, S., Borreca, A., Laurenti, D., Marullo, F., Bernardi, G., . . . Fusco, F. R. (2009). Phosphodiesterase 10 inhibition reduces striatal excitotoxicity in the quinolinic acid model of Huntington's disease. *Neurobiol Dis, 34*(3), 450-456. doi: 10.1016/j.nbd.2009.02.014

Gil, J. M., Mohapel, P., Araujo, I. M., Popovic, N., Li, J. Y., Brundin, P., & Petersen, A. (2005). Reduced hippocampal neurogenesis in R6/2 transgenic Huntington's disease mice. *Neurobiol.Dis., 20*(3), 744-751.

Giralt, A., Saavedra, A., Alberch, J., & Perez-Navarro, E. (2012). Cognitive Dysfunction in Huntington's Disease: Humans, Mouse Models and Molecular Mechanisms. *J Huntingtons Dis, 1*(2), 155-173. doi: 10.3233/JHD-120023

Glass, M., Dragunow, M., & Faull, R. L. (2000). The pattern of neurodegeneration in Huntington's disease: a comparative study of cannabinoid, dopamine, adenosine and GABA(A) receptor alterations in the human basal ganglia in Huntington's disease. *Neuroscience, 97*(3), 505-519.

Gomez-Sanchez, E., & Gomez-Sanchez, C. E. (2014). The multifaceted mineralocorticoid receptor. *Compr Physiol, 4*(3), 965-994. doi: 10.1002/cphy.c130044

Goodman, A. O., & Barker, R. A. (2011). Body composition in premanifest Huntington's disease reveals lower bone density compared to controls. *PLoS Curr, 3*, RRN1214. doi: 10.1371/currents.RRN1214

Goodman, A. O., Murgatroyd, P. R., Medina-Gomez, G., Wood, N. I., Finer, N., Vidal-Puig, A. J., . . . Barker, R. A. (2008). The metabolic profile of early Huntington's disease--a combined human and transgenic mouse study. *Exp Neurol, 210*(2), 691-698. doi: 10.1016/j.expneurol.2007.12.026

Gorski, J. A., Talley, T., Qiu, M., Puelles, L., Rubenstein, J. L., & Jones, K. R. (2002). Cortical excitatory neurons and glia, but not GABAergic neurons, are produced in the Emx1-expressing lineage. *J Neurosci, 22*(15), 6309-6314. doi: 20026564

Gould, E., Cameron, H. A., Daniels, D. C., Woolley, C. S., & McEwen, B. S. (1992). Adrenal hormones suppress cell division in the adult rat dentate gyrus. *J Neurosci, 12*(9), 3642-3650.

Gourfinkel-An, I., Cancel, G., Duyckaerts, C., Faucheux, B., Hauw, J. J., Trottier, Y., . . . Hirsch, E. C. (1998). Neuronal distribution of intranuclear inclusions in Huntington's disease with adult onset. *Neuroreport, 9*(8), 1823-1826.

Graveland, G. A., Williams, R. S., & DiFiglia, M. (1985). Evidence for degenerative and regenerative changes in neostriatal spiny neurons in Huntington's disease. *Science, 227*(4688), 770-773.

Gray, M., Shirasaki, D. I., Cepeda, C., Andre, V. M., Wilburn, B., Lu, X. H., . . . Yang, X. W. (2008). Full-length human mutant huntingtin with a stable polyglutamine repeat can elicit progressive and selective neuropathogenesis in BACHD mice. *J Neurosci, 28*(24), 6182-6195. doi: 10.1523/JNEUROSCI.0857-08.2008

Graybiel, A. M., & Rauch, S. L. (2000). Toward a neurobiology of obsessive-compulsive disorder. *Neuron, 28*(2), 343-347.

Green, K. N., Billings, L. M., Roozendaal, B., McGaugh, J. L., & LaFerla, F. M. (2006). Glucocorticoids increase amyloid-beta and tau pathology in a mouse model of Alzheimer's disease. *J Neurosci, 26*(35), 9047-9056. doi: 10.1523/JNEUROSCI.2797-06.2006

Grondin, R., Kaytor, M. D., Ai, Y., Nelson, P. T., Thakker, D. R., Heisel, J., . . . Kaemmerer, W. F. (2012). Six-month partial suppression of Huntingtin is well tolerated in the adult rhesus striatum. *Brain, 135*(Pt 4), 1197-1209. doi: 10.1093/brain/awr333

Grossberg, A. J., Scarlett, J. M., & Marks, D. L. (2010). Hypothalamic mechanisms in cachexia. *Physiol Behav., 100*(5), 478-489.

Gruver-Yates, A. L., & Cidlowski, J. A. (2013). Tissue-specific actions of glucocorticoids on apoptosis: a double-edged sword. *Cells, 2*(2), 202-223. doi: 10.3390/cells2020202

Gu, X., Greiner, E. R., Mishra, R., Kodali, R., Osmand, A., Finkbeiner, S., . . . Yang, X. W. (2009). Serines 13 and 16 are critical determinants of full-length human mutant huntingtin induced disease pathogenesis in HD mice. *Neuron, 64*(6), 828-840. doi: 10.1016/j.neuron.2009.11.020

Gusella, J. F., Wexler, N. S., Conneally, P. M., Naylor, S. L., Anderson, M. A., Tanzi, R. E., . . . et al. (1983). A polymorphic DNA marker genetically linked to Huntington's disease. *Nature, 306*(5940), 234-238.

Hannan, A. J., & Ransome, M. I. (2012). Deficits in spermatogenesis but not neurogenesis are alleviated by chronic testosterone therapy in R6/1 Huntington's disease mice. *J Neuroendocrinol, 24*(2), 341-356. doi: 10.1111/j.1365-2826.2011.02238.x

Hansson, O., Nylandsted, J., Castilho, R. F., Leist, M., Jaattela, M., & Brundin, P. (2003). Overexpression of heat shock protein 70 in R6/2 Huntington's disease mice has only modest effects on disease progression. *Brain Res, 970*(1-2), 47-57.

Harper, S. Q., Staber, P. D., He, X., Eliason, S. L., Martins, I. H., Mao, Q., . . . Davidson, B. L. (2005). RNA interference improves motor and neuropathological abnormalities in a Huntington's disease mouse model. *Proc.Natl.Acad.Sci.U.S.A, 102*(16), 5820-5825.

Harrington, D. L., Liu, D., Smith, M. M., Mills, J. A., Long, J. D., Aylward, E. H., & Paulsen, J. S. (2014). Neuroanatomical correlates of cognitive functioning in prodromal Huntington disease. *Brain Behav., 4*(1), 29-40.

Hastings, T. G. (2009). The role of dopamine oxidation in mitochondrial dysfunction: implications for Parkinson's disease. *J Bioenerg Biomembr, 41*(6), 469-472. doi: 10.1007/s10863-009-9257-z

Hay, D. G., Sathasivam, K., Tobaben, S., Stahl, B., Marber, M., Mestril, R., . . . Bates, G. P. (2004). Progressive decrease in chaperone protein levels in a mouse model of Huntington's disease and induction of stress proteins as a therapeutic approach. *Hum Mol Genet, 13*(13), 1389-1405. doi: 10.1093/hmg/ddh144

Hefter, H., Homberg, V., Lange, H. W., & Freund, H. J. (1987). Impairment of rapid movement in Huntington's disease. *Brain, 110 (Pt 3)*, 585-612.

Heinsen, H., Strik, M., Bauer, M., Luther, K., Ulmar, G., Gangnus, D., . . . Gotz, M. (1994). Cortical and striatal neurone number in Huntington's disease. *Acta Neuropathol, 88*(4), 320-333.

Herbst, K. L., & Bhasin, S. (2004). Testosterone action on skeletal muscle. *Curr Opin Clin Nutr Metab Care, 7*(3), 271-277.

Hersch, S. M., Schifitto, G., Oakes, D., Bredlau, A. L., Meyers, C. M., Nahin, R., . . . Coordinators. (2017). The CREST-E study of creatine for Huntington disease: A randomized controlled trial. *Neurology, 89*(6), 594-601. doi: 10.1212/WNL.0000000000004209

Heuser, I. J., Chase, T. N., & Mouradian, M. M. (1991). The limbic-hypothalamic-pituitary-adrenal axis in Huntington's disease. *Biol.Psychiatry, 30*(9), 943-952.

Heyder, K., Suchan, B., & Daum, I. (2004). Cortico-subcortical contributions to executive control. *Acta Psychol (Amst), 115*(2-3), 271-289. doi: 10.1016/j.actpsy.2003.12.010

Hickey, M. A., Gallant, K., Gross, G. G., Levine, M. S., & Chesselet, M. F. (2005). Early behavioral deficits in R6/2 mice suitable for use in preclinical drug testing. *Neurobiol Dis, 20*(1), 1-11. doi: 10.1016/j.nbd.2005.01.024

Ho, A. K., Gilbert, A. S., Mason, S. L., Goodman, A. O., & Barker, R. A. (2009). Health-related quality of life in Huntington's disease: Which factors matter most? *Mov Disord., 24*(4), 574-578.

Hobbs, N. Z., Pedrick, A. V., Say, M. J., Frost, C., Dar, S. R., Coleman, A., . . . Scahill, R. I. (2011). The structural involvement of the cingulate cortex in premanifest and early Huntington's disease. *Mov Disord.*

Hockly, E., Woodman, B., Mahal, A., Lewis, C. M., & Bates, G. (2003). Standardization and statistical approaches to therapeutic trials in the R6/2 mouse. *Brain Res Bull, 61*(5), 469-479.

Hodges, A., Strand, A. D., Aragaki, A. K., Kuhn, A., Sengstag, T., Hughes, G., . . . Luthi-Carter, R. (2006). Regional and cellular gene expression changes in human Huntington's disease brain. *Hum Mol Genet, 15*(6), 965-977. doi: 10.1093/hmg/ddl013

Hubers, A. A., van der Mast, R. C., Pereira, A. M., Roos, R. A., Veen, L. J., Cobbaert, C. M., . . . Giltay, E. J. (2015). Hypothalamic-pituitary-adrenal axis functioning in Huntington's disease and its association with depressive symptoms and suicidality. *J.Neuroendocrinol., 27*(3), 234-244.

Hult Lundh, S., Nilsson, N., Soylu, R., Kirik, D., & Petersen, A. (2013). Hypothalamic expression of mutant huntingtin contributes to the development of depressive-like behavior in the BAC transgenic mouse model of Huntington's disease. *Hum Mol Genet, 22*(17), 3485-3497. doi: 10.1093/hmg/ddt203

Hult, S., Soylu, R., Bjorklund, T., Belgardt, B. F., Mauer, J., Bruning, J. C., . . . Petersen, A. (2011). Mutant huntingtin causes metabolic imbalance by disruption of hypothalamic neurocircuits. *Cell Metab, 13*(4), 428-439.

Huntington Disease Collaborative Research Group. (1993). A novel gene containing a trinucleotide repeat that is expanded and unstable on Huntington's disease chromosomes. The Huntington's Disease Collaborative Research Group. *Cell, 72*(6), 971-983.

Huntington Study Group. (1996). Unified Huntington's Disease Rating Scale: reliability and consistency. Huntington Study Group. *Mov Disord, 11*(2), 136-142. doi: 10.1002/mds.870110204

Huntington Study Group. (2006). Tetrabenazine as antichorea therapy in Huntington disease: a randomized controlled trial. *Neurology, 66*(3), 366-372. doi: 10.1212/01.wnl.0000198586.85250.13

Huntington Study Group, Frank, S., Testa, C. M., Stamler, D., Kayson, E., Davis, C., . . . Christopher, E. (2016). Effect of Deutetrabenazine on Chorea Among Patients With Huntington Disease: A Randomized Clinical Trial. *JAMA, 316*(1), 40-50. doi: 10.1001/jama.2016.8655

Huntington Study Group, D. I. (2010). A futility study of minocycline in Huntington's disease. *Mov Disord, 25*(13), 2219-2224. doi: 10.1002/mds.23236

Ille, R., Schafer, A., Scharmuller, W., Enzinger, C., Schoggl, H., Kapfhammer, H. P., & Schienle, A. (2011). Emotion recognition and experience in Huntington disease: a voxel-based morphometry study. *J Psychiatry Neurosci, 36*(6), 383-390. doi: 10.1503/jpn.100143

Jakel, R. J., & Maragos, W. F. (2000). Neuronal cell death in Huntington's disease: a potential role for dopamine. *Trends Neurosci, 23*(6), 239-245.

Joel, D. (2001). Open interconnected model of basal ganglia-thalamocortical circuitry and its relevance to the clinical syndrome of Huntington's disease. *Mov Disord, 16*(3), 407-423.

Johnson, P. L., Potts, G. F., Sanchez-Ramos, J., & Cimino, C. R. (2017). Self-reported impulsivity in Huntington's disease patients and relationship to executive dysfunction and reward responsiveness. *J Clin Exp Neuropsychol, 39*(7), 694-706. doi: 10.1080/13803395.2016.1257702

Julien, C. L., Thompson, J. C., Wild, S., Yardumian, P., Snowden, J. S., Turner, G., & Craufurd, D. (2007). Psychiatric disorders in preclinical Huntington's disease. *J Neurol Neurosurg Psychiatry, 78*(9), 939-943. doi: 10.1136/jnnp.2006.103309

Kalliolia, E., Silajdzic, E., Nambron, R., Hill, N. R., Doshi, A., Frost, C., . . . Warner, T. T. (2014). Plasma melatonin is reduced in Huntington's disease. *Mov Disord., 29*(12), 1511-1515.

Kim, E. H., Thu, D. C., Tippett, L. J., Oorschot, D. E., Hogg, V. M., Roxburgh, R., . . . Faull, R. L. (2014). Cortical interneuron loss and symptom heterogeneity in Huntington disease. *Ann Neurol, 75*(5), 717-727. doi: 10.1002/ana.24162

Kipps, C. M., Duggins, A. J., McCusker, E. A., & Calder, A. J. (2007). Disgust and happiness recognition correlate with anteroventral insula and amygdala volume respectively in preclinical Huntington's disease. *J.Cogn Neurosci., 19*(7), 1206-1217.

Kirkwood, S. C., Su, J. L., Conneally, P., & Foroud, T. (2001). Progression of symptoms in the early and middle stages of Huntington disease. *Arch Neurol, 58*(2), 273-278.

Klapstein, G. J., Fisher, R. S., Zanjani, H., Cepeda, C., Jokel, E. S., Chesselet, M. F., & Levine, M. S. (2001). Electrophysiological and morphological changes in striatal spiny neurons in R6/2 Huntington's disease transgenic mice. *J Neurophysiol, 86*(6), 2667-2677.

Kordasiewicz, H. B., Stanek, L. M., Wancewicz, E. V., Mazur, C., McAlonis, M. M., Pytel, K. A., . . . Cleveland, D. W. (2012). Sustained therapeutic reversal of Huntington's disease by transient repression of huntingtin synthesis. *Neuron, 74*(6), 1031-1044. doi: 10.1016/j.neuron.2012.05.009

Kosinski, C. M., Schlangen, C., Gellerich, F. N., Gizatullina, Z., Deschauer, M., Schiefer, J., . . . Lindenberg, K. S. (2007). Myopathy as a first symptom of Huntington's disease in a Marathon runner. *Mov Disord., 22*(11), 1637-1640.

Kremer, B., Goldberg, P., Andrew, S. E., Theilmann, J., Telenius, H., Zeisler, J., . . . et al. (1994). A worldwide study of the Huntington's disease mutation. The sensitivity and specificity of measuring CAG repeats. *N Engl J Med, 330*(20), 1401-1406. doi: 10.1056/NEJM199405193302001

Kudwa, A. E., Menalled, L. B., Oakeshott, S., Murphy, C., Mushlin, R., Fitzpatrick, J., . . . Brunner, D. (2013). Increased Body Weight of the BAC HD Transgenic Mouse Model of Huntington's Disease Accounts for Some but Not All of the Observed HD-like Motor Deficits. *PLoS Curr, 5*. doi: 10.1371/currents.hd.0ab4f3645aff523c56ecc8ccbe41a198

Labbadia, J., Cunliffe, H., Weiss, A., Katsyuba, E., Sathasivam, K., Seredenina, T., . . . Bates, G. P. (2011). Altered chromatin architecture underlies progressive impairment of the heat shock response in mouse models of Huntington disease. *J Clin Invest, 121*(8), 3306-3319. doi: 10.1172/JCI57413

Landles, C., Sathasivam, K., Weiss, A., Woodman, B., Moffitt, H., Finkbeiner, S., . . . Bates, G. P. (2010). Proteolysis of mutant huntingtin produces an exon 1 fragment that accumulates

as an aggregated protein in neuronal nuclei in Huntington disease. *J Biol Chem, 285*(12), 8808-8823. doi: 10.1074/jbc.M109.075028

Lanska, D. J., Lanska, M. J., Lavine, L., & Schoenberg, B. S. (1988). Conditions associated with Huntington's disease at death. A case-control study. *Arch Neurol, 45*(8), 878-880.

Lawrence, A. D., Sahakian, B. J., Hodges, J. R., Rosser, A. E., Lange, K. W., & Robbins, T. W. (1996). Executive and mnemonic functions in early Huntington's disease. *Brain, 119 (Pt 5)*, 1633-1645.

Lawrence, A. D., Sahakian, B. J., & Robbins, T. W. (1998). Cognitive functions and corticostriatal circuits: insights from Huntington's disease. *Trends Cogn Sci, 2*(10), 379-388.

Leblhuber, F., Peichl, M., Neubauer, C., Reisecker, F., Steinparz, F. X., Windhager, E., & Maschek, W. (1995). Serum dehydroepiandrosterone and cortisol measurements in Huntington's chorea. *J.Neurol.Sci., 132*(1), 76-79.

Lee, M. C., Wee, G. R., & Kim, J. H. (2005). Apoptosis of skeletal muscle on steroid-induced myopathy in rats. *J Nutr, 135*(7), 1806S-1808S.

Levy, M. L., Cummings, J. L., Fairbanks, L. A., Masterman, D., Miller, B. L., Craig, A. H., . . . Litvan, I. (1998). Apathy is not depression. *J.Neuropsychiatry Clin.Neurosci., 10*(3), 314-319.

Li, J. Y., Popovic, N., & Brundin, P. (2005). The use of the R6 transgenic mouse models of Huntington's disease in attempts to develop novel therapeutic strategies. *NeuroRx., 2*(3), 447-464.

Li, L., Murphy, T. H., Hayden, M. R., & Raymond, L. A. (2004). Enhanced striatal NR2B-containing N-methyl-D-aspartate receptor-mediated synaptic currents in a mouse model of Huntington disease. *J Neurophysiol, 92*(5), 2738-2746. doi: 10.1152/jn.00308.2004

Li, W., Silva, H. B., Real, J., Wang, Y. M., Rial, D., Li, P., . . . Chen, J. F. (2015). Inactivation of adenosine A2A receptors reverses working memory deficits at early stages of Huntington's disease models. *Neurobiol Dis, 79*, 70-80. doi: 10.1016/j.nbd.2015.03.030

Linden, T., Kalimo, H., & Wieloch, T. (1987). Protective effect of lesion to the glutamatergic cortico-striatal projections on the hypoglycemic nerve cell injury in rat striatum. *Acta Neuropathol, 74*(4), 335-344.

Lione, L. A., Carter, R. J., Hunt, M. J., Bates, G. P., Morton, A. J., & Dunnett, S. B. (1999). Selective discrimination learning impairments in mice expressing the human Huntington's disease mutation. *J Neurosci, 19*(23), 10428-10437.

Lofberg, E., Gutierrez, A., Wernerman, J., Anderstam, B., Mitch, W. E., Price, S. R., . . . Alvestrand, A. (2002). Effects of high doses of glucocorticoids on free amino acids, ribosomes and protein turnover in human muscle. *Eur J Clin Invest, 32*(5), 345-353.

Lopez-Rubalcava, C., & Lucki, I. (2000). Strain differences in the behavioral effects of antidepressant drugs in the rat forced swimming test. *Neuropsychopharmacology, 22*(2), 191-199. doi: 10.1016/S0893-133X(99)00100-1

Lu, J., Goula, D., Sousa, N., & Almeida, O. F. (2003). Ionotropic and metabotropic glutamate receptor mediation of glucocorticoid-induced apoptosis in hippocampal cells and the neuroprotective role of synaptic N-methyl-D-aspartate receptors. *Neuroscience, 121*(1), 123-131.

Luk, K. C., Mills, I. P., Trojanowski, J. Q., & Lee, V. M. (2008). Interactions between Hsp70 and the hydrophobic core of alpha-synuclein inhibit fibril assembly. *Biochemistry, 47*(47), 12614-12625. doi: 10.1021/bi801475r

Luo, W., Sun, W., Taldone, T., Rodina, A., & Chiosis, G. (2010). Heat shock protein 90 in neurodegenerative diseases. *Mol Neurodegener, 5*, 24. doi: 10.1186/1750-1326-5-24

Lupien, S. J., de Leon, M., de Santi, S., Convit, A., Tarshish, C., Nair, N. P., . . . Meaney, M. J. (1998). Cortisol levels during human aging predict hippocampal atrophy and memory deficits. *Nat Neurosci, 1*(1), 69-73. doi: 10.1038/271

Luthi-Carter, R., Hanson, S. A., Strand, A. D., Bergstrom, D. A., Chun, W., Peters, N. L., . . . Olson, J. M. (2002). Dysregulation of gene expression in the R6/2 model of polyglutamine disease: parallel changes in muscle and brain. *Hum.Mol.Genet., 11*(17), 1911-1926.

Magnusson-Lind, A., Davidsson, M., Silajdzic, E., Hansen, C., McCourt, A. C., Tabrizi, S. J., & Bjorkqvist, M. (2014). Skeletal muscle atrophy in R6/2 mice - altered circulating skeletal muscle markers and gene expression profile changes. *J Huntingtons Dis, 3*(1), 13-24. doi: 10.3233/JHD-130075

Maheshwari, M., Bhutani, S., Das, A., Mukherjee, R., Sharma, A., Kino, Y., . . . Jana, N. R. (2014). Dexamethasone induces heat shock response and slows down disease progression in mouse and fly models of Huntington's disease. *Hum Mol Genet, 23*(10), 2737-2751. doi: 10.1093/hmg/ddt667

Makino, S., Hashimoto, K., & Gold, P. W. (2002). Multiple feedback mechanisms activating corticotropin-releasing hormone system in the brain during stress. *Pharmacol Biochem Behav, 73*(1), 147-158.

Mangelsdorf, D. J., Thummel, C., Beato, M., Herrlich, P., Schutz, G., Umesono, K., . . . Evans, R. M. (1995). The nuclear receptor superfamily: the second decade. *Cell, 83*(6), 835-839.

Mangiarini, L., Sathasivam, K., Seller, M., Cozens, B., Harper, A., Hetherington, C., . . . Bates, G. P. (1996). Exon 1 of the HD gene with an expanded CAG repeat is sufficient to cause a progressive neurological phenotype in transgenic mice. *Cell, 87*(3), 493-506.

Marder, K., Zhao, H., Myers, R. H., Cudkowicz, M., Kayson, E., Kieburtz, K., . . . Shoulson, I. (2000). Rate of functional decline in Huntington's disease. Huntington Study Group. *Neurology, 54*(2), 452-458.

Mason, S. L., Zhang, J., Begeti, F., Guzman, N. V., Lazar, A. S., Rowe, J. B., . . . Hampshire, A. (2015). The role of the amygdala during emotional processing in Huntington's disease: from pre-manifest to late stage disease. *Neuropsychologia, 70*, 80-89. doi: 10.1016/j.neuropsychologia.2015.02.017

McBride, J. L., Boudreau, R. L., Harper, S. Q., Staber, P. D., Monteys, A. M., Martins, I., . . . Davidson, B. L. (2008). Artificial miRNAs mitigate shRNA-mediated toxicity in the brain: implications for the therapeutic development of RNAi. *Proc.Natl.Acad.Sci.U.S.A, 105*(15), 5868-5873.

McBride, J. L., Pitzer, M. R., Boudreau, R. L., Dufour, B., Hobbs, T., Ojeda, S. R., & Davidson, B. L. (2011). Preclinical safety of RNAi-mediated HTT suppression in the rhesus macaque as a potential therapy for Huntington's disease. *Mol Ther, 19*(12), 2152-2162. doi: 10.1038/mt.2011.219

McColgan, P., Razi, A., Gregory, S., Seunarine, K. K., Durr, A., R, A. C. R., . . . Track On, H. D. I. (2017). Structural and functional brain network correlates of depressive symptoms in premanifest Huntington's disease. *Hum Brain Mapp, 38*(6), 2819-2829. doi: 10.1002/hbm.23527

McColgan, P., & Tabrizi, S. J. (2017). Huntington's disease: a clinical review. *Eur J Neurol*. doi: 10.1111/ene.13413

McEwen, B. S. (1999). Stress and hippocampal plasticity. *Annu.Rev.Neurosci., 22*, 105-122.

McGarry, A., Kieburtz, K., Abler, V., Grachev, I. D., Gandhi, S., Auinger, P., . . . Hayden, M. (2017). Safety and Exploratory Efficacy at 36 Months in Open-HART, an Open-Label Extension Study of Pridopidine in Huntington's Disease. *J Huntingtons Dis, 6*(3), 189-199. doi: 10.3233/JHD-170241

McGarry, A., McDermott, M., Kieburtz, K., de Blieck, E. A., Beal, F., Marder, K., . . . Coordinators. (2017). A randomized, double-blind, placebo-controlled trial of coenzyme Q10 in Huntington disease. *Neurology, 88*(2), 152-159. doi: 10.1212/WNL.0000000000003478

Menalled, L., El-Khodor, B. F., Patry, M., Suarez-Farinas, M., Orenstein, S. J., Zahasky, B., . . . Brunner, D. (2009). Systematic behavioral evaluation of Huntington's disease transgenic and knock-in mouse models. *Neurobiol Dis, 35*(3), 319-336. doi: 10.1016/j.nbd.2009.05.007

Mihm, M. J., Amann, D. M., Schanbacher, B. L., Altschuld, R. A., Bauer, J. A., & Hoyt, K. R. (2007). Cardiac dysfunction in the R6/2 mouse model of Huntington's disease. *Neurobiol Dis, 25*(2), 297-308. doi: 10.1016/j.nbd.2006.09.016

Milad, M. R., & Rauch, S. L. (2007). The role of the orbitofrontal cortex in anxiety disorders. *Ann N Y Acad Sci, 1121*, 546-561. doi: 10.1196/annals.1401.006

Milakovic, T., & Johnson, G. V. (2005). Mitochondrial respiration and ATP production are significantly impaired in striatal cells expressing mutant huntingtin. *J Biol Chem, 280*(35), 30773-30782. doi: 10.1074/jbc.M504749200

Milakovic, T., Quintanilla, R. A., & Johnson, G. V. (2006). Mutant huntingtin expression induces mitochondrial calcium handling defects in clonal striatal cells: functional consequences. *J Biol Chem, 281*(46), 34785-34795. doi: 10.1074/jbc.M603845200

Miller, J., Arrasate, M., Shaby, B. A., Mitra, S., Masliah, E., & Finkbeiner, S. (2010). Quantitative relationships between huntingtin levels, polyglutamine length, inclusion body formation, and neuronal death provide novel insight into huntington's disease molecular pathogenesis. *J Neurosci, 30*(31), 10541-10550. doi: 10.1523/JNEUROSCI.0146-10.2010

Milnerwood, A. J., Gladding, C. M., Pouladi, M. A., Kaufman, A. M., Hines, R. M., Boyd, J. D., . . . Raymond, L. A. (2010). Early increase in extrasynaptic NMDA receptor signaling and expression contributes to phenotype onset in Huntington's disease mice. *Neuron, 65*(2), 178-190. doi: 10.1016/j.neuron.2010.01.008

Mo, C., Pang, T. Y., Ransome, M. I., Hill, R. A., Renoir, T., & Hannan, A. J. (2014). High stress hormone levels accelerate the onset of memory deficits in male Huntington's disease mice. *Neurobiol.Dis., 69*, 248-262.

Mo, C., Renoir, T., & Hannan, A. J. (2014). Effects of chronic stress on the onset and progression of Huntington's disease in transgenic mice. *Neurobiol.Dis., 71*, 81-94.

Mo, C., Renoir, T., Pang, T. Y., & Hannan, A. J. (2013). Short-term memory acquisition in female Huntington's disease mice is vulnerable to acute stress. *Behav.Brain Res., 253*, 318-322.

Mochel, F., Charles, P., Seguin, F., Barritault, J., Coussieu, C., Perin, L., . . . Durr, A. (2007). Early energy deficit in Huntington disease: identification of a plasma biomarker traceable during disease progression. *PLoS.One., 2*(7), e647.

Moffitt, H., McPhail, G. D., Woodman, B., Hobbs, C., & Bates, G. P. (2009). Formation of polyglutamine inclusions in a wide range of non-CNS tissues in the HdhQ150 knock-in mouse model of Huntington's disease. *PLoS One, 4*(11), e8025. doi: 10.1371/journal.pone.0008025

Monteys, A. M., Ebanks, S. A., Keiser, M. S., & Davidson, B. L. (2017). CRISPR/Cas9 Editing of the Mutant Huntingtin Allele In Vitro and In Vivo. *Mol Ther, 25*(1), 12-23. doi: 10.1016/j.ymthe.2016.11.010

Morgan, F. H., & Laufgraben, M. J. (2013). Mifepristone for management of Cushing's syndrome. *Pharmacotherapy, 33*(3), 319-329. doi: 10.1002/phar.1202

Morton, A. J. (2013). Circadian and sleep disorder in Huntington's disease. *Exp.Neurol., 243*, 34-44.

Morton, A. J., Wood, N. I., Hastings, M. H., Hurelbrink, C., Barker, R. A., & Maywood, E. S. (2005). Disintegration of the sleep-wake cycle and circadian timing in Huntington's disease. *J.Neurosci., 25*(1), 157-163.

Moutsatsou, P., Kassi, E., & Papavassiliou, A. G. (2012). Glucocorticoid receptor signaling in bone cells. *Trends Mol Med, 18*(6), 348-359. doi: 10.1016/j.molmed.2012.04.005

Myers, R. H., Sax, D. S., Koroshetz, W. J., Mastromauro, C., Cupples, L. A., Kiely, D. K., . . . Bird, E. D. (1991). Factors associated with slow progression in Huntington's disease. *Arch.Neurol., 48*(8), 800-804.

Nagai, Y., Inui, T., Popiel, H. A., Fujikake, N., Hasegawa, K., Urade, Y., . . . Toda, T. (2007). A toxic monomeric conformer of the polyglutamine protein. *Nat Struct Mol Biol, 14*(4), 332-340. doi: 10.1038/nsmb1215

Nasir, J., Floresco, S. B., O'Kusky, J. R., Diewert, V. M., Richman, J. M., Zeisler, J., . . . Hayden, M. R. (1995). Targeted disruption of the Huntington's disease gene results in embryonic lethality and behavioral and morphological changes in heterozygotes. *Cell, 81*(5), 811-823.

Nehl, C., & Paulsen, J. S. (2004). Cognitive and psychiatric aspects of Huntington disease contribute to functional capacity. *J.Nerv.Ment.Dis., 192*(1), 72-74.

Nieuwenhuizen, A. G., & Rutters, F. (2008). The hypothalamic-pituitary-adrenal-axis in the regulation of energy balance. *Physiol Behav, 94*(2), 169-177. doi: 10.1016/j.physbeh.2007.12.011

Novak, M. J., & Tabrizi, S. J. (2010). Huntington's disease. *BMJ, 340*, c3109. doi: 10.1136/bmj.c3109

Nucifora, F. C., Jr., Sasaki, M., Peters, M. F., Huang, H., Cooper, J. K., Yamada, M., . . . Ross, C. A. (2001). Interference by huntingtin and atrophin-1 with cbp-mediated transcription leading to cellular toxicity. *Science, 291*(5512), 2423-2428. doi: 10.1126/science.1056784

Oakeshott, S., Farrar, A., Port, R., Cummins-Sutphen, J., Berger, J., Watson-Johnson, J., . . . Brunner, D. (2013). Deficits in a Simple Visual Go/No-go Discrimination Task in Two Mouse Models of Huntington's Disease. *PLoS Curr, 5*. doi: 10.1371/currents.hd.fe74c94bdd446a0470f6f905a30b5dd1

Oakeshott, S., Port, R. G., Cummins-Sutphen, J., Watson-Johnson, J., Ramboz, S., Park, L., . . . Brunner, D. (2011). HD mouse models reveal clear deficits in learning to perform a simple instrumental response. *PLoS Curr, 3*, RRN1282. doi: 10.1371/currents.RRN1282

Orth, D. N. (1995). Cushing's syndrome. *N.Engl.J.Med., 332*(12), 791-803.

Pang, T. Y., Du, X., Zajac, M. S., Howard, M. L., & Hannan, A. J. (2009). Altered serotonin receptor expression is associated with depression-related behavior in the R6/1 transgenic mouse model of Huntington's disease. *Hum Mol Genet, 18*(4), 753-766. doi: 10.1093/hmg/ddn385

Papalexi, E., Persson, A., Bjorkqvist, M., Petersen, A., Woodman, B., Bates, G. P., . . . Popovic, N. (2005). Reduction of GnRH and infertility in the R6/2 mouse model of Huntington's disease. *Eur.J.Neurosci., 22*(6), 1541-1546.

Pardridge, W. M., & Mietus, L. J. (1979). Transport of steroid hormones through the rat blood-brain barrier. Primary role of albumin-bound hormone. *J Clin Invest, 64*(1), 145-154. doi: 10.1172/JCI109433

Parfitt, G. M., Nguyen, R., Bang, J. Y., Aqrabawi, A. J., Tran, M. M., Seo, D. K., . . . Kim, J. C. (2017). Bidirectional Control of Anxiety-Related Behaviors in Mice: Role of Inputs Arising from the Ventral Hippocampus to the Lateral Septum and Medial Prefrontal Cortex. *Neuropsychopharmacology, 42*(8), 1715-1728. doi: 10.1038/npp.2017.56

Paulsen, J. S., Langbehn, D. R., Stout, J. C., Aylward, E., Ross, C. A., Nance, M., . . . Hayden, M. (2008). Detection of Huntington's disease decades before diagnosis: the Predict-HD study. *J.Neurol.Neurosurg.Psychiatry, 79*(8), 874-880.

Paulsen, J. S., Nehl, C., Hoth, K. F., Kanz, J. E., Benjamin, M., Conybeare, R., . . . Turner, B. (2005). Depression and stages of Huntington's disease. *J Neuropsychiatry Clin Neurosci, 17*(4), 496-502. doi: 10.1176/jnp.17.4.496

Paulsen, J. S., Ready, R. E., Hamilton, J. M., Mega, M. S., & Cummings, J. L. (2001). Neuropsychiatric aspects of Huntington's disease. *J Neurol Neurosurg Psychiatry, 71*(3), 310-314.

Peavy, G. M., Jacobson, M. W., Goldstein, J. L., Hamilton, J. M., Kane, A., Gamst, A. C., . . . Corey-Bloom, J. (2010). Cognitive and functional decline in Huntington's disease: dementia criteria revisited. *Mov Disord, 25*(9), 1163-1169. doi: 10.1002/mds.22953

Petersen, A., & Bjorkqvist, M. (2006). Hypothalamic-endocrine aspects in Huntington's disease. *Eur J Neurosci, 24*(4), 961-967. doi: 10.1111/j.1460-9568.2006.04985.x

Petersen, A., Gil, J., Maat-Schieman, M. L., Bjorkqvist, M., Tanila, H., Araujo, I. M., . . . Brundin, P. (2005). Orexin loss in Huntington's disease. *Hum.Mol.Genet., 14*(1), 39-47.

Pflanz, S., Besson, J. A., Ebmeier, K. P., & Simpson, S. (1991). The clinical manifestation of mental disorder in Huntington's disease: a retrospective case record study of disease progression. *Acta Psychiatr.Scand., 83*(1), 53-60.

Phan, J., Hickey, M. A., Zhang, P., Chesselet, M. F., & Reue, K. (2009). Adipose tissue dysfunction tracks disease progression in two Huntington's disease mouse models. *Hum.Mol.Genet., 18*(6), 1006-1016.

Pla, P., Orvoen, S., Saudou, F., David, D. J., & Humbert, S. (2014). Mood disorders in Huntington's disease: from behavior to cellular and molecular mechanisms. *Front Behav Neurosci, 8*, 135. doi: 10.3389/fnbeh.2014.00135

Porsolt, R. D., Bertin, A., & Jalfre, M. (1977). Behavioral despair in mice: a primary screening test for antidepressants. *Arch Int Pharmacodyn Ther, 229*(2), 327-336.

Porsolt, R. D., Le Pichon, M., & Jalfre, M. (1977). Depression: a new animal model sensitive to antidepressant treatments. *Nature, 266*(5604), 730-732.

Pouladi, M. A., Graham, R. K., Karasinska, J. M., Xie, Y., Santos, R. D., Petersen, A., & Hayden, M. R. (2009). Prevention of depressive behaviour in the YAC128 mouse model of Huntington disease by mutation at residue 586 of huntingtin. *Brain, 132*(Pt 4), 919-932.

Pratley, R. E., Salbe, A. D., Ravussin, E., & Caviness, J. N. (2000). Higher sedentary energy expenditure in patients with Huntington's disease. *Ann Neurol, 47*(1), 64-70.

Pratt, W. B. (1993). The role of heat shock proteins in regulating the function, folding, and trafficking of the glucocorticoid receptor. *J Biol Chem, 268*(29), 21455-21458.

Pringsheim, T., Wiltshire, K., Day, L., Dykeman, J., Steeves, T., & Jette, N. (2012). The incidence and prevalence of Huntington's disease: a systematic review and meta-analysis. *Mov Disord, 27*(9), 1083-1091. doi: 10.1002/mds.25075

Ransome, M. I., Renoir, T., & Hannan, A. J. (2012). Hippocampal neurogenesis, cognitive deficits and affective disorder in Huntington's disease. *Neural Plast., 2012*, 874387.

Ratovitski, T., Gucek, M., Jiang, H., Chighladze, E., Waldron, E., D'Ambola, J., . . . Ross, C. A. (2009). Mutant huntingtin N-terminal fragments of specific size mediate aggregation and toxicity in neuronal cells. *J Biol Chem, 284*(16), 10855-10867. doi: 10.1074/jbc.M804813200

Rebec, G. V., Conroy, S. K., & Barton, S. J. (2006). Hyperactive striatal neurons in symptomatic Huntington R6/2 mice: variations with behavioral state and repeated ascorbate treatment. *Neuroscience, 137*(1), 327-336. doi: 10.1016/j.neuroscience.2005.08.062

Reddy, T. E., Pauli, F., Sprouse, R. O., Neff, N. F., Newberry, K. M., Garabedian, M. J., & Myers, R. M. (2009). Genomic determination of the glucocorticoid response reveals unexpected

mechanisms of gene regulation. *Genome Res, 19*(12), 2163-2171. doi: 10.1101/gr.097022.109

Renoir, T., Zajac, M. S., Du, X., Pang, T. Y., Leang, L., Chevarin, C., . . . Hannan, A. J. (2011). Sexually dimorphic serotonergic dysfunction in a mouse model of Huntington's disease and depression. *PLoS One, 6*(7), e22133. doi: 10.1371/journal.pone.0022133

Ressler, K. J., & Nemeroff, C. B. (2000). Role of serotonergic and noradrenergic systems in the pathophysiology of depression and anxiety disorders. *Depress Anxiety, 12 Suppl 1*, 2-19. doi: 10.1002/1520-6394(2000)12:1+<2::AID-DA2>3.0.CO;2-4

Reyes, A., Cruickshank, T., Ziman, M., & Nosaka, K. (2014). Pulmonary function in patients with Huntington's disease. *BMC Pulm Med, 14*, 89. doi: 10.1186/1471-2466-14-89

Ribchester, R. R., Thomson, D., Wood, N. I., Hinks, T., Gillingwater, T. H., Wishart, T. M., . . . Morton, A. J. (2004). Progressive abnormalities in skeletal muscle and neuromuscular junctions of transgenic mice expressing the Huntington's disease mutation. *Eur J Neurosci, 20*(11), 3092-3114. doi: 10.1111/j.1460-9568.2004.03783.x

Richfield, E. K., Maguire-Zeiss, K. A., Vonkeman, H. E., & Voorn, P. (1995). Preferential loss of preproenkephalin versus preprotachykinin neurons from the striatum of Huntington's disease patients. *Ann Neurol, 38*(6), 852-861. doi: 10.1002/ana.410380605

Rockabrand, E., Slepko, N., Pantalone, A., Nukala, V. N., Kazantsev, A., Marsh, J. L., . . . Thompson, L. M. (2007). The first 17 amino acids of Huntingtin modulate its sub-cellular localization, aggregation and effects on calcium homeostasis. *Hum Mol Genet, 16*(1), 61-77. doi: 10.1093/hmg/ddl440

Rodda, R. A. (1981). Cerebellar atrophy in Huntington's disease. *J.Neurol.Sci., 50*(1), 147-157.

Rodrigues, F. B., & Wild, E. J. (2017). Clinical Trials Corner: September 2017. *J Huntingtons Dis, 6*(3), 255-263. doi: 10.3233/JHD-170262

Rosas, H. D., Koroshetz, W. J., Chen, Y. I., Skeuse, C., Vangel, M., Cudkowicz, M. E., . . . Goldstein, J. M. (2003). Evidence for more widespread cerebral pathology in early HD: an MRI-based morphometric analysis. *Neurology, 60*(10), 1615-1620.

Rosas, H. D., Salat, D. H., Lee, S. Y., Zaleta, A. K., Pappu, V., Fischl, B., . . . Hersch, S. M. (2008). Cerebral cortex and the clinical expression of Huntington's disease: complexity and heterogeneity. *Brain, 131*(Pt 4), 1057-1068.

Ross, C. A., Aylward, E. H., Wild, E. J., Langbehn, D. R., Long, J. D., Warner, J. H., . . . Tabrizi, S. J. (2014). Huntington disease: natural history, biomarkers and prospects for therapeutics. *Nat Rev Neurol, 10*(4), 204-216. doi: 10.1038/nrneurol.2014.24

Ross, C. A., & Tabrizi, S. J. (2011). Huntington's disease: from molecular pathogenesis to clinical treatment. *Lancet Neurol, 10*(1), 83-98. doi: 10.1016/S1474-4422(10)70245-3

Rub, U., Hoche, F., Brunt, E. R., Heinsen, H., Seidel, K., Del Turco, D., . . . den Dunnen, W. F. (2013). Degeneration of the cerebellum in Huntington's disease (HD): possible relevance for the clinical picture and potential gateway to pathological mechanisms of the disease process. *Brain Pathol, 23*(2), 165-177. doi: 10.1111/j.1750-3639.2012.00629.x

Rub, U., Vonsattel, J. P., Heinsen, H., & Korf, H. W. (2015). The Neuropathology of Huntington s disease: classical findings, recent developments and correlation to functional neuroanatomy. *Adv Anat Embryol Cell Biol, 217*, 1-146.

Sadler, A. M., & Bailey, S. J. (2013). Validation of a refined technique for taking repeated blood samples from juvenile and adult mice. *Lab Anim, 47*(4), 316-319.

Saleh, N., Moutereau, S., Durr, A., Krystkowiak, P., Azulay, J. P., Tranchant, C., . . . Maison, P. (2009). Neuroendocrine disturbances in Huntington's disease. *PLoS One, 4*(3), e4962. doi: 10.1371/journal.pone.0004962

Samaranch, L., Blits, B., San Sebastian, W., Hadaczek, P., Bringas, J., Sudhakar, V., . . . Bankiewicz, K. S. (2017). MR-guided parenchymal delivery of adeno-associated viral vector serotype 5 in non-human primate brain. *Gene Ther, 24*(4), 253-261. doi: 10.1038/gt.2017.14

Sanberg, P. R., Fibiger, H. C., & Mark, R. F. (1981). Body weight and dietary factors in Huntington's disease patients compared with matched controls. *Med.J.Aust., 1*(8), 407-409.

Sapolsky, R. M., Krey, L. C., & McEwen, B. S. (1985). Prolonged glucocorticoid exposure reduces hippocampal neuron number: implications for aging. *J Neurosci, 5*(5), 1222-1227.

Sapolsky, R. M., Romero, L. M., & Munck, A. U. (2000). How do glucocorticoids influence stress responses? Integrating permissive, suppressive, stimulatory, and preparative actions. *Endocr Rev, 21*(1), 55-89. doi: 10.1210/edrv.21.1.0389

Sapolsky, R. M., Uno, H., Rebert, C. S., & Finch, C. E. (1990). Hippocampal damage associated with prolonged glucocorticoid exposure in primates. *J Neurosci, 10*(9), 2897-2902.

Sapp, E., Kegel, K. B., Aronin, N., Hashikawa, T., Uchiyama, Y., Tohyama, K., . . . DiFiglia, M. (2001). Early and progressive accumulation of reactive microglia in the Huntington disease brain. *J Neuropathol.Exp.Neurol., 60*(2), 161-172.

Sauer, B. (1998). Inducible gene targeting in mice using the Cre/lox system. *Methods, 14*(4), 381-392. doi: 10.1006/meth.1998.0593

Schaffar, G., Breuer, P., Boteva, R., Behrends, C., Tzvetkov, N., Strippel, N., . . . Hartl, F. U. (2004). Cellular toxicity of polyglutamine expansion proteins: mechanism of transcription factor deactivation. *Mol.Cell, 15*(1), 95-105.

Schilling, B., Gafni, J., Torcassi, C., Cong, X., Row, R. H., LaFevre-Bernt, M. A., . . . Ellerby, L. M. (2006). Huntingtin phosphorylation sites mapped by mass spectrometry. Modulation of cleavage and toxicity. *J Biol Chem, 281*(33), 23686-23697. doi: 10.1074/jbc.M513507200

Schilling, G., Becher, M. W., Sharp, A. H., Jinnah, H. A., Duan, K., Kotzuk, J. A., . . . Borchelt, D. R. (1999). Intranuclear inclusions and neuritic aggregates in transgenic mice expressing a mutant N-terminal fragment of huntingtin. *Hum.Mol.Genet., 8*(3), 397-407.

Schilling, G., Coonfield, M. L., Ross, C. A., & Borchelt, D. R. (2001). Coenzyme Q10 and remacemide hydrochloride ameliorate motor deficits in a Huntington's disease transgenic mouse model. *Neurosci Lett., 315*(3), 149-153.

Schilling, G., Klevytska, A., Tebbenkamp, A. T., Juenemann, K., Cooper, J., Gonzales, V., . . . Borchelt, D. R. (2007). Characterization of huntingtin pathologic fragments in human Huntington disease, transgenic mice, and cell models. *J Neuropathol Exp Neurol, 66*(4), 313-320. doi: 10.1097/nen.0b013e318040b2c8

Shah, N., Ruiz, H. H., Zafar, U., Post, K. D., Buettner, C., & Geer, E. B. (2017). Proinflammatory cytokines remain elevated despite long-term remission in Cushing's disease: a prospective study. *Clin Endocrinol (Oxf), 86*(1), 68-74. doi: 10.1111/cen.13230

Sharp, A. H., Loev, S. J., Schilling, G., Li, S. H., Li, X. J., Bao, J., . . . et al. (1995). Widespread expression of Huntington's disease gene (IT15) protein product. *Neuron, 14*(5), 1065-1074.

She, P., Zhang, Z., Marchionini, D., Diaz, W. C., Jetton, T. J., Kimball, S. R., . . . Lynch, C. J. (2011). Molecular characterization of skeletal muscle atrophy in the R6/2 mouse model of Huntington's disease. *Am.J.Physiol Endocrinol.Metab, 301*(1), E49-E61.

Shin, J. W., Kim, K. H., Chao, M. J., Atwal, R. S., Gillis, T., MacDonald, M. E., . . . Lee, J. M. (2016). Permanent inactivation of Huntington's disease mutation by personalized allele-specific CRISPR/Cas9. *Hum Mol Genet, 25*(20), 4566-4576. doi: 10.1093/hmg/ddw286

Shin, L. M., & Liberzon, I. (2010). The neurocircuitry of fear, stress, and anxiety disorders. *Neuropsychopharmacology, 35*(1), 169-191. doi: 10.1038/npp.2009.83

Shirbin, C. A., Chua, P., Churchyard, A., Hannan, A. J., Lowndes, G., & Stout, J. C. (2013). The relationship between cortisol and verbal memory in the early stages of Huntington's disease. *J Neurol, 260*(3), 891-902. doi: 10.1007/s00415-012-6732-y

Shirbin, C. A., Chua, P., Churchyard, A., Lowndes, G., Hannan, A. J., Pang, T. Y., . . . Stout, J. C. (2013). Cortisol and depression in pre-diagnosed and early stage Huntington's disease. *Psychoneuroendocrinology, 38*(11), 2439-2447.

Shirendeb, U. P., Calkins, M. J., Manczak, M., Anekonda, V., Dufour, B., McBride, J. L., . . . Reddy, P. H. (2012). Mutant huntingtin's interaction with mitochondrial protein Drp1 impairs mitochondrial biogenesis and causes defective axonal transport and synaptic degeneration in Huntington's disease. *Hum Mol Genet, 21*(2), 406-420. doi: 10.1093/hmg/ddr475

Shoulson, I., & Fahn, S. (1979). Huntington disease: clinical care and evaluation. *Neurology, 29*(1), 1-3.

Slow, E. J., van Raamsdonk, J., Rogers, D., Coleman, S. H., Graham, R. K., Deng, Y., . . . Hayden, M. R. (2003). Selective striatal neuronal loss in a YAC128 mouse model of Huntington disease. *Hum Mol Genet, 12*(13), 1555-1567.

Snowden, J. S., Craufurd, D., Thompson, J., & Neary, D. (2002). Psychomotor, executive, and memory function in preclinical Huntington's disease. *J Clin Exp Neuropsychol, 24*(2), 133-145. doi: 10.1076/jcen.24.2.133.998

Snowden, M. B., Atkins, D. C., Steinman, L. E., Bell, J. F., Bryant, L. L., Copeland, C., & Fitzpatrick, A. L. (2015). Longitudinal Association of Dementia and Depression. *Am J Geriatr Psychiatry, 23*(9), 897-905. doi: 10.1016/j.jagp.2014.09.002

Soneson, C., Fontes, M., Zhou, Y., Denisov, V., Paulsen, J. S., Kirik, D., . . . Huntington Study Group, P.-H. D. i. (2010). Early changes in the hypothalamic region in prodromal Huntington disease revealed by MRI analysis. *Neurobiol Dis, 40*(3), 531-543. doi: 10.1016/j.nbd.2010.07.013

Soylu-Kucharz, R., Baldo, B., & Petersen, A. (2016). Metabolic and behavioral effects of mutant huntingtin deletion in Sim1 neurons in the BACHD mouse model of Huntington's disease. *Sci Rep, 6*, 28322. doi: 10.1038/srep28322

Spargo, E., Everall, I. P., & Lantos, P. L. (1993). Neuronal loss in the hippocampus in Huntington's disease: a comparison with HIV infection. *J.Neurol.Neurosurg.Psychiatry, 56*(5), 487-491.

Sprengelmeyer, R., Orth, M., Muller, H. P., Wolf, R. C., Gron, G., Depping, M. S., . . . Landwehrmeyer, G. B. (2014). The neuroanatomy of subthreshold depressive symptoms in Huntington's disease: a combined diffusion tensor imaging (DTI) and voxel-based morphometry (VBM) study. *Psychol Med, 44*(9), 1867-1878. doi: 10.1017/S003329171300247X

Squitieri, F., Di Pardo, A., Favellato, M., Amico, E., Maglione, V., & Frati, L. (2015). Pridopidine, a dopamine stabilizer, improves motor performance and shows neuroprotective effects in Huntington disease R6/2 mouse model. *J Cell Mol Med, 19*(11), 2540-2548. doi: 10.1111/jcmm.12604

Squitieri, F., Gellera, C., Cannella, M., Mariotti, C., Cislaghi, G., Rubinsztein, D. C., . . . Donato, S. D. (2003). Homozygosity for CAG mutation in Huntington disease is associated with a more severe clinical course. *Brain, 126*(Pt 4), 946-955.

Stack, E. C., & Ferrante, R. J. (2007). Huntington's disease: progress and potential in the field. *Expert Opin Investig Drugs, 16*(12), 1933-1953. doi: 10.1517/13543784.16.12.1933

Stack, E. C., Kubilus, J. K., Smith, K., Cormier, K., Del Signore, S. J., Guelin, E., . . . Ferrante, R. J. (2005). Chronology of behavioral symptoms and neuropathological sequela in R6/2

Huntington's disease transgenic mice. *J Comp Neurol, 490*(4), 354-370. doi: 10.1002/cne.20680

Stack, E. C., Smith, K. M., Ryu, H., Cormier, K., Chen, M., Hagerty, S. W., . . . Ferrante, R. J. (2006). Combination therapy using minocycline and coenzyme Q10 in R6/2 transgenic Huntington's disease mice. *Biochim.Biophys.Acta, 1762*(3), 373-380.

Stanek, L. M., Sardi, S. P., Mastis, B., Richards, A. R., Treleaven, C. M., Taksir, T., . . . Shihabuddin, L. S. (2014). Silencing Mutant Huntingtin by Adeno-Associated Virus-Mediated RNA Interference Ameliorates Disease Manifestations in the YAC128 Mouse Model of Huntington's Disease. *Hum.Gene Ther., 25*(5), 461-474.

Starkman, M. N., Schteingart, D. E., & Schork, M. A. (1981). Depressed mood and other psychiatric manifestations of Cushing's syndrome: relationship to hormone levels. *Psychosom Med, 43*(1), 3-18.

Stout, J. C., Paulsen, J. S., Queller, S., Solomon, A. C., Whitlock, K. B., Campbell, J. C., . . . Aylward, E. H. (2011). Neurocognitive signs in prodromal Huntington disease. *Neuropsychology, 25*(1), 1-14. doi: 10.1037/a0020937

Strand, A. D., Aragaki, A. K., Shaw, D., Bird, T., Holton, J., Turner, C., . . . Olson, J. M. (2005). Gene expression in Huntington's disease skeletal muscle: a potential biomarker. *Hum.Mol.Genet., 14*(13), 1863-1876.

Strong, T. V., Tagle, D. A., Valdes, J. M., Elmer, L. W., Boehm, K., Swaroop, M., . . . Albin, R. L. (1993). Widespread expression of the human and rat Huntington's disease gene in brain and nonneural tissues. *Nat.Genet., 5*(3), 259-265.

Sun, L., Chang, J., Kirchhoff, S. R., & Knowlton, A. A. (2000). Activation of HSF and selective increase in heat-shock proteins by acute dexamethasone treatment. *Am J Physiol Heart Circ Physiol, 278*(4), H1091-1097.

Sun, Y., Savanenin, A., Reddy, P. H., & Liu, Y. F. (2001). Polyglutamine-expanded huntingtin promotes sensitization of N-methyl-D-aspartate receptors via post-synaptic density 95. *J Biol Chem, 276*(27), 24713-24718. doi: 10.1074/jbc.M103501200

Swaab, D. F., Raadsheer, F. C., Endert, E., Hofman, M. A., Kamphorst, W., & Ravid, R. (1994). Increased cortisol levels in aging and Alzheimer's disease in postmortem cerebrospinal fluid. *J Neuroendocrinol, 6*(6), 681-687.

Tabrizi, S. J., Langbehn, D. R., Leavitt, B. R., Roos, R. A., Durr, A., Craufurd, D., . . . Stout, J. C. (2009). Biological and clinical manifestations of Huntington's disease in the longitudinal TRACK-HD study: cross-sectional analysis of baseline data. *Lancet Neurol., 8*(9), 791-801.

Tabrizi, S. J., Scahill, R. I., Durr, A., Roos, R. A., Leavitt, B. R., Jones, R., . . . Investigators, T.-H. (2011). Biological and clinical changes in premanifest and early stage Huntington's disease in the TRACK-HD study: the 12-month longitudinal analysis. *Lancet Neurol, 10*(1), 31-42. doi: 10.1016/S1474-4422(10)70276-3

Tabrizi, S. J., Workman, J., Hart, P. E., Mangiarini, L., Mahal, A., Bates, G., . . . Schapira, A. H. (2000). Mitochondrial dysfunction and free radical damage in the Huntington R6/2 transgenic mouse. *Ann Neurol, 47*(1), 80-86.

Takahashi, T., Kikuchi, S., Katada, S., Nagai, Y., Nishizawa, M., & Onodera, O. (2008). Soluble polyglutamine oligomers formed prior to inclusion body formation are cytotoxic. *Hum Mol Genet, 17*(3), 345-356. doi: 10.1093/hmg/ddm311

Takatsu-Coleman, A. L., Patti, C. L., Zanin, K. A., Zager, A., Carvalho, R. C., Borcoi, A. R., . . . Frussa-Filho, R. (2013). Short-term social isolation induces depressive-like behaviour and reinstates the retrieval of an aversive task: mood-congruent memory in male mice? *J Psychiatry Neurosci, 38*(4), 259-268. doi: 10.1503/jpn.120050

Thompson, P. D., Berardelli, A., Rothwell, J. C., Day, B. L., Dick, J. P., Benecke, R., & Marsden, C. D. (1988). The coexistence of bradykinesia and chorea in Huntington's disease and its implications for theories of basal ganglia control of movement. *Brain, 111 (Pt 2)*, 223-244.

Thomson, S., Koren, G., Fraser, L. A., Rieder, M., Friedman, T. C., & Van Uum, S. H. (2010). Hair analysis provides a historical record of cortisol levels in Cushing's syndrome. *Exp.Clin.Endocrinol.Diabetes, 118*(2), 133-138.

Thu, D. C., Oorschot, D. E., Tippett, L. J., Nana, A. L., Hogg, V. M., Synek, B. J., . . . Faull, R. L. (2010). Cell loss in the motor and cingulate cortex correlates with symptomatology in Huntington's disease. *Brain, 133*(Pt 4), 1094-1110.

Timmers, H. J., Swaab, D. F., van de Nes, J. A., & Kremer, H. P. (1996). Somatostatin 1-12 immunoreactivity is decreased in the hypothalamic lateral tuberal nucleus of Huntington's disease patients. *Brain Res., 728*(2), 141-148.

Todd, T. W., & Lim, J. (2013). Aggregation formation in the polyglutamine diseases: protection at a cost? *Mol Cells, 36*(3), 185-194. doi: 10.1007/s10059-013-0167-x

Tomlinson, J. W., & Stewart, P. M. (2001). Cortisol metabolism and the role of 11beta-hydroxysteroid dehydrogenase. *Best Pract Res Clin Endocrinol Metab, 15*(1), 61-78. doi: 10.1053/beem.2000.0119

Toth, M., & Grossman, A. (2013). Glucocorticoid-induced osteoporosis: lessons from Cushing's syndrome. *Clin.Endocrinol.(Oxf), 79*(1), 1-11.

Travessa, A. M., Rodrigues, F. B., Mestre, T. A., & Ferreira, J. J. (2017). Fifteen Years of Clinical Trials in Huntington's Disease: A Very Low Clinical Drug Development Success Rate. *J Huntingtons Dis, 6*(2), 157-163. doi: 10.3233/JHD-170245

Trejo, A., Boll, M. C., Alonso, M. E., Ochoa, A., & Velasquez, L. (2005). Use of oral nutritional supplements in patients with Huntington's disease. *Nutrition, 21*(9), 889-894.

Trejo, A., Tarrats, R. M., Alonso, M. E., Boll, M. C., Ochoa, A., & Velasquez, L. (2004). Assessment of the nutrition status of patients with Huntington's disease. *Nutrition, 20*(2), 192-196.

Trottier, Y., Devys, D., Imbert, G., Saudou, F., An, I., Lutz, Y., . . . Mandel, J. L. (1995). Cellular localization of the Huntington's disease protein and discrimination of the normal and mutated form. *Nat Genet, 10*(1), 104-110. doi: 10.1038/ng0595-104

Tsvetkov, A. S., Arrasate, M., Barmada, S., Ando, D. M., Sharma, P., Shaby, B. A., & Finkbeiner, S. (2013). Proteostasis of polyglutamine varies among neurons and predicts neurodegeneration. *Nat Chem Biol, 9*(9), 586-592. doi: 10.1038/nchembio.1308

Tunez, I., Collado, J. A., Medina, F. J., Pena, J., Del, C. M. M., Jimena, I., . . . Montilla, P. (2006). 17 beta-Estradiol may affect vulnerability of striatum in a 3-nitropropionic acid-induced experimental model of Huntington's disease in ovariectomized rats. *Neurochem Int, 48*(5), 367-373. doi: 10.1016/j.neuint.2005.11.011

Ulrich-Lai, Y. M., Arnhold, M. M., & Engeland, W. C. (2006). Adrenal splanchnic innervation contributes to the diurnal rhythm of plasma corticosterone in rats by modulating adrenal sensitivity to ACTH. *Am J Physiol Regul Integr Comp Physiol, 290*(4), R1128-1135. doi: 10.1152/ajpregu.00042.2003

Ulrich-Lai, Y. M., & Herman, J. P. (2009). Neural regulation of endocrine and autonomic stress responses. *Nat.Rev.Neurosci., 10*(6), 397-409.

Unmack Larsen, I., Vinther-Jensen, T., Gade, A., Nielsen, J. E., & Vogel, A. (2015). Assessing impairment of executive function and psychomotor speed in premanifest and manifest Huntington's disease gene-expansion carriers. *J Int Neuropsychol Soc, 21*(3), 193-202. doi: 10.1017/S1355617715000090

Valadao, P. A., de Aragao, B. C., Andrade, J. N., Magalhaes-Gomes, M. P., Foureaux, G., Joviano-Santos, J. V., . . . Guatimosim, C. (2017). Muscle atrophy is associated with cervical spinal motoneuron loss in BACHD mouse model for Huntington's disease. *Eur J Neurosci, 45*(6), 785-796. doi: 10.1111/ejn.13510

Valassi, E., Crespo, I., Santos, A., & Webb, S. M. (2012). Clinical consequences of Cushing's syndrome. *Pituitary., 15*(3), 319-329.

van der Burg, J. M., Bacos, K., Wood, N. I., Lindqvist, A., Wierup, N., Woodman, B., . . . Bjorkqvist, M. (2008). Increased metabolism in the R6/2 mouse model of Huntington's disease. *Neurobiol.Dis., 29*(1), 41-51.

van der Burg, J. M., Bjorkqvist, M., & Brundin, P. (2009). Beyond the brain: widespread pathology in Huntington's disease. *Lancet Neurol., 8*(8), 765-774.

van der Burg, J. M., Winqvist, A., Aziz, N. A., Maat-Schieman, M. L., Roos, R. A., Bates, G. P., . . . Wierup, N. (2011). Gastrointestinal dysfunction contributes to weight loss in Huntington's disease mice. *Neurobiol.Dis.*

van Duijn, E., Kingma, E. M., Timman, R., Zitman, F. G., Tibben, A., Roos, R. A., & van der Mast, R. C. (2008). Cross-sectional study on prevalences of psychiatric disorders in mutation carriers of Huntington's disease compared with mutation-negative first-degree relatives. *J Clin Psychiatry, 69*(11), 1804-1810.

van Duijn, E., Kingma, E. M., & van der Mast, R. C. (2007). Psychopathology in verified Huntington's disease gene carriers. *J Neuropsychiatry Clin Neurosci, 19*(4), 441-448. doi: 10.1176/jnp.2007.19.4.441

van Duijn, E., Selis, M. A., Giltay, E. J., Zitman, F. G., Roos, R. A., van, P. H., & van der Mast, R. C. (2010). Hypothalamic-pituitary-adrenal axis functioning in Huntington's disease mutation carriers compared with mutation-negative first-degree controls. *Brain Res.Bull., 83*(5), 232-237.

Van Raamsdonk, J. M., Murphy, Z., Selva, D. M., Hamidizadeh, R., Pearson, J., Petersen, A., . . . Leavitt, B. R. (2007). Testicular degeneration in Huntington disease. *Neurobiol.Dis., 26*(3), 512-520.

van Vugt, J. P., van Hilten, B. J., & Roos, R. A. (1996). Hypokinesia in Huntington's disease. *Mov Disord, 11*(4), 384-388. doi: 10.1002/mds.870110406

van Wamelen, D. J., Aziz, N. A., Anink, J. J., van, S. R., Angeloni, D., Fraschini, F., . . . Swaab, D. F. (2013). Suprachiasmatic nucleus neuropeptide expression in patients with Huntington's Disease. *Sleep, 36*(1), 117-125.

Vining, R. F., McGinley, R. A., Maksvytis, J. J., & Ho, K. Y. (1983). Salivary cortisol: a better measure of adrenal cortical function than serum cortisol. *Ann.Clin.Biochem., 20 (Pt 6)*, 329-335.

Vogt, B. A., & Paxinos, G. (2014). Cytoarchitecture of mouse and rat cingulate cortex with human homologies. *Brain Struct Funct, 219*(1), 185-192. doi: 10.1007/s00429-012-0493-3

Vonsattel, J. P., Myers, R. H., Stevens, T. J., Ferrante, R. J., Bird, E. D., & Richardson, E. P., Jr. (1985). Neuropathological classification of Huntington's disease. *J Neuropathol.Exp.Neurol., 44*(6), 559-577.

Wacker, J. L., Huang, S. Y., Steele, A. D., Aron, R., Lotz, G. P., Nguyen, Q., . . . Muchowski, P. J. (2009). Loss of Hsp70 exacerbates pathogenesis but not levels of fibrillar aggregates in a mouse model of Huntington's disease. *J Neurosci, 29*(28), 9104-9114. doi: 10.1523/JNEUROSCI.2250-09.2009

Wang, N., Gray, M., Lu, X. H., Cantle, J. P., Holley, S. M., Greiner, E., . . . Yang, X. W. (2014). Neuronal targets for reducing mutant huntingtin expression to ameliorate disease in a mouse model of Huntington's disease. *Nat.Med., 20*(5), 536-541.

Weikum, E. R., Knuesel, M. T., Ortlund, E. A., & Yamamoto, K. R. (2017). Glucocorticoid receptor control of transcription: precision and plasticity via allostery. *Nat Rev Mol Cell Biol, 18*(3), 159-174. doi: 10.1038/nrm.2016.152

Weinstein, S. P., Paquin, T., Pritsker, A., & Haber, R. S. (1995). Glucocorticoid-induced insulin resistance: dexamethasone inhibits the activation of glucose transport in rat skeletal muscle by both insulin- and non-insulin-related stimuli. *Diabetes, 44*(4), 441-445.

Wexler, N. S., Young, A. B., Tanzi, R. E., Travers, H., Starosta-Rubinstein, S., Penney, J. B., . . . et al. (1987). Homozygotes for Huntington's disease. *Nature, 326*(6109), 194-197. doi: 10.1038/326194a0

Whitnall, M. H. (1993). Regulation of the hypothalamic corticotropin-releasing hormone neurosecretory system. *Prog Neurobiol, 40*(5), 573-629.

Wild, E. J., & Tabrizi, S. J. (2017). Therapies targeting DNA and RNA in Huntington's disease. *Lancet Neurol, 16*(10), 837-847. doi: 10.1016/S1474-4422(17)30280-6

Wong, E. Y., & Herbert, J. (2004). The corticoid environment: a determining factor for neural progenitors' survival in the adult hippocampus. *Eur J Neurosci, 20*(10), 2491-2498. doi: 10.1111/j.1460-9568.2004.03717.x

Wood, N. I., Carta, V., Milde, S., Skillings, E. A., McAllister, C. J., Ang, Y. L., . . . Morton, A. J. (2010). Responses to environmental enrichment differ with sex and genotype in a transgenic mouse model of Huntington's disease. *PLoS One, 5*(2), e9077. doi: 10.1371/journal.pone.0009077

Wood, N. I., Goodman, A. O., van der Burg, J. M., Gazeau, V., Brundin, P., Bjorkqvist, M., . . . Morton, A. J. (2008). Increased thirst and drinking in Huntington's disease and the R6/2 mouse. *Brain Res.Bull., 76*(1-2), 70-79.

Wu, J., Ryskamp, D. A., Liang, X., Egorova, P., Zakharova, O., Hung, G., & Bezprozvanny, I. (2016). Enhanced Store-Operated Calcium Entry Leads to Striatal Synaptic Loss in a Huntington's Disease Mouse Model. *J Neurosci, 36*(1), 125-141. doi: 10.1523/JNEUROSCI.1038-15.2016

Xie, Y., Hayden, M. R., & Xu, B. (2010). BDNF overexpression in the forebrain rescues Huntington's disease phenotypes in YAC128 mice. *J Neurosci, 30*(44), 14708-14718. doi: 10.1523/JNEUROSCI.1637-10.2010

Xu, C., He, J., Jiang, H., Zu, L., Zhai, W., Pu, S., & Xu, G. (2009). Direct effect of glucocorticoids on lipolysis in adipocytes. *Mol Endocrinol, 23*(8), 1161-1170. doi: 10.1210/me.2008-0464

Yanai, A., Huang, K., Kang, R., Singaraja, R. R., Arstikaitis, P., Gan, L., . . . Hayden, M. R. (2006). Palmitoylation of huntingtin by HIP14 is essential for its trafficking and function. *Nat Neurosci, 9*(6), 824-831. doi: 10.1038/nn1702

Yang, W., Dunlap, J. R., Andrews, R. B., & Wetzel, R. (2002). Aggregated polyglutamine peptides delivered to nuclei are toxic to mammalian cells. *Hum Mol Genet, 11*(23), 2905-2917.

Yero, T., & Rey, J. A. (2008). Tetrabenazine (Xenazine), An FDA-Approved Treatment Option For Huntington's Disease-Related Chorea. *P.T., 33*(12), 690-694.

You, S. C., Geschwind, M. D., Sha, S. J., Apple, A., Satris, G., Wood, K. A., . . . Possin, K. L. (2014). Executive functions in premanifest Huntington's disease. *Mov Disord, 29*(3), 405-409. doi: 10.1002/mds.25762

Yu, I. T., Lee, S. H., Lee, Y. S., & Son, H. (2004). Differential effects of corticosterone and dexamethasone on hippocampal neurogenesis in vitro. *Biochem Biophys Res Commun, 317*(2), 484-490. doi: 10.1016/j.bbrc.2004.03.071

Zala, D., Benchoua, A., Brouillet, E., Perrin, V., Gaillard, M. C., Zurn, A. D., . . . Deglon, N. (2005). Progressive and selective striatal degeneration in primary neuronal cultures using lentiviral vector coding for a mutant huntingtin fragment. *Neurobiol.Dis., 20*(3), 785-798.

Zhang, J., Peng, Q., Li, Q., Jahanshad, N., Hou, Z., Jiang, M., . . . Duan, W. (2010). Longitudinal characterization of brain atrophy of a Huntington's disease mouse model by automated morphological analyses of magnetic resonance images. *Neuroimage, 49*(3), 2340-2351. doi: 10.1016/j.neuroimage.2009.10.027

Zielonka, D., Piotrowska, I., Marcinkowski, J. T., & Mielcarek, M. (2014). Skeletal muscle pathology in Huntington's disease. *Front Physiol, 5*, 380. doi: 10.3389/fphys.2014.00380

Zuccato, C., Ciammola, A., Rigamonti, D., Leavitt, B. R., Goffredo, D., Conti, L., . . . Cattaneo, E. (2001). Loss of huntingtin-mediated BDNF gene transcription in Huntington's disease. *Science, 293*(5529), 493-498.

Zweig, R. M., Ross, C. A., Hedreen, J. C., Peyser, C., Cardillo, J. E., Folstein, S. E., & Price, D. L. (1992). Locus coeruleus involvement in Huntington's disease. *Arch.Neurol., 49*(2), 152-156.